The University of Nottingham

Carbon Dioxide Capture and Storage by Mineralisation Using Recyclable Ammonium Salts

Xiaolong Wang, MSc

Thesis submitted to the University of Nottingham for

the degree of Doctor of Philosophy

October 2011

Abstract

Carbon dioxide capture and storage by mineralisation (CCSM) is considered to be an alternative solution for reducing anthropogenic CO_2 in some regions, where geological storage is not possible or considered uneconomically viable. However, low efficiency of mineral dissolution and use of unrecyclable additives are two key barriers for the development of CCSM.

A novel CCSM process with recyclable ammonium salts is proposed to overcome these barriers in this study. This process integrates mineral carbonation with CO_2 capture by employing NH_3, NH_4HSO_4 and CO_2 containing ammonium salts in the capture step, mineral dissolution and carbonation steps, respectively. The NH_4HSO_4 and NH_3 can then be regenerated by thermal decomposition of $(NH_4)_2SO_4$, which is the by-product from the process. The use of CO_2 containing ammonium salts as the source of CO_2 can avoid desorption and compression of CO_2, which account for 70 % of the total energy consumption in the whole CCS chain.

In this work, a CCSM process route at low solid to liquid ratio (50 g/l) was experimentally investigated to validate the process concept. It was found that the dissolution efficiency of magnesium (Mg) can achieve 100 % by using NH_4HSO_4 and the carbonation efficiency can

reach 96.5 % by using CO_2 containing ammonium salts from the capture step and addition of aqueous NH_3. Three products, including Si rich residue, Fe rich residue and pure hydromagnesite were obtained from the process. The TGA studies reported that the regeneration efficiency of NH_4HSO_4 and NH_3 in this process was 95 %. Both dissolution and carbonation efficiencies achieved in this work are higher than the values reported in previous work.

In order to reduce the water usage, a CCSM process at high solid to liquid ratio (200-300 g/l) was developed. It was found that the dissolution efficiency of Mg was 64 and 72 % at 200 and 300 g/l, respectively. The increase of dissolution efficiency with a solid to liquid ratio could be explained by the removal of passive product layer caused by particle-particle interaction. At a solid to liquid ratio of 300 g/l, the highest carbonation efficiency achieved was 65.4 %. Magnesite instead of hydromagnesite was found after carbonation due to the CO_2 pressure caused by the decomposition of ammonium salts above 70 °C. Additionally, the carbonation efficiency was doubled by using $(NH_4)_2CO_3$ compared to that using NH_4HCO_3.

A preliminary evaluation was conducted to estimate the OPEX, including energy consumption, chemical costs and feedstock cost, based on the experimental results from the two process routes developed. In order to get low OPEX, the optimization process conditions, such as solid to liquid ratio and reaction time, were

determined. Then, experiments at these optimized conditions were conducted. The dissolution efficiency of Mg from serpentine with particle size 75-150 μm using 2.8 M NH_4HSO_4 at 100 g/l solid to liquid ratio for 1 h was around 80 %. The carbonation efficiency was 96 % when the molar ratio of Mg: CO_2 containing NH^{4+} salts: NH_3 was 1:1.5:2. Thus, the mass balance of the process showed that 3.0 t[1] of serpentine, 0.2 t of NH_4HSO_4 and 0.1 t of NH_3 were required to sequester 1 t of CO_2 and produce 1.9 t of magnesite. Moreover, 1.7 t of high Si content (46.9 wt. %) and 0.3 t of high Fe content (60 wt. %) were produced.

Finally, a cost evaluation study including CAPEX and OPEX was made using Aspen plus software to simulate the optimized CCSM process with recyclable ammonium salts for a 100 MW coal-fired power plant. For the input of 60 t/h CO_2, 93 % of them can be sequestered by the process with 29.5 % energy consumption and the total carbon capture and storage costs was 71.8 US$/t CO_2 sequestered, excluding the product sale.

[1] Metric tonne throughout thesis

Acknowledgements

Firstly, I would like to acknowledge and tank my supervisor Professor Mercedes Maroto-Valer for her support, continuous guidance and excellent supervision throughout my PhD. Thank you for giving me the chance to be part of a fantastic research group and for having faith in me.

The financial support of the Center for Innovation in Carbon Capture and Storage (CICCS) through the Engineering and Physical Science Research Council, EPSRC (EP/F012098/1), as well as the Department of Chemical and Environmental Engineering at the University of Nottingham are gratefully acknowledged. Also, thank you to the Graduate School for the travel award to support my attendance at a conference in US.

I would like to thank technicians who keep the place running and take care of the postgraduate labs, and to all the staff in the Department of Chemical and Environmental Engineering.

I would like to thank Dr. David Cliff for his time, expertise and help with XRD and SEM analysis. I would also like to thank to Dr. Scout Young at Department of Biology for his help with ICP-MS, Ron Perry for his help with ICP-AES, Nick Marsh at Department of Geology at University of Leicester for their help with XRF.

I am very grateful to all those postgraduates who I have shared office and labs with during my PhD. Thank you for a great office and lab environment. Special thanks go to my dear friends and colleagues who supported me during this time: Susana Garcia, Mark Kennedy, Mara Olivares, Steve Bouzalakos, Sarah Mackintosh, Ania Kaminska, Qi Liu, Dong Liu... Thank you for all the laughs, good moments, and friendship.

I would love to thank my family, my mother Xueqin Wang and father Min Wang, who I missed a lot and means everything to me in my life.

Of course, THANK YOU Yukun Wang for just being you and being so incredibly special. Thank you for been always there for me.

Publication list

Journal publications

Xiaolong Wang, Mercedes Maroto-Valer, Dissolution of serpentine using recyclable ammonium salts for CO_2 mineral carbonation, Fuel, 90(3):1229-1237, 2011

Xiaolong Wang, Mercedes Maroto-Valer, Combination of CO_2 capture and pH-swing mineral sequestration by using recyclable ammonium salts, Energy Procedia 4: 4930-4936, 2011

Xiaolong Wang, Mercedes Maroto-Valer, Integration of CO_2 capture and mineral carbonation by using recyclable ammonium salts, ChemSusChem, 4(9):1291-1300, 2011

Journal publications in preparation

Xiaolong Wang, Mercedes Maroto-Valer, Evaluation of reaction variables in carbon capture, storage and mineralisation (CCSM) process with recyclable ammonium salt, International Journal of Greenhouse Gas Control (In preparation)

Xiaolong Wang, Mercedes Maroto-Valer, Cost evaluation of carbon capture, storage and mineralisation (CCSM) process with recyclable ammonium salt, Environmental Science Technology (In preparation)

Refereed conference proceedings

Xiaolong Wang, Mercedes Maroto-Valer, Integrated CO_2 capture and production of hydromagnesite from serpentine by using recyclable ammonium salts, Proceedings Accelerated Carbonation for Environmental and Material Engineering 2010 (ACEME-10), Turku, Finland, 29 November-1 December 2010

Xiaolong Wang, Mercedes Maroto-Valer, Combination of CO_2 capture and pH-swing mineral sequestration by using recyclable ammonium salts, The 10th International Conference on Greenhouse Gas Control Technologies (GHGT-10), Amsterdam, Netherland, 19-23 September, 2010, 31

Xiaolong Wang, Sean Casey, Steve Bouzalakos, Ameena Camps, Ron Perry, M. Mercedes Maroto-Valer, Matthew Hall and Mark Gillott, Mineral sequestration of CO_2 by aqueous carbonation of Incinerator Sewage Sludge Ash, the 8th European Conference on Coal Research & Its Application, Leeds, UK, 6-9 September, 2010, 49

Xiaolong Wang, Teyssie Guillaume, Lulla Amrita, Steve Bouzalakos and M. Mercedes Maroto-Valer, Development of a new CO_2 mineral carbonation process utilizing Recycled Concrete Aggregate, the 9th Annual Conference on Carbon Capture and Sequestration, Pittsburgh, U.S., 10-13 May 2010, CD-Rom publication

Xiaolong Wang, Mercedes Maroto-Valer, Ex-situ mineral carbonation with regenerative ammonium salts, The 8th Annual Conference on Carbon Capture and Sequestration, Pittsburgh, U.S, 4-7 May, 2009, CD-Rom publication

Xiaolong Wang, Mercedes Maroto-Valer, Dissolution kinetics of minerals for advanced mineral carbonation, The 7th European Conference on Coal Research & Its Application, Cardiff, UK, 3-5 September 2008, 91

Table of Contents

List of Figures

List of tables

Chapter 1. Introduction

1.1 Climate change mitigation and CO_2 abatement

Concerns about climate change and its possible effects have risen during the past decade. It has been widely accepted that carbon dioxide (CO_2) emissions reduction is necessary for climate change mitigation (IPCC, 2007), with most of the CO_2 emissions coming from the combustion of fossil fuels. CO_2 abatement solutions include improvement of energy efficiency, alternative energy resources (such as renewables and nuclear energy) and carbon dioxide capture and storage (CCS). The replacement of fossil fuels by renewable energy or nuclear power is not an easy task, since fossil fuels dominate in the current energy supply (e.g., 70% in China and 50 % in U.S.; IPCC, 2005). Moreover, renewable energy, such as wind, solar and tidal, is still less economical than fossil fuels and thus the replacement of fossil fuel energy has a high cost attached (IEA, 2008). Nuclear power suffers limitations due to potential safety risks and the problem of waste disposal (IPCC, 2005). The contribution from improvement of energy efficiency could be slowed down due to the "ceiling effect". For example, recent new technologies, such as integrated gasification combined cycle (IGCC)

and natural gas combined cycle (NGCC), are already getting close to the maximum efficiency boundary (40-50 %). For these reasons, fossil fuels will still provide the majority of energy for the foreseeable future; CCS is then the only solution to allow for this continued use of fossil fuels while reducing CO_2 emissions. Therefore, CCS will play an important role in the portfolio of CO_2 emission reduction. It is predicted that CCS CO_2 abatement contribution can reach 19 % by 2050 (IEA, 2008).

1.2 Carbon dioxide capture and storage and mineralisation

CCS consists of three main steps: capture and separation of CO_2 from industrial and energy-related sources, compressing of CO_2 and transportation to a storage location, and long-term isolation from the atmosphere. The most promising CCS approach is carbon capture and geological storage (CCGS) (IPCC, 2005). However, the development of CO_2 geological storage has been slow in respect of potential environmental impacts and regulation for CO_2 injection and monitoring (Class *et al.*, 2009). Moreover, some countries, such as Finland and India, do not have sufficient storage capacity or lack suitable storage formations (Teir *et al.*, 2007c). Besides, sometimes the construction of pipeline is very expensive due to the long distance between CO_2 emission sources and storage sites. For example, some small and medium emitters in southwest England

are far from the suitable storage site in the North Sea. Therefore, there has been an increasing interest in alternatives to CCGS, including mineral carbonation.

Mineral carbonation or mineralisation is a promising strategy to permanently and safely store anthropogenic CO_2 in solid magnesium (Mg) and calcium (Ca) carbonates. The advantages of mineral carbonation include large storage capacity, worldwide availability feedstock, permanent and inherently safe sequestration of CO_2 and theoretical exothermic process (Lackner *et al.*, 1995). However, mineral sequestration also faces barriers such as low efficiency of mineral dissolution, slow kinetics, and energy intensive pre-treatment processes (Lackner *et al.*, 1995). Even though, some barriers such as low efficiency and slow kinetics have been solved by swinging the pH (Teir *et al.*, 2007c; Park and Fan, 2004), the addition of large amounts of acid and base required for the dissolution and subsequent carbonation limit the development of mineral sequestration.

O'Connor *et al.* (2002) have reported that mineral dissolution is the rate-limiting step in direct aqueous mineral carbonation, since the acidity produced by pressurised CO_2 in aqueous solution was not sufficient for mineral dissolution. In a second step, the carbonation of the leached solution was promoted by using a basic medium. This

indirect process is called pH-swing[2]. Park et al. (2004) proposed a pH-swing process using mixed weak acid solvents with 1 vol% H_3PO_4, 0.9 wt% of oxalic acid and 0.1 wt% EDTA to promote mineral leaching. Nesquehonite ($MgCO_3 \cdot 3H_2O$) was obtained from the carbonation of a Mg-rich solution by raising the pH of the solution to 9.5 with NH_4OH. The overall conversion to $MgCO_3$ was ~65%. However, the additives used in Park's process were not recycled and the dissolution efficiency was still low. Teir *et al.* (2007a) dissolved serpentine in HCl or HNO_3, and then hydromagnesite ($4MgCO_3 \cdot Mg(OH)_2 \cdot 4H_2O$) was obtained by controlling the Mg-rich solution pH to 9 with addition of NaOH (Teir *et al.*, 2007b). Although high carbonation conversion efficiency of Mg (80 - 90%) was obtained, the chemicals involved, such as HCl and NaOH, could not be reused. For Teir's process, 2.4 t NaOH and 2.1 t HCl acid (or 3.6 t HNO_3) were consumed per tonne of CO_2. The cost for make-up chemicals alone (600 - 1600 US$/t CO_2) is much larger than the budget for CO_2 emission allowances (30-40 US$/t CO_2) (IPCC, 2005). Thus, recycling of all chemicals involved is crucial to make CO_2 mineral carbonation viable.

Kodama *et al.* (2008) reported a pH swing CO_2 mineralisation process with recyclable additives. In their study, steel slags were reacted with $(NH_4)_2SO_4$ to extract Ca and produce NH_3. CO_2 was

[2] Change the pH of the solution from acid to base condition

then purged to the Ca-rich solution to precipitate $CaCO_3$ and recycle $(NH_4)_2SO_4$. Kodama *et al.* (2008) reported a 62 % dissolution efficiency but the effect of important parameters such as temperature, pressure and reaction time was not reported. Moreover, the value of 80% for the carbonation conversion efficiency was only derived from theoretical calculations and not from experimental work. Furthermore, the CO_2 storage capacity of steel slags is only 60-80 $MtCO_2$/year (Weber, 2000), which is very small compared with the vast capacity of mineral silicates, like serpentine and olivine that is estimated to be 100,000 $GtCO_2$ (Lackner, 2002).

Pundsack *et al.* (1967) used 1.4 M NH_4HSO_4 to dissolve serpentine at 95°C for 5 hours and obtained 92.8% Mg extraction efficiency, but the carbonation efficiency was only 35 %. Pundsack's process aimed to produce pure magnesium carbonate and more work is needed to understand the dissolution kinetics, optimize reaction conditions of this process, improve the carbonation efficiency and investigate its potential application for mineral carbonation to store CO_2.

Krevor *et al.* (2009) tested NH_4Cl, NaCl, sodium citrate, sodium EDTA, sodium oxalate, and sodium acetate to dissolve serpentine. All experiments were carried out at 120 °C and 20 bars of CO_2 in a batch autoclave. When using 0.1 M citrate, EDTA and oxalate

solutions, 60 % dissolution efficiency of Mg from serpentine was achieved within 2 hours, rising to 80 % after 7 hours and reaching nearly 100 % between 10 and 20 hours. Therefore, the mineral dissolution with organic solvents is promising in terms of dissolution efficiency, but the dissolution rate is relatively slow and needs a long reaction time of up to 20 hours.

Fagerlund *et al.* (2009) proposed a process for production of $Mg(OH)_2$ from serpentine using $(NH_4)_2SO_4$. Solid-solid reaction of serpentine with $(NH_4)_2SO_4$ was carried out at above 440 °C to generate $MgSO_4$, that was then put into ammonia water to precipitate $Mg(OH)_2$ and regenerate $(NH_4)_2SO_4$. The $Mg(OH)_2$ was then carbonated with CO_2 directly in a pressurized fluidized bed (PFB) reactor at 470-550 °C and 20 bar. However, only 20-60 % extraction efficiency of Mg from serpentine was reported (Nduagu, 2010), and the carbonation efficiency of $Mg(OH)_2$ only achieved a maximum value of 45 %. This was due to the conversion of $Mg(OH)_2$ to MgO at the temperature range used, where the produced MgO cannot react with CO_2 to produce carbonates at the above temperature range (Zevenhoven, 2010). Therefore, work is needed to improve both dissolution and carbonation efficiencies of this indirect gas solid mineralisation process.

1.3 Aim and objectives

The aim of this research is to develop a pH swing mineral carbonation process using recyclable salts. It is hypothesised that ammonium salts would provide high efficiency of mineral dissolution and carbonation and can be recovered at the end of process. The research objectives are:

- To investigate the mineral dissolution of selected feedstock (serpentine) with ammonium salts, such as ammonium bisulphate, and to maximize the magnesium dissolution efficiency by changing temperature, reaction time, solid/liquid ratio, particle size and additive concentration.
- To investigate the precipitation of magnesium carbonates by reacting ammonium bicarbonate/carbonate with Mg^{2+} rich solution, and to maximize the carbonation efficiency by changing temperature, reaction time and mass ratio between $Mg:NH_4HCO_3:NH_3$.
- In order to reduce the water usage so that lower the energy cost, a process route at high solid/liquid ratio is proposed to understand the effects of solid to liquid ratio in the dissolution and carbonation efficiencies.
- To study the thermal decomposition of ammonium sulphate and maximize the regenerative rate of ammonia and ammonia bisulphate.

- To estimate the OPEX of the two process routes by using an excel spreadsheet tool, and to optimize process conditions (solid to liquid ratio, reaction time, Mg:CO_2 containing NH^{4+} salts:NH_3) according to the triggers from cost estimation.
- To study the dissolution and carbonation efficiency at these optimized process conditions, and maximize the efficiencies by changing the ratio of Mg:CO_2 containing NH^{4+} salts:NH_3.
- To evaluate the CAPEX and OPEX of the optimized process using the chemical process simulation software (Aspen plus), including sensitivity analysis to understand the relationship between process conditions and cost.

This thesis presents the following structure. The literature review is presented in Chapter 2, followed by the introduction of two process routes for CCSM process with recyclable ammonium salts in Chapter 3. Chapters 4 and 5 describe the experimental work on dissolution and carbonation at low and high solid to liquid ratio, respectively. The process evaluation of the two process routes is discussed in Chapter 6 and then optimization experiments are presented in Chapter 7. Finally, Chapter 8 focuses on the cost evaluation and sensitivity analysis of the CCSM process with ammonium salts.

Chapter 2. Literature review

2.1 Climate change mitigation and CO_2 emissions

Climate change mitigation and global climate change negotiation

Fossil fuels combustion dominates energy production, and is likely to remain the key energy source for the foreseeable future (IPCC, 2005). However, large amounts of greenhouse gases (GHG) emissions, mainly CO_2, are associated with fossil fuel combustion and cause increasing CO_2 atmospheric concentrations from approximately 280 ppmv in the pre-industrial times to the current levels of 389.6 ppmv (Fig 2-1).

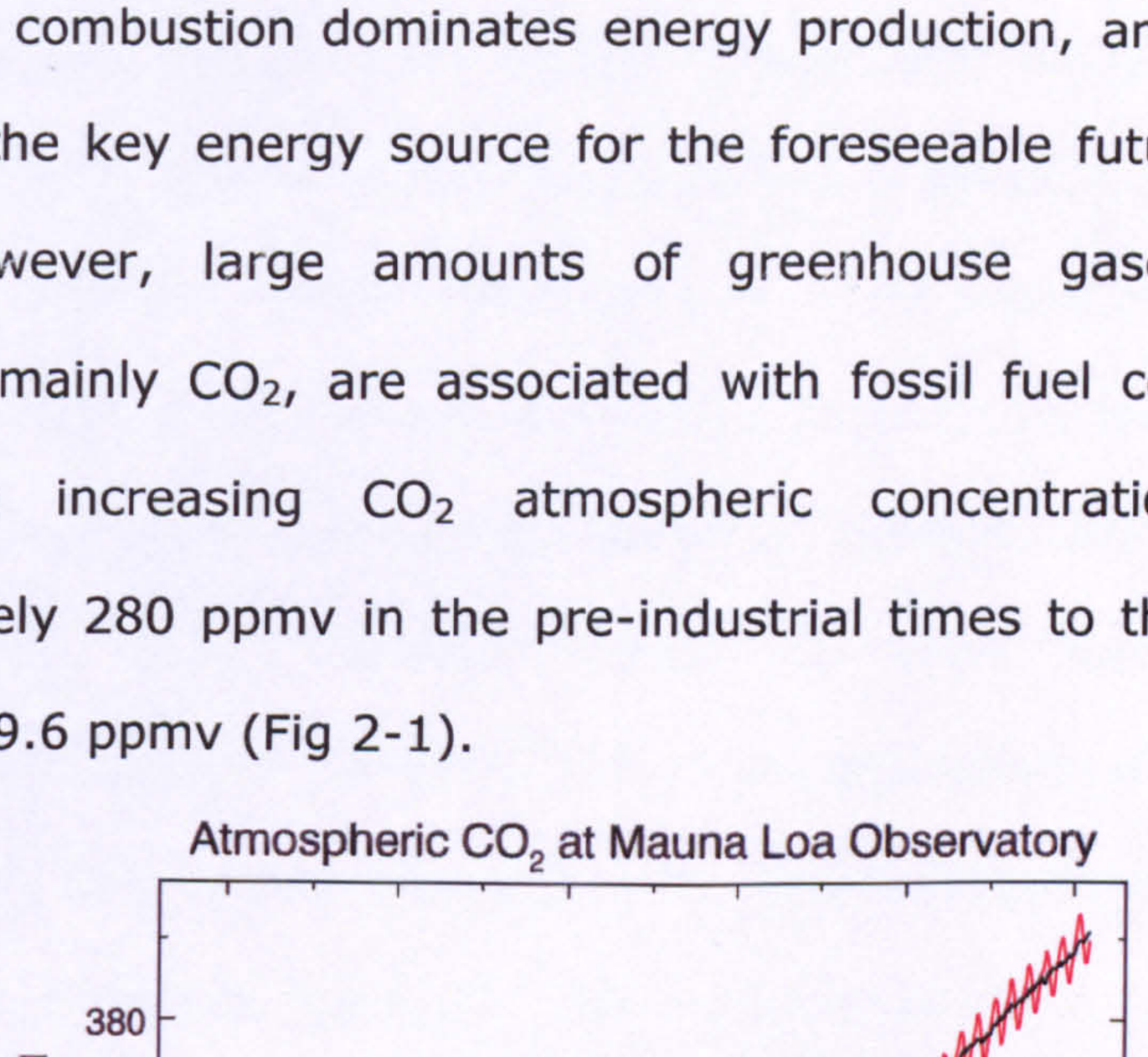

Figure 2-1: Average annual atmospheric CO_2 concentration based on direct measurements at Mauna Loa Observatory from 1960-2010 (Dr Pieter Tans, NOAA/ESRL, www.esrl.noaa.gov/gmd/ccgg/trends, accessed on 15th March, 2011)

Records of temperature and atmospheric CO_2 concentration have been reconstructed from ice-cores drilled in Antarctica for the last 400,000 years (ADIAC, 2004). Atmospheric CO_2 concentrations never exceeded 300 ppmv before 1950, and temperature increase presents the same trend as seen with the change of atmospheric CO_2 concentration. To date, the most credible estimation of future climate from mathematical models based on physical approximations predicts that climate change with greenhouse gas increases (IPCC, 2007). Although uncertainties remain, there is no doubt that without drastic reductions in GHG emissions climate change will occur, leading to severe consequences. According to the United Nations Intergovernmental Panel on Climate Change (IPCC) report (IPCC, 2007), "climate change has been proven to be unequivocally linked to human activity from observation of increases in global air and ocean temperatures, rising global average sea levels and widespread melting of sea-ice in the Arctic". Irreversible impacts are likely to occur in the near future as follows (IPCC, 2007):

- Approximately 20-30 % of species assessed so far are likely to be at increased risk of extinction.
- Between 75 and 250 million people projected to be exposed to increased water stress in Africa by 2020.
- Many of the world's major cities (22 of the top 50) are at risk of flooding from coastal surges, including Tokyo, Shanghai,

Hong Kong, Mumbai, Calcutta, Karachi, Buenos Aires, St Petersburg, New York, Miami and London.

Numerous international efforts are being made to control climate change, including the United Nations Framework Convention on Climate Change (UNFCCC) in 1994 and the Kyoto Protocol in 1997 that entered into force in 2005 to reduce GHG emissions by 5.2 % of 1990 levels by the year 2010. In 2006, the Stern review (2006) showed the need to stabilize greenhouse gas concentrations between 450 and 500 ppm CO_2-eq[3] in order to substantially reduce the worst impacts of climate change. In November 2008, the UK Climate Change Act set a target of 80% reduction of CO_2 emission with respect to 1990 levels by 2050 (DECC, 2009).

CO_2 emissions

The major emissions of GHGs worldwide in 2004 were 56.6 % CO_2 from fossil fuel use, 17.3 % CO_2 from deforestation and decay of biomass, 14.3 % methane (CH_4) and 7.9 % nitrous oxide (N_2O) (IPCC, 2007). Therefore, CO_2 is the most important anthropogenic greenhouse gas.

Global CO_2 emissions were 28.4 Gt in 2008 (IEA, 2010a). In terms of worldwide CO_2 emissions by fuel, 43 % were produced from coal, 37 % from oil and 20% from gas. In terms of CO_2 emission by

[3] CO_2-equivalent emissions are the amount of CO_2 emissions that would cause the same time-integrated radioactive forcing, over a given time horizon.

region, two-thirds of world emissions for 2008 originated from just ten countries, where China and U.S. produced 6. 5 $GtCO_2$ and 5.6 $GtCO_2$, respectively (Fig. 2-2). In terms of CO_2 emission by sectors, two sectors, electricity and heat generation (41 %) and transport (22 %), produced two-thirds of global CO_2 in 2008 (Fig. 2-3).

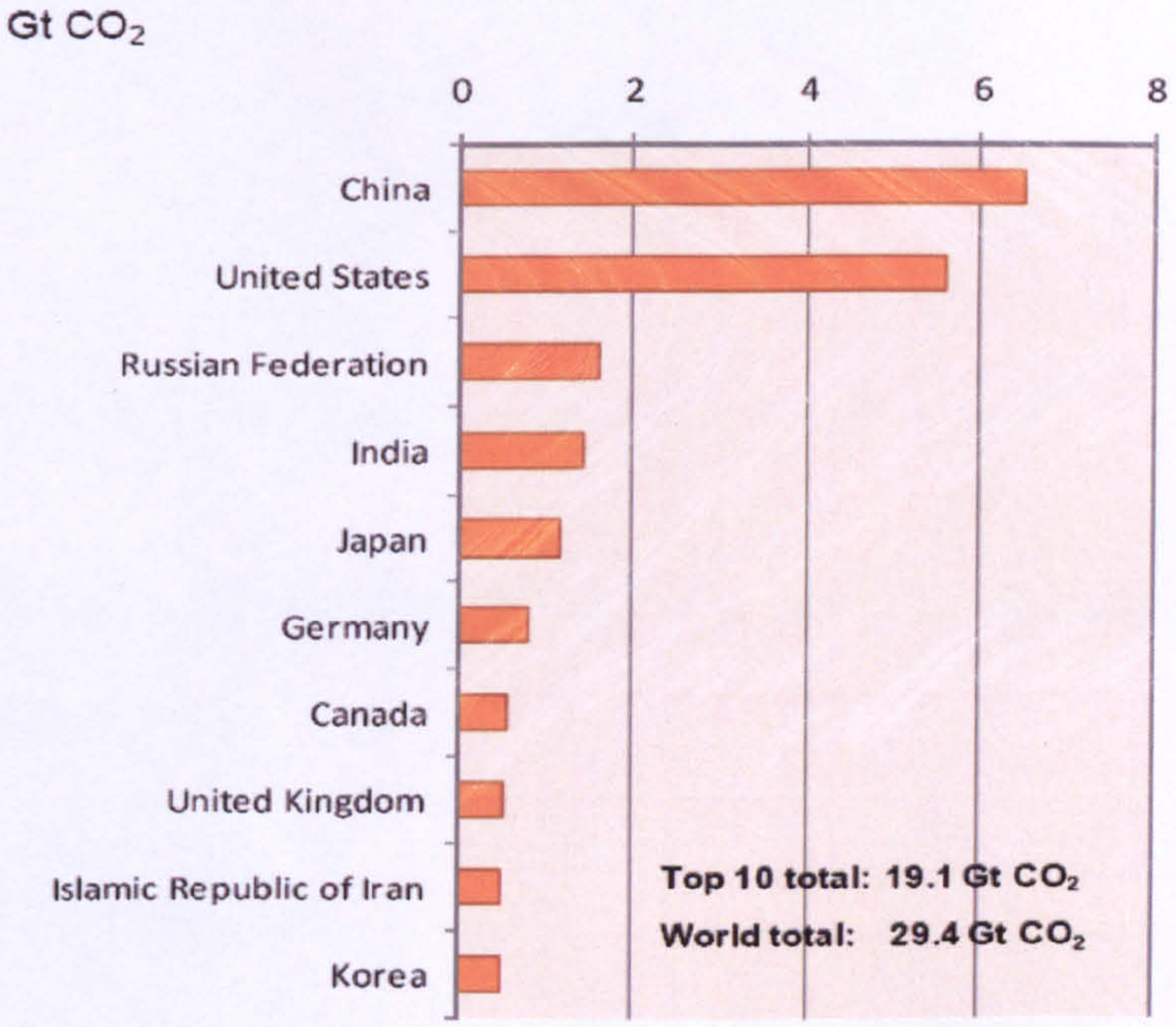

Figure 2-2: The top 10 CO_2 emitting countries (IEA, 2010a).

The World Energy Outlook 2009 predicts that demand for electricity will be almost twice as high as current demand by 2030 and global demand for transport appears unlikely to decrease in the foreseeable future (IEA, 2009). The urgent need to reduce CO_2 emissions and increasing energy demand drive the development of CO_2 abatement technologies in a low carbon society.

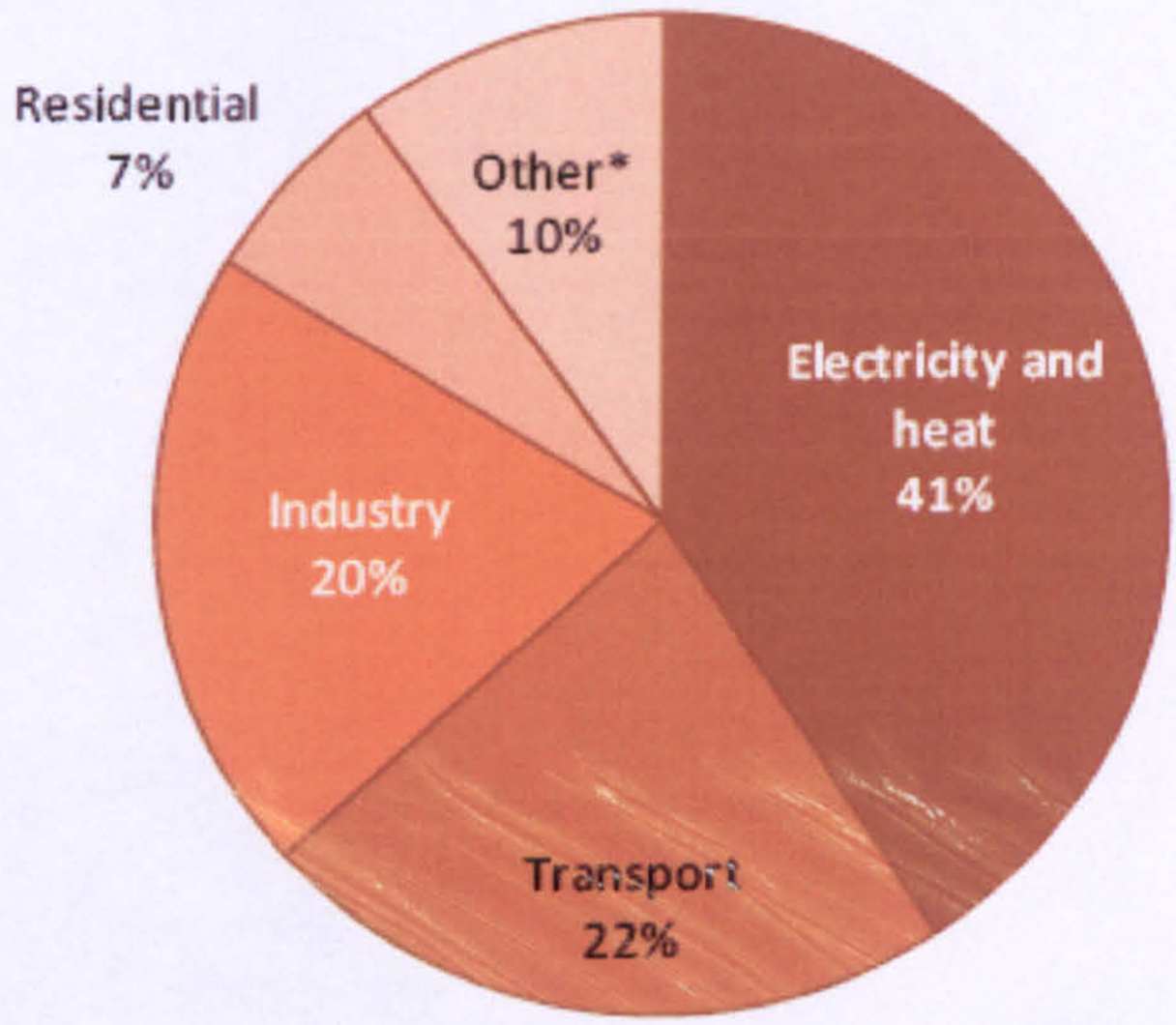

Figure 2-3: World CO_2 emissions by sector in 2008 (IEA, 2010a).

2.2 Carbon dioxide abatement and carbon dioxide capture and storage

2.2.1 CO_2 abatement

Efficiency improvement, alternative energy resources (such as renewable and nuclear energy) and carbon dioxide capture and storage (CCS) are considered to be the three most important CO_2 emissions abatement strategies (IPCC, 2005). According to the International Energy Agency's (IEA) Energy Technology Perspectives in 2008, in the 450 ppm scenario, efficiency enhancement technology will constitute 65 %, 57 % and 54 % in the global emissions abatement portfolio by 2020, 2030 and 2050, respectively (Fig. 2-4). However, with the ceiling effect of efficiency enhancement (large increase of cost only resulting in small increase

of efficiency) and the difficulties in replacing fossil fuels with alternative energy resources, CCS abatement contribution has to grow from 3 % of the global abatement portfolio in 2020 to 10 % in 2030 and finally reach 19 % in 2050 to stabilize the CO_2 atmospheric concentration at 450 ppm (Fig. 2-4) (IEA, 2008).

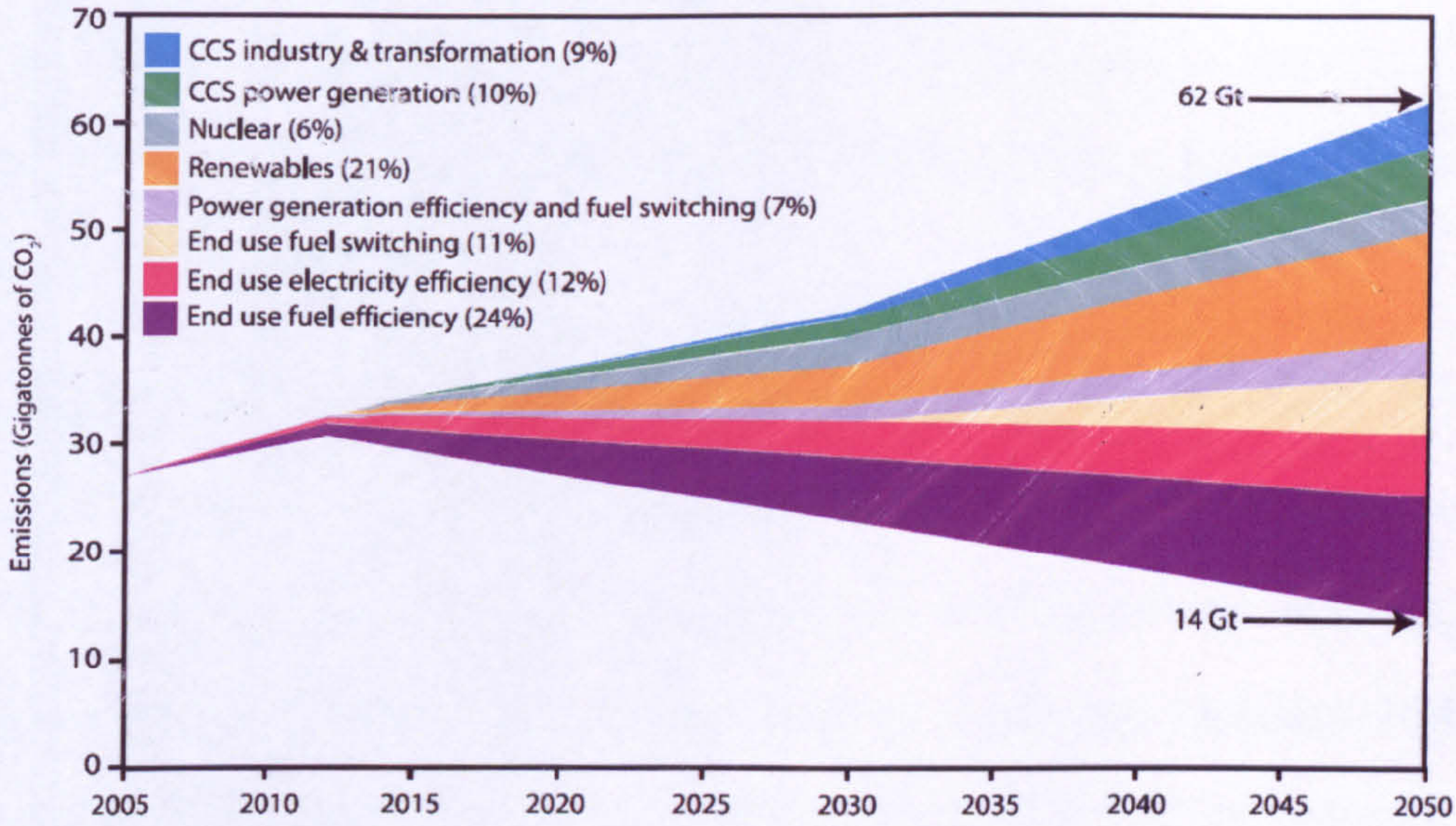

Figure 2-4: Shares of contributions to CO_2 emission reductions by technologies from 2005-2050 (IEA, 2008)

Furthermore, according to an IEA study (2008) on the costs of various emissions abatement technologies, implementing CCS will contribute to the least-cost route of emissions abatement. To reach the 450 ppm scenario[4] without utilizing CCS would lead to a 70 %

[4] 450 ppm scenario is to control the atmosphere CO_2 concentration under below 450 ppm so that limit the global temperature rising below 2 °C (Stern, 2006). In Copenhagen conference, all countries reached a consensus on the 2 °C target.

increase in the total cost of emissions abatement by 2050 compared with that of utilizing CCS (IEA, 2008).

In addition, CCS can reduce anthropogenic CO_2 emissions from large point sources, and particularly fossil fuel fired power plants, by up to 90 % (IPCC, 2005). The most important key feature of CCS is that it allows for the continued use of fossil fuels. On a global scale, CCS could potentially reduce between 1.4 $GtCO_2$ (Stern, 2006) and 4 $GtCO_2$ (IEA, 2007) by 2030.

2.2.2 Carbon dioxide capture and storage

CCS is defined as a process consisting of three main steps: capture and separation of CO_2 from industrial and energy-related sources, compression of CO_2 and transportation to a storage location, and long-term isolation from the atmosphere by a variety of methods (Fig. 2-5). The main storage formations include oceans, depleted gas, oil and coal reservoirs, and saline aquifers. In addition, mineral carbonation, which was first described by Seifritz (1990), refers to the fixation of the CO_2 using binary oxides such as magnesium oxide (MgO) and calcium oxide (CaO) into carbonate for long term CO_2 storage. Mineral carbonation also has the potential to convert CO_2 into beneficial products, for example, carbonates used as construction materials.

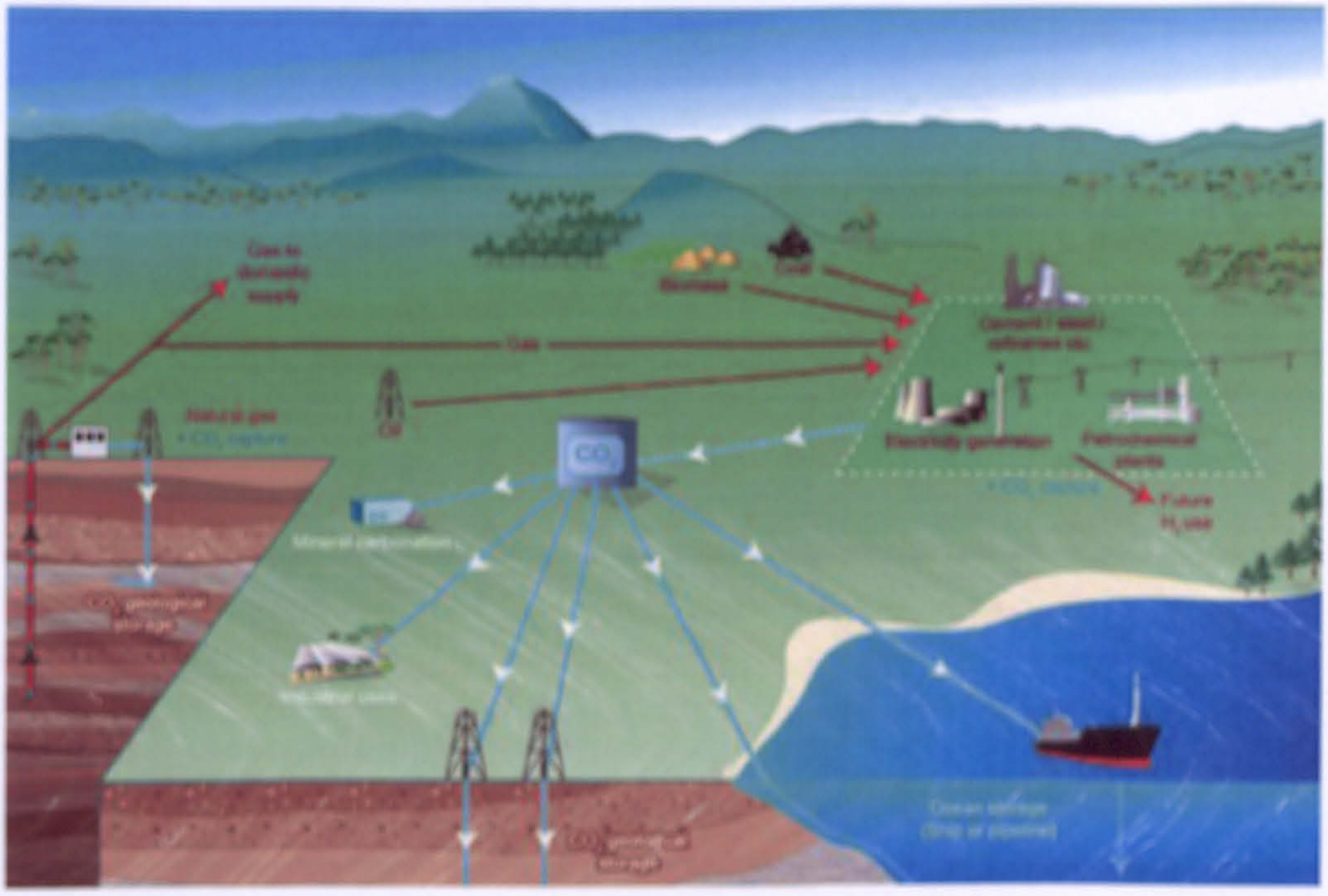

Figure 2-5: Overview of carbon capture and storage technologies (IPCC, 2005)

CCS combines three separate technologies: capture, transportation and storage, where each technology seems relatively mature (IPCC, 2005). For example, CO_2 storage is not new, and uses similar technologies applied in enhanced oil recovery (EOR), which is a mature technology in the oil industry. However, the integration of individual technologies in CCS attracts public concerns on the maturity of the technology and potential health and safety impacts. Moreover, the development of individual technologies in the CCS chain are at different stages of technology readiness level (TRL), as shown in Table 2-1. It can be seen that mineral carbonation is currently in the research stage and demands more research work.

CCS component	CCS technology	Research phase	Demonstration phase	Economically feasible under specific conditions	Mature market
Capture	Post-combustion			X	
	Pre-combustion			X	
	Oxyfuel combustion		X		
	Industrial separation (natural gas processing, ammonia production)				X
Transportation	Pipeline				X
	Shipping			X	
Geological storage	Enhanced Oil Recovery (EOR)				X
	Gas or oil fields			X	
	Saline formations			X	
	Enhanced Coal Bed Methane recovery (ECBM)		X		
Ocean storage	Direct injection (dissolution type)	X			
	Direct injection (lake type)	X			
Mineral carbonation	Natural silicate minerals	X			
	Waste materials		X		
Industrial uses of CO_2					X

Table 2-1: The current development stages of individual CCS technologies (IPCC, 2005)

In order to prove the feasibility of CCS and accumulate experience in operation and management, there are 77 pilot-scale CCS projects around the world (GCCSI, 2010). Governments and energy corporations are developing and implementing incentives to facilitate widespread deployment of CCS technologies in the near future. The UK government has planned to build one of the first commercial-scale CCS projects by 2014 (BERR, 2008; BERR, 2009; APGTF, 2009). The EU has implemented a programmed of 10-12 demonstration CCS projects to be in operation by 2015 (APGTF, 2009). China is also making significant progress in CCS. For example, the GreenGen project led by eight Chinese energy companies and Peabody Energy plan to develop a 400 MW

integrated gas cycle combustion (IGCC) power plant with CCS by 2020; Shenhua Group, the largest coal production company in China, has implemented a 1 Mt CO_2 project in Ordos, Inner Mongolia, and has started to inject CO_2 into a saline aquifer from January, 2011. In April 2009, the Australian government launched the Global Carbon Capture and Storage Institute (GCCSI), which aims at accelerating the worldwide commercial development of CCS technologies. The Department of Energy (DOE) in the U.S. has formed a national network of Regional Carbon Sequestration Partnership (RCSP) to help determine the best approach for CCS. In May 2011, Canadian authorities approved a fund of US$ 1.3 billion for a CCS demonstration plant in Saskatchewan, which aims to reduce annual greenhouse gas emissions by around 1 Mt CO_2.

However, some difficulties in developing CCS technologies include the absence of financial support, regulations and policy frameworks and potential lack of public support. The major barriers are probably the high energy penalties, costs and potential impacts due to CO_2 leakage (IPCC, 2005).

The IPCC's CCS special report (IPCC, 2005) presents the costs of the different CCS technologies. It can be seen in Table 2-2 that capture technologies are very expensive and account for 75% of the total cost of CCS. The cost of geological storage is relatively low at 0.6-8.3 US$/t$CO_2$. The cost of mineral carbonation was based on

the direct aqueous process developed by O'Connor (2005), where 185 °C and 150 P_{CO2}[5] pressure were used. It must be pointed out that estimating the cost of CCS technologies involves a high degree of uncertainty on how these costs may develop over time and in terms of potential variations in the technical requirement, scale and application of projects. McKinsey & Company (2008) released a report on CCS predicted costs based on a case-study approach. According to the findings of the report, early commercial CCS projects by 2020, are estimated to cost 45-65 US$/$tCO_2$ with CO_2 capture being the most expensive step and accounting for 33-42 US$/$tCO_2$.

Table 2-2: The costs of current CCS technologies (IPCC, 2005).

CCS system components	Cost range	Remarks
Capture from a coal- or gas-fired power plant	15-75 US$/$tCO_2$ net captured	Net costs of captured CO_2, compared to the same plant without capture.
Capture from hydrogen and ammonia production or gas processing	5-55 US$/$tCO_2$ net captured	Applies to high-purity sources requiring simple drying and compression.
Capture from other industrial sources	25-115 US$/$tCO_2$ net captured	Range reflects use of a number of different technologies and fuels.
Transportation	1-8 US$/$tCO_2$ transported	Per 250 km pipeline or shipping for mass flow rates of 5 (high end) to 40 (low end) $MtCO_2$ yr^{-1}.
Geological storage[a]	0.5-8 US$/$tCO_2$ net injected	Excluding potential revenues from EOR or ECBM.
Geological storage: monitoring and verification	0.1-0.3 US$/$tCO_2$ injected	This covers pre-injection, injection, and post-injection monitoring, and depends on the regulatory requirements.
Ocean storage	5-30 US$/$tCO_2$ net injected	Including offshore transportation of 100-500 km, excluding monitoring and verification.
Mineral carbonation	50-100 US$/$tCO_2$ net mineralized	Range for the best case studied. Includes additional energy use for carbonation.

[5] CO_2 partial pressure in autoclave reactor

2.2.3 The shortages of carbon capture and geological storage (CCGS)

The most promising CCS approach is carbon capture and geological storage (CCGS) (IPCC, 2005). However, the development of CO_2 geological storage has been slow recently in respect of avoiding leaking risk and lacking of regulation for CO_2 injection and monitoring. Some countries, such as Finland and India, do not have sufficient geological storage capacity or lack suitable storage formations (Teir *et al.*, 2009; Devleena Mani, 2008). Moreover, the distance from the emission point source to a suitable geological storage location sometimes may be thousands of kilometres away, e.g., the main power plants in China located in Huabei area, the suitable geological sites are more than 1000 km away in Bohai (NZEC, 2009). Therefore, the construction and maintenance of a high pressure CO_2 pipeline may be relatively costly up to 1.6 million US$/mile (ZEP, 2011). Furthermore, Oman wants to use their abundant natural resources of ophiolite to mineralize CO_2, since Oman has mineral capacity large enough to store the world CO_2 emissions from fossil fuels for 200 years (Matter et. al., 2009). Another example is Singapore, where they want to use the carbonate products from CO_2 mineralisation for land reclamation (AStar/ICES, 2009). Geological storage might not be able to offer the necessary capacity soon enough to match the urgent emission reduction targets. In a recent international conference, it was

reported that the total worldwide capacity of geological storage (identified and surveyed) increased ~7 Mt CO_2/y in 2008 and is expected to increase to 24 Mt CO_2/y in 2012 (Thambimuthu, 2009). It may be hard to match the sequestration rate of many Gt CO_2/y within near future, putting pressure on the development of alternatives, such as mineralisation.

2.3 Mineral carbonation

Mineral carbonation or mineralisation is a promising strategy to permanently and safely store anthropogenic generated CO_2 in solid magnesium (Mg) and calcium (Ca) carbonates. The reaction of mineral carbonation can be expressed by the following equation:

$$MO + CO_2 \rightarrow MCO_3 + heat$$

Equation 2-1

Where M refers to a metallic element such as calcium, magnesium or iron.

Mineral carbonation can be classified into in-situ mineral carbonation and accelerated mineral carbonation. In-situ mineral carbonation is closely related to geological storage as it involves the injection of CO_2 underground, but it differs from geological storage, in that it explicitly aims at enhancing the formation of carbonates with alkaline-minerals present in the geological formation. The mineral trapping in geological storage is same to mineral carbonation, but it

requires very long times (Fig. 2-6). The first in-situ mineral carbonation project, called Carbfix, started at Hellisheidi (Iceland) in 2008 (Oelkers *et al.*, 2008). In order to speed up the reaction rate, the Carbfix project firstly dissolves the CO_2 from a geothermal power plant in water at elevated pressure and then injects it through wells down to a basalt formation below 400-800 m (Matter *et al.*, 2009). Recently, Kelemen *et al.* (2010) finished the geological survey work on a ophiolite complex in Oman and plan to launch a in-situ mineral carbonation project in future. Although the timescale of in-situ mineral carbonation is shorter than that for solubility trapping and mineral trapping in CO_2 geological storage (Fig. 2-6), it still take hundreds of years to permanently store CO_2 into carbonates (Matter *et al.*, 2009). In contrast, the timescale of accelerated mineral carbonation is only in the order of hours, or even minutes. It must be pointed out that accelerated mineral carbonation may produce some beneficial by-products, and therefore it is also classified as a CO_2 utilization process. For the purpose of this thesis, mineral carbonation is the term used to refer to accelerated mineral carbonation.

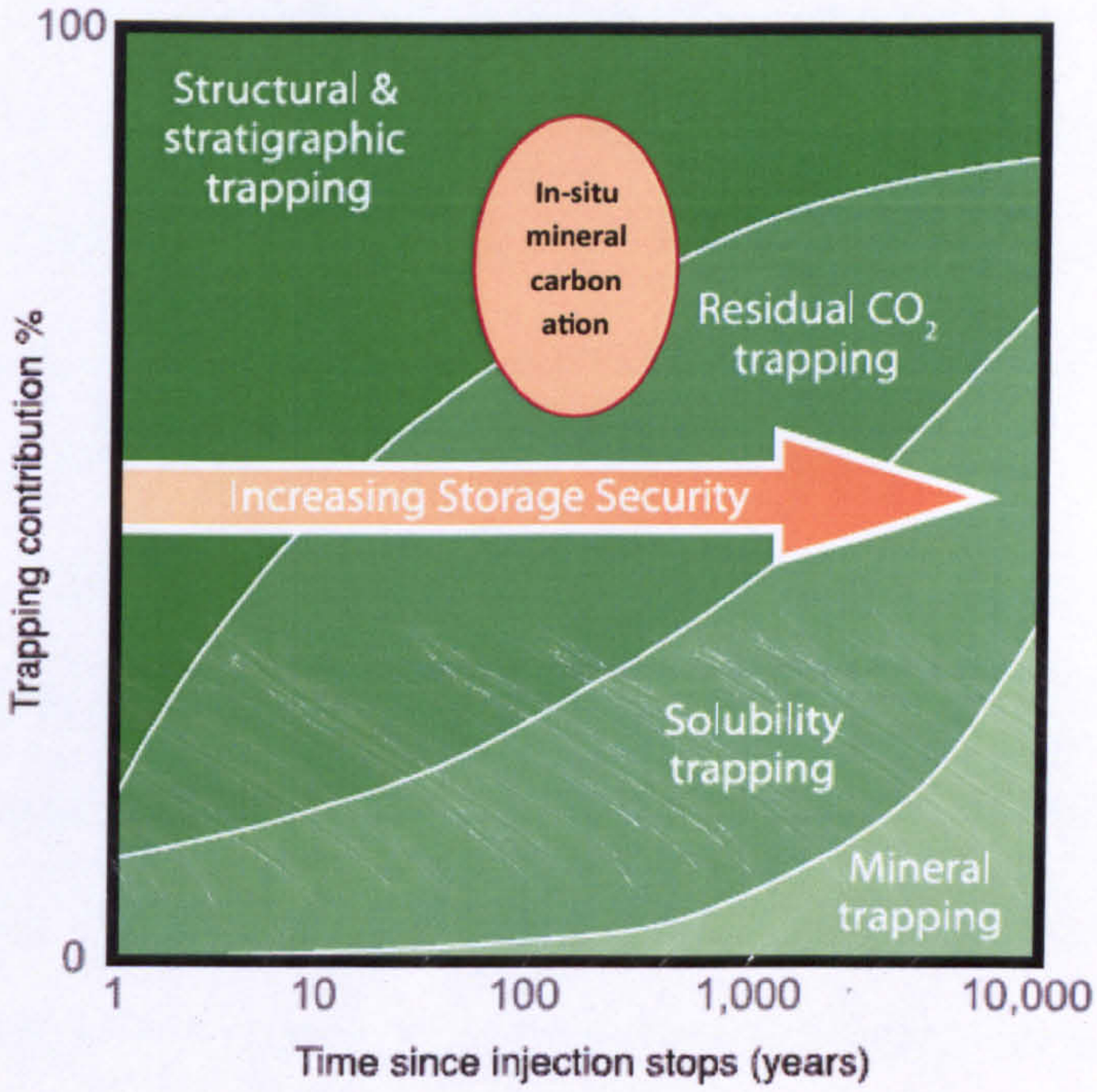

Figure 2-6: Time scale with trapping contribution by different mechanisms in CO_2 geological storage (modified from IPCC, 2005)

The first advantage of mineral carbonation compared to geological storage is the environmentally benign and permanent trapping of CO_2. Unlike geological storage, there is no need for post-storage monitoring for potential environmental impacts. In a recent study, Teir *et al.* (2006) investigated the stability of Ca and Mg carbonate formed from mineralisation when subjected to an acidic aqueous environment (similar to acidic rain, pH 3-5) and concluded that Ca and Mg carbonates are resistant from corrosion from local environmental effects.

The second advantage of mineral carbonation is the significant large capacity and worldwide availability of the minerals required. The

estimated capacity of various CO_2 storage options are summarized in Table 2-3, which states that mineral carbonation is capable of fixing all the CO_2 worldwide output from combustion of fossil fuels. The most abundant feedstocks are magnesium silicate minerals such as serpentine and olivine, while there are some other interesting feedstocks such as calcium-rich silicate minerals (wollastonite), waste materials from steel, cement and water sewage industries and brine water (see Section 2.3.1.). CO_2 mineralisation for storing several Mt of CO_2 per year will involve solids handling of a scale similar to a typical metal ore or mineral mining and processing activity (IPCC, 2005). An example of a large-scale processing of solids is the mining and processing of oil sands in Alberta, Canada, where 1 Mt oil sands are moved each day (Kunzig, 2009).

Table 2-3: Estimated Capacity of CO_2 storage and utilization options

Options	Estimated global capacity [GtC]	Reference
Coal reserves worldwide	*>10,000*	Lackner, 2002
Total CO_2 output during the 21st century	*2,300*	Lackner, 2002
CO_2 Mineral sequestration	Very large (more than the total output of carbon from fossil fuel); Mg/Ca silicates > 30,000	Kohlmann, 2001; Lackner, 2002
Ocean disposal	>1,000; 300-600	Kohlmann, 2001;

		Lackner, 2002
Saline aquifers	1,000-20,000	IPCC, 2005; IEA, 2008
Depleted gas reservoirs	>140	Kohlmann, 2001
Depleted oil reservoirs	>40	Kohlmann, 2001
Improved forestry and reforestation	50-100	Kohlmann, 2001
Enhanced oil recovery	65	Kohlmann, 2001
Bio fixation	1.35	Kohlmann, 2001
Chemicals	0.09	Kohlmann, 2001

The third advantage of mineral carbonation is that theoretically the carbonation reaction could proceed without energy input, since carbonates have a lower thermodynamic energy state than CO_2 (Fig. 2-7), but this has not been accomplished. However, the carbonation process takes a geological time (thousands of years) to complete, the reaction rate must be improved to industry time (hours). A high energy penalty is caused from the pre-treatment of minerals and the high temperature and pressure conditions applied to accelerate the kinetics of carbonation process. It is expected that optimisation and process integration should allow reducing the net energy input.

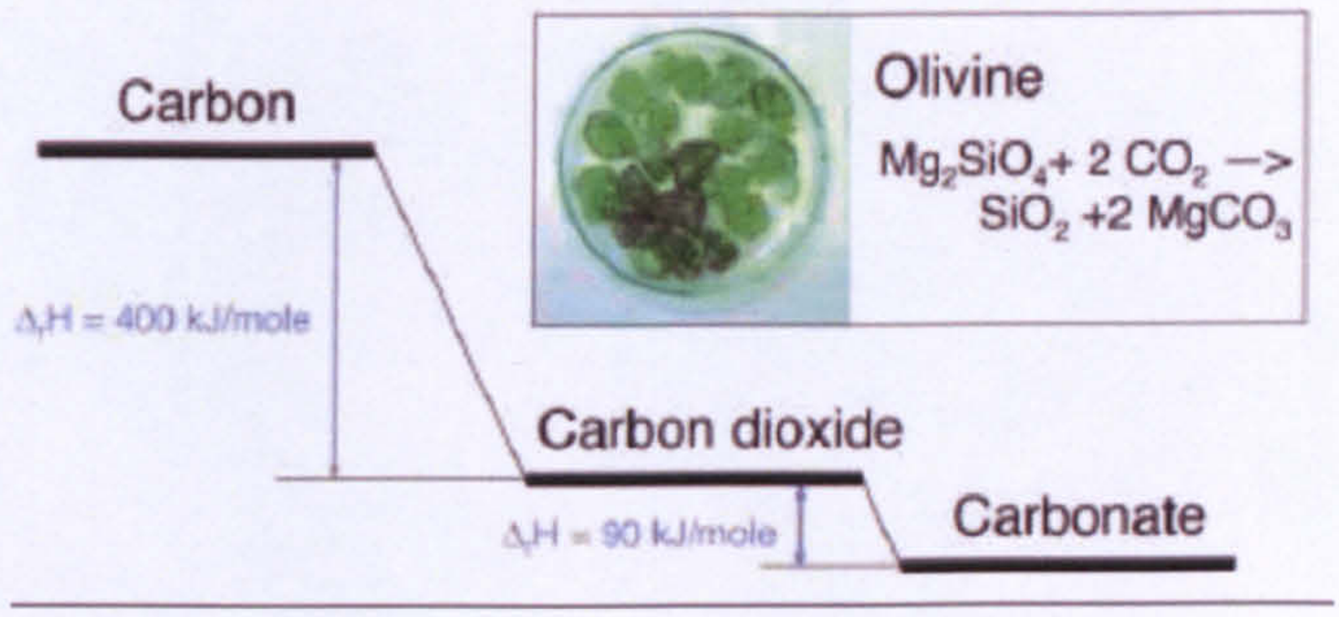

Figure 2-7: Thermodynamic energy state of carbon, carbon dioxide and carbonate. (Baciocchi, 2008)

The fourth advantage of mineral carbonation is that it can provide a CO_2 sequestration solution to some countries, where large geological reservoirs do not exist and ocean storage is not feasible. Finland, Korea and India have started studies on mineral sequestration of CO_2 due to the lack of suitable geological formations (Kohlmann, 2001; Devleena Mani, 2008; Lee *et al.*, 2005). In Lithuania and the Baltic region, mineral sequestration of CO_2 is also being studied, as the saline aquifers in Lithuania have been found unsuitable for CO_2 storage (Stasiulaitiene *et al.*, 2007; Shogenova *et al.*, 2009). Moreover, the distance from the emission source to a suitable storage location sometimes may be hundreds or thousands of kilometres away, such as hundreds of coal fired power plants in South China, central of India, southwest of U.S., east of Russia and south of Europe (Fig. 2-8).

Figure 2-8: Geographical relationship between CO_2 emission sources and prospective geological storage sites (Bradshaw, 2004)

The last advantage of mineral carbonation is the potential use of products from the process. Recent papers have investigated the use of Mg carbonates in building materials or flame retardants (Teir *et al.*, 2007b; Laoutid *et al.*, 2006), applications of Ca carbonates in paper production (Eloneva *et al.*, 2009) and the use of by-products, such as high purity silica from mineral dissolution as aggregates and high Fe contain products from pH-swing as feedstock for the steel industry (Teir *et al.*, 2007b; Xiaolong Wang, 2010a). In addition, mineralisation is receiving increased attention from mineral, cement, metal, paper and power plant industries, where the waste materials produced could be a good feedstock for mineralisation to avoid the transportation of minerals. In addition, the high reactivity of many calcium-containing industrial wastes could avoid the high energy penalty from mineral pre-treatment.

Although the advantages of mineral carbonation include vast

storage capacity, permanent storage and the fact that mineralisation is exothermic, mineral sequestration also faces many problems such as low efficiency of mineral dissolution, slow kinetics, and energy intensive pre-treatment processes (Lackner *et al.*, 1995). Even though, some barriers such as low efficiency and slow kinetics have been solved by swinging the pH (Teir *et al.*, 2007c; Park and Fan, 2004), the addition of large amounts of acid and base required for the dissolution and subsequent carbonation limit the development of mineral sequestration.

2.3.1 Raw materials and capacity

Table 2-4, lists various materials investigated for mineral carbonation. Alkaline earth metals, Ca, Mg and Fe, can be used for mineral carbonation. Fe has been suggested for carbonation, but as it is a valuable mineral resource it is sought after for other purposes. Mg and Ca metals comprise 2.0% and 2.1% of the Earth's crust, respectively (Goff *et al.*, 1998), and therefore they are generally selected as feedstock for mineral CO_2 sequestration. Carbonation of Ca is easier, but Mg minerals are favoured, because Mg silicates are widely available worldwide. Furthermore, the ratio of magnesium oxide required to bind CO_2 is 3.3:1, compared with calcium oxide's 4.7:1. Therefore, magnesium-containing minerals are the most promising feedstock for mineral carbonation. In addition, there are

also industrial solid wastes that contain large amounts of Mg, Ca and even Fe, such as steel slags, fly ash and waste cement.

Table 2-4: Raw materials studied in literature and associated references.

Material	Formula/Composition	Reference
Basalt[a]		Oelkers *et al.*, 2008; Matter *et al.*, 2009; Gislason *et al.*, 2010
Forsterite	Mg_2SiO_4	Giammar *et al.*, 2005
Olivine	$(Mg,Fe)_2SiO_4$	Hänchen *et al.*, 2006; Hänchen *et al.*, 2007; Hänchen *et al.*, 2008; Prigiobbe *et al.*, 2009b; Gerdemann *et al.*, 2007; Krevor and Lackner, 2009; Jarvis *et al.*, 2009; Dufaud *et al.*, 2009; O'Connor, 2005; Prigiobbe *et al.*, 2009a; Munz *et al.*, 2009; Haug *et al.*, 2010
Serpentine[b]	$Mg_3Si_2O_5(OH)_4$	Blencoe *et al.*, 2003; Ron Zevenhoven, 2002; Zevenhoven *et al.*, 2006; Zevenhoven *et al.*, 2008; Teir *et al.*, 2009; Teir *et al.*, 2007b; Teir *et al.*, 2007c; Mercedes Maroto-Valer *et al.*, 2005; Alexander *et al.*, 2007; Xiaolong Wang, 2011a; Xiaolong Wang, 2011b; Park and Fan, 2004; Van Essendelft and Schobert, 2009a; Van Essendelft and Schobert, 2009b; Van Essendelft and Schobert, 2010; McKelvy *et al.*, 2004; Fouda *et*

		al., 1996; O'Connor, 2001; Li *et al.*, 2009
Feldspar	$CaAl_2Si_2O_8$	O'Connor, 2005
Pyroxene	CaMgSi2O6+(Fe, Al)	O'Connor, 2005
Talc	$Mg_3Si_4O_{10}(OH)_2$	O'Connor, 2005
Wollastonite	$CaSiO_3$	Teir *et al.*, 2005; Huijgen *et al.*, 2006; Daval *et al.*, 2009; Kakizawa *et al.*, 2001
Brucite	$Mg(OH)_2$	Blencoe *et al.*, 2003; Ron Zevenhoven, 2010

[a] Basalt (%): SiO_2: 49.2, TiO_2: 1.84, Al_2O_3: 15.74, Fe_2O_3: 3.79, FeO: 7.13, MnO: 0.2, MgO: 6.73, CaO: 9.47, Na_2O: 2.91

[b] Further categorized into different mineral types: chrysotile, lizardite and antigorite

From the Table 2-4 above it can be concluded that the most investigated minerals are olivine, serpentine and wollastonite. Magnesium-rich silicate minerals, especially serpentine, are found in large deposits worldwide (see Fig. 2-9), with large reservoirs being known, for example, on both the East and West coast of North America and in Scandinavia. Previous studies of mineral reserves in the U.S. have concluded that there is enough mineral volume to sequester the total US (2006 level) CO_2 emissions of 7 Gt/year for more than 500 years (Krevor, 2009). Lackner (2000) reported a deposit in Oman of 30,000 km^3 (350×40×5 km, 30 % pure, i.e. 25000-30000 km^3 of olivine) magnesium silicates which alone would be able to store most of the CO_2 generated by the combustion of the

world's coal reserves. Serpentinites in eastern Finland (Outokumpu-Kainuu ultramafic rock belt) alone could provide 2.5-3.5 $GtCO_2$ storage capacity (Teir *et al.*, 2009). Kelemen *et al.* (2008) also found large mineral deposits in Oceania and around the Adriatic Sea. Therefore, serpentine and olivine occur in sufficient magnitude to be considered viable candidates for mineral carbonation; however the abundant and wide availability of serpentine makes it particularly attractive.

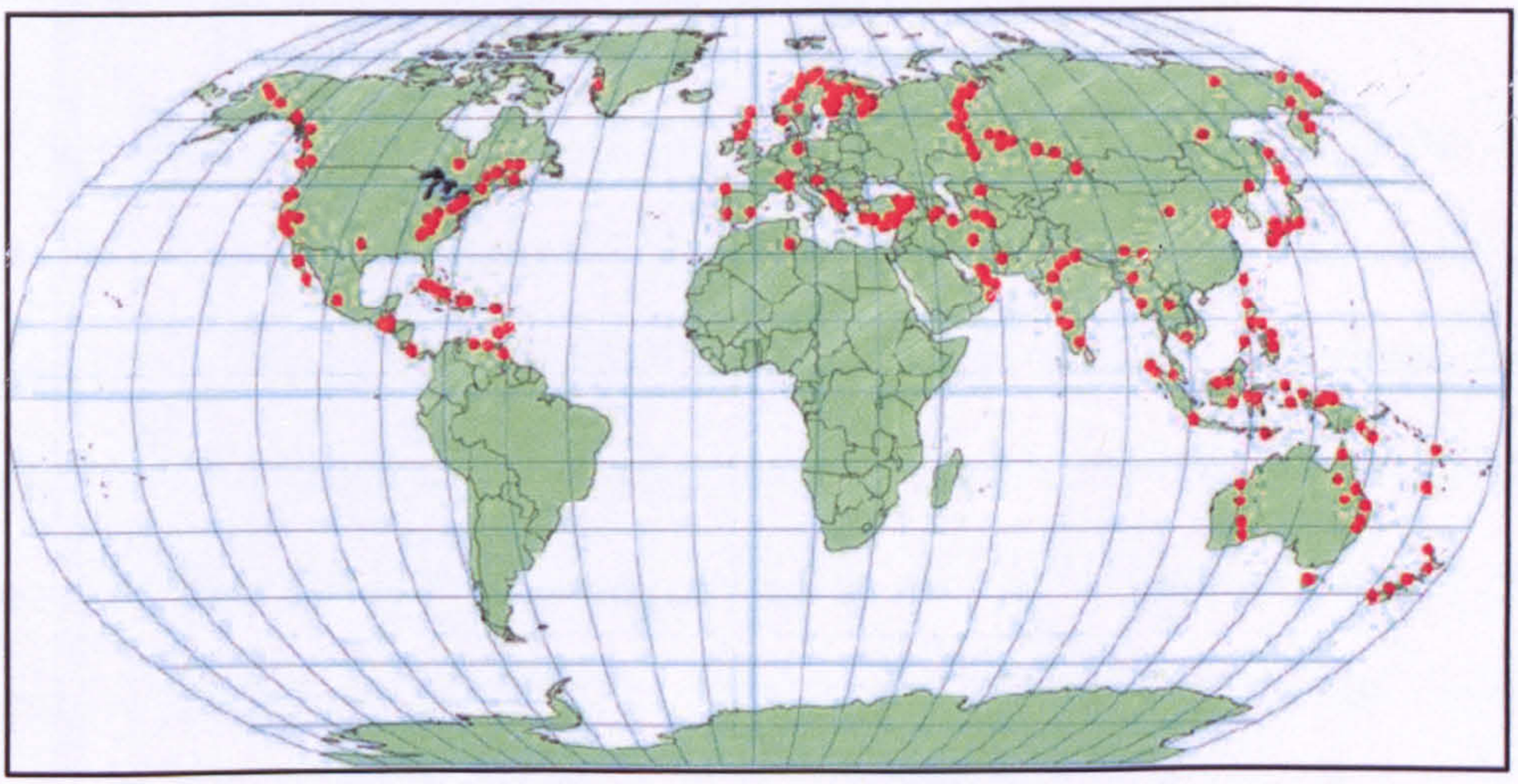

Figure 2-9: Distribution of magnesium silicate mineral deposits worldwide (Ron Zevenhoven, 2001)

R_{CO2} gives the theoretical mass amount of a given material necessary to convert a unit mass of CO_2 into mineral carbonate. The typical composition of various minerals, their specific R_{CO2} and the capacities of feedstock are given in Table 2-5. The main Mg ultramafic rocks, such as olivine and serpentine have much higher MgO wt. % values than waste materials. The main Ca ultramafic

rocks, such as wollastonite have similar CaO wt. % values to waste materials.

Table 2-5: Composition of various materials and carbon dioxide sequestration characteristics R_{CO2}.

Material	MgO [wt%]	CaO [wt%]	FeO [wt%]	R_{CO2} [kg/kg]	Capacity
Olivine[a]	45-50	0.1-0.5	6-10	1.8	10000 Gt [c]
Serpentine[a]	38-45	0	5-8	2.3	10000 Gt [c]
Wollastonite[b]	-	35-48	-	3.6	Small [c]

[a] O'Connor, 2001; [b] Daval *et al.*, 2009; [c] Lackner, 2002.

Magnesium and calcium rarely occur as binary oxides in nature, and they are typically found as silicate minerals. These minerals are capable of being carbonated because carbonic acid is stronger than silicic acid (H_4SiO_4). The reactions of Mg and Ca silicates (olivine, serpentine and wollastonite) with CO_2 and the thermodynamic data are described in Table 2-6. The carbonation reactions of olivine, serpentine and wollastonite can generate 89, 64 and 90 kJ/mol CO_2.

Table 2-6: Thermodynamic data of reaction for various carbonation reactions of typical minerals.

Mineral	Reaction	ΔH(kJ/ mol)[a]
Olivine	$Mg_2SiO_4 + 2CO_2 \rightarrow 2MgCO_3 + SiO_2$	-89
Serpentine	$Mg_3Si_2O_5(OH)_4 + 3CO_2 \rightarrow 3MgCO_3 + 2SiO_2 + 2H_2O$	-64
Wollastonite	$CaSiO_3 + CO_2 \rightarrow CaCO_3 + SiO_2$	-90

[a] IPCC, 2005.

2.3.2 Historical development

The concept of mineral carbonation was first mentioned by Seifritz (1990). A few years later, CO_2 storage by conversion of Ca-rich brine into carbonates was conducted by Dunsmore (1992). Detailed investigations of abundant and cheap natural silicate minerals such as olivine, serpentine and wollastonite, and also basalt rock were then conducted by Lackner and co-workers at Los Alamos National Laboratory (LANL) and the National Energy Technology Laboratory (NETL) (Lackner *et al.*, 1995). From then, mineral carbonation research developed quickly and can be divided into two different approaches: direct carbonation, where the carbonation of the mineral takes place in a single process step; and indirect carbonation, where calcium or magnesium is first dissolved from the mineral and subsequently carbonated (Fig 2-10).

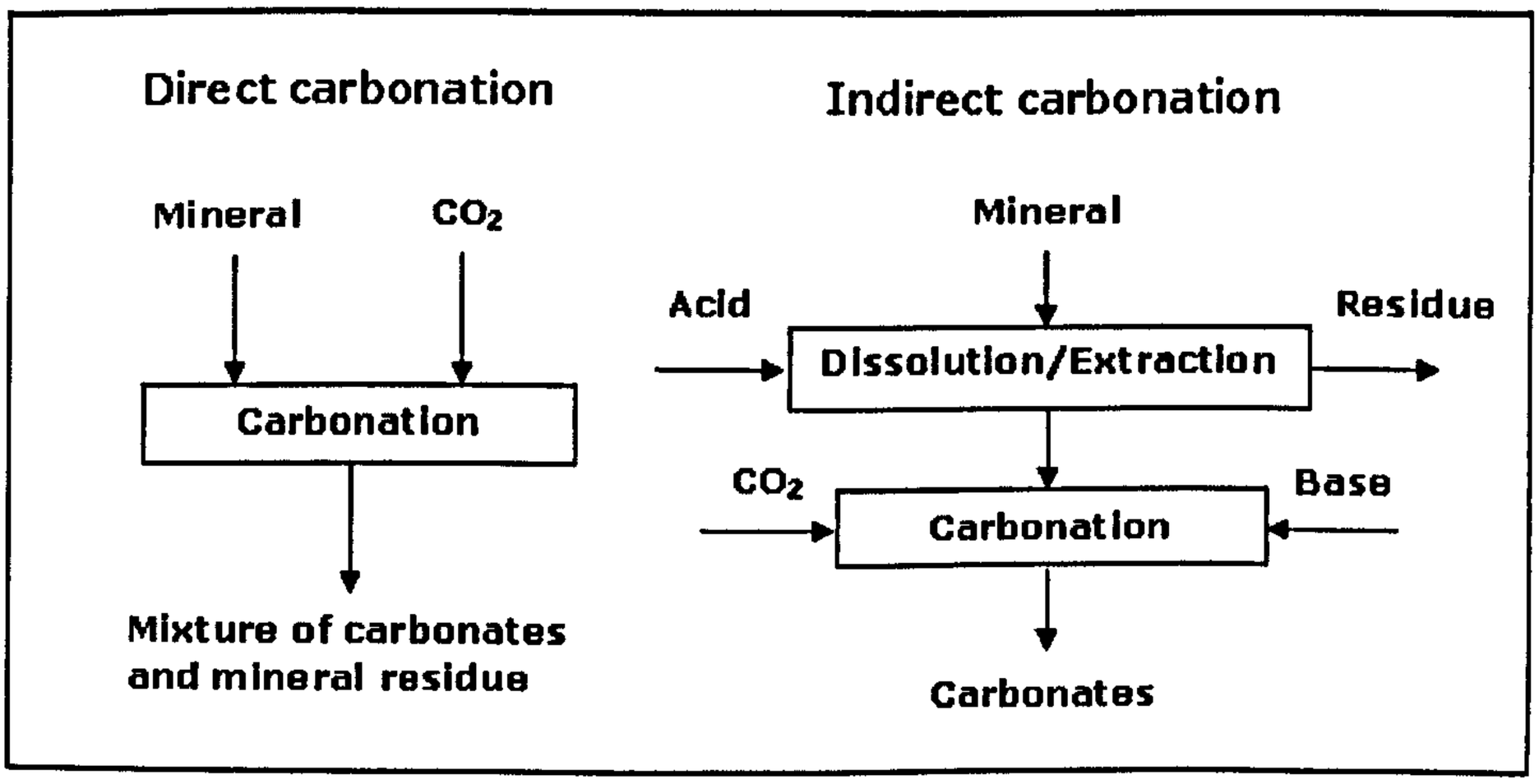

Figure 2-10: Schematic representation of the principles of direct and indirect carbonation.

Direct gas-solid carbonation using pressurised CO_2 at high temperature (25 % carbonation conversion at 340 bars, 500 °C after 2 h with 50-100 μm serpentine) was studied by Lackner *et al.* (1998). In addition, Butt and Lackner *et al.* (2002) reported an indirect gas-solid process, which produced $Mg(OH)_2$ from Mg silicates by using hydrochloric acid (HCl), followed by gas-solid carbonation of $Mg(OH)_2$ and then regeneration of HCl from $MgCl_2 \bullet nH_2O$ or Mg(OH)Cl. The carbonation of $Mg(OH)_2$ was found to be significantly faster than carbonation of MgO, where 90% conversion from $Mg(OH)_2$ to carbonates was obtained after 30 mins at 565 °C and 52 bar. Due to the complexity and energy penalty of this process, work started on a direct aqueous route.

O'Connor *et al.* (2001) at Albany Research Center (ARC) in the U.S. studied a direct aqueous process with optimisation of solution chemistry, heat treatment and grinding. They reported 84 % carbonation conversion within 6 h at 185 °C and 150 bar for ground olivine with particle size less than 38 μm; for heat treated serpentine the carbonation conversion was 60 % within 6 h at 155 °C and 115 bar using 0.64 M $NaHCO_3$ and 1 M NaCl solution; and for wollastonite the carbonation conversion reached 80 % within 30 mins at 100 °C and 40 bar in distilled water (O'Connor, 2005; Gerdemann *et al.*, 2007). This process was considered to be the most successful route for mineral carbonation and the cost of CO_2 sequestration by mineral carbonation based on this process was

estimated to be 54, 78 and 64 US$/t CO_2 sequestered (excluding CO_2 capture and transportation) for olivine, serpentine and wollastonite, respectively. Herzog (2002) gave a critical assessment of this method and concluded that this process would cause a 20 % energy penalty for a coal-fired power plant. The IPCC's special report on CCS used the highest cost of the ARC's process to compare mineralisation to other CCS approaches that presented a much lower cost. Nonetheless, mineralisation still received attention and improvements were made by using high-alkali bicarbonate concentrated (5.5 M $KHCO_3$) solutions, fluid-flow conditions and sonication (McKelvy *et al.*, 2006; Jarvis *et al.*, 2009). Zevenhoven (2008) reported that the costs of the ARC process were overestimated partly due to unrealistic calculation of energy efficiency and costs, where the costs of process heat input were significantly over-estimated when charged the same way as power input, giving a false impression of overall process economics. However, it remains unclear whether the CO_2 carbonated comes from the target CO_2 injected or from the $NaHCO_3$ added to the solution (see Section 2.3.4).

CO_2 mineral sequestration studies were initiated in Finland in 2000 and started with direct gas-solid route at elevated temperatures. The objective of this work was to make use of the possibility of covering process energy requirements with the heat from the carbonation reaction (Zevenhoven, 2002). Then, stepwise gas-solid

carbonation with Finnish serpentine and calcined $Mg(OH)_2$ powder was investigated in a pressurised thermogravimetric analyser (PTGA) (Zevenhoven *et al.*, 2008). Still, the chemical kinetics of gas-solid carbonation are relatively slower than aqueous carbonation. In order to improve the carbonation kinetics by increasing the intra-particle mechanical effects, a fluidised bed (FB) reactor was designed working at 20-40 bar of CO_2 pressure and 400-600 °C of temperature conditions. With the CO_2 acting as a fluidising gas, the carbonate product that built up on the reacting particles ($Mg(OH)_2$ powder) was removed as fines from the reactor with the exit gas flow. However, the production of $Mg(OH)_2$ became the limiting step, since $Mg(OH)_2$ is not naturally available in large quantities. Recently, Experience *et al.* (2010) proposed a solid-solid reaction process for production of $Mg(OH)_2$ from serpentine using $(NH_4)_2SO_4$ at 440 °C to generate $MgSO_4$, following addition of ammonia water to precipitate $Mg(OH)_2$ (Fagerlund *et al.*, 2009; Nduagu, 2010). $Mg(OH)_2$ was then carbonated with CO_2 directly in a pressurized fluidized bed (PFB) reactor at 470-550 °C and 20 bar. However, only 20-50 % dissolution efficiency of Mg from serpentine was reported (Nduagu, 2010). Moreover, the carbonation efficiency of $Mg(OH)_2$ only achieved a maximum value of 50 % due to the conversion from $Mg(OH)_2$ to MgO at the temperature range used, and the produced MgO could not be carbonated at the above

reaction temperature (Zevenhoven, 2010). Therefore, work is needed to improve both dissolution and carbonation efficiencies.

In order to avoid energy-intensive pre-treatment, research teams worldwide embarked on indirect aqueous routes, where Mg or Ca were dissolved from minerals or industrial wastes by using strong or weak acids, alkali or ligands solutions (Maroto-Valer *et al.*, 2005; McKelvy *et al.*, 2004; Park and Fan, 2004; Blencoe *et al.*, 2003). However, a problem with these routes is that the chemicals used could not be recovered and re-used. For example, Teir and co-workers dissolved serpentinite with strong HNO_3 and HCl solution, and the prepared Mg-rich solutions were used to precipitate pure hydromagnesite ($Mg_5(CO_3)_4(OH)_2 \bullet 4H_2O$), while regulating the pH by adding NaOH, which is needed for precipitation (Teir *et al.*, 2007b and 2007c). However, the energy and costs of makeup acids and NaOH (using 2 t NaOH and 2-3 t acid per tonne CO_2 sequestered) made this process uneconomic with costs of 600-1600 US$/t CO_2 sequestered (Teir *et al.*, 2009). Another example of such indirect aqueous process is the pH-swing process suggested by Kodama *et al.* (2008), where steel slags were dissolved with ammonium chloride (NH_4Cl), followed by carbonation with NH_3, which was produced from the dissolution, and recovery of NH_4Cl from the carbonation. The energy penalty of this process was reported to be 300 kWh/t CO_2 sequestered. Meanwhile, much work is currently carried out on enhancing carbonation chemistry of magnesium

silicates in aqueous systems using weak acids and additives such as citrates, oxalates and ethylenediamine tetraacetic acid (EDTA) (Park, 2008; Krevor and Lackner, 2009; Prigiobbe *et al.*, 2010). The organic acid dissolution proceeds rapidly, achieving dissolution greater than 60% and 80% within 2 and 7 hours, respectively, and near 100% dissolution is achieved between 10 and 20 hours. Although the use of organic acids can minimise the use of chemicals, their complete recovery and reuse is not feasible (Krevor, 2011).

Various pre-treatment methods (chemical, mechanical and thermal) have been developed (McKelvy *et al.*, 2004; Musvoto *et al.*, 2000; Maroto-Valer *et al.*, 2005). In the UK, Alexander *et al.* (2007) studied the effect of process parameters, such as solvent concentration, temperature, reaction time, CO_2 pressure and particle size on serpentine mineralisation. In Switzerland, Mazzotti, Hanchen and co-workers at Eldgenossische Technische Hochschule Zurich (ETH) investigated the reaction kinetics and modelling of dissolution and carbonation reactions (Hänchen *et al.*, 2006 and 2008). In Netherlands, Huijgen and Comans (2006 and 2007) at the Energy Research Center of the Netherlands (ECN) conducted experimental work on direct aqueous carbonation of wollastonitie and steel slags.

Many researchers (Teir *et al.*, 2007c; Huijgen *et al.*, 2006; Bearat *et al.*, 2006; Xiaolong Wang, 2010a) have reported that the rate-

limiting step of mineral carbonation is mineral dissolution, when a passive silicate layer is formed and prevents further dissolution. Chemical reaction control dominates the fast initial dissolution, while product layer diffusion control dominates further dissolution and the produced passive layer becomes the barrier preventing further dissolution. Intensive particle-particle (mechanical) interactions inside a reactor or the presence of abrasion can enhance the kinetics of dissolution.

Recently, the Global Institute of Carbon Capture and Storage (GICCS) in Australia and CO_2 Technology Centre (TCM) in Norway have provided funding for mineralisation projects. Dlugogorski *et al.* (2010) at the University of Newcastle in Australia and Munz (2009) at the Institute for Energy Technology in Norway are further developing the ARC's direct aqueous carbonation.

Despite these recent developments, little progress has been made when it comes to the recovery and recycling of additives, which is a key issue for the development of mineral carbonation. In general, the additive-free process is not able to match the additive-enhanced process in terms of dissolution and carbonation efficiencies. Moreover, there is a risk that the cost of additives may make the process uneconomic.

2.3.3 Process routes classification

The CO_2 mineral sequestration technology is likely to be conducted in a dedicated processing plant (Fig. 2-11). The CO_2 is captured at the power plant or other emission source. In order to minimize transportation costs, the location of a mineral carbonation plant can be sited either within the power plant or close to the mine or industry plant, where solid wastes are produced. The CO_2 can be transported by pipeline, minerals and wastes can be transported by shipping or railway. After carbonation, the Mg or Ca carbonates can either be reused in construction or other purposes, or landfilled at a storage site.

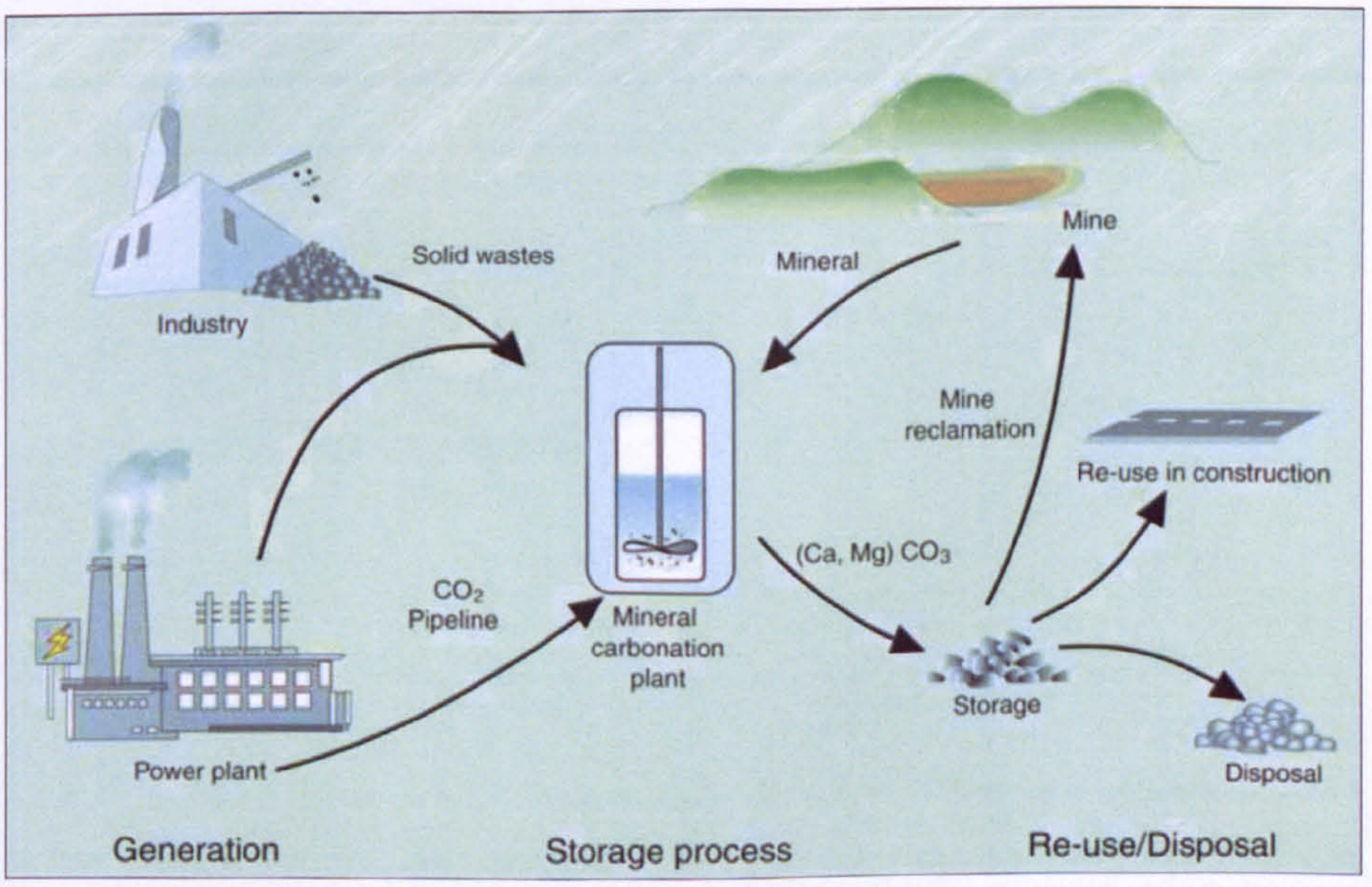

Figure 2-11: Material fluxes and process steps of mineral carbonation (IPCC, 2005)

The mineral carbonation technology applied in the plant will be one of the various process routes described in Fig. 2-12, ranging from the most basic accelerated weathering of minerals to advanced

multi-step processes. As described here, some of the process routes suggested earlier have been abandoned, such as molten salts and pressure swing, and are not included here. The definitions of direct and indirect processes have been explained in Figure 2-10. For the direct aqueous mineral carbonation, various pre-treatment methods are presented. For the indirect aqueous mineral carbonation, research mainly focuses on different additives.

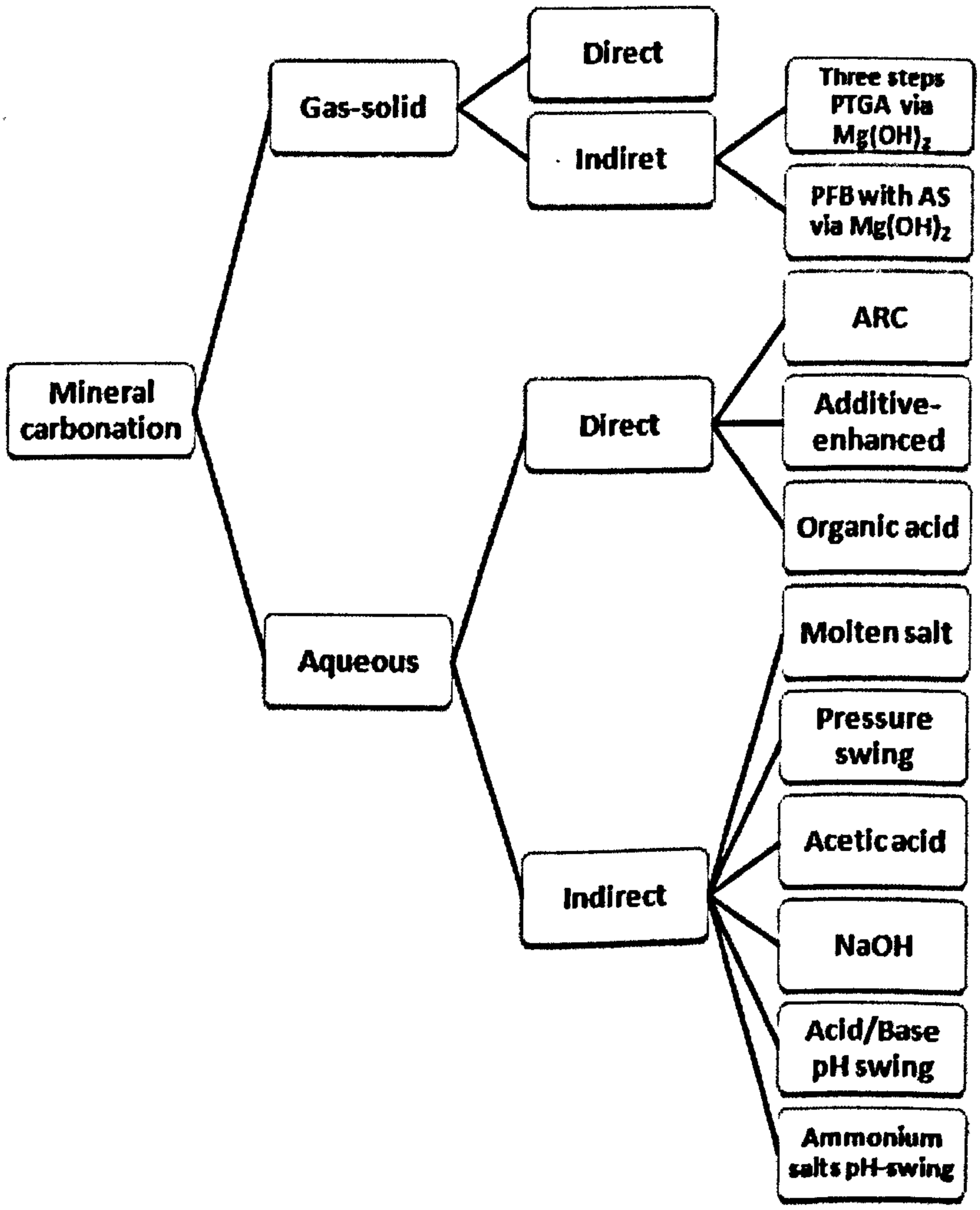

Figure 2-12: Process routes of mineral carbonation.

2.3.4 Direct and indirect gas-solid mineral carbonation

Gas–solid mineral carbonation is the most straightforward approach in mineral carbonation, where gaseous CO_2 reacts with solid Ca/Mg silicates at an elevated temperature and pressure (Lackner *et al.*, 1997; Zevenhoven, 2002):

$$Ca/Mg-silicate(s)+CO_2(g)\rightarrow (Ca/Mg)CO_3(s)+SiO_2(s)$$

Equation 2-2

2.3.4.1 Direct gas-solid carbonation

The dry process of direct gas-solid carbonation has the potential of producing high temperature steam or electricity, while converting CO_2 into carbonates and producing silica. However, the reaction rates of this process have been too slow (7 days) and the process suffers from thermodynamic limitations. Activation of minerals by heat treatment can improve the carbonation rate, but it is energy prohibitive. Therefore, most of the studies about this process have been abandoned. In a previous literature review conducted by Huijgen and Comans (2003), it was concluded that the direct gas-solid carbonation route does not have the potential to become an industrially viable process.

However, developments suggest that there are still significant improvements to be made in the process when using waste materials (Rendek *et al.*, 2006; Baciocchi, 2006a and 2006b). The

advantages of CO_2 storage and lowering the hazardous nature of waste make this carbonation route interesting. However, the potential CO_2 storage capacity of this waste is limited.

2.3.4.2 Indirect gas-solid carbonation

i. Three steps pressurised thermogravimetric analyser (PTGA) process via $Mg(OH)_2$.

Indirect gas-solid carbonation, involving dissolution of magnesium oxide or hydroxide and subsequent dry carbonation at elevated temperature and pressure, could be more attractive than direct gas-solid carbonation for reasons of better kinetics. Butt *et al.* (1998) found that the gas-solid carbonation of $Mg(OH)_2$ can be considered feasible and faster than the carbonation of MgO. But since hydroxides do not occur in a significant amount in nature, these have to be produced from Mg-silicates. Zevenhoven *et al.* (2008) firstly suggested a three steps process using serpentine as follows (Fig. 2-13): a) MgO production in a high temperature (>500 °C) reactor, b) MgO hydration and c) carbonation of $Mg(OH)_2$ at elevated pressure. The experimental results showed that 40~60 % carbonation conversion was achieved at 495-540 °C and at 35-45 bar for 6 h in a PTGA. Although this process enhanced the reaction rates compared to the two step carbonation of MgO (Butt *et al.*, 1998), it is still too slow (6 hrs) to produce $Mg(OH)_2$ from serpentine.

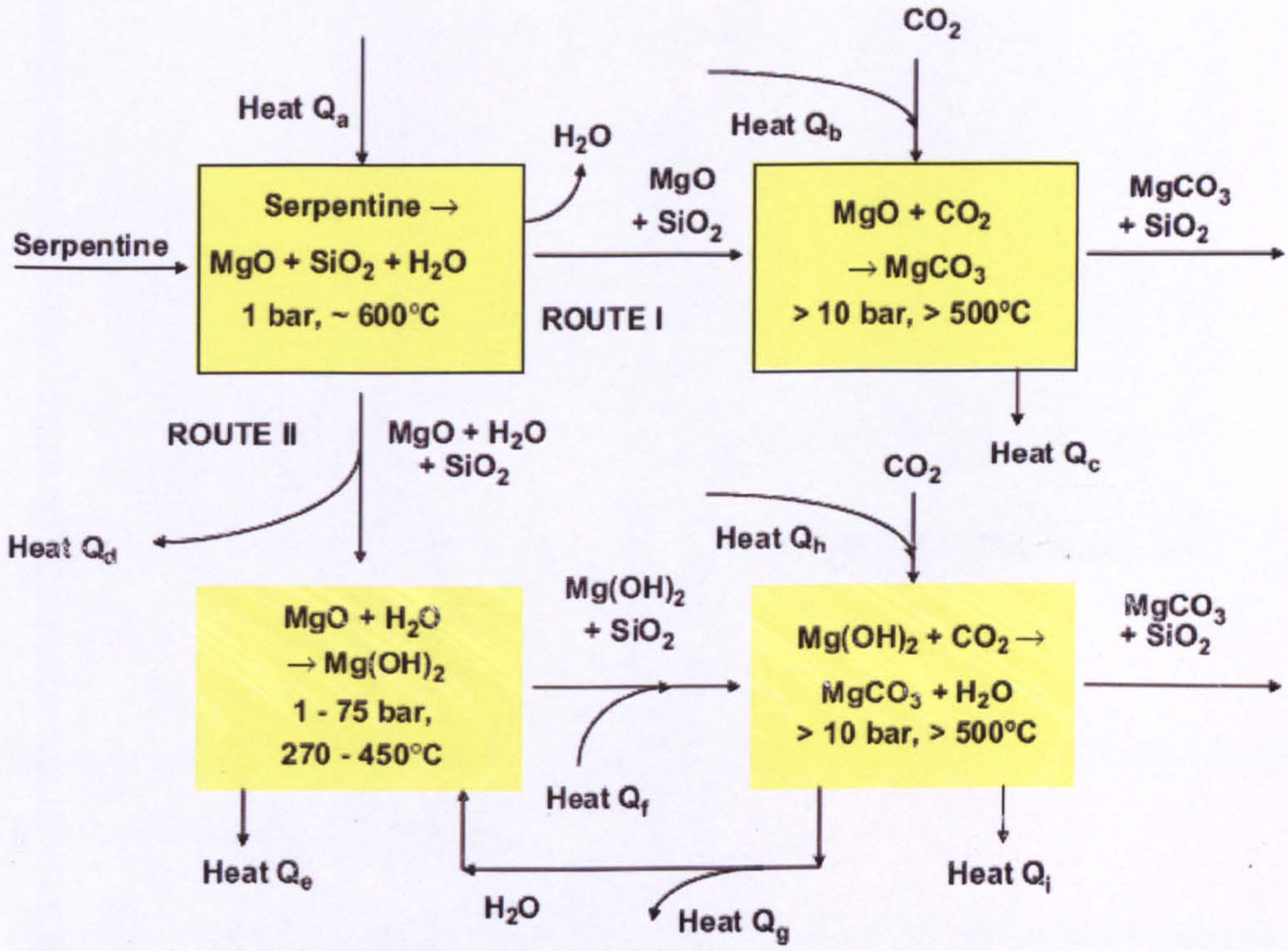

Figure 2-13: Two alternative routes for serpentine carbonation: via MgO or via $Mg(OH)_2$. (Zevenhoven *et al.*, 2008)

ii. Pressurised fluidised bed (PFB) with ammonium sulphate (AS) via $Mg(OH)_2$.

Fagerlund *et al.* (2009) developed the use of gas/solid PFB reactors (see Fig. 2-14), where carbonate removal is possible due to particle collisions (attrition or abrasion) and the flue gas can carry the particles out of the reactor. Moreover, particle collisions can improve the overall carbonation reaction rate since product layer diffusion has been shown to be the rate limiting step and this can be partly overcome by particle collisions (Bearat *et al.*, 2006).

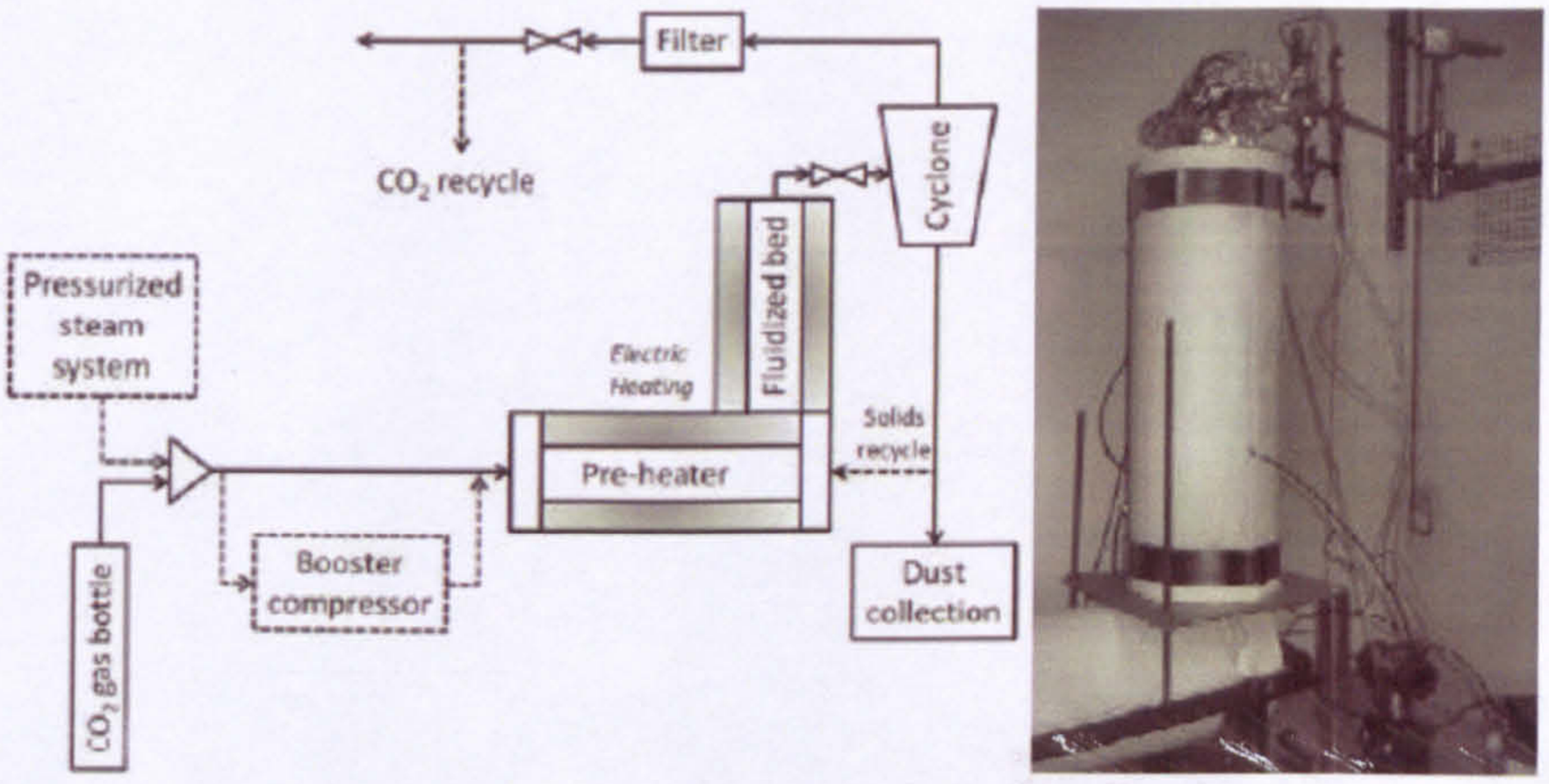

Figure 2-14: Schematic diagram of the fluidised bed together with actual (work-in-progress) setup. (Fagerlund *et al.*, 2009)

Recently, Nduagu *et al.* (2010) developed a new method to produce $Mg(OH)_2$ from serpentine. Firstly, solid-solid reaction of serpentine with ammonium sulphate (AS) $(NH_4)_2SO_4$) was carried out at above 440 °C for 20-60 mins to generate $MgSO_4$, that was then put into ammonia water to precipitate $Mg(OH)_2$ and regenerate $(NH_4)_2SO_4$, and finally $Mg(OH)_2$ was carbonated with CO_2 directly in a PFB reactor at 470-550 °C and 20 bar for 15-60 mins (shown in Fig. 2-15). Interestingly, most of the carbonation took place at only 30 minutes. However, only 20-60 % dissolution efficiency of Mg from serpentine was reported (Nduagu, 2010), and the carbonation efficiency of $Mg(OH)_2$ only achieved a maximum value of 50 % (see Fig. 2-16). The low carbonation efficiency was due to the conversion of $Mg(OH)_2$ to MgO at the temperature range used (470-550 °C), and the produced MgO could not react with CO_2 to produce

carbonates at the above temperature range (Zevenhoven, 2010). Therefore, work is needed to improve both dissolution and carbonation efficiencies.

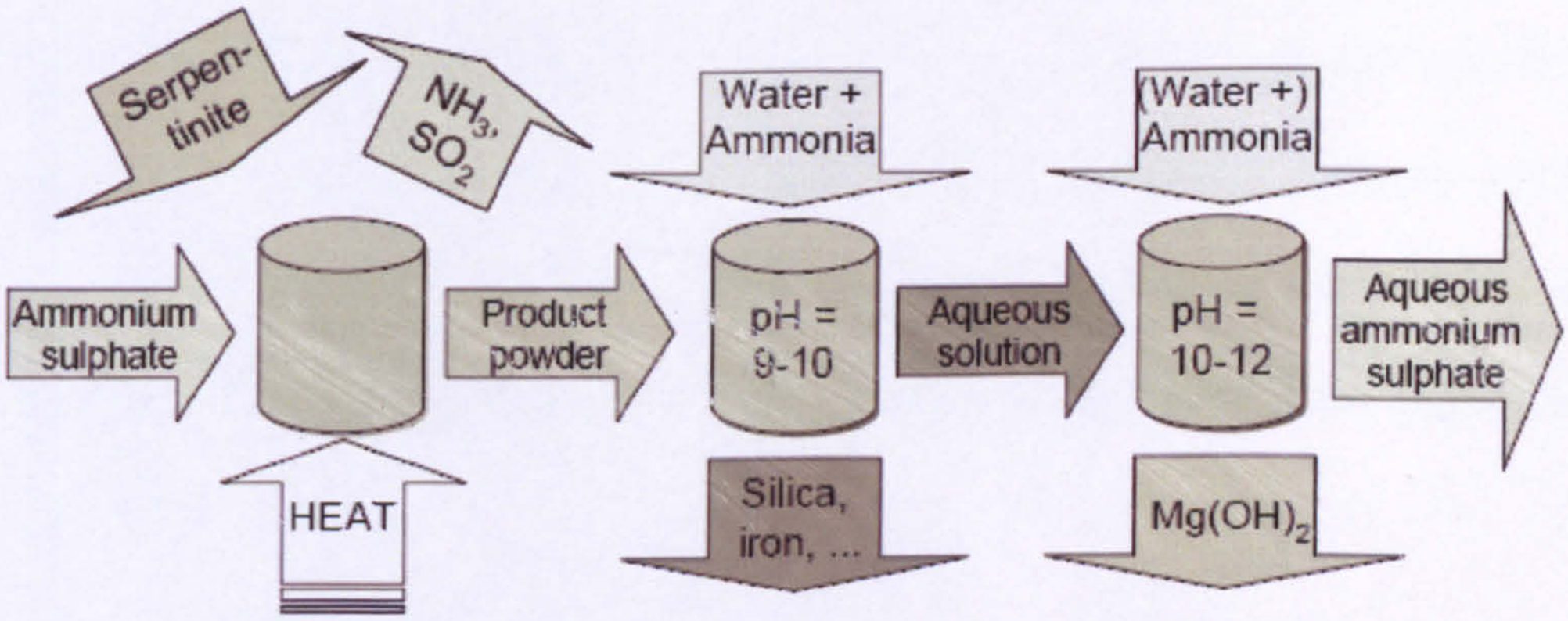

Figure 2-15: Flow diagram of the $Mg(OH)_2$ production process from serpentine with ammonium salts (Fagerlund *et al.*, 2009).

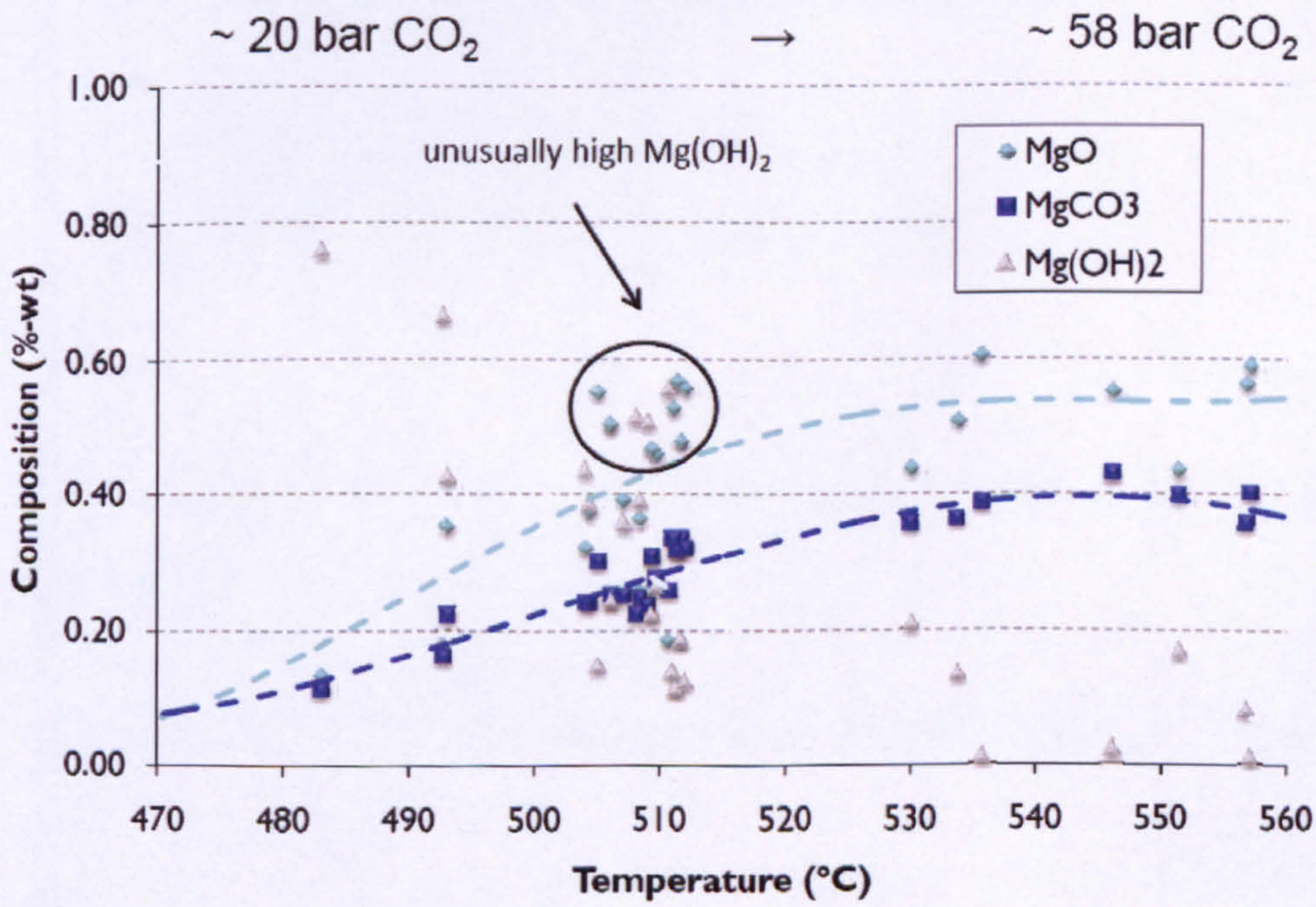

Figure 2-16: The composition of MgO, $Mg(OH)_2$ and $MgCO_3$ with temperature in FB reactor (Zevenhoven, 2010).

2.3.5 Direct aqueous mineral carbonation

The presence of water can significantly enhance the reaction rate of carbonation processes (O'Connor, 2001). The direct aqueous mineral carbonation process is performed in an aqueous solution and in single step, but there are three reactions taking place simultaneously. Firstly, CO_2 dissolves into water and dissociates to bicarbonate and H^+ resulting in a pH of about 4.0-5.5 at high CO_2 pressure:

$$CO_2(g) + H_2O(l) \Leftrightarrow H_2CO_3 \Leftrightarrow H^+(aq) + HCO_3^-(aq)$$

Equation 2-3

Secondly, Ca/Mg leached from the mineral matrix by H^+:

$$Ca/Mg - silicates(s) + 2H^+(aq) \rightarrow$$
$$(Ca/Mg)^{2+}(aq) + SiO_2(s) + H_2O(l)$$

Equation 2-4

Finally, the $(Ca/Mg)^{2+}$ reacts with HCO_3^- and precipitates as Ca/Mg carbonates:

$$(Ca/Mg)^{2+}(aq) + HCO_3^-(aq) \rightarrow (Ca/Mg)CO_3(s) + H^+(aq)$$

Equation 2-5

2.3.5.1 ARC process.

The Albany Research Centre's process was regarded as a state-of-art technology in direct aqueous mineral carbonation. Various pre-treatment methods were developed for this process to improve the reaction rate of both dissolution and carbonation. Thermodynamic studies were also conducted to understand the controlling mechanism of reactions. Additionally, further additive-enhanced processes and organic acid processes were investigated as the continuous work of ARC's process.

In order to maximise the reaction rate, a careful selection of process conditions such as particle size, temperature and CO_2 pressure was made by O'Connor *et al.* at ARC (O'Connor, 2001). The process diagram of the direct aqueous mineral carbonation process is presented in Fig. 2-17 and the optimum conditions and the carbonation conversions are listed in Table 2-7.

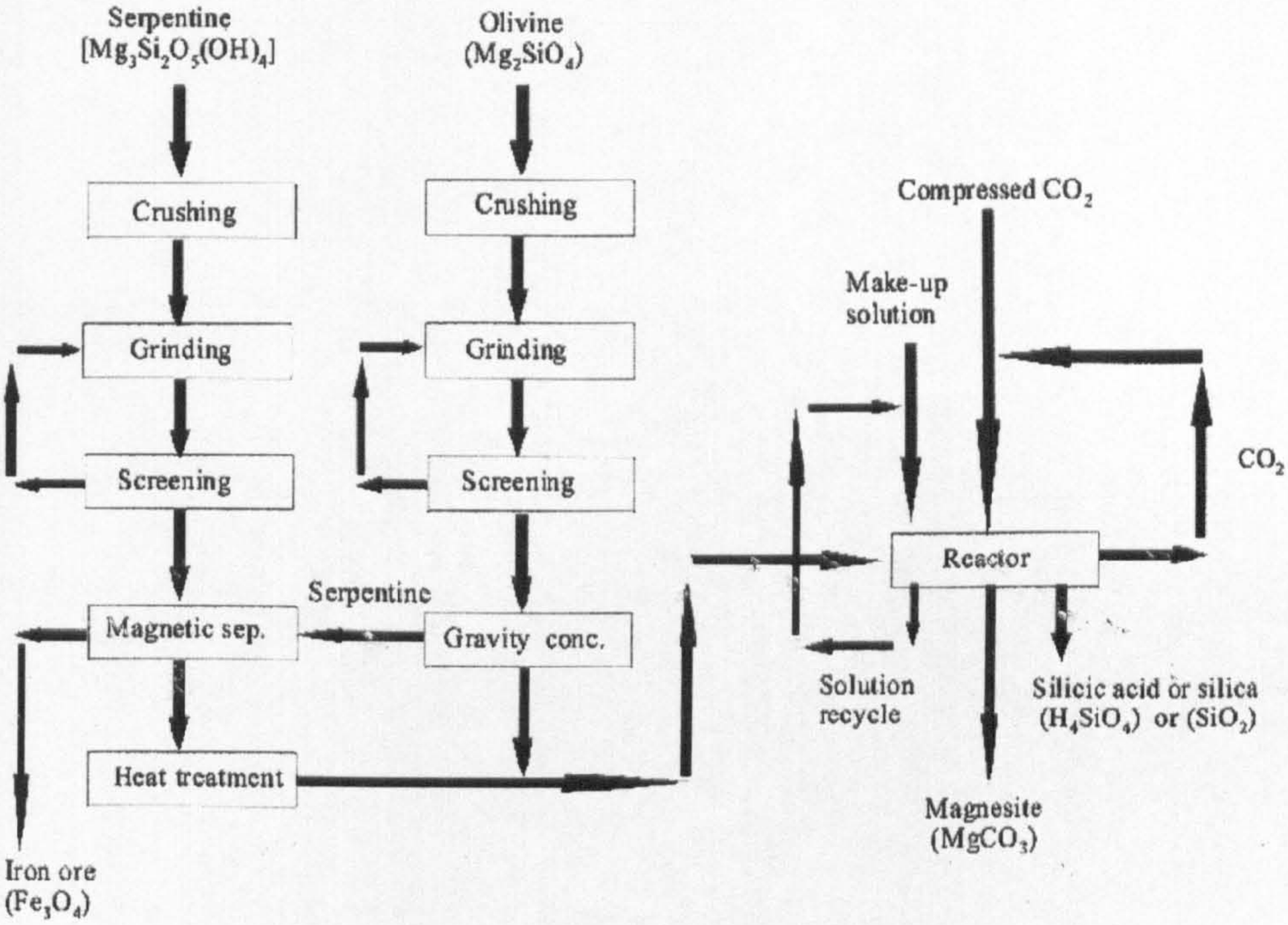

Figure 2-17: Process flow diagram for the direct carbonation process (O'Connor, 2001)

Table 2-7: Optimum carbonation conditions and carbonation conversion (Gerdemann *et al.*, 2007)

Mineral	T (°C)	P_{CO2} (bar)	Carrier solution	Reaction time (h)	Carbonation conversion (%)	Carbonation conversion, 1 h (%)
Olivine	185	150	0.64 M $NaHCO_3$, 1 M NaCl	6	91.0	49.5
Wollastonite	100	40	distilled water	-	97.8	81.8
HT serpentine	155	115	0.64 M $NaHCO_3$, 1 M NaCl	-	80.0	73.5

In O'Connor's work, particle size reduction (<4 μm), by intensive grinding for olivine and heat treatment at high temperature (above 600 °C) for serpentine were studied to improve the reaction rate. However, the energy intensive pre-treatment became a barrier for large-scale application. Bicarbonate/salt ($NaHCO_3$/NaCl) mixture solution was found to accelerate the reaction (O'Connor, 2001). The $NaHCO_3$ increased the HCO_3^- concentration, which in turn lowered the Mg^{2+} concentration required to precipitate $MgCO_3$. The solution was then buffered at a pH of 7.7-8.0, resulting in the improvement of absorption of CO_2. NaCl can increase the release of Ca/Mg^{2+} from silicate by creating soluble complexes and thus lowering the activity of Ca/Mg^{2+} in solution, in the other words, thereby increasing the solubility of Ca/Mg-silicates and decreasing the solubility of Ca/Mg carbonates (Fauth *et al.*, 2001). The reactions of olivine in $NaHCO_3$/NaCl solution are presented below:

$$Mg_2SiO_4(s) + 2HCO_3^-(aq) \rightarrow 2MgCO_3(s) + SiO_2(s) + 2OH^-(aq)$$

Equation 2-6

The bicarbonate can be regenerated by the reaction of OH^- with $CO_2(g)$:

$$OH^-(aq) + CO_2(g) \rightarrow HCO_3^-$$

Equation 2-7

It was assumed that the HCO_3^- concentration and pH of the solution were kept constant and the process did not consume $NaHCO_3$. However, experiments conducted by O'Connor *et al.* (2004), showed that when 0.64 M $NaHCO_3$ solution was used the carbonation conversion measured was 19%. However, when the solution was recycled and reused the final carbonation conversion was only 0.3%-0.7%. These results substantiated that production of magnesium carbonates demand fresh addition of sodium bicarbonate. This provides a considerable limitation as producing sodium bicarbonate (or sodium carbonate) from gaseous CO_2 greatly increases the energy and economic penalties for this process.

O'Connor *et al.* (2005) and Gerdemann *et al.* (2007) reported a 91 % carbonation conversion was achieved in 6 h at 185 °C and 150 P_{CO2} bar and 15 % solid/liquid ratio in 0.64 M $NaHCO_3$ + 1 M NaCl solution for olivine; for heat treated (HT) serpentine, 80 % carbonation conversion was achieved in 6 h at 155 °C and 115 P_{CO2} bar and 15 % solid/liquid ratio in 0.64 M $NaHCO_3$ + 1 M NaCl solution; and for wollastonite, 80 % carbonation conversion was reached in 1 h at 100 °C and 40 P_{CO2} bar and 15 % solid/liquid ratio in distilled water (O'Connor, 2001; Gerdemann *et al.*, 2007). Wollastonite reacts faster, and a lower CO_2 pressure and no additive are required to obtain high conversion compared to Mg-silicates. However, less CO_2 can be sequestered per kilo feedstock than Mg-silicates due to the higher molar mass of Ca. In addition, the

worldwide availability of wollastonite is limited compared to Mg-silicates (O'Connor, 2004).

Direct aqueous carbonation is thus far the only process that has shown a detailed energy and economic evaluation (Gerdemann *et al.*, 2007; O'Connor, 2004). The evaluation is based on the ARC's process using an autoclave reactor. A 27 % energy penalty was reported for a 1.3 GW coal-fired power, where 75 % of the energy penalty was due to the grinding of the feedstock. Seven regions in the U.S. were studied where both large ultramafic ores and large amounts of CO_2 are present. For the best case, the sequestration cost were 54, 91 and 250 US$/t CO_2 sequestered[6] (78, 112 and 309 US$/t CO_2 avoid[7]) for olivine, wollastonite and HT serpentine, respectively. These costs have to be reduced significantly in order to become economically competitive with other sequestration options.

Due to the non-complete conversion of the minerals, the mineral amounts required significantly exceed the theoretical amount. Gerdemann *et al.* (2007) reposted that in the best-case scenario 5.3 tonnes of olivine, 6.5–8.9 tonnes of serpentine or around 8.9 tonnes of wollastonite are required for each tonnes of coal. Therefore it is very important to consider the environmental and economic impacts of the products disposal and utilization.

[6] This cost excludes the chemical make-up.

[7] Excluding energy consumption from the CO_2 mineralisation process.

In the Netherlands, Huijgen *et al.* (2006) studied a similar direct aqueous mineral carbonation process using wollastonite and steel slag. For the optimised conditions, a 70 % carbonation conversion was achieved after 15 min at 200 °C, 20 bar CO_2 and particle size of <38 µm. The cost evaluation of the process using chemical simulation software (ASPEN PLUS) was reported to be 125 and 93 US$/t CO_2 sequestered for wollastonite and steel slag, respectively (Huijgen *et al.*, 2007). The major costs were associated with the feedstock and the grinding and compression. It was suggested that further cost reduction should focus on the liquid/solid ratio and offset by the sale of the carbonated product.

2.3.5.2 Pre-treatment studies and silica passive layer.

High pressure CO_2, fine grinding of minerals and high temperature heat treatment in the direct aqueous route are expensive and energy prohibitive. Therefore, research has been performed on understanding the controlling mechanism of reactions. Aqueous carbonation of Ca/Mg silicates occurs in two steps, 1) dissolution of $(Ca/Mg)^{2+}$ from mineral and 2) precipitation of Ca/Mg carbonate. The rate limiting step is the dissolution since a passive layer is formed, which hinders further leaching of Ca/Mg.

A fundamental study of aqueous carbonation was conducted by Wolf *et al.* (2004), who developed a micro-reaction system with in-situ

observation of aqueous CO_2 mineral carbonation reaction using synchronotron X-ray diffraction and Raman spectroscopy. The experimental results showed that magnesite precipitated directly when the HT serpentine slurry was exposed at 150 bar CO_2 and 150 °C. McKelvy *et al.* (2004) developed a system of simultaneous thermogravimetric and differential thermal analysis (TGA/DTA) to study the effect of heat treatment on the serpentine mineral lizardite. Meta-serpentine materials were observed to form above 600 °C by removal of 90 % of hydroxide groups and the carbonation from meta-serpentine directly into magnesite was observed. Bearat *et al.* (2006) found the formation of a passive silica-rich layer around the mineral particles that hindered further dissolution of Mg from mineral matrix and slowed the carbonate formation. Thus, improvement of carbonation conversion could be achieved by maximizing particle interaction and mechanical stirring (attrition or abrasion). It is interesting to find that the demonstration of intergrowth of carbonate minerals within an olivine matrix. In considering the separation of the products from the un-reacted feedstocks, Bearat *et al.* (2006) observed that the carbonate precipitated as a coating on the minerals hindering further carbonation and making recycling of un-reacted feedstocks very difficult.

The possibility of reducing the expenses associated with particle size reduction by enhancing particle-particle interaction was studied

using a flow-loop reactor, where a mixture of large particles (75-150 μm) and ultrafine particles (<4 μm) were carbonated at the optimum solution and conditions (see Table 2-7) (Penner, 2004). A 53 % conversion was achieved compared to 40 % in an autoclave reactor since the intensive mixing removed the silica passive layer and enhanced the reaction rate. Further research in new reactor design, such as fluidised bed reactor and continuous pipeline reactor, is expected to further improve the dissolution efficiency and rate.

2.3.5.3 Thermodynamic studies of dissolution rate and precipitation studies.

The dissolution rate of olivine and serpentine in aqueous solutions has been studied extensively (Oelkers, 2001; Pokrovsky and Schott, 2000; Rosso and Rimstidt, 2000; Chen and Brantley, 2000). The dissolution of minerals has been found to occur in two stages: first, a rapid dissolution stage, followed by a relatively slow dissolution stage (Hänchen *et al.*, 2006). The latter stage is most relevant to enhance the mineral carbonation process. Dissolution is affected by temperature, CO_2 pressure and pH. Many geochemistry studies have focuses on dissolution of Ca/Mg silicates, but unfortunately, the majority of these studies were performed at ambient conditions (Oelkers, 2001; Pokrovsky and Schott, 2000; Rosso and Rimstidt, 2000; Chen and Brantley, 2000). Hanchen *et al.* (2006), however, critically analysed earlier studies and performed experiments at 90,

120 and 150 °C. Hänchen *et al.* (2006) developed the shrinking core model[8] to describe the dissolution of olivine at high temperature (up to 150 °C). Later, Hanchen *et al.* (2007) developed a population balance model[9] to better describe the dissolution of olivine and concluded that the previous model could be used as a good approximation for narrow size distributions, while the improved model was able to handle a much wider range of particle sizes. Hanchen *et al.* (2008) have extensively studied the chemistry of aqueous mineral carbonation of olivine in order to better understand magnesium carbonate precipitation. An H_2O-CO_2-Na_2CO_3-$MgCl_2$ system at various temperature and CO_2 pressures (25 °C and 1 bar, 120 °C and 3 bar, 120 °C and 100 bar) was investigated. The results concluded that the formation of magnesium carbonate species depended on temperature and pressure. Nesquehonite ($MgCO_3 \bullet 3H_2O$) precipitated from aqueous solutions at ambient temperature, while at higher temperatures (50 and 100 °C), nesquehonite was transformed into hydromagnesite ($4MgCO_3 \bullet Mg(OH)_2 \bullet 5H_2O$). When the temperature was above 100 °C, hydromagnesite was transformed into magnesite ($MgCO_3$).

[8] Shrinking core model describes the particle size and the reacting core shrink simultaneously.

[9] Particle population balance describes the time-varying particle size distribution. Assuming particles with constant shape, it is possible to describe the particle size evolution using one characteristic length.

2.3.5.4 Additive-enhanced process.

McKelvy *et al.* (2006) suggested that the reaction rates can be significantly improved by further increasing the bicarbonate ($NaHCO_3$, $KHCO_3$) concentration. Adding bicarbonate salts increased the ionic strength of the solution and therefore facilitated the formation of complexes with dissolved Ca or Mg. Thus, the Ca/Mg-activity in solution was lowered and the release of $(Ca/Mg)^{2+}$ ions from the silicate was enhanced. McKelvy *et al.* (2006) showed that adding 5.5 M $KHCO_3$ resulted in an increase of the olivine and HT serpentine carbonation to 81% and 92% after 1 hour, respectively, compared to 91% after 6 h for olivine without additives at the same conditions (185 °C, 150 bar CO_2, <38 μm and 1500 rpm). However, Jarvis *et al.* (2009) reported that, only 63 % conversion was obtained using 5.5 M $KHCO_3$ after 1 h. Chen *et al.* (2006) explained the effects of bicarbonate concentration, temperature and pressure to carbonation conversions in fundamental chemistry.

2.3.5.5 Organic acid process.

In order to overcome the pH conflict between dissolution and carbonation, organic acid solutions with neutral pH have been sought to overcome slow dissolution kinetics without inherently being consumed in reactions. Several additives such as acetic acid and citric acid have been studied (Park and Fan, 2004; Lackner, 2002). A combination of orthophosphoric acid, oxalic acid and EDTA

has been reported to increase the dissolution of serpentine most effectively (65 % dissolution efficiency) (Park and Fan, 2004). Krevor *et al.* (2011) conducted a solvent selection study, including sodium oxalate, EDTA, trisodium citrate, NH_4Cl, NaCl and sodium acetate at the conditions of 0.1 M salt conc., 90 °C, 20 bar CO_2 and 3g serpentine in 1kg water. They reported that 50 % dissolution efficiency was achieved after 6 h for oxalate, EDTA and citrate, and 100 % dissolution efficiency was obtained after 24 h by using citrate. It is important to point out that neutral pH, while enhancing the dissolution rate, inhibits carbonate precipitation due to the formation of strong complexes. Moreover, there is no evidence to prove the feasibility of recycling organic acid solution and the cost of make-up organic acid solutions is expensive. Furthermore, the un-recycled organic solvent may cause serious environmental impacts. Therefore expensive organic solvents can only be applied practically when the complete solvent recycling is achieved.

2.3.6 Indirect aqueous mineral carbonation

Indirect aqueous mineral carbonation comprises several steps, as described here. Normally, the reactive component (Ca/Mg) is first dissolved from the feedstocks and then reacts with CO_2 to form the desired carbonates (see Fig. 2-10). Various additives are used to enhance the reaction rate and efficiency of each step. Indirect

mineral carbonation has been widely investigated, and the main processes are presented here.

2.3.6.1 NaOH

Blencoe *et al.* (2004) developed an approach to overcome the disadvantages associated with the elevated temperatures and pressures of the direct aqueous route. Their process using NaOH was tested using various feedstocks. There are four major drawbacks of this process as follows: (1) reaction times reported were too long (3 days) for industrial application, (2) the feedstock needed to be milled to <10 μm resulting in a high energy penalty, (3) process conditions required 200 °C and 15 bar, and (4) large quantities of NaOH were required as recycling of NaOH was not proved. There is no progress of this process reported since 2004.

2.3.6.2 Acetic acid

In order to reduce the energy requirements, the use of acetic acid for the dissolution of calcium from a calcium-rich feedstock was investigated by Kakizawa *et al.* (2001). The route consisted of two steps, dissolution and carbonation, as described in Eq.2-8 and 2-9, respectively:

$$CaSiO_3(s) + 2CH_3COOH(l) \rightarrow Ca^{2+}(aq) + 2CH_3COO^-(aq) + H_2O(l) + SiO_2(s)$$

Equation 2-8

$$Ca^{2+}(aq) + 2CH_3COO^-(aq) + CO2(g) + H_2O(l) \rightarrow$$
$$CaCO_3(s) + 2CH_3COOH(l)$$

Equation 2-9

The acetic acid used in the dissolution step was recovered in the following carbonation step. A schematic diagram of the process is given in Fig. 2-18.

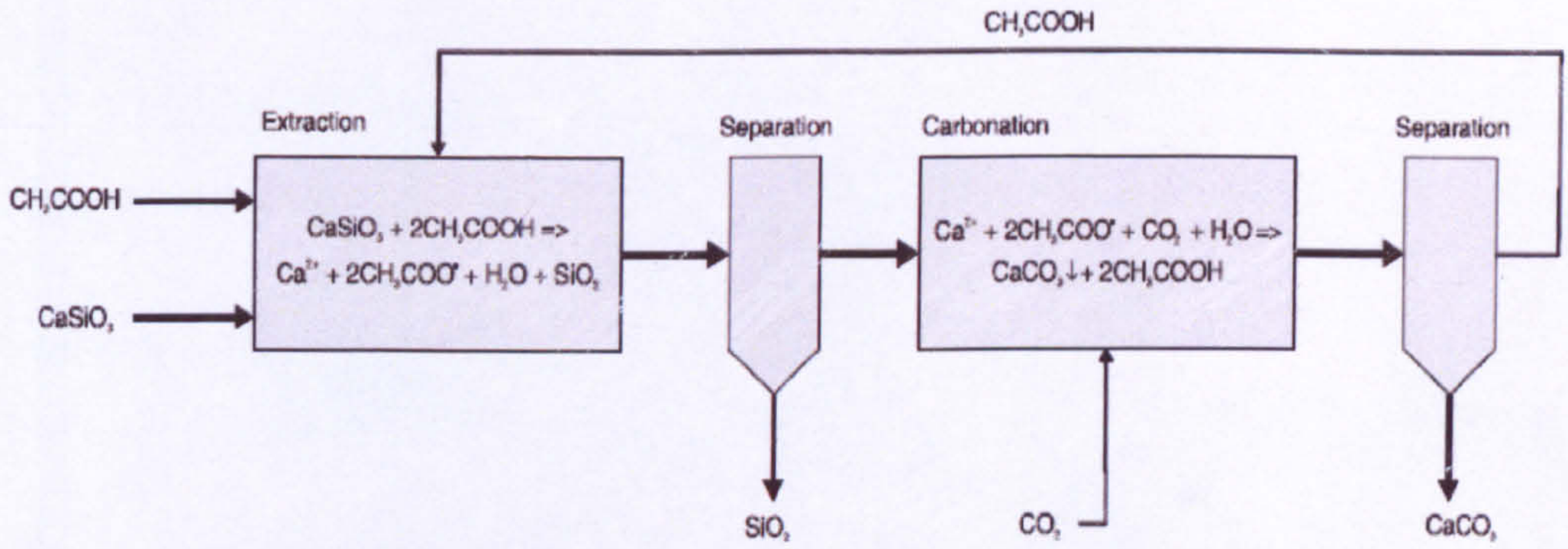

Figure 2-18: Process scheme of acetic acid route (Teir *et al.*, 2005).

According to Kakizawa's (2001) experimental results, 48 % Ca dissolution was achieved at 60°C and atmospheric pressure after 250 mins when using 20 μm wollatonite particles. 20 % $CaCO_3$ conversion was obtained at 30 °C and 30 bar CO_2 after 60 mins. However, there is no study on the recovery of acetic acid.

Teir *et al.* (2005 and 2007a) studied the process proposed by Kakizawa (2001) to produce precipitated calcium carbonate (PCC) from both wollastonite and steel slags. According to Teir's energy penalty evaluation results (ASPEN PLUS), PCC production via the conventional route (calcination process) emitted 0.21 kg CO_2 /kg

PCC, whereas PCC production via the acetic acid process route using wollastonite gave a net fixation of 0.34 kg CO_2/kg PCC (Teir *et al.*, 2005). Teir also found that the principal problem of unsuccessful recycling of acetic acid. The complete recycling of the acid is necessary for this process to become feasible in large scale and that has not yet been demonstrated.

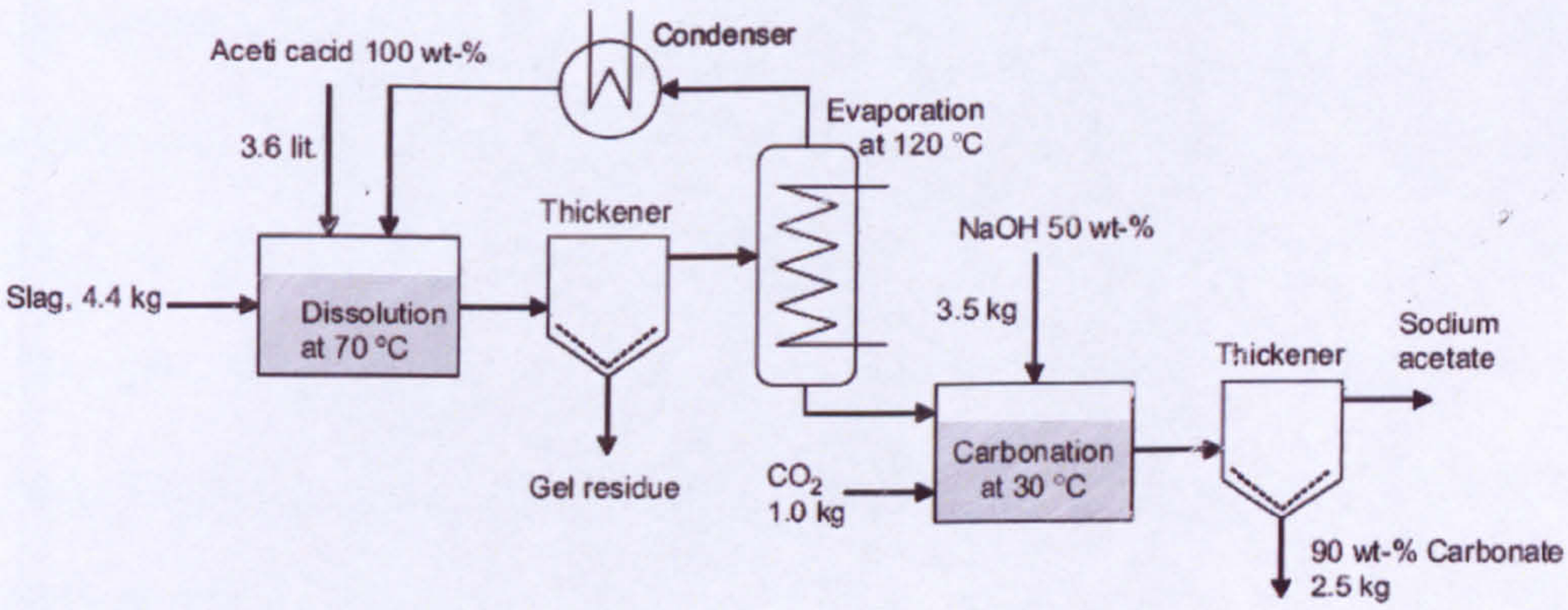

Figure 2-19: A process scheme for binding 1 kg of carbon dioxide by carbonating acetate produced from blast furnace slag (Eloneva *et al.*, 2008).

Inspired by the concept of CO_2 fixation of wollastonite using acetic acid, Teir *et al.* (2007a) and Eloneva *et al.* (2008) investigated a similar process using steelmaking slags, which contain significant amounts of CaO. Teir *et al.* (2007a) reported that over 84 % Ca can be dissolved from blast furnace slags, steel converter slag, electric arc furnace slag and argon oxygen decarburization (AOD) process slag at 50 °C using 33.3 wt% acetic acid after 20 mins, compared to 41 % from wollastonite under the same conditions. Subsequently,

Eloneva *et al.* (2008) reported 19 - 74% Ca carbonation efficiency was obtained from blast furnace slag using acetic acid at 1-30 bar CO_2 and 30-70 °C (see Fig. 2-19). However, significant amounts of sodium hydroxide (28 g/l) were required to promote the carbonation. The mass balance of this process showed that 4.4 kg of blast furnace slag, 26 l (100 wt %) of acetic acid [10], and 3.5 kg of NaOH would be required to bind 1 kg of CO_2, resulting in a maximum of 2.5 kg of 90% pure calcium carbonate. The world steelmaking slag production was estimated to be around 255-345 Mt steel making slags in 2003 (Teir *et al.*, 2007a). Thus, the annual CO_2 storage potential of steelmaking slags is in the order of 70 - 180 Mt CO_2 by using the process investigated by Eloneva (2008). Although the CO_2 sequestration potential for this option compared to the global CO_2 emissions is small, the process could provide a significant alternative solution. Nevertheless, a problem being investigated related to the acetic acid route is the co-leaching of heavy metals, and the demand for NaOH in order to precipitate carbonates. The additional NaOH makes recycling of acetic acid impossible and as a result the chemical costs for this process route are too high.

2.3.6.3 Acid/base pH swing

In order to overcome the different pH requirement for dissolution and carbonation, Park *et al.* (2004) studied an indirect aqueous

[10] 22.5 l acetic acid could be recycled after evaporation.

mineral carbonation process called pH swing process. The pH swing process consisted of a first step at low pH to dissolve the Mg from the serpentine by using a combination of organic acids and ammonium bisulphate, and a second step at higher pH by adding ammonia water to form carbonates. Internal grinding in combination with organic acids proved to be the most effective dissolution. The process conditions required to obtain a significant conversion (70 °C and 1 bar) were milder than those for direct aqueous carbonation (185 °C and 150 bar). However, a detailed study of costs and environmental impact was not provided.

Maroto-Valer *et al.* (2005) proposed another process with serpentine based on acid/base pH swing. However, the chemicals used in this process could not be regenerated. In a follow-up study by Alexander *et al.* (2007), the effects of reaction time, particle size, temperature and solvent concentration on serpentine dissolution efficiencies were reported under the conditions of atmospheric pressure and low temperatures (25 - 50 °C). The results of Alexander's study were in agreement with previous findings (Park and Fan, 2004). Magnesium dissolution improved with increasing acid concentration (1.5-5 M) and decreasing particle size (163, 125 and 63 μm).

Teir *et al.* (2007a, c and 2009) studied the possibility of CO_2 mineral sequestration using serpentinite in Finland, where there is no

suitable geological formation, but there are abundant magnesium silicates. In their serpentine dissolution studies (Teir *et al.*, 2007c), various acids and bases were tested (HCl, H_2SO_4, HNO_3, HCOOH, CH_3COOH, NaOH, KOH, NH_3, NH_4Cl, $(NH_4)_2SO_4$, and NH_4NO_3). Sulfuric acid was found to be the best dissolution agent of all the chemicals tested, however ammonium salts were able to extract Mg selectively but with low dissolution efficiency. The effect of the particle size in the range of 125 - 500 μm did not influence the Mg dissolution rate significantly in 2 h and at 70 °C. All mineral acids (2 M HCl, H_2SO_4, HNO_3) extracted 100% Mg from the serpentinite sample after 3 h. Product layer diffusion was found to be the rate limiting step for Mg dissolution. In their subsequent work, the process was fully developed and described in Fig. 2-20 (Teir *et al.*, 2007b).

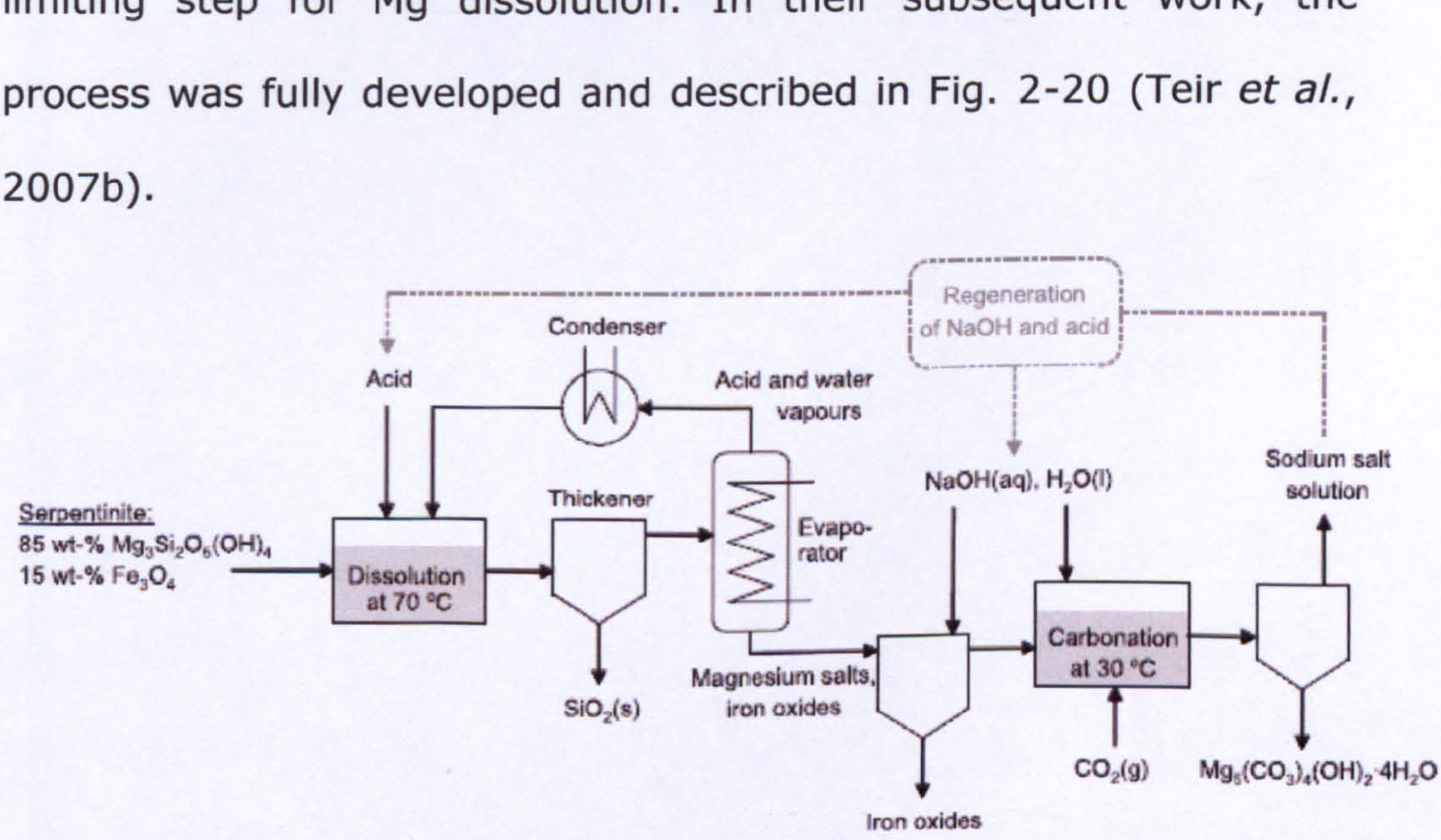

Figure 2-20: Process scheme for production of hydromagnesite from serpentinite using HCl or HNO_3 (Teir *et al.*, 2009)

Firstly, HCl and HNO_3 solution were selected as the dissolution solvents due to their low boiling point (the boiling point for nitric acid is 83 °C, hydrochloric acid is 48 - 110 °C (38 - 20 wt. % and sulfuric acid is 338 °C). 88 % and 93 % of Mg, 37 % and 87 % of Fe were dissolved from serpentine (100 g/l) at 70 °C after 2 h by HNO_3 and HCl, respectively. The residue after dissolution, a high silica by-product, was separated by filtering. The solution was then evaporated to get solid magnesium salts and recover the acids. After dissolving magnesium salts into water, NaOH was added into the solution to raise the pH of solution from dissolution. Magnetite (Fe_3O_4) and goethite ($Fe_2O_3 \bullet H_2O$) precipitated when the pH was controlled to 4-6. After separating the precipitates, CO_2 was bubbled through the solution with pH regulation by adding NaOH, and hydromageniste ($Mg_5(CO_3)_4(OH)_2 \bullet 4H_2O$) was precipitated at pH 8-11 at 30 °C. A solution pH of 9 was found to be the optimum value for precipitation. At this pH, the highest purity of hydromagnesite (99 wt.%) and lowest net requirements of NaOH (0.9-1.2 g NaOH / g hydromagnesite) were achieved, as well as the highest conversion (94 %) of magnesium ions to carbonate were obtained. Besides, relatively pure iron oxide (88 wt.%) and amorphous silica (82 wt.%) were obtained in this process. So far, this indirect aqueous process is the only one with detailed studies of mass balance, energy and cost evaluation (Teir *et al.*, 2009). The mass balance is presented in Fig. 2-21.

	Amounts when using HNO_3 (t)	Amounts when using HCl (t)
Input		
CO_2	1.0	1.0
Serpentinite	3.1	3.1
HNO_3	3.6[a]	–
HCl	–	2.1[a]
NaOH	2.3[a]	2.3[a]
Total	10.0	8.5
Output		
SiO_2	1.1	1.1
Fe_2O_3	0.5	–
Fe_3O_4	–	0.5
$Mg_5(CO_3)_4(OH)_2 \cdot 4H_2O$	2.7	2.7
NaCl	–	3.3[b]
$NaNO_3$	4.8[b]	–
H_2O	0.9	0.9
	10.0	8.5

[a] Unless regenerated from the spent sodium salt solution, these are the amounts of make-up chemicals required for each ton of CO_2 fixed as hydromagnesite.

[b] Unless used for regeneration of NaOH and acids, these are additional by-products from the process.

Figure 2-21: Mass balance of Teir's process (Teir *et al.*, 2009).

Teir *et al.* (2009) reported that the energy required for grinding the serpentinite to below 74 μm is about 160-190 MJ/t (44-53 kWh/t) CO_2 sequestered. The evaporation of the water released would require at least 1908 MJ/t (530 kWh/t) CO_2 sequestered. Based on the mass balance, the chemical make-up used in this process would cost 1300 US$/t CO_2 sequestered for a process based on HCl and 1600 US$/t CO_2 sequestered for a process based on HNO_3. Teir *et al.* (2009) proposed that electrolysis could be one option for recycling the resulting aqueous NaCl or $NaNO_3$ solution. In the chlor-alkali industry, NaCl is electrolysed producing chlorine gas, sodium hydroxide and hydrogen gas (see Eq. 2-10 and 2-11):

$$2NaCl(aq) + 2H_2O(l) \rightarrow Cl_2(g) + H_2(g) + 2NaOH(aq)$$

ΔG=208 kJ/mol NaCl

Equation 2-10

$$H_2(g)+Cl_2(g)\rightarrow 2HCl(g)$$

ΔH=-352 kJ/mol

Equation 2-11

However, this regeneration process suffered from a high energy penalty, where the energy consumption for electrolysis of the NaCl is 3277 kWh/t CO_2 sequestered when using HCl and 4361 kWh/t CO_2 sequestered when using HNO_3, respectively. Teir *et al.* (2009) concluded that the process studied might be suitable for producing valuable mineral and metal products from serpentinite, but probably not for CO_2 sequestration. However, the thermal stability study of the hydromagnesite produced shows that it should be a stable storage medium for CO_2 up to 300 °C.

2.3.6.4 Ammonium salts

It is imperative to recycle the additives in carbonation processes due to the large scale of any industrial application. Recently, ammonium salts have received growing attention due to their weak base and strong acid properties and the feasibility of recovery with low energy requirements.

Kodama *et al.* (2008) developed a pH swing CO_2 mineral carbonation process using recyclable ammonium salts. The schematic picture of this process is presented in Fig. 2-22.

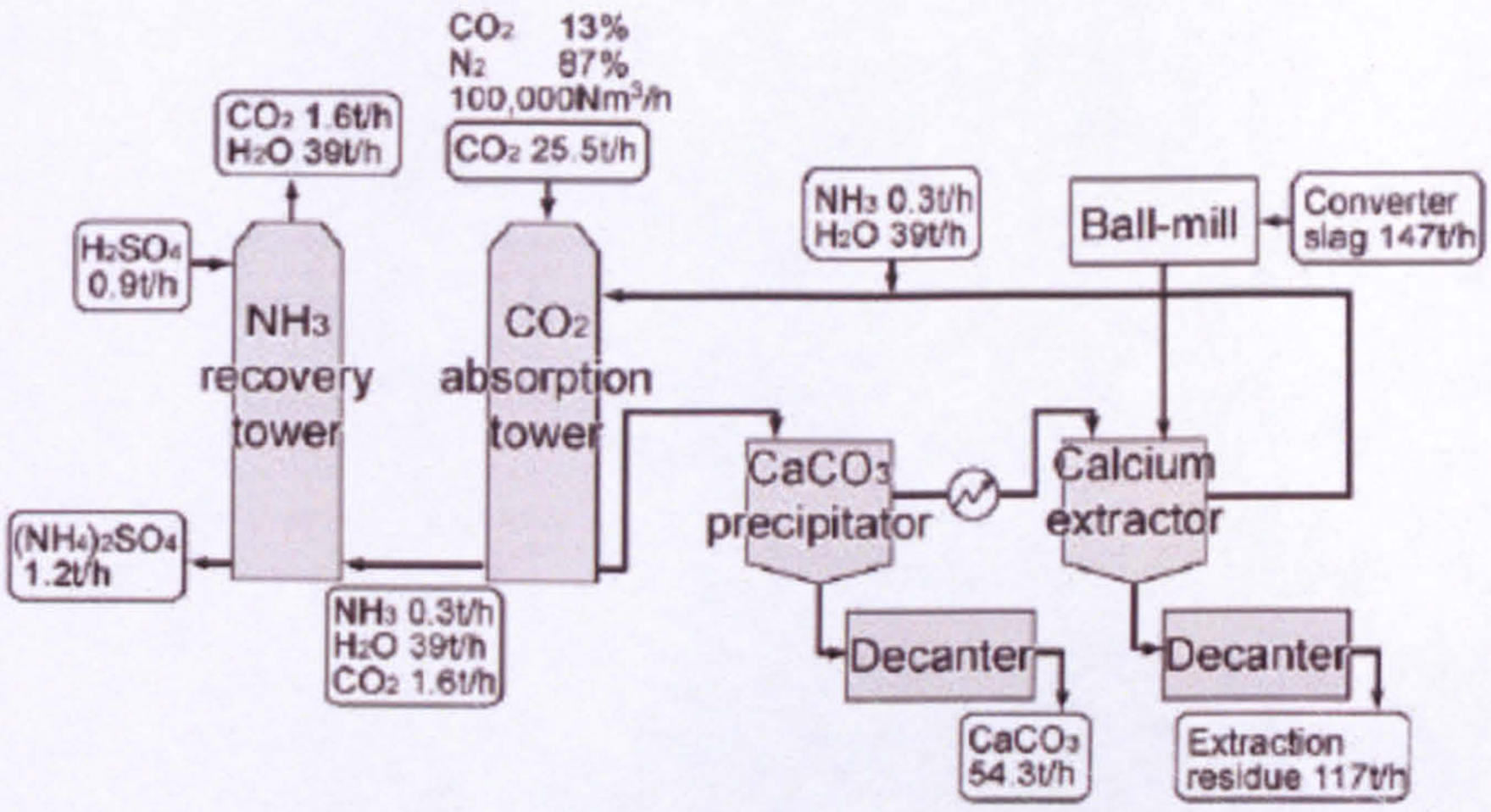

Figure 2-22: schematic picture of a pH swing CO_2 mineral carbonation process using recyclable ammonium salts (Kodama *et al.*, 2008)

Steel slags were firstly dissolved by NH_4Cl to leach Ca and produce ammonia gas (Eq. 2-12). The Ca-rich slurry with ammonia was injected into the absorption tower to absorb CO_2 and produce ammonium carbonate (Eq. 2-13). This is followed by the precipitation of calcium carbonate in another reactor and the recovery of ammonium chloride (Eq. 2-14). In their experimental work, 72 % dissolution efficiency was achieved at 80 °C for 60 mins, and the precipitation was theoretically calculated to be 70 % at 80 °C. The energy input requirement for this process was estimated at around 300 kWh/t CO_2 [11], but the loss of NH_3 presented a problem. More experimental work is need on precipitation and to prove the recovery of ammonium salts.

[11] Include CO_2 absorption

$$4NH_4Cl(aq)+2CaO\bullet SiO_2(s)\rightarrow$$
$$2CaCl_2(aq)+4NH_3(g)+2H_2O(l)$$

Equation 2-12

$$2NH_3(g)+CO_2(g)+H_2O(l)\rightarrow(NH_4)_2CO_3$$

Equation 2-13

$$CaCl_2(aq)+(NH_4)_2CO_3(aq)\rightarrow$$
$$CaCO_3\downarrow+2NH_4Cl(aq)$$

Equation 2-14

Eloneva *et al.* (2010) studied the CO_2 emissions reduction by mineral carbonation of steel making slags using ammonium salts. In their study, ammonium chloride, ammonium nitrate and ammonium acetic were firstly selected as the most promising solvents. These ammonium salts effectively dissolved 50-80 % Ca at 30 °C and atmospheric pressure. Close to 100 wt% pure calcium carbonate was precipitated from the Ca-NH_4 salt solution by bubbling through CO_2 at 30 °C with conversion efficiencies of 50-70 % after separation of the slag residue. Then, the effects of particle size, solid to liquid ratio and solvent concentration on dissolution efficiencies were experimentally studied. The results indicated that the grain size of the steel converter slag should not be increased to above 500 μm and solid to liquid ratio over 100 g/l (in 2 M solution)

should be avoided. Based on the experimental results, the mass balance of the process was estimated and presented in Fig. 2-23.

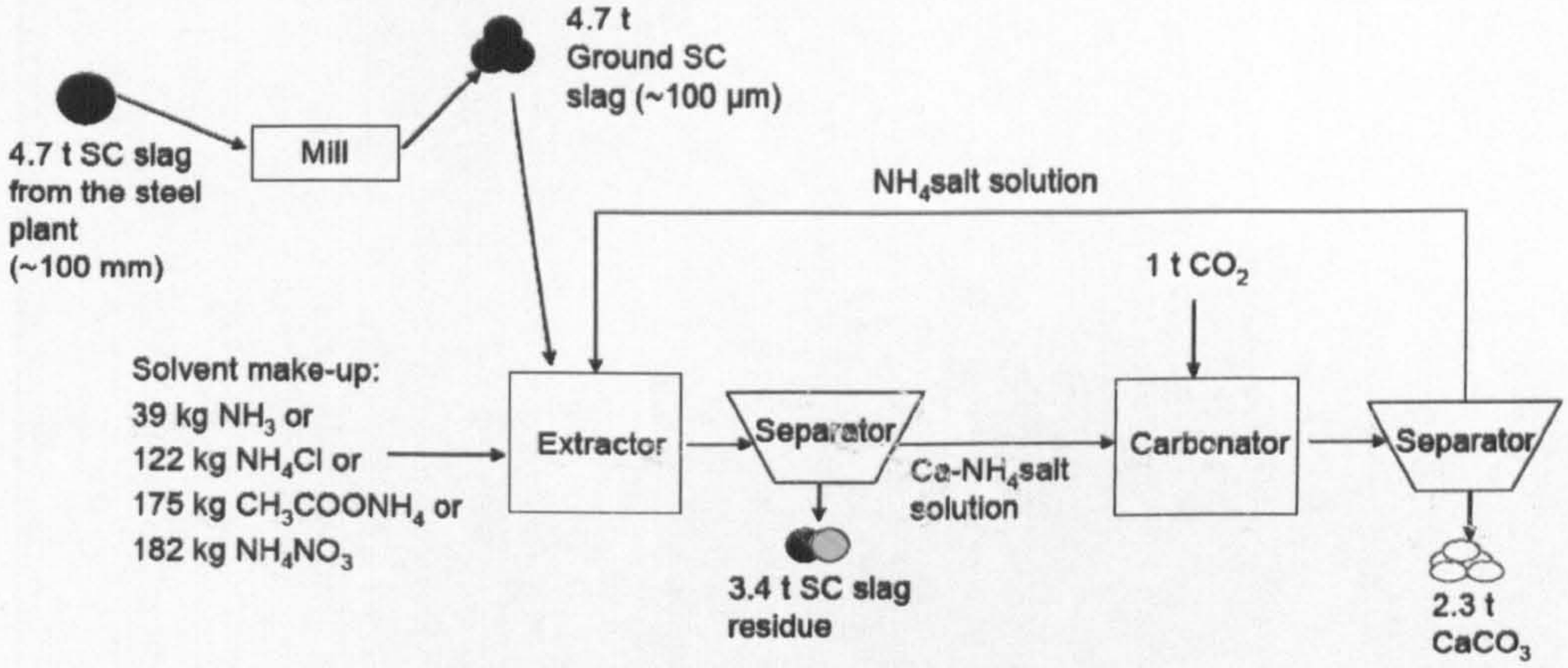

Figure 2-23: A simplified process scheme for sequestering 1 t of CO_2 by producing pure calcium carbonate from steel converter (SC) slag using aqueous solution of ammonium salt as a solvent (Eloneva *et al.*, 2010).

1 t of sequestered CO_2 requires 4.7 t of steel converter slag (33 wt % Ca) and produces 2.3 t of $CaCO_3$, as well as 3.4 t of residue slag. Assuming that 5 wt % of ammonium would be lost, 39 kg of NH_3, 122 kg of NH_4Cl, 182 kg of NH_4NO_3, or 175 kg of CH_3COONH_4 are consumed per tonnes of CO_2 sequestered. The cost for chemical make-up would be 38 US$/t CO_2 sequestered (26 €/t CO_2 sequestered) for NH_4Cl and 58 US$/t CO_2 sequestered (40 €/t CO_2 sequestered) for both NH_4NO_3 and CH_3COONH_4. The energy penalty in grinding, extraction and carbonation was estimated to be 140 kWh/t CO_2 sequestered (<100 µm), 5-200 kWh/t CO_2 sequestered depending on the particle size and 5 kWh/t CO_2 sequestered, respectively. On the other hand, the sale of produced calcium

carbonates as PCC can generate a profit of 329 US$/t CO_2 sequestered (227 €/t CO_2 sequestered) (Nordkaly, 2004) and the selling of CO_2 emission allowance can earn 19 US$/t CO_2 sequestered (13 €/t CO_2 sequestered). Accordingly, this process shows promise to be potentially economical feasible. However, the minimization of ammonium losses is extremely important and the suitability of the products for use as commercial products has to be explored further. In addition, the raw materials studied thus far do not have enough CO_2 storage capacity potential for climate change mitigation purposes.

2.4 Products from CCSM and applications

The successful development of applications of products with marketable value from mineralisation processes can help to offset the cost of CO_2 sequestration. The products of CO_2 mineral sequestration can be utilised in many applications such as building materials or high value commercial products. In addition to the final carbonates, several by-products from the indirect aqueous process, where by-products could be separated, can have industrial applications. However, the purity levels of products from the process, diversity of application, the size of market and market value are significant factors to the successful application of products from CCSM. In addition, the products from CCSM may need post-processing to get smaller particle size and higher purity, and the

energy penalty of CCSM plus post-processing may be higher than that for producing these products by conventional process.

The different CCSM process routes illustrated (Section 2.3.3-2.3.6) produce a range of different products, which can be divided into two main groups: low value mixed products (mixtures of carbonates with silica sand, iron oxides and silicate rock residue in the ARC process) and high value pure products (carbonates, silica and iron oxide like in indirect pH-swing process). Taking Teir's pH-swing indirect aqueous process route (Teir *et al.*, 2007b) as an example, 1.1 t/t CO_2 of silica sand with 82-88% purity, 0.5 t/t CO_2 of iron oxides and 2.7 t/ t CO_2 of 99% pure hydromagnesite, with uniformly sized and spherical crystals with a lamellar structure are produced. Due to the limitations on applications and market value of low value mixed products, only high value pure products are investigated in this study.

The main products of CO_2 mineralisation are Ca or Mg carbonates, while the by-products include silicon, iron precipitates and other heavy metals. These products could be further post-processed to achieve high purity and increase their commercial value. Table 2-8 presents the main products from CO_2 mineralisation and their purity as reported from the literature, as well as the applications, size of current market and commercial values.

Table 2-8: Products from CO_2 mineralisation, and their purity, market size and value of potential applications.

Products	Purity	Market size	Applications	Value
PCC	>97% ($CaCO_3$ %)	13 Mt[12]	Filler and coating pigment in plastics, rubbers , paints and papers	145-402 US$/t [13] (fine grade)
Magnesite or hydromagnesite	>90% ($MgCO_3$ %)	18.3 Mt	paper industry, cement industry, civil engineering and production of fire retardant, a reinforcing agent in rubber, a drying agent, a laxative, supplement in food	200-1200 US$/t (technical grade-pharma grade)
Silica	82-88% (SiO_2)	112 Mt	electronic, automotive, chemical, and ceramic industries	10-134 £/t (grain-fine ground grade)
Iron oxide	24-36% (FeO)	1.4 Mt (pigment) 1414 Mt (crude steel production)	iron industry and the manufacture of pigments	219-235 US$/t (pigment) 2.12 US$/t (iron ore)

In considering the large amount of CO_2 emissions (around 33 Gt in 2010), the amount of products from CO_2 mineralisation is significantly large, in the order of thousands of Million t per year. The current market is not large enough to take up these quantities,

[12] 13 Mt in 2007, 16 Mt prospected in 2012. ROSKILL INFORMATION SERVICES, L. 2008. The Economics of Precipitated Calcium Carbonate, 7th Edition, 2008.
[13] Price increase 30 % in 2008, NORDKALY, O. 2004. Price data. Supplied by Nordkalk Oy, June 2004.

and new applications must be found. Recently, Calera Corporation proposed to use the end product of their CO_2 mineralisation process as supplementary cementitious material (SCM). The cement industry produces 5 % of the total global CO_2 emissions (Gunning *et al.*, 2010), and if the product from mineralisation could be used as a substitute for cement. The cement industry would be replaced then by the mineralisation industry, which has negative CO_2 emissions and helps to store CO_2 from other sources such as power plants. In addition, the Fe-rich precipitate (iron oxide) from indirect aqueous processes could be used as feedstock for a steel-making plant. If the mineralisation process is scaled up to millions of tonnes per year, the trace elements should be paid more attention. For example, Ni and Mn are valuable metals and are widely used in high efficiency batteries.

2.5 Summary.

There has been an increasing interest in mineral carbonation. Obviously, one of the main advantages of this process is the permanent safe storage of CO_2 due to the thermodynamically stable nature of the solid carbonates formed (Goff, 1998). Moreover, carbonation is an exothermic process, which may reduce the overall energy penalty and costs (Lackner, 2000). However, mineral sequestration also faces some barriers such as low efficiency of mineral dissolution, slow kinetics, and energy intensive pre-treatment processes (Lackner *et al.*, 1995). Although, low efficiency

and slow kinetics have been solved by swinging the pH (Teir *et al.*, 2007c; Park and Fan, 2004), the addition of large amounts of acid and base required for the dissolution and subsequent carbonation limit the development of mineral sequestration. Therefore, there is a need to find low cost recyclable solvents that can provide high efficiency of mineral dissolution and carbonation.

Chapter 3. Carbon dioxide capture and storage by mineralisation using recyclable ammonium salts

Ammonium salts have received increasing attention in CCSM due to their properties to form efficient acid and base in dissolution and carbonation reactions and ability of being recycled. Kodama *et al.* (2008) reported a pH-swing CO_2 mineralisation process with steel slags using recyclable ammonium salts. Pundsack *et al.* (1967) also reported using a recyclable ammonium salts for serpentine dissolution. In this study, the author developed a new pH-swing mineral carbonation process by using recyclable ammonium salts. The process developed here overcomes the two barriers of low efficiency of mineral dissolution and unrecyclable use of additives.

Moreover, mineral sequestration has been considered as a separate process from capture. In the capture process, the CO_2 is first absorbed by chemicals, such as monoethanolamine or NH_3 (Yang *et al.*, 2008). The CO_2 is then thermally desorbed to recover the sorbents and release concentrated CO_2. The CO_2 is then compressed for transportation; however, compression consumes a lot of energy, which nearly accounts for 25% of the total energy penalty of the whole CCS process (IPCC, 2005). The process developed here combines capture and mineralisation by employing ammonium salts. In this Chapter, two process routes of CCSM process with recyclable

ammonium salts are described in Section 3.1, the characterization of raw materials used in this study is reported in Section 3.2 and the solvent selection studies is presented in Section 3.3.

3.1 Description of process

In this work, two process routes were developed using different solid to liquid ratio. The first process route is at low solid/liquid ratio (<100 g/l) and three products are obtained (Si rich product with residual serpentine, Fe-rich products and hydromagnesite). The second process applies high solid/liquid ratio (>200 g/l) in order to reduce the water usage and energy requirement in evaporation, and only one product (mixture of residual serpentine and carbonates) is obtained. It is not possible to separate products in the high solid to liquid ratio experiments since $MgSO_4$ exceeds the solubility limit and precipitates during mineral dissolution. These two process routes are described in the following sections.

3.1.1 CCSM process route at low solid to liquid ratio

The multistep process route with pure products for carbon dioxide capture storage and mineralisation consists of five main steps, and the main reactions are presented in Figure 3-1 and Table 3-1.

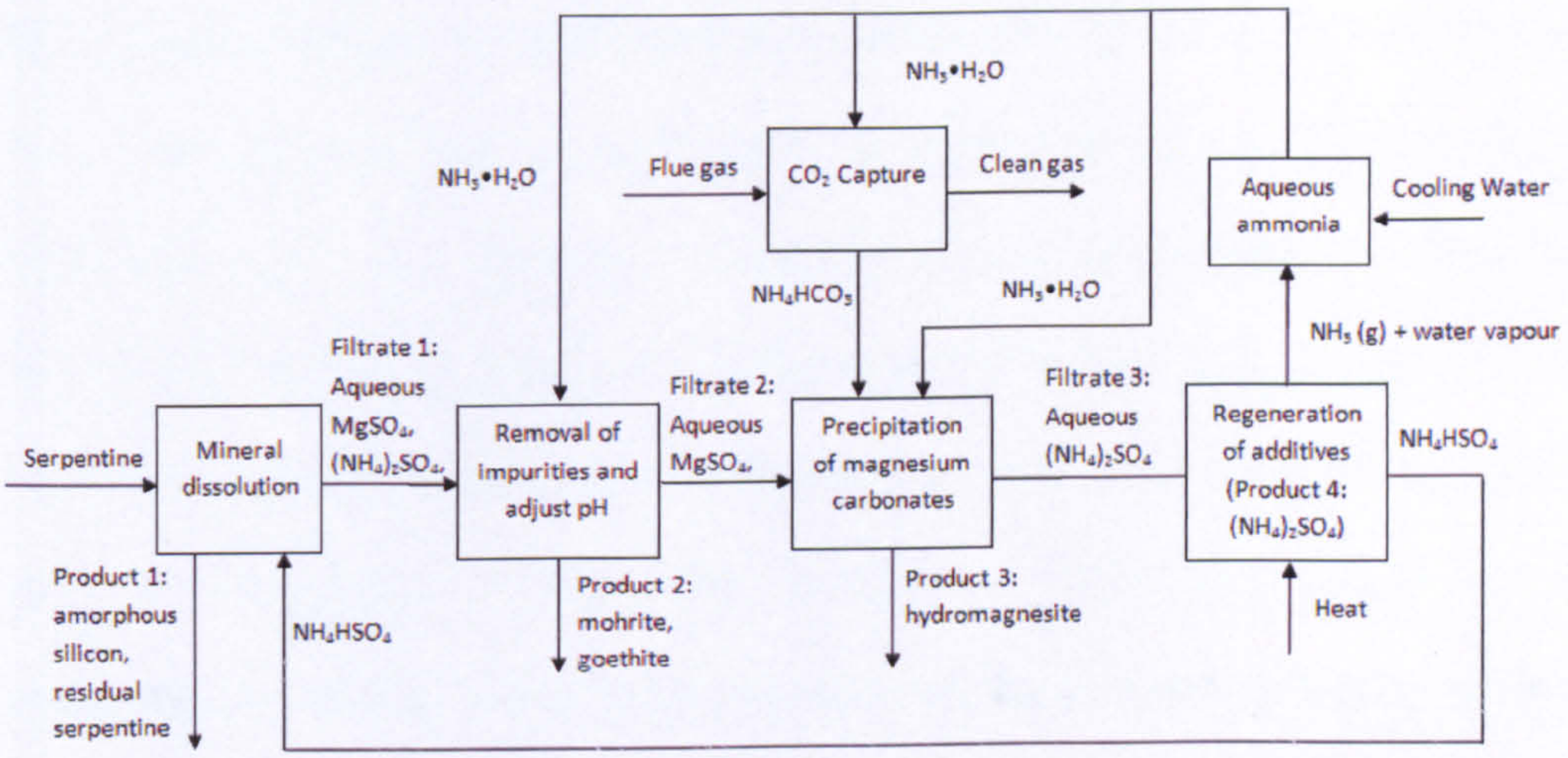

Figure 3-1: Schematic of CCSM process route at low solid to liquid ratio.

Table 3-1: Chemical reactions and thermodynamic data of the different steps of the process.

	Reaction equations	T(°C)	ΔH (kJ)
CO_2 capture	$NH_3 + CO_2 + H_2O \rightarrow NH_4HCO_3$	10	-127.0
Mineral dissolution	$Mg_3Si_2O_5 \bullet (OH)_4 + 6NH_4HSO_4 \rightarrow 3MgSO_4 + 2SiO_2 + 5H_2O + 3(NH_4)_2SO_4$	90	-141.1
pH adjustment	$NH_4HSO_4 + NH_4OH \rightarrow (NH_4)_2SO_4 + H_2O$	25	-116.0
Removal of impurities	$(Fe,Al,Cr)_2(SO_4)_3 + 6NH_4OH \rightarrow 2(Fe,Al,Cr)(OH)_3 \downarrow + 3(NH_4)_2SO_4$	25	-673.0
	$(Zn,Cu,Mn)SO_4 + 2NH_4OH \rightarrow (Zn,Cu,Mn)(OH)_2 \downarrow + (NH_4)_2SO_4$	25	-191.4
Carbonation	$MgSO_4 + NH_4HCO_3 + NH_3 + 3H_2O \rightarrow MgCO_3 \bullet 3H_2O \downarrow + (NH_4)_2SO_4$ $5MgCO_3 \bullet 3H_2O + 2H_2O \rightarrow 4MgCO_3 \bullet Mg(OH)_2 \bullet 3H_2O + CO_2 \uparrow$	80	-6.6
Regeneration of additives	$(NH_4)_2SO_4 \rightarrow NH_4HSO_4 + NH_3 \uparrow$	300	111.6

Firstly, NH_3 is used to capture CO_2 from power plant's flue gas and produces NH_4HCO_3. Secondly, the NH_4HSO_4 is used to extract Mg from serpentine at mild heating conditions in the mineral dissolution step. Thirdly, the Mg-rich solution produced from mineral dissolution is regulated to neutral pH by adding NH_4OH; then, the impurities in the leaching solution are removed by adding NH_4OH. After that, the solution reacts with the intermediate product (NH_4HCO_3) from the

CO_2 capture step to precipitate carbonates at mild temperature. Since the formation of carbonate is determined by temperature (Hänchen *et al.*, 2008), nesquehonite ($MgCO_3 \bullet 3H_2O$) can be converted to hydromagnesite ($4MgCO_3 \bullet Mg(OH)_2 \bullet 4H_2O$) above 70°C. With the precipitation of hydromagnesite, the final solution contains mainly $(NH_4)_2SO_4$. Finally, the $(NH_4)_2SO_4$ could be recovered by evaporation and subsequently heated up to regenerate NH_3 which returns to the capture step and NH_4HSO_4 which is then reused for the mineral dissolution step.

The thermodynamic data for this process was calculated by using HSC 5.0 thermal calculation software and the enthalpy and Gibbs free energy values for the different steps are presented in Table 3-1. It can be seen that all reactions in this process are spontaneous, with the exception of the regeneration reaction. The dissolution and carbonation reactions are exothermic, while the reaction of carbonate formation is endothermic.

This process is unique in using NH_4HCO_3 instead of direct CO_2 gas for indirect aqueous mineral carbonation. The advantages of using NH_4HCO_3 include avoiding CO_2 desorption in the capture step and subsequent CO_2 compression for transportation that are energy intensive steps of the conventional CCS process (70 % of the total energy penalty in whole CCS process; IPCC, 2005).

3.1.2 CCSM process route at high solid to liquid ratio

The CCSM process route at high solid to liquid ratio also consists of five main steps (see Fig. 3-2), and the main reactions are the same as those presented in Table 3-1.

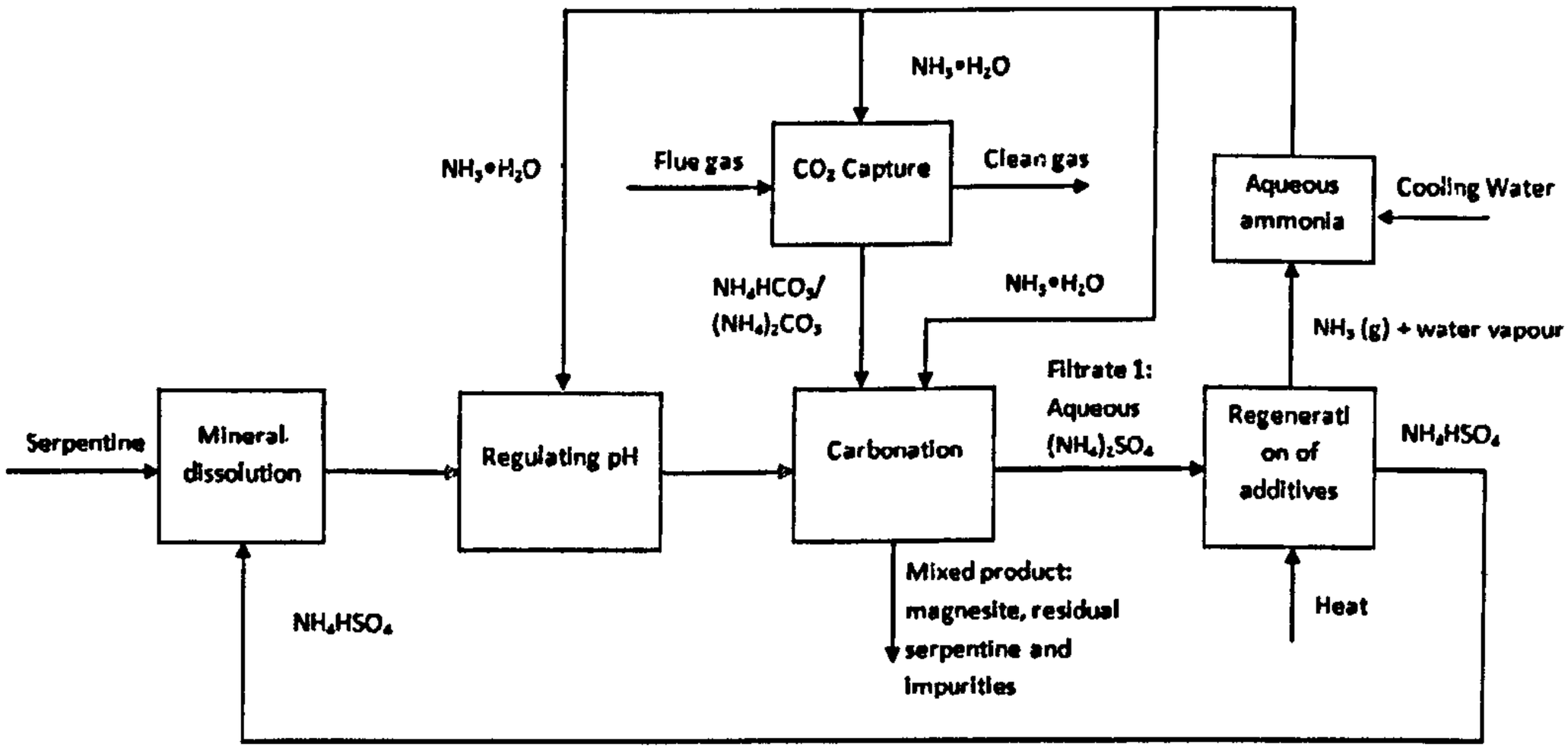

Figure 3-2: Schematic of CCSM process route at high solid to liquid ratio.

Firstly, NH_3 is used to capture CO_2 from power plant's flue gas and produces NH_4HCO_3. Secondly, the NH_4HSO_4 is used to extract Mg from serpentine at mild temperature (100 °C) in the mineral dissolution step, where the dissolved Mg ions exist in both the liquid phase and also as precipitated $MgSO_4$. Thirdly, the mixed slurry produced from mineral dissolution is regulated to neutral pH by adding NH_4OH. After that, the solution reacts in a closed autoclave with the intermediate product (NH_4HCO_3 or $(NH_4)_2CO_3$) from the CO_2 capture step to precipitate carbonates at mild temperature (80 °C). The pressure evolved from the decomposition of NH_4HCO_3 or $(NH_4)_2CO_3$ helps the carbonation reaction and transforms

hydromagnesite into magnesite (Hänchen *et al.*, 2008). After filtering the slurry, the final solution contains mainly $(NH_4)_2SO_4$ and a mixed product solid consisting of magnesite, residual serpentine and high Fe content impurities. Finally, the $(NH_4)_2SO_4$ can be recovered by evaporation and subsequently heated up to regenerate NH_3 which goes back to the capture step, while the regenerated NH_4HSO_4 is then reused for the mineral dissolution step.

3.2 Characterization of raw materials

A serpentinite sample from Cedar Hills quarry in southeast Pennsylvania, USA and supplied by Albany Research Center (U.S.), was selected for this study. A batch of 10 kg serpentinite was ground and sieved. A coarse portion of the sample was ground initially in a jaw crusher in order to get small particles. Then, the crushed sample was ground to a smaller particle size using a Tema mill for a short time (30 s). Once the grinding process was completed, the samples were sieved using an automatic shaker to generate sample with particle size fraction of 75-150 μm. Particle size distribution (PSD) tests were performed to measure the particle size. To identify the mineral phases present, 1 gram sample was analyzed using a Philips Analytical 1050 X-Ray Diffraction (XRD) at scan speed 3°2θ/minute from 5° to 65°under 40 kV / 40 mA. To determine the elemental composition of the serpentinite sample, 0.5 gram sample was completely dissolved using HF solution by

microwave digestion. The solutions were diluted 100-fold and acidified by 10% HNO_3, and then analyzed by Inductively Coupled Plasma-Atomic Emission Spectrometry (Perkin-Elmer's Optima 3000 series) using two different wave lengths to give a more exact reference number for the concentrations of Mg, Si, Fe, Ca, Al, Ni, Mn, Cr, Cu, Al, Sr, Na, Ti and Ba. The inherent carbonate content of the sample was determined using a thermal gravimetric analyzer (TGA Q500, TA Instrument). Representative samples (10-20 mg) were heated in a ceramic cup under nitrogen atmosphere at 20°C/min from ambient to 950 °C. The weight loss in the temperature region of 450°C to 650 °C was determined to be carbonates (Huijgen *et al.*, 2006). The loss on ignition (LOI) was determined by drying the sample at 950°C for 1 hour in argon. The elemental composition of the original mineral sample determined by microwave digestion and ICP-AES is presented in Table 3-2.

Table 3-2: Elemental analysis of original mineral serpentine

	Element/Oxide, wt%	Element, wt% (w)
Fe_3O_4	7.4	5.3
Al_2O_3	0.2	0.1
MgO	40.1	24.0
MnO	0.1	0.1
CaO	0.1	0.1
NiO	0.3	0.2
Na_2O	0.1	0.1
SiO_2	38.1	17.8
CO_2	1.1	
Water [1]	0.6	
Water, bonded [2]	11.9	
TOTAL	100.00	
LOI	13.6	

1 Free moisture, measured as the weight loss after 1 hour at 105 °C, in nitrogen.
2 Chemically-bonded water, measured as the difference between the LOI and all other volatiles.

The major elements were Mg (24.0 wt. %), Si (17.8 wt. %) and Fe (5.3 wt. %), and minor elements were Mn, Ca, Al and Ni (concentrations of 0.1–0.3 wt.%). The sample contained trace carbonate (1.1 wt.%). The loss on ignition at 950 °C was 13.6 wt.%, which consists of 0.6 wt.% moisture content (number 1) and 11.9 wt.% chemical-bound water (number 2). This can be confirmed by the TGA analysis (Fig. 3-3).

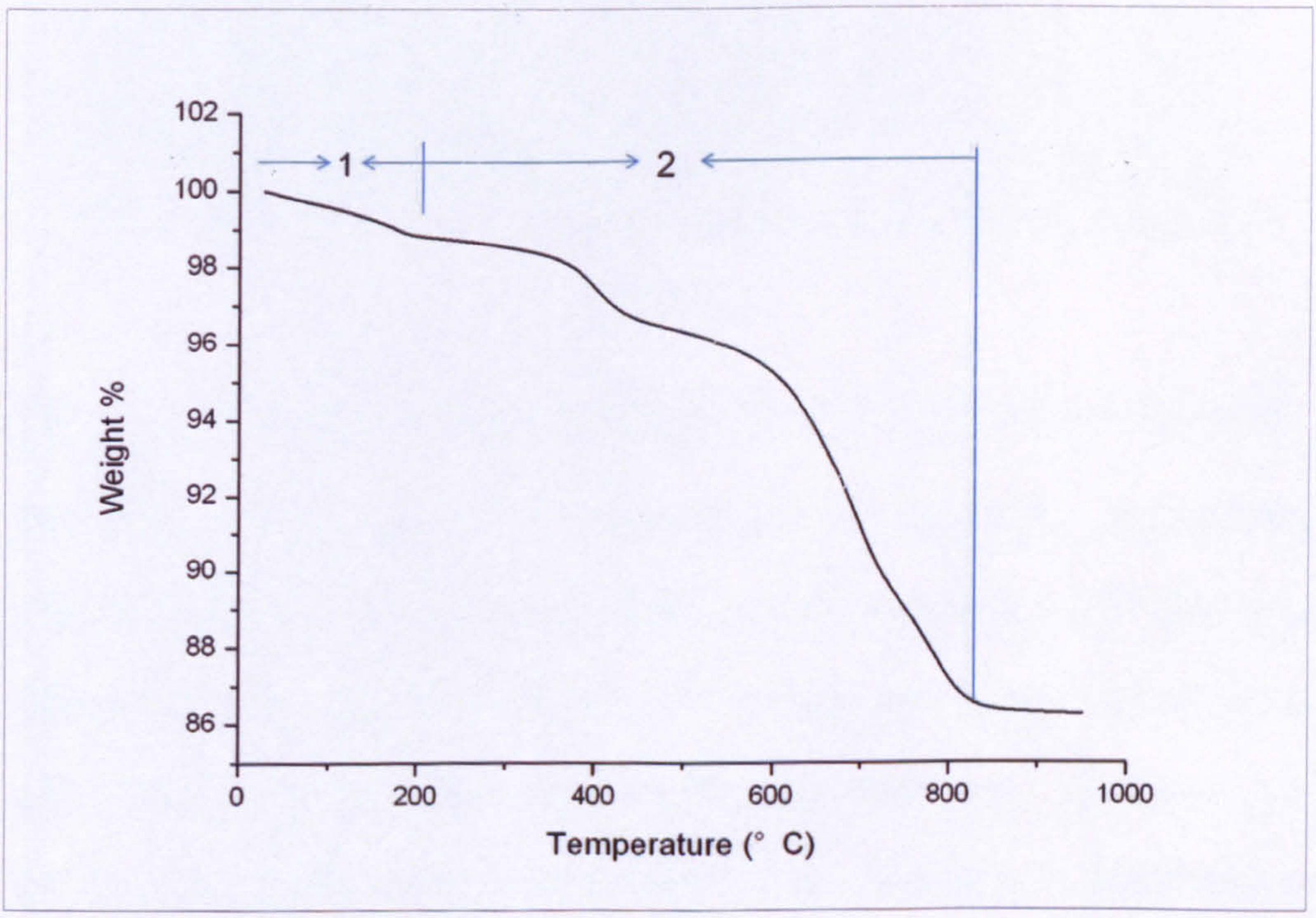

Figure 3-3: TGA graph of the original mineral serpentine sample.

The particle size distribution (PSD) graph of the original mineral serpentine with particle size fraction of 75-150 μm is described in Fig 3-4. The d_{50} is 87 μm and d_{90} is 105.9 μm. In this study, particle size fraction of 75-150 μm is selected as the base line in order to

compare with other researchers' work, where this same particle size fraction was used (Teir *et al.*, 2007c).

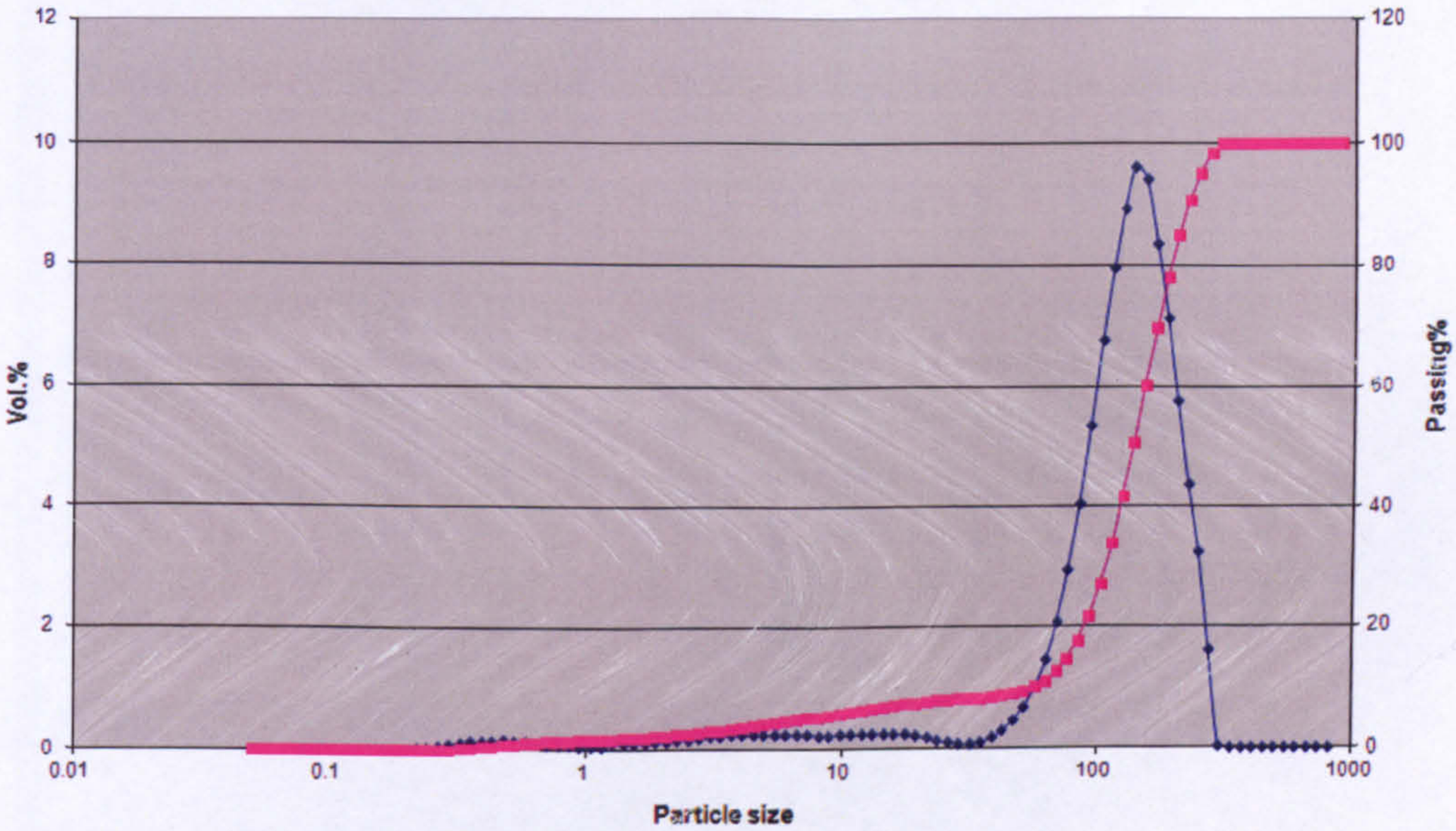

Figure 3-4: PSD graph of original mineral serpentine with particle size fraction of 75-150 µm.

The XRD pattern (Fig. 3-5) reveals that it is mainly serpentine, ($Mg_3Si_2O_5(OH)_4$; antigorite), and small amounts of forsterite (Mg_2SiO_4) and magnetite (Fe_3O_4). It should be noted that different polymorphic forms may have different dissolution behavior, as already discussed by Van Essendelft *et al.* (2009a). A summary of the results from serpentine characterization indicate that this serpentine sample is representative and similar to that used in Teir (2007c) and Alexander *et al.* (2007) studies. The high levels of Mg indicate that this serpentine sample is suitable for CO_2 mineralization.

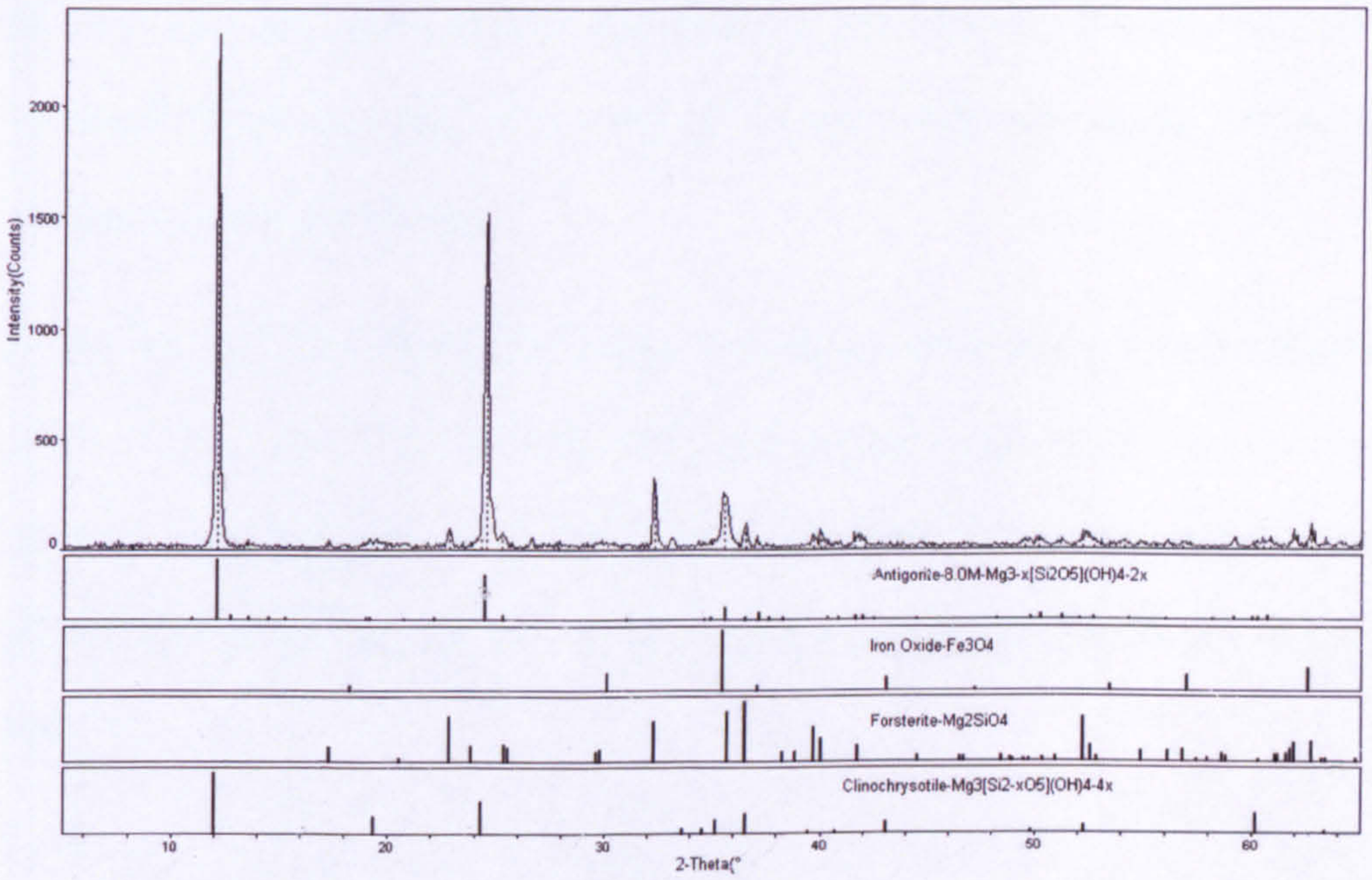

Figure 3-5: XRD pattern of the original mineral serpentine.

3.3 Solvent selection studies

In order to find a suitable ammonium salt for leaching Mg from serpentine, NH_4Cl, $(NH_4)_2SO_4$ and NH_4HSO_4 (which cover a wide range of pKa from -3 to 10) were tested alongside previously used solvents for comparison of dissolution efficiencies. Maroto-Valer *et al.* (2005) have reported dissoltion of serpentine using acids (e.g. HCl, H_2SO_4, HNO_3), where a 2M H_2SO_4 gave the highest dissolution efficiency of Mg, 70 % at 75°C after 6 hours. A batch of 20 g of serpentine (75–150 μm) was dissolved in 400 ml aqueous solutions of 2M concentrations of the respective solvent in a sealed flask. This concentration of solvent was chosen as it represents 100 % excess of the required stoichiometric amount. The solutions were stirred at 800 rpm at a temperature of 70 °C. The solutions were immediately

filtered with 0.7 µm Pall syringe filters after 3 hours dissolution. The concentrations of Mg, Fe, and Si in the filtered solutions were measured using ICP-AES.

Since the original mineral sample contained very low concentrations of Ca (0.09 wt%, Table 3-2), only the concentrations of Mg, Fe and Si are reported for the dissolution studies. The Mg dissolution efficiencies ($Mg_{Dissolution}$ %) using different solvents are shown in Fig. 3-6.

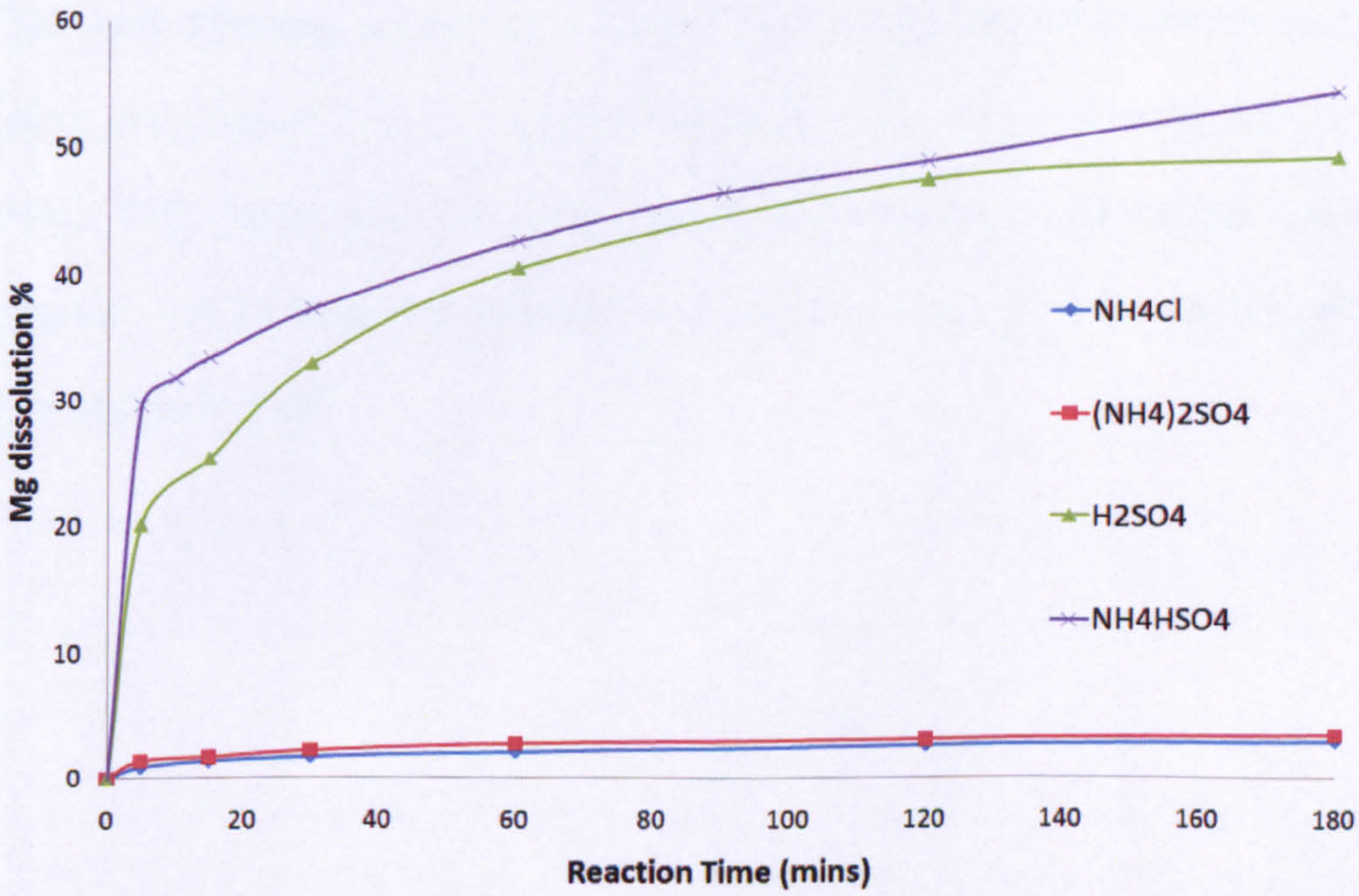

Figure 3-6: Mg dissolution from serpentine using different ammonium salts and H_2SO_4 (2M concentration at 70°C for 3 hours)

After 3 hours NH_4HSO_4 can extract significant amounts of Mg from serpentine (52 %), while NH_4Cl and $(NH_4)_2SO_4$ can only extract smaller amounts (3–5 %). A dissolution experiment using H_2SO_4 was carried out to compare with that using ammonium salts. The

results indicated that NH_4HSO_4 can extract slightly more Mg than H_2SO_4 acid (52 vs. 47 %). Both NH_4HSO_4 and H_2SO_4 perform better than $(NH_4)_2SO_4$ and NH_4Cl. This can be due to the pKa values of NH_4HSO_4 and H_2SO_4 that are both -3.00 and much lower than 9.24 and 8.74 for NH_4Cl and $(NH_4)_2SO_4$, respectively. Moreover, NH_4HSO_4 is preferred over H_2SO_4 because ammonium salts have the potential to be regenerated.

3.4 Summary

The two process routes of CCSM with recyclable ammonium salts were described. The serpentine sample used was characterized by TGA, PSD, XRD and ICP-AES. Solvent selection experiments were carried out to find the suitable ammonium slats and compare with the sulpuric acid.

Chapter 4. CCSM process route at low solid to liquid ratio

4.1 Dissolution of serpentine using recyclable ammonium salts at low solid/liquid ratio

This section presents the dissolution of serpentine using a series of ammonium salts at different temperatures. Therefore, in this work the kinetics of serpentine dissolution were investigated and the rate-limiting step was identified. The understanding of dissolution kinetics can help to improve the dissolution rate. Van Essendelft et al (2009a and 2009b) have found that the dissolution mechanism of serpentine with sulfuric acid changes with particle size as the reaction progresses. Their work suggests that the dissolution rate-limiting step may be a combination of several control factors as the reaction progresses. The author developed a model that considered surface reaction, surface speciation, the electrical double layer, particle size distribution, temperature, concentration and grinding energy input (Van Essendelft *et al.*, 2009b).

4.1.1 Experimental methods

Dissolution experiments were carried out in a 600ml 3 neck glass flask reactor, which was heated by a temperature-controlled silicone

oil bath and equipped with a water-cooled condenser to minimise solution losses due to evaporation (Fig. 4-1). The 400 ml 1.4 M NH_4HSO_4 solution was well mixed by using a magnetic stirrer at 800 rpm. The solution was heated up to the temperature required, and then 20 grams of 75-150 µm fraction of serpentine were added. For the kinetics studies, the t_0 started after adding the solid serpentine sample. After that, 1 ml liquid samples were dissolved with a syringe at given interval times, such as 5 min, 15 min, 30 min, 1 h, 2 h, and 3 h. The samples were immediately filtered using a 0.45 µm syringe filter unit. The Mg, Fe and Si concentrations of the samples were measured using ICP-AES. The dissolution efficiency of a specific element X (Mg, Fe or Si) in solution sample at a given time y (at 5, 15, 30 mins...) was calculated as follows:

$$X_{Dissolution}\% = \frac{C_y \times V}{m_{batch} \times w_x} \times 100\% \quad \text{Equation 4-1}$$

C_y is the concentration of element x in the solution sampled at y time, V is the volume of the solution in the reactor (V is considered constant as only 6ml are dissolved throughout the course of the experiment), m_{batch} is the mass of serpentine sample added. w_x is the initial weight percentage of mass of element x over the total mass of solid present in the original mineral sample. The reproducibility of the results from the experimental work was approximately 1%. The uncertainty stems from errors in three

measured quantities, i.e., the solvent concentrations, the mass of the solid and the analysis error of liquid sample by ICP-AES.

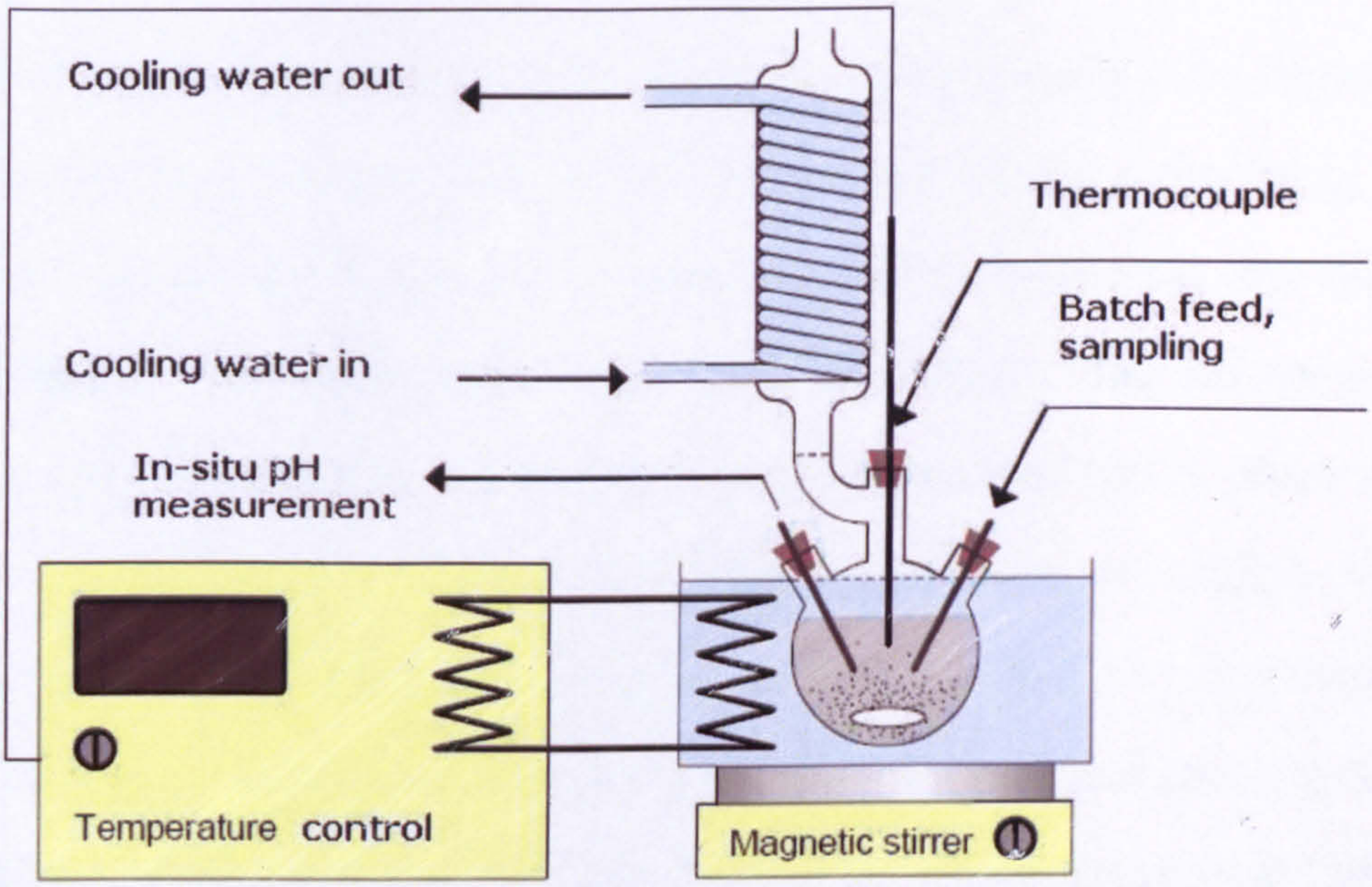

Figure 4-1: Experimental setup for dissolution experiments.

4.1.2 Results and discussion

Based on the dissolution experiments described previously (Section 3.3), NH_4HSO_4 was selected for further studies. The dissolution rate of serpentine with a particle size fraction of 75–150 µm was tested at temperatures of 70, 80, 90, and 100 °C. The concentration used was 1.4 M NH_4HSO_4 following earlier work by Pundsack et al (1967), where this represents 40 % excess of the stoichiometric amount. The effect of temperature upon the dissolution of serpentine is shown in Figures 4-2 to 4-4. As expected, temperature has a significant effect upon the solubility of magnesium (and other

elements as well) from serpentine, and higher temperatures yield higher dissolution efficiencies for each element tested. At 100 °C and 3 hours, NH_4HSO_4 was able to extract 100 % of Mg and 98 % of the Fe, but only 17.6 % of Si (Figure 4-2). The Mg:Si ratio remains greater than the stoichiometric 3:2 by more than a factor of 5, as the mineral leaching is an incongruent process, which has also been confirmed by previous work (Bearat *et al.*, 2006). This incongruent leaching is probably due to the secondary precipitation of dissolved silicon back to the surface of particles (Bearat *et al.*, 2006). The formation of a silica-rich passive layer can inhibit the continuous leaching of magnesium and iron from the inside of particles and this probably explains why the dissolution rate slows down over time. The formation of a silica passive layer has been previously reported on direct mineral carbonation, where dissolution and carbonation are studied concurrently (Bearat *et al.*, 2006). They observed that the presence of this passive layer inhibited the dissolution reaction.

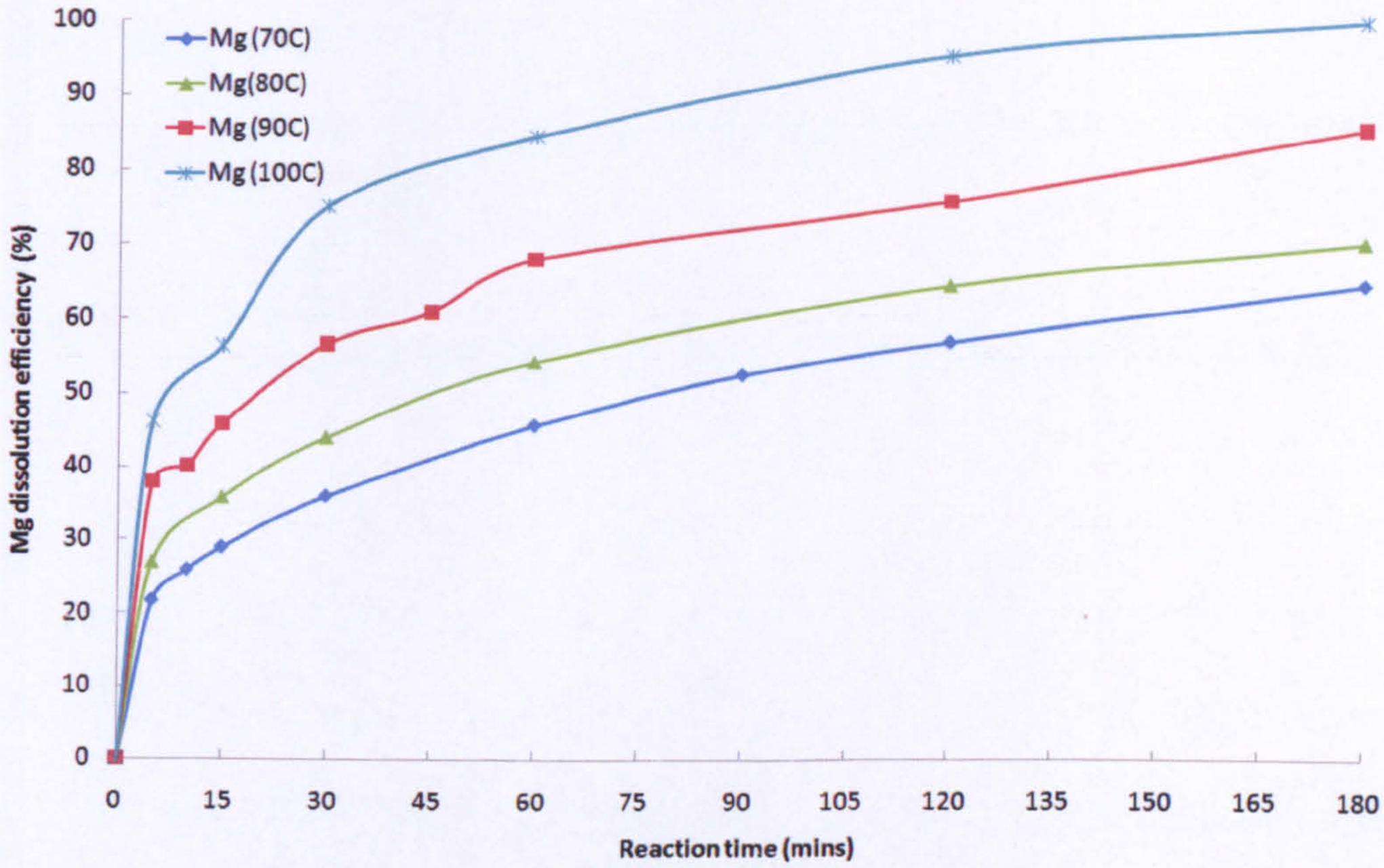

Figure 4-2: Mg dissolution from serpentine in 1.4 M NH_4HSO_4 solution at 70, 80, 90 and 100°C for 3 hours.

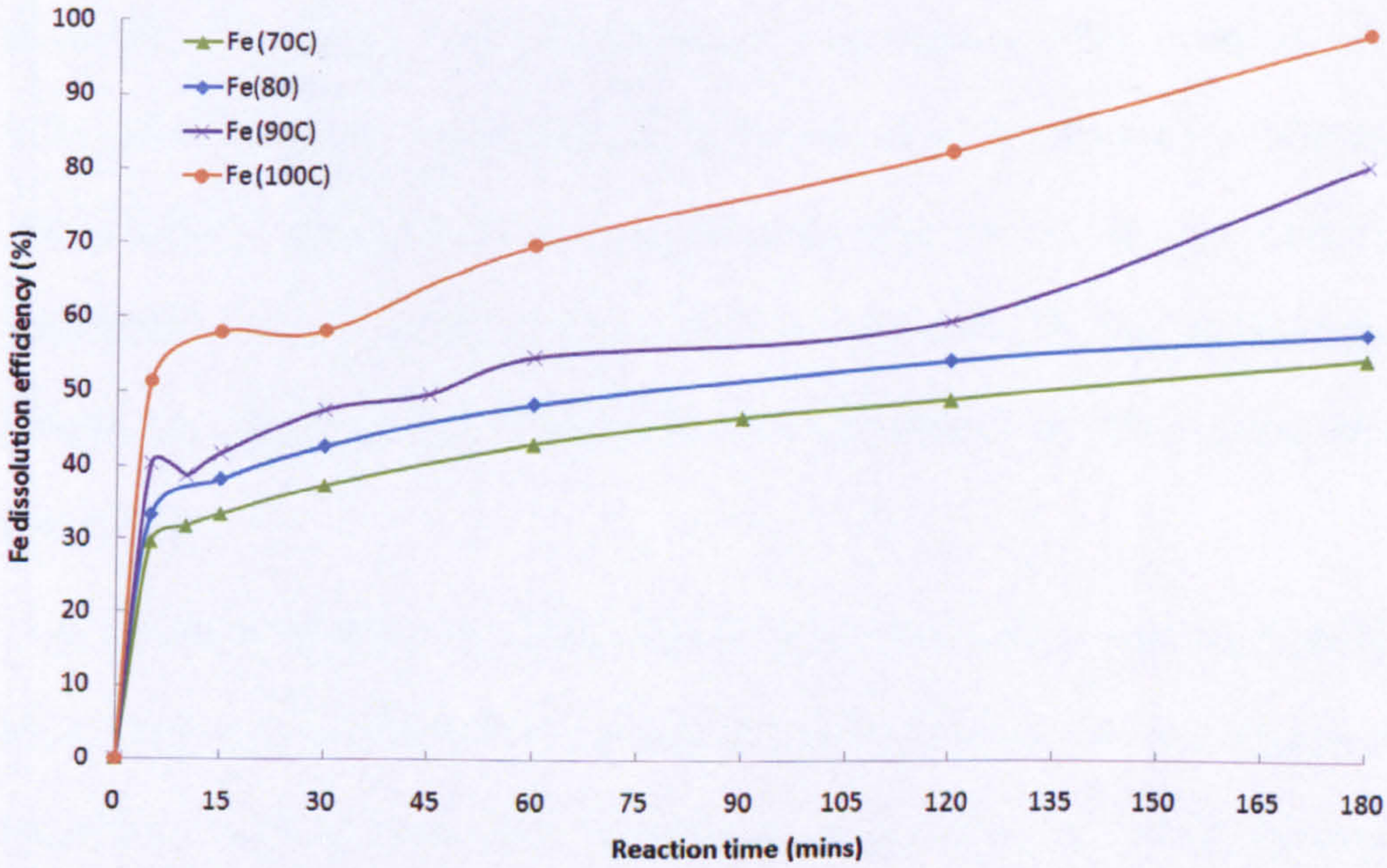

Figure 4-3: Fe dissolution from serpentine in 1.4 M NH_4HSO_4 solution at 70, 80, 90 and 100°C for 3 hours.

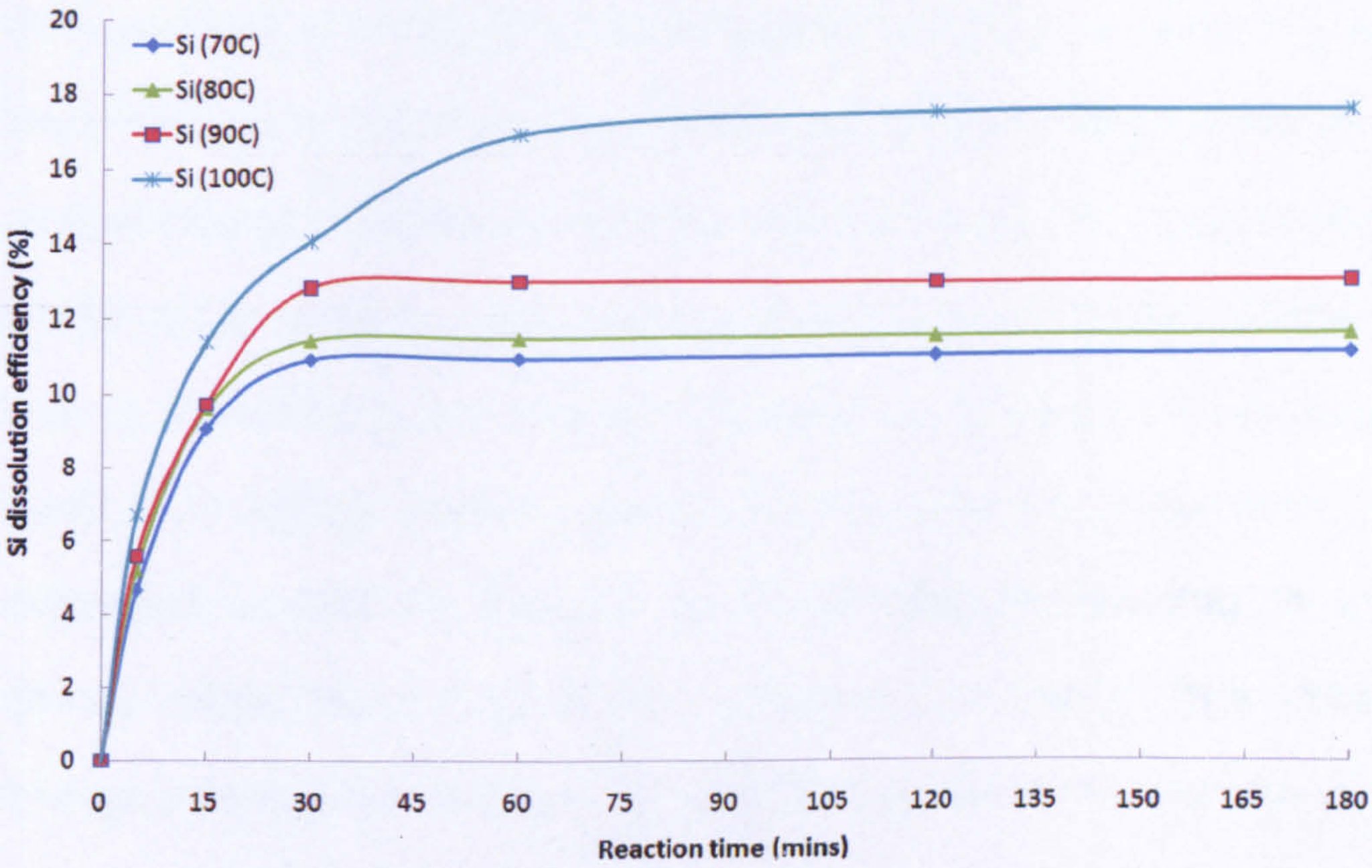

Figure 4-4: Si dissolution from serpentine in 1.4 M NH_4HSO_4 solution at 70, 80, 90 and 100°C for 3 hours.

NH_4HSO_4 provided a 100 % dissolution efficiency after 3 hours and this value is higher than that of 72 % reported by Park et al (2004) using H_3PO_4, oxalic acid and EDTA and that of 70 % reported by Alexander *et al.* (2007) using H_2SO_4. A 100 % Mg dissolution efficiency has also been reported by Teir *et al.* (2007c) using HCl and HNO_3.

It is anticipated that the dissolution rate ($mol/m^2/s$) can be further improved by increasing the additive concentration in the aqueous solution. Furthermore, pre-treatment of serpentine could further enhance the dissolution rate. For example, studies have shown that heat-treatment at 650 °C increases reactivity greatly (McKelvy *et al.*, 2004). However, physical and thermal activation of the mineral increases considerably the energy demand of the process.

Gerdemannet *et al.* (2007) have studied the energy penalty of pre-treatment of serpentine. The theoretical energy required for the heat-activation process to heat the mineral to 630 °C is up to 326 kWh/t for serpentine. The energy required for the initial crushing step is estimated to be 2 kWh/t and grinding to minus 75 μm adds another 11 kWh/t. Further grinding to minus 38 μm in ball mills is estimated to add 70 kWh/to, and high-intensity grinding in an stirred media detritor adds an estimated 150 kWh/t. The extra energy penalty can increase CO_2 emissions and decrease the net power generated of power plants. More recently, it has been reported that concurrent grinding could effectively remove the silica layer from the particles (Van Essendelft *et al.*, 2009a).

4.1.3 Kinetic analysis

In a liquid-solid reaction, the reaction rate is generally controlled by one of the following sequential steps: diffusion through the fluid film, diffusion through the layer on the particle surface, or the chemical reaction at the surface. The rate of the reaction is controlled by the slowest of these steps (Levenspiel, 1972.).

In order to determine the kinetic parameters, including reaction constant and activation energy, and the rate-limiting step in the dissolution of serpentine using ammonium salts, the experimental data were analyzed according to the standard integral analysis method (Levenspiel, 1972.). The unreacted-core model of constant

size particles (Levenspiel, 1972.) was selected since previous studies have reported incongruent dissolution of serpentine and proved the existence of a silicon layer after dissolution (Fauth *et al.*, 2001). Experimental data were fitted into integral rate equations of film diffusion control, product layer diffusion control, and reaction control for constant size particles (flat plate, cylinder and sphere). The multiple regression correlation coefficients (R) were calculated for each equation and checked graphically. The rate-limiting step of the reaction was identified as that reaction with the highest multiple regression correlation coefficient.

Kinetic analysis was performed using the magnesium dissolution data (Table 4-1). When fitting the experimental data to the integral rate equations, product layer diffusion gave the best match based on the regression correlation coefficients calculated (Figure 4-5).

Table 4-1: Multiple regression coefficients for experimental kinetic data fitted to constant size particles models.

Model	Equation	R^2
Film diffusion	$kt = X_B$	-0.279 — 0.2016
Product layer diffusion	$kt = 1 - 3(1 - X_B)^{2/3} + 2(1 - X_B)$	0.9324 — 0.9643
Chemical reaction controls	$kt = 1 - (1 - X_B)^{1/3}$	0.4228 — 0.8562

The results (Figure 4-5) indicate that the rate limiting step for dissolution of serpentine in NH_4HSO_4 is more likely to be product layer diffusion. Luce (1972) found that a product layer is the rate-controlling mechanism for dissolution of magnesium silicates by using HNO_3 and KOH. Apostolidis and Distin (1978) also found that the rate was limited by diffusion through a silica passive layer when

the magnesium dissolution is above 25% by using H_2SO_4. This study is in agreement with these studies and the finding that low concentration of Si in solution supports the theory of a build up of a product layer of silica on the particles. It should be noted that the rate-limiting control mechanism probably changes with particle size, and if a smaller particle size sample was chosen, pure chemical reaction control may have become dominant.

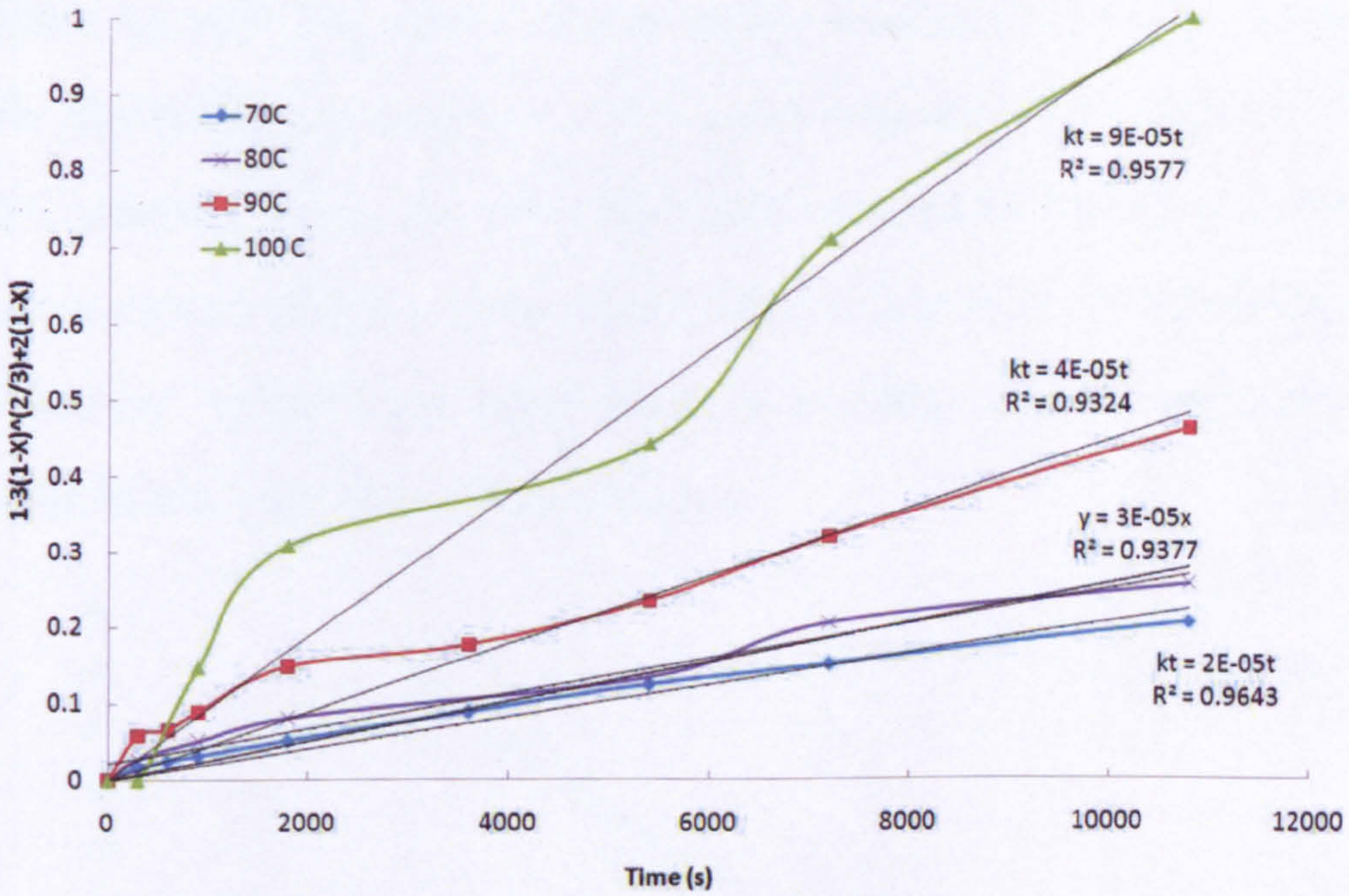

Figure 4-5: Kinetic analysis of the dissolution of Mg from serpentine using 1.4 M NH_4HSO_4

The apparent rate constant (k) was determined from the slope of the lines in Figure 4-5. The apparent rate constant can be used for determining the activation energy (E) by Arrhenius' law:

$$k = k_0 e^{-E/RT} \quad \text{(Eq. 2)}$$

The activation energy was determined by plotting the apparent rate constants for each experiment at different temperatures (Fig. 4-6). As there are no previous studies of dissolution of serpentine using ammonium salts, studies for dissolution of serpentine in strong acids were selected for comparison and the activation energies reported are presented in Table 4. The activation energy found in this study (40.9 kJ mol^{-1}) is similar to the value calculated by Fouda (1996) for dissolution of serpentine in 3M H_2SO_4 between 30-75°C (Table 4-2). However, it is much lower than that reported by Teir *et al.* (2007) when using 2M H_2SO_4 between 30-70°C (Table 4-2). The difference between Fouda's and Teir's work is probably due to heat pre-treatment of samples in Fouda's work.

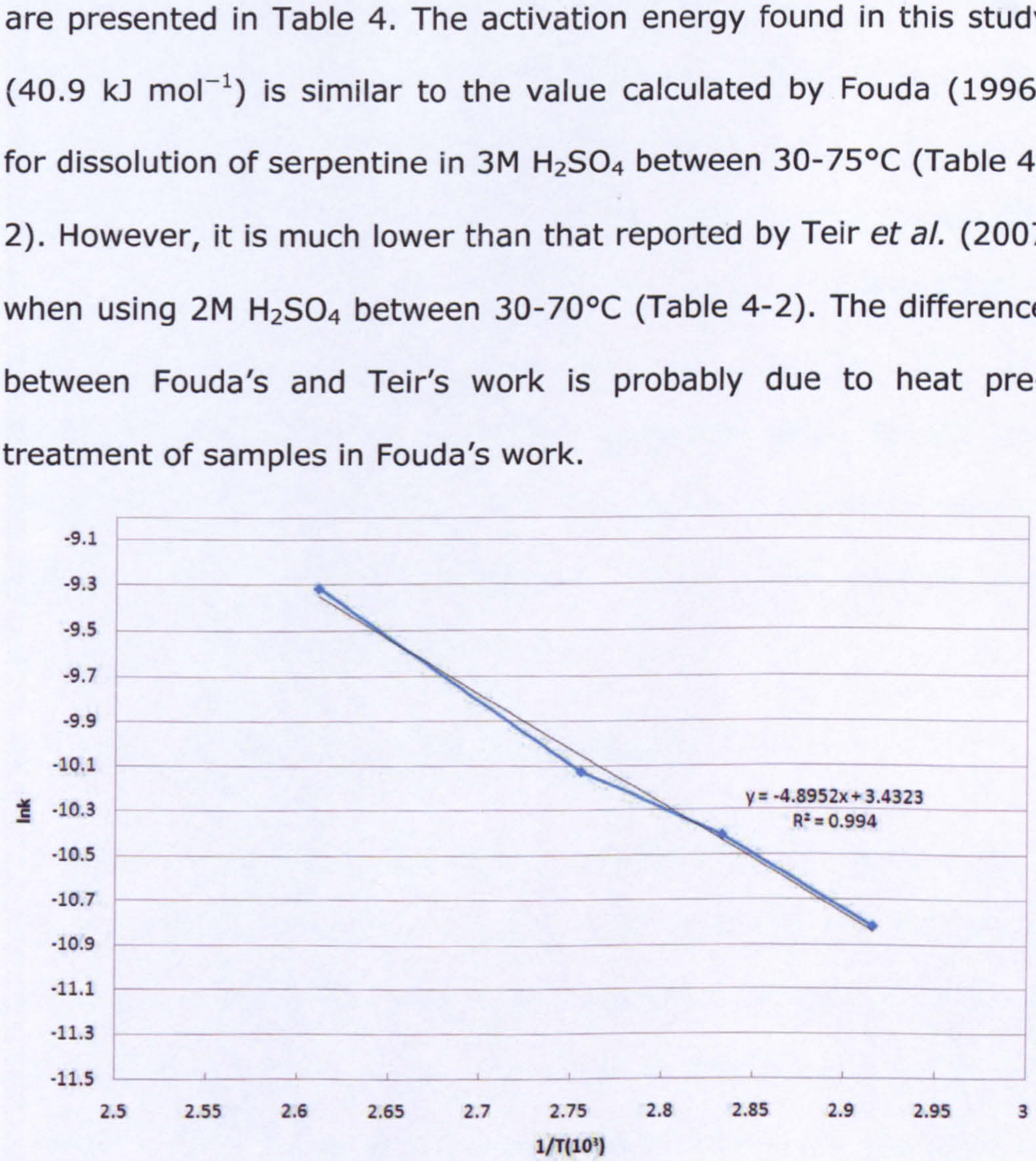

Figure 4-6: Arrhenius plot for dissolution of Mg from serpentine using 1.4 M NH_4HSO_4

Table 4-2: Data on dissolution of serpentine from literature

	Feedstock	Solution	Activation energy E (kJ mol^{-1})
Fouda et al. (1996b)	Serpentine pre-heated at 800°C for 2-3 hours	3 M H2SO4, T=30-75°C	35.6
Teir et al. (2007)	Serpentine with particle size fraction of 74-125 µm	2 M H2SO4, T=30-70°C	68.1
Present study	Serpentine with particle size fraction of 75-150 µm	1.4 M NH4HSO4. T=70-110°C	40.9

Teir *et al.* (2007c) proposed that chemical reaction is the initial rate limiting step, and product layer diffusion gradually becomes rate limiting, because of the build up of a product layer of silica and the decrease of unreacted surface area. The observed activation energy here is higher than the value of typical layer diffusion controlled process, and is roughly one half of that of a pure chemical reaction controlled process (Levenspiel, 1972.). In summary, the rate limiting mechanism of serpentine dissolution with 75-150 µm particle size using NH_4HSO_4 is a combination of chemical reaction control and product layer diffusion control. This explains the derivations observed from Figure 4-5.

4.1.4 The effect of solvent concentration

The effect of solvent concentration was tested by dissolving 20 g of original mineral serpentine (75-150 µm) in a 400 ml solution of ammonium bisulphate with concentration values of 0.7, 1 (stoichiometric value), 1.4, 2 and 2.8 M at 100 °C for 1 h. The Mg concentrations of the solutions after dissolution were analyzed by

ICP-AES. The equipment and procedure used were same to those described in Section 4.1.1.

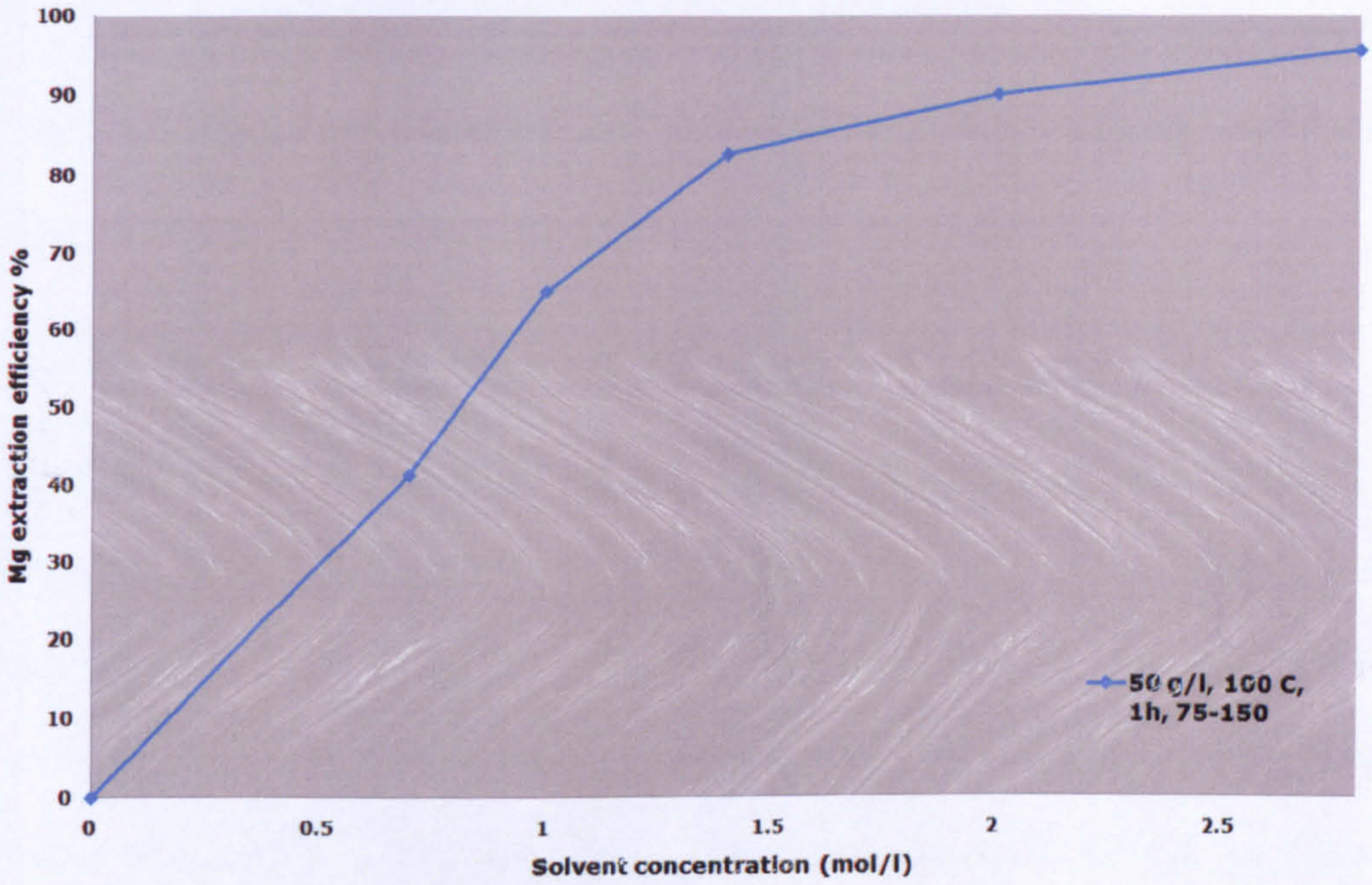

Figure 4-7: The effect of solvent concentration on dissolution of Mg from serpentine in aqueous solution of ammonium bisulphate.

According to the stoichiometry of dissolution of Mg and NH_4HSO_4, 2 parts of NH_4HSO_4 is required to dissolve one part of Mg. A 20 g serpentine dissolving in 400 ml solution theoretically contains 0.5 M Mg ions, thus 1 M NH_4HSO_4 aqueous solution is required. However, due to the limitation of the diffusion of NH_4HSO_4 in pore space of mineral particles, only 65.0 % Mg dissolution efficiency was obtained when using the 1 M stoichiometry concentration, compared to 41.2, 82.5 and 89.9 % when using 0.7, 1.4 and 2 M, respectively (Fig. 4-7). Therefore, the excess of NH_4HSO_4 concentration can maximise the Mg dissolution efficiency. Although the highest Mg dissolution efficiency (95.5 %) was achieved at highest solvent

concentration (2.8 M), 1.4 M was considered to be the optimized solvent concentration since more excess cannot promote the dissolution efficiency significantly. However, it must be noted that when using excess NH_4HSO_4 more ammonia water was consumed to regulate the pH to neutral value.

4.1.5 The effect of particle size

The effect of particle size was tested by dissolving 20 g of original mineral serpentine in a 400 ml solution of 1.4 M ammonium bisulphate at 90 °C for 2 h. The particle size values selected were <38, 75-150 and 150-300 μm, as these values allow for comparison with previous published work. The Mg concentrations of the solutions after dissolution were analyzed by ICP-AES. The equipment and procedure used were identical to those described in section 4.1.1.

Figure 4-8 shows that dissolution rate of Mg in all three particle size within the first 15 minutes is higher than that after 15 minutes. The smallest particle size (<38 μm) presents the slightly highest Mg dissolution efficiency (68.1 % in 60 mins) (Fig. 4-8). Moreover, the Mg dissolution efficiency does not decrease significantly with increasing particle size, where 67.8 % (60 mins) is achieved when using the 75-150μm compared to 65.4 % (60 mins) for that using 150-300 μm. After 2 h, the Mg dissolution efficiency of that using 75-150 μm is nearly same to that using <38 μm. Alexander *et al.*

(2007) reported 38 and 25 % were obtained in their H_2SO_4 extraction experiments when using 75-150 and 150-300 µm. In terms of energy saving on grinding, the high particle size fraction of 75-150 µm should be used.

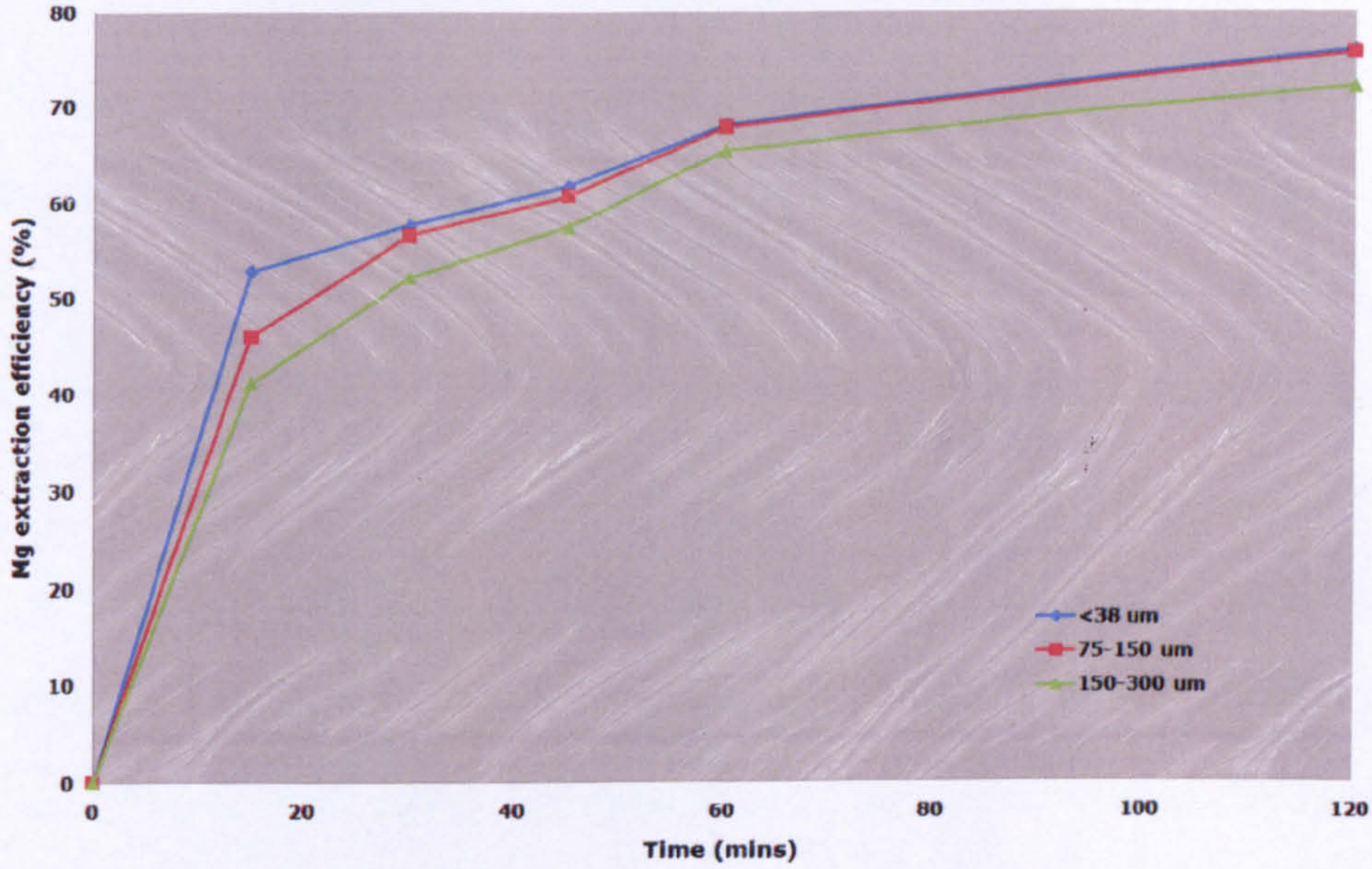

Figure 4-8: The effect of particle size on dissolution of Mg from serpentine in aqueous solution of ammonium bisulphate.

4.1.6 The effect of solid to liquid ratio

High solid to liquid ratio is preferred to reduce water usage and save energy during the evaporation. Accordingly, the dissolution of Mg from serpentine using different solid to liquid ratios was tested by adding a sample (20, 40, 80 and 120 g) of serpentine (75-150 µm) to 400 ml of 1.4 M ammonium bisulphate solution at 100 °C for 3 h. The Mg concentrations of the solutions after dissolution were analyzed by ICP-AES. The equipment and procedure used were identical to those described in Section 4.1.1. For the solid to liquid

ratio above 100 g/l, $MgSO_4$ precipitated during the dissolution, and excess water was added at the end of dissolution to dissolve all the Mg into the solution. After filtering, the Mg concentration and the volume of solution were measured.

The highest Mg dissolution efficiency (100 %) was reached with the lowest solid to liquid ratio (50 g/l) (Fig. 4-9). The Mg dissolution efficiency did not decrease significantly (91 %) when the solid to liquid ratio increased to 100 g/l. The Mg dissolution efficiency decreased from 91 % to 75 % as the solid to liquid ratio increased from 100 g/l to 200 g/l. However, when solid to liquid ratio continuously increase to 300 g/l, the Mg dissolution efficiency increased to 85 %. Because increasing of high solid to liquid ratio enhances the probability of interactions between particles. Once the product layer is exfoliated by collision of particles, the fresh mineral located below the product layer can react with the reactive reagent (NH_4HSO_4). This results in increasing of dissolution efficiency with increasing the diffusion of reactive reagent in the pore space of particles. The increase of dissolution efficiency by the intensive particle-particle interaction resulted from the removal of silica passive layer have been reported by Bearat *et al.* (2006) and Park and Fan (2004).

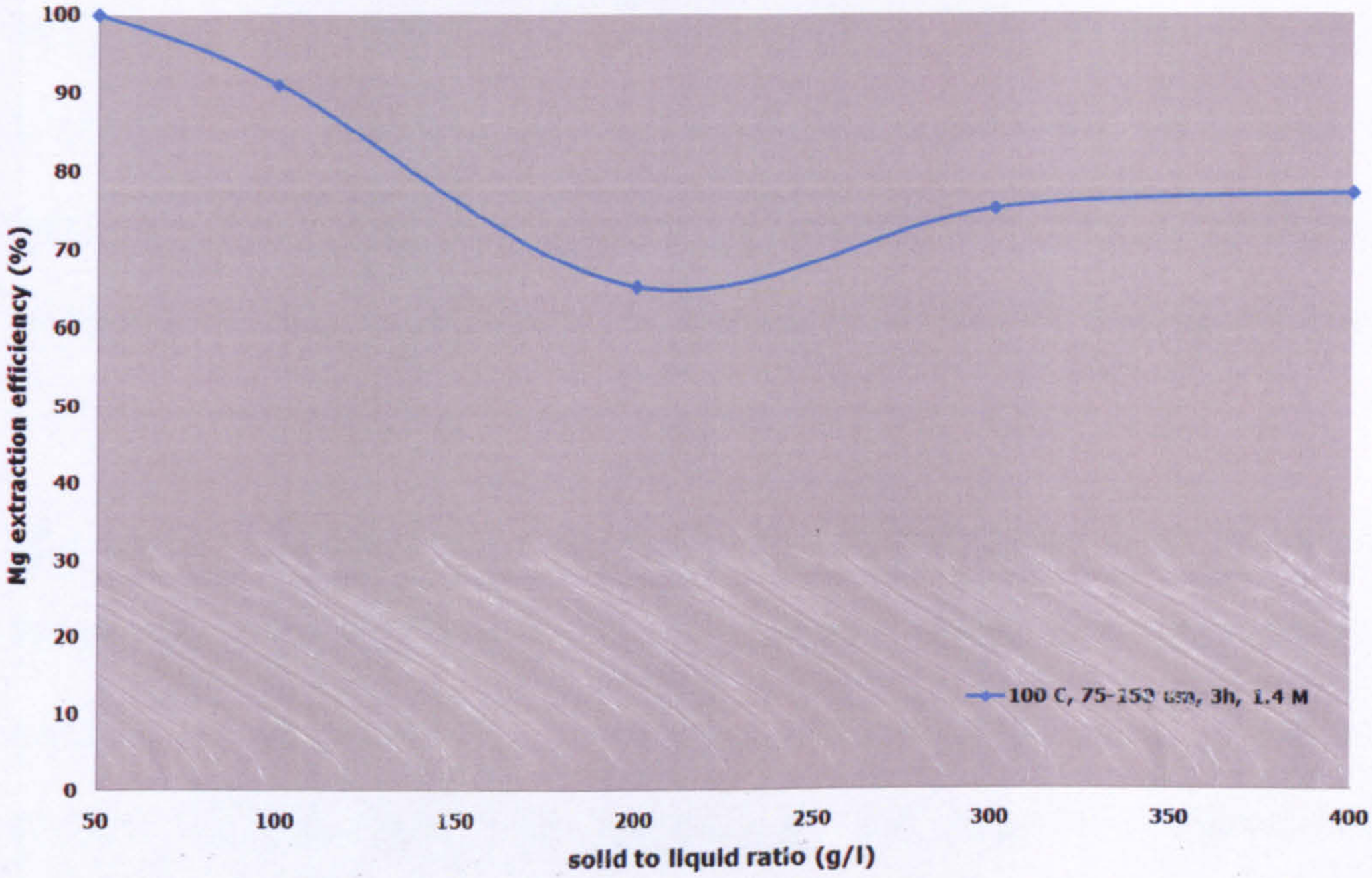

Figure 4-9: Effect of solid to liquid ratio on dissolution of Mg from serpentine in aqueous solution of ammonium bisulphate.

Consequently, the solid to liquid ratio of 50 g/l in the dissolution of Mg from serpentine is favoured and ratios over 100 g/l should be avoided. Application of internal grinding in serpentine dissolution at a fluidised bed is a potential solution to provide intensive particle-particle interaction and thus remove passive layer (Park and Fan, 2004).

4.1.7 Summary

This work reports the dissolution of serpentine using ammonium salts. It has been shown that NH_4HSO_4 can extract significant amounts of Mg from serpentine and its dissolution efficiency is higher than that reported using H_2SO_4. The results from dissolution experiments show that at 100 °C 1.4 M NH_4HSO_4 extracted 100% of

Mg from serpentine in 3 hours, as well as 98% of Fe, but only 17.6% of Si. This incongruent leaching would lead to create a passive silicon layer on the surface of particle that blocks continuous leaching of Mg. In addition, it was found that the Mg dissolution from serpentine increases with higher temperatures.

The dissolution kinetics of serpentine with NH_4HSO_4 were found to follow the model of constant size particles, where the rate limiting mechanism is a chemical reaction with product layer diffusion control. In this study, the results show that serpentine dissolution with NH_4HSO_4 is very temperature dependent with activation energy of 40.9 kJ mol^{-1}, which is in agreement with the previous kinetic studies of magnesium dissolution from serpentine.

The effect of solvent concentration, particle size and solid to liquid ratio were investigated. The Mg dissolution from serpentine was favoured at when using particle size fraction of 75-150 µm, 1.4 M ammonium bisulfate solution at 50 g/l solid to liquid ratio.

4.2 Production of hydromagnesite with recyclable ammonium salts

The dissolution of serpentine with NH_4HSO_4 has been reported in Section 4.1. In this section, the carbonation with NH_4HCO_3 and the regeneration of NH_4HSO_4 and NH_3 are reported. The carbonation experiments were conducted at different molar ratio of Mg-

NH_4HCO_3-NH_3. Finally, the mass balance of all streams in this process is presented.

4.2.1 Experimental methods

4.2.1.1 Preparation of magnesium salt solutions from serpentine using NH_4HSO_4

Previous dissolution experiments conducted have shown that NH_4HSO_4 is suitable for extracting magnesium from serpentine (Section 3.3). The dissolution of magnesium from serpentine using NH_4HSO_4 is presented in Eq. 4-2:

$$Mg_3Si_2O_5 \bullet (OH)_4(s) + 6NH_4HSO_4(aq) \rightarrow 3MgSO_4(aq) + 2SiO_2(s) + 5H_2O(l) + 3(NH_4)_2SO_4(aq)$$

Equation 4-2

For the dissolution experiments, the same procedure and serpentine sample was used as in Section 4.1.1. Different temperatures (80 °C, 90 °C and 100 °C) and reaction times (1 h, 2 h and 3 h) were used for the preparation of $MgSO_4$ solutions. After dissolution, the solution was cooled down to room temperature and filtered using a 0.45 µm Pall syringe filters. The filtrate is referred to as filtrate 1 (Figure 3-1) and was used for the pH regulation studies described in Section 4.2.1.2. The solid residue was dried at 105 °C overnight and is referred to as product 1 (Figure 3-1). The filtrate 1 was analysed by ICP-AES to measure the concentration of dissolved Mg, Fe and Si.

For the purpose of this analysis, filtrate 1 was acidified by 70 wt. % HNO_3 for preventing precipitation of Mg and Fe. The product 1 was sampled and sent for XRF analysis to determine the weight % of Mg, Fe and Si. The reproducibility of these analyses is found to be around 1 % according to duplicate experiments.

4.2.1.2 pH regulation and removal of impurities

About 40 % excess NH_4HSO_4 was used for the dissolution of serpentine in order to maximise the magnesium dissolution. After the dissolution, the pH values of the solution were about 0.9~1.2. Because the carbonation reaction is favored at high pH values, it was necessary to increase the pH of the solution to alkaline values. The chemical reaction of the pH regulation is presented in Eq. 4-3:

$$NH_4HSO_4(aq) + NH_3 \bullet H_2O(aq) \rightarrow (NH_4)_2SO_4(aq) + H_2O(l)$$

Equation 4-3

The reason of using ammonia water is because the above reaction produces ammonium sulphate, which can be converted back to NH_3 and NH_4HSO_4 in the regeneration step in order to achieve the recycle of the additives (Figure 3-1).

If a high value product (pure magnesium carbonate) is desired, some impurities, such as Fe, Al, Cr, Zn, Cu and Mn, need to be precipitated out from the system firstly by increasing the pH. In order to optimize the removal of impurities, extra ammonia water

was added into filtrate 1 after pH regulation, and the reactions of impurities removal are presented in Eq.4-4 and 4-5:

$$(Fe,Al,Cr)_2(SO_4)_3(aq)+6NH_3\bullet H_2O(aq)\rightarrow$$
$$2(Fe,Al,Cr)(OH)_3(s)\downarrow+3(NH_4)_2SO_4(aq)$$

Equation 4-4

$$(Zn,Cu,Mn,Fe)SO_4(aq)+2NH_3\bullet H_2O(aq)\rightarrow$$
$$(Zn,Cu,Mn,Fe)(OH)_2(s)\downarrow+(NH_4)_2SO_4(aq)$$

Equation 4-5

During the pH regulation and removal of impurities, ammonia water (35 wt. %) was added into filtrate 1 until the pH value was neutral. During this process, the solution was stirred and an in-situ pH probe was used to measure the pH value. The solution was filtered with 0.7 μm Pall syringe filters. The filtrate is referred to as filtrate 2 (Figure 3-1) and was used for the carbonation experiments described in Section 4.2.1.3. The solid residue was dried at 105 °C overnight and is referred to as product 2 (Figure 3-1). The filtrate 2 was analyzed by ICP-AES to quantify the concentration of different elements, including Mg, Si, Fe, Mn, Zn, Cu, Al and Cr. The product 2 was analyzed by XRF and XRD to quantify its composition and identify the mineral phases present.

4.2.1.3 Precipitation of hydromagnesite using NH_4HCO_3

The precipitation of hydromagnesite by reacting $MgSO_4$ with NH_4HCO_3 and NH_3 is presented in Eq. 4-6 and 4-7:

$$MgSO_4(aq) + NH_4HCO_3(aq) + NH_3 \bullet H_2O(aq)$$
$$+2H_2O(l) \rightarrow MgCO_3 \bullet 3H_2O(s)\downarrow + (NH_4)_2SO_4(aq)$$

Equation 4-6

$$5MgCO_3 \bullet 3H_2O(s) \rightarrow 4MgCO_3 \bullet Mg(OH)_2 \bullet 4H_2O(s)\downarrow$$
$$+10H_2O(l) + CO_2(g)\uparrow$$

Equation 4-7

The formation of magnesium carbonate species depends on temperature and pressure (Hänchen *et al.*, 2008). Nesquehonite ($MgCO_3 \bullet 3H_2O$) can precipitate from aqueous solutions at ambient temperature as described in Eq. 4-6, while at higher temperatures (50 and 100 °C), nesquehonite is transformed into hydromagnesite ($4MgCO_3 \bullet Mg(OH)_2 \bullet 5H_2O$) as presented in Eq. 4-7. For temperatures above 100 °C, hydromagnesite is transformed into magnesite ($MgCO_3$). In this study, hydromagnesite was produced as the experiments were conducted at 85 °C.

For the carbonation experiments, the filtrate 2 was put in a 500 ml 3 neck glass vessel and heated up to 60 °C using a silicon oil bath. The experimental setup was as previously reported in Section 4.1.1.

The time, temperature and pH values were recorded every 5 mins. Before starting heating, ammonia water (35 wt. %) was added into filtrate 2. When the temperature reached 60 °C, NH_4HCO_3 (as CO_2 source) was added and the solution was heated to 90 °C. After the solution was stabilised at 90 °C, the solution was kept at that temperature for 30 mins. 2 ml aliquots were sampled using a needle syringe at 5, 10, 15, 30, 45 and 60 mins. The liquid samples were filtered by a mini filter unit and acidified with HNO_3 for subsequent ICP-AES analysis to measure the Mg concentration. At the end of the experiment, the solution was cooled down and filtered with 0.7 µm Pall syringe filters and the filtrate is referred to as filtrate 3 (Figure 3-1). The solid residue was dried at 105 °C overnight and is referred to as product 3 (Figure 3-1). The composition of the product 3 was analyzed using XRF and the mineral phases were identified by XRD. Experiments were conducted at different mass ratios of Mg : NH_3 : NH_4HCO_3, where Mg is the mass of Mg in filtrate 2, and NH_3 and NH_4HCO_3 represent the mass of ammonia water and the mass of NH_4HCO_3 added, respectively. In addition, a preliminary experiment was conducted where no NH_3 was added. The matrix of the experiments conducted at different mass ratios is listed in Table 4-3.

Table 4-3: Matrix of the molar ratios Mg:NH_4HCO_3:NH_3 and carbonation efficiency (For experiments 3 and 4, ammonia water was added at ambient temperature, therefore double ammonium magnesium was precipitated. For all the other experiments, ammonia water was added when the temperature reached 60 °C)

	Mg	NH_4HCO_3	NH_3	Carbonation %
Preliminary	1	3	0	25.5
Experiment 1	1	3	1	71. 6
Experiment 2	1	3	0.5	53.0
Experiment 3	1	3.5	1.5	46.5
Experiment 4	1	4	1.5	53.4
Experiment 5	1	2	1	41.5
Experiment 6	1	4	1	77.9
Experiment 7	1	5	1	89.9
Experiment 8	1	4	2	95.9
Experiment 9	1	4	1.5	91.5
Experiment 10	1	4	3	91.3

The carbon content of the product 3 was measured by a TGA Q500 analyzer. The temperature programme was from 30 °C to 950 °C at 20 °C/min under nitrogen atmosphere. The carbonation efficiency from soluble magnesium sulphate to hydromagnesite is defined as follows:

$$Carbonation\ efficiency\ (\%) = \frac{CO_2\ content\ (wt\%) \times 24 \times m_3}{44 \times c_2 \times V_2} \times 100$$

Equation 4-8

Where CO_2 content (wt. %) is the weight loss of product 3 during the temperature range from 300 °C to 500 °C corresponding to carbonate decomposition from the TGA studies (Huijgen *et al.*,

2006). m_3 is the mass (grams) of product 3 from carbonation experiment, c_2 is the magnesium concentration in filtrate 2 from ICP-AES and V_2 is the volume of filtrate 2, 24 and 44 is the total molecular weight of Mg and CO_2 in hydromagnesite.

4.2.1.4 Thermal decomposition of $(NH_4)_2SO_4$

The filtrate 3 was evaporated by using a rotary evaporator at 60 °C for 15 mins. The solid collected from the rotary evaporator is referred to as product 4. The regeneration of NH_4HSO_4 and NH_3 was conducted by thermal decomposition of product 4 in an oven at 330 °C and the reaction is presented in Eq. 4-9:

$$(NH_4)_2SO_4(s) \rightarrow NH_4HSO_4(s) + NH_3(g)\uparrow$$

Equation 4-9

The thermal decomposition of product 4 was characterised by performing thermal gravimetric studies using a TGA Q500 in the temperature range of 30-530 °C under nitrogen atmosphere. The temperature programme was as follows: from 30 °C to 230 °C at 10 °C/min, hold for 10 mins at 230 °C, up to 330 °C at 10 °C/min, hold for 10 mins at 330 °C and finally up to 530 °C at 10 °C/min. The choice of these three heating steps was to avoid the mixture of products decomposition. In order to ascertain the decomposition from the TGA analysis of product 4, pure $(NH_4)_2SO_4$ and NH_4HSO_4

were also characterised by TGA analysis using the same heating procedure.

4.2.2 Results and discussion

4.2.2.1 Preparation of magnesium salts solutions from serpentine using NH_4HSO_4

The results from the ICP-AES analyses (Table 4-4) of the filtrate 1 solutions from all experiments show that high concentrations of Mg and Fe were dissolved, while most of the Si remained in the serpentine. The dissolution efficiency is calculated as the percentage of dissolved elements in filtrate 1 solution over elements in original mineral serpentine. The values for the original mineral serpentine are also reported in Table 4-4. Taking experiment 3 as an example, using the data in Table 4-4, the dissolution efficiency of Mg from serpentine was 91 % using 1.4 M NH_4HSO_4 at 100 °C for 2 h. The dissolution efficiency of other elements for experiment 3 is presented in Figure 4-10.

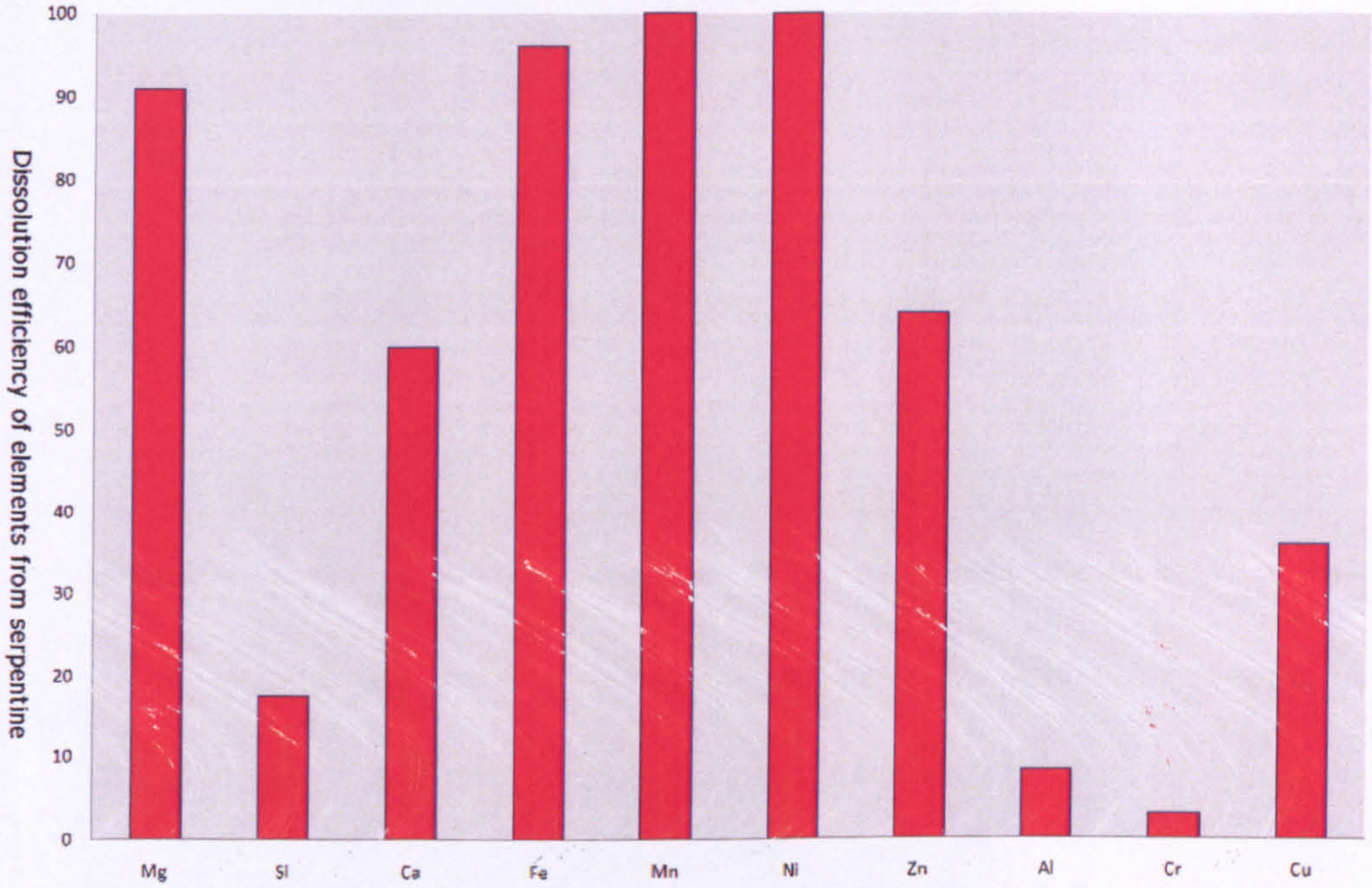

Figure 4-10: Dissolution efficiency of different elements after serpentine dissolution by NH_4HSO_4 (Experiment 3, 100 °C, 2 h)

It was found that 96 % Fe, 17 % Si, 100 % Ni and Mn, and some Ca, Zn, Cu and Al were also dissolved from serpentine. This result is consistent with the previous dissolution studies, where the dissolution efficiencies of Mg, Fe and Si from serpentine were 95 %, 83 % and 17 %, respectively, under the same experimental conditions (Section 4.1.2). The dissolution efficiencies for Ni, Mn, Ca, Zn, Cu and Al were very similar for all experiments conducted. As high purity $MgCO_3$ is desired, all the other cations are considered as impurities, with Fe and Si being identified as the main impurities and are reported in Table 4-4. In conclusion, Mg was removed from serpentine, leaving behind amorphous silica. This can be explained by incongruent dissolution of Mg and Si as previously discussed (Section 4.1.2), where chemical reaction with product layer diffusion

control was found to be the rate limiting step of serpentine dissolution in NH_4HSO_4.

Table 4-4: Summary from ICP-AES analyses of original mineral serpentine and filtrate samples produced in the experiments (units: mg/l).

		Mg	Si	Fe	Dissolution%	Carbonation%
Serpentine		11970.0	3680.0	2050.0		
Experiment 1	Filtrate 1	8851.0	505.2	1179.0	73.8	71.56
	Filtrate 2	8252.0	74.1	600.0		
	Filtrate 3	2347.0	11.2	1.0		
Experiment 2	Filtrate 1	9052.0	447.0	1284.0	75.4	53.0
	Filtrate 2	8290.0	110.0	244.0		
	Filtrate 3	3219.0	20.2	0.5		
Experiment 3	Filtrate 1	10957	621.0	1964.0	91.3	46.5
	Filtrate 2	9629.0	98.0	337.0		
	Filtrate 3	2983.0	5.2	0.3		
Experiment 4	Filtrate 1	8497.0	399.0	1131.0	70.8	53.4
	Filtrate 2	7840.0	105.0	187.0		
	Filtrate 3	2914.0	21.0	0.2		
Experiment 5	Filtrate 1	9550.0	411.0	1133.0	79.6	41.5
	Filtrate 2	8690.0	154.0	145.0		
	Filtrate 3	4097.0	35.2	0.9		
Experiment 6	Filtrate 1	8261.0	478.0	1175.0	68.8	77.9
	Filtrate 2	7866.0	132.0	206.0		
	Filtrate 3	1625.0	19.4	0.2		
Experiment 7	Filtrate 1	8960.0	463.0	1084.0	74.7	89.9
	Filtrate 2	8123.0	98.0	133.1		
	Filtrate 3	865.0	15.2	0.4		
Experiment 8	Filtrate 1	8487.0	422.0	1064.0	70.7	95.9
	Filtrate 2	7679.0	68.5	97.0		
	Filtrate 3	889.2	6.9	0.6		
Experiment 9	Filtrate 1	6311.0	289.5	738.3	52.6	91.5
	Filtrate 2	5784.0	58.5	80.0		
	Filtrate 3	589.8	12.5	0.3		
Experiment 10	Filtrate 1	8264.0	311.0	1135.0	68.9	91.3
	Filtrate 2	7794.0	82.5	98.0		
	Filtrate 3	780.6	8.5	0.7		

Finally, in order to compare this work with Pundsack's (1967), carbonation experiments were carried out following his procedure. CO_2 was bubbled into the prepared high Mg concentration solution from serpentine and excess ammonia water was added to adjust the pH until the value of 9. Only 35 % carbonation efficiency was obtained. In comparison, the carbonation efficiency from this work can achieve a maximum of 95.9 % (experiment 8) due to the faster reaction rate between NH_4HCO_3 and Mg.

4.2.2.2 pH regulation and removal of impurities

It was found that after adding ammonia water (35 wt. %) to the filtrate 1 solution, some particles precipitated. After filtering and drying overnight at 105 °C, the resulting solid and filtrate were labelled as product 2 and filtrate 2 (Figure 3-1), respectively. Ammonia water (35 wt. %) was then added to filtrate 2 until the pH value reached 8.5. Table 4-5 presents the XRF results of the products and the mass balance for Mg, Si and Fe will be discussed in Section 4.2.2.6. Taking experiment 7 as an example, it can be seen that product 2 consists of 19 % Fe, 8 % Si and 3 % Mg. The XRD pattern of product 2 for the experiment 7 (Figure 4-11) identified double ammonium salts, $(NH_4)_2Fe_2(SO_4)2{\bullet}6H_2O$, $(NH_4)_2Mg_2(SO_4)_2{\bullet}6H_2O$ and $(NH_4)_2Zn_2(SO_4)_2{\bullet}6H_2O$, to be the major phases. The presence of these double ammonium salts resulted from the excess of ammonia water. Hot water flashing can

decompose these double ammonium salts into ammonium sulphate and insoluble hydroxide salts (Everingham, 1976).

Table 4-5: XRF analyses of solids produced in the experiments (units: wt. %), and the CO_2 content from TGA analysis. The mass balance for Mg, Si and Fe for the three products in relation to patent serpentine is also presented as mass ratio (%).

		Mass Mg	Mass ratio (%)	Si	Mass ratio (%)	Fe	Mass ratio (%)	CO_2
Serpentine		23.9	100	22.2	100	5.7	100	N/A
Experiment 1	Product 1	10.5	26.2	42.3	86.3	5.6	42.5	N/A
	Product 2	2.7	5.0	6.3	11.7	20.4	28.2	N/A
	Product 3	21.5	49.2	0.2	1.7	2.2	29.2	38.8
Experiment 2	Product 1	9.8	24.6	43.6	87.9	5.3	37.4	N/A
	Product 2	2.0	6.6	6.4	9.2	21.2	50.7	N/A
	Product 3	16.5	42.3	0.3	2.4	0.8	11.9	30.1
Experiment 3	Product 1	3.5	8.7	45.7	83.1	3.0	4.2	N/A
	Product 2	5.4	11.1	11.0	14.2	27.5	79.2	N/A
	Product 3	21.9	55.4	0.2	2.5	1.1	16.4	39.5
Experiment 4	Product 1	11.8	29.2	42.4	89.2	5.8	44.8	N/A
	Product 2	2.5	5.5	8.8	8.0	18.5	46.0	N/A
	Product 3	20.1	41.1	0.3	2.3	0.8	9.1	37.5
Experiment 5	Product 1	8.2	20.4	42.8	88.8	5.8	44.7	N/A
	Product 2	3.4	7.2	5.8	7.0	20.1	48.2	N/A
	Product 3	23.8	38.3	0.4	3.2	0.8	7.0	40.9
Experiment 6	Product 1	12.5	31.2	42.2	87.0	5.6	42.7	N/A
	Product 2	3.9	3.3	6.4	9.4	21.3	47.3	N/A
	Product 3	19.8	52.0	0.4	3.1	0.7	1.0	35.5
Experiment 7	Product 1	10.1	25.3	40.7	87.4	5.9	47.1	N/A
	Product 2	2.8	7.0	8.2	9.9	19.3	46.4	N/A
	Product 3	20.5	60.5	0.3	2.3	0.4	6.2	36.7
Experiment 8	Product 1	11.7	29.3	42.0	88.5	6.0	48.1	N/A
	Product 2	1.6	6.7	9.6	9.6	19.8	47.2	N/A
	Product 3	17.7	56.6	0.2	1.7	0.3	4.7	26.51
Experiment 9	Product 1	18.7	47.4	35.4	92.1	7.1	64.0	N/A
	Product 2	4.8	4.4	13.9	6.3	20.2	32.1	N/A
	Product 3	18.2	43.3	0.1	1.3	0.3	3.9	27.0
Experiment 10	Product 1	12.5	31.1	43.4	91.5	5.8	44.6	N/A
	Product 2	4.6	3.9	4.7	60.2	16.3	50.6	N/A
	Product 3	21.3	58.5	0.1	2.0	0.3	4.7	38.5

Table 4-4 clearly shows that the concentration of Fe in filtrate 2 decreased significantly compared to filtrate 1. This decrease of Fe concentration indicates that Fe precipitates. The results of XRF, ICP-

AES and XRD analysis in Tables 4-4 and 4-5 and Figure 48 are consistent with this observation, indicating that a high Fe content precipitate was produced. Some Mg also precipitated during this procedure, causing filtrate 2 to contain 5 % less dissolved magnesium than filtrate 1. All experiments presented similar XRF, ICP-AES and XRD results on product 2 and filtrate 2 samples. Moreover, the Fe content of product 2 was measured by XRF to be between 16 wt. % to 28 wt. % (Table 4-5). Furthermore, the picture of product 2 could be seen in Figure 4-11

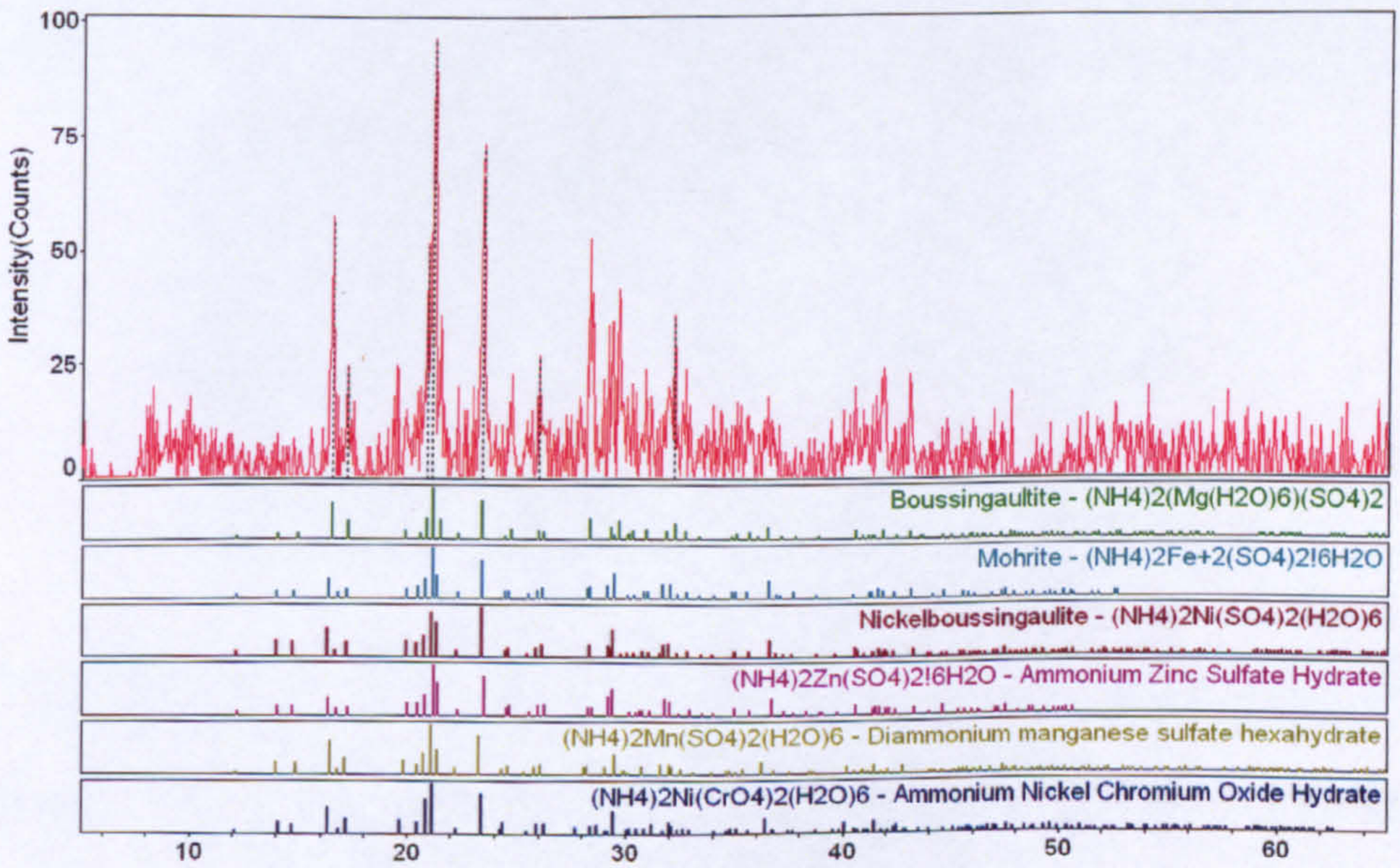

Figure 4-11: XRD pattern of product 2 of experiment 7.

4.2.2.3 Precipitation studies

10 precipitation experiments were carried out at different mass ratio of Mg:NH_3:NH_4HCO_3, as shown in Table 4-3. The observations and

findings from these 10 experiments were similar in terms of carbonation and morphology of the product 1, 2, 3 and 4 (Pictures of products can be seen in Figure 4-12). Taking product 3 of experiment 7 as an example, Figure 4-13 shows the presence of magnesium carbonate. This corresponds to the decrease of Mg concentration in solution for ICP-AES results presented in Table 4-4.

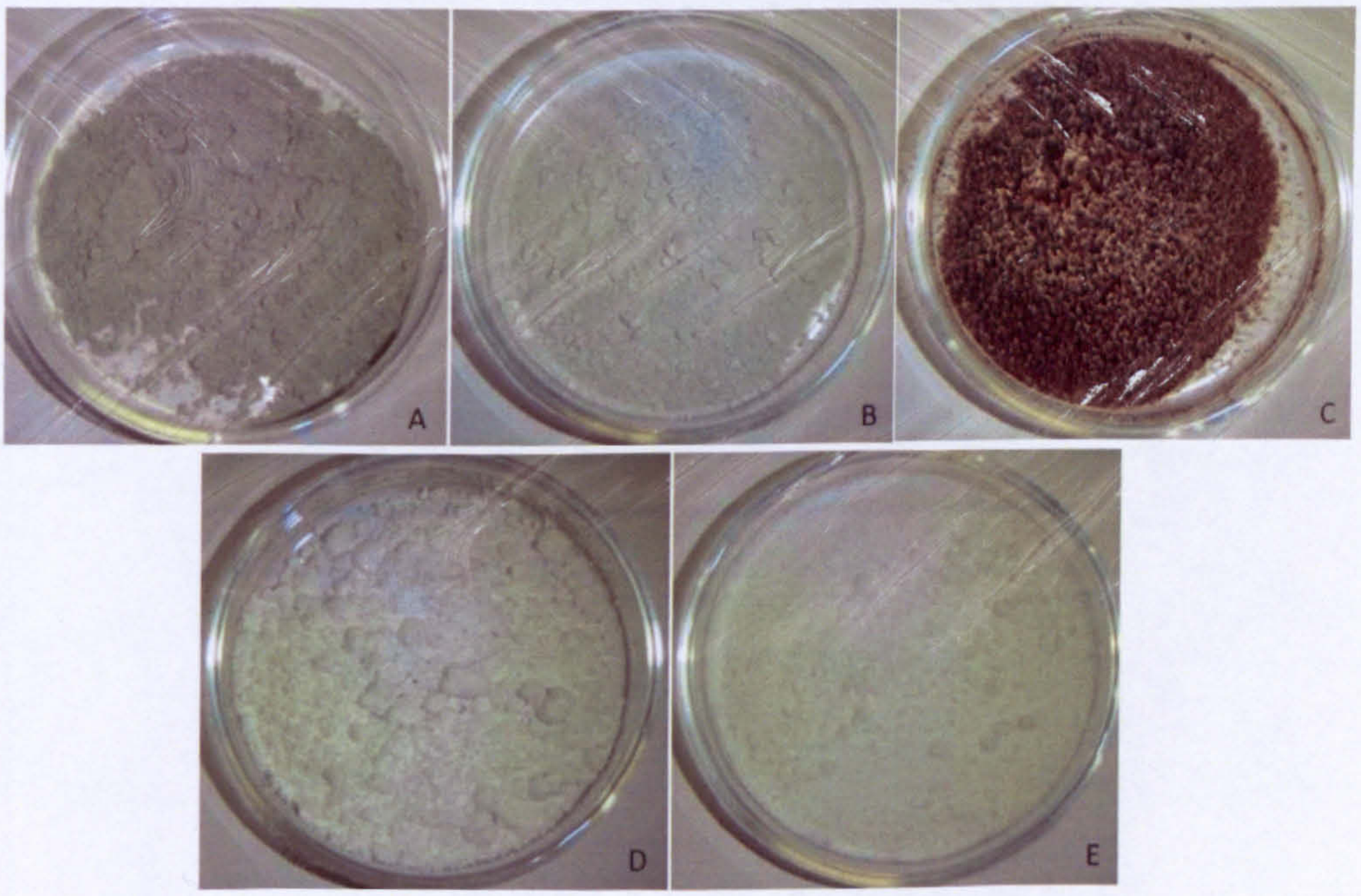

Figure 4-12: Pictures of original mineral sample and products in the process route. (A. patent serpentine; B. product 1; C. product 2; D. product 3; E. product 4)

Figure 4-13 shows the Mg concentration variation with time and temperature for experiment 7. The starting time is recorded when heating starts. It can be seen that the pH of filtrate 2 decreased from 8.5 to 7.3 when the temperature increases during the first 20 mins. When the temperature reached 60 °C, NH_4HCO_3 was added and the pH increased slightly to 7.6. No precipitate was formed

before adding NH_4HCO_3. The concentration of magnesium started to drop when the temperature went up to 70°C at 25 minutes. In the following 5 mins, half of the Mg ions precipitated at a very high rate of 33.3 mmol/min. When the temperature was stabilised at 85 °C after the 40 minutes, the pH became stable and the Mg precipitated at a constant rate of 7.9 mmol/min. After 25 mins counted from the addition of NH_4HCO_3, the concentration of Mg in solution became constant and finally went below 1000 mg/l.

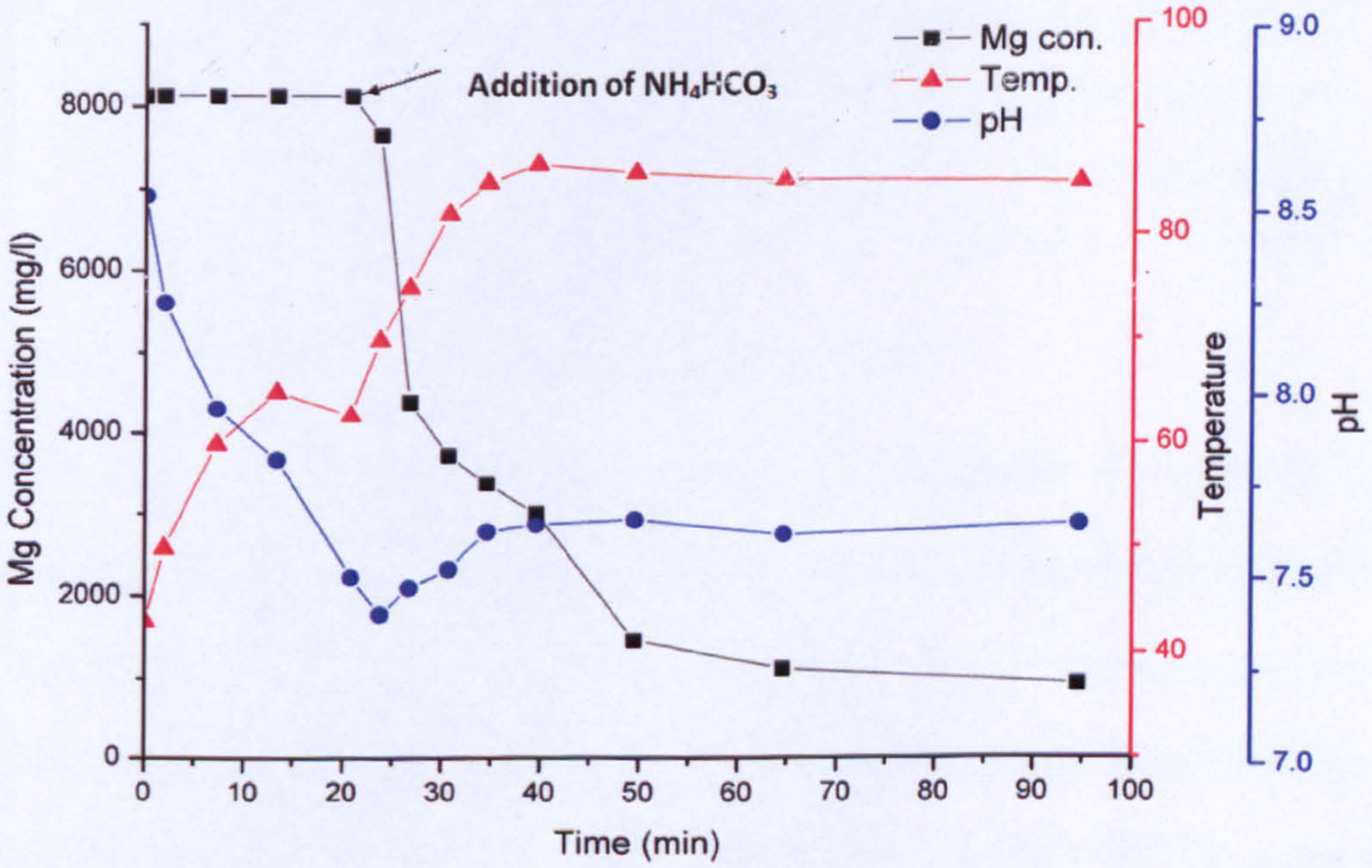

Figure 4-13: Temperature, time, pH and concentration of Mg in solution during the course of a typical carbonation experiment (Experiment 7)

For product 3 of experiment 7, the XRD pattern of product 3 (Figure 4-14) showed that the Mg precipitated as hydromagnesite, $Mg_5(CO_3)_4(OH)_2 \bullet 4H_2O$. Combining the results from XRF of product 3 (Table 4-5) and ICP-AES of filtrate 3 (Table 4-4), it can be

concluded that product 3 is a 80 % purity hydromagnesite with only 0.79 wt. % of Fe and 0.29 wt. % Si.

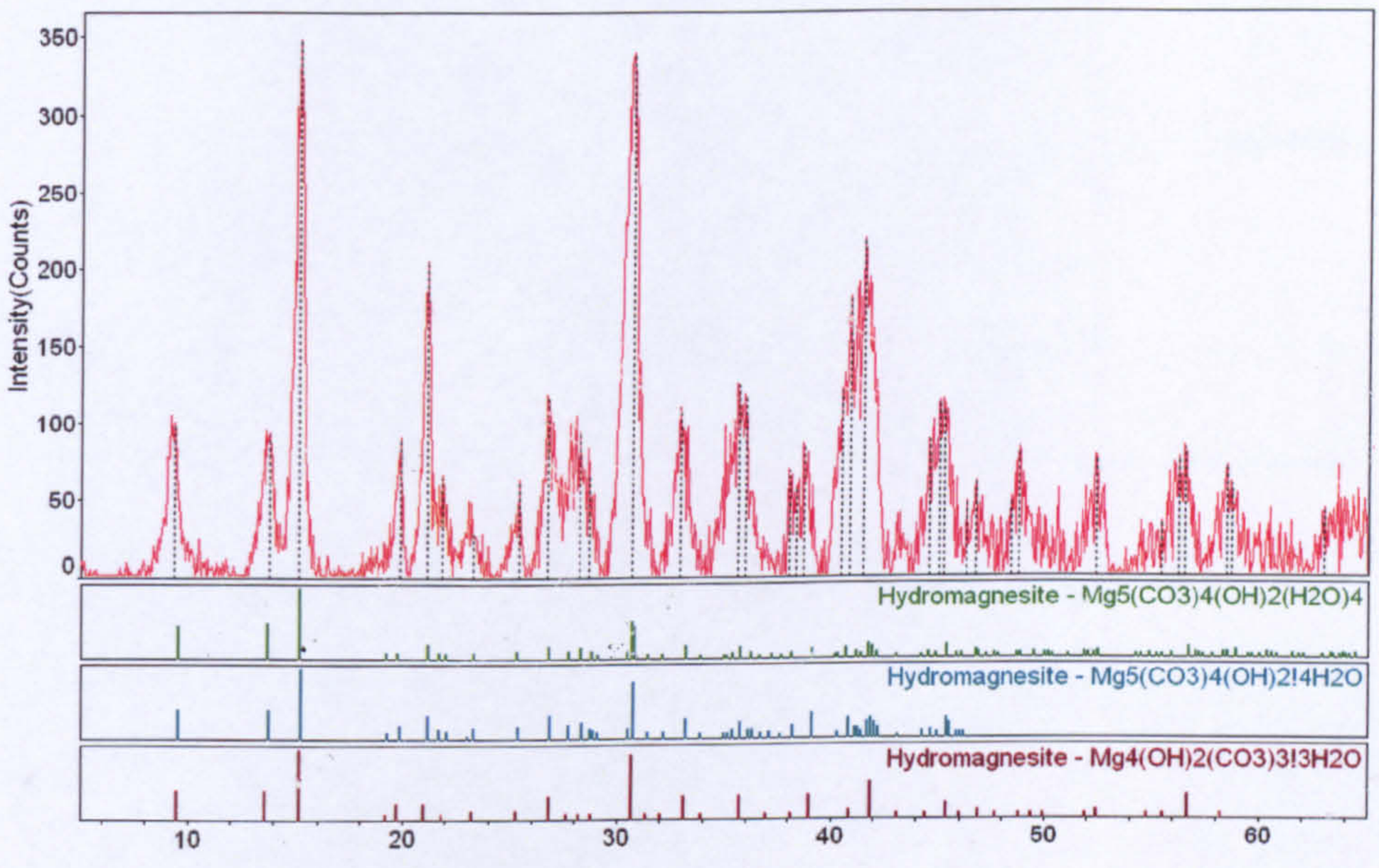

Figure 4-14: XRD pattern of product 3 of experiment 7

The carbon content of product 3 can be calculated from the TGA profiles (Figure 4-15 (a)), as described in the experimental methods (Section 4.2.1.3). All samples presented one carbonate phase according to the XRD studies. Therefore, the mass of the identified carbonate phase was estimated based on the corresponding weight loss from the TGA studies. As an example, Figure 4-15 (a) shows two peaks, where the first peak below 250 °C is about 12 wt. % and corresponds to the release of crystal water (Huijgen *et al.*, 2006). The second peak located between 250 °C to 500 °C accounts for 37 wt. % and is due to the decomposition of hydromagnesite (Hänchen *et al.*, 2008). Finally, based on the CO_2 content (Table 4-5) and the

Mg concentration in filtrate 2 (Table 4-4), it can be calculated that the carbonation efficiency of experiment 7 is 90 %.

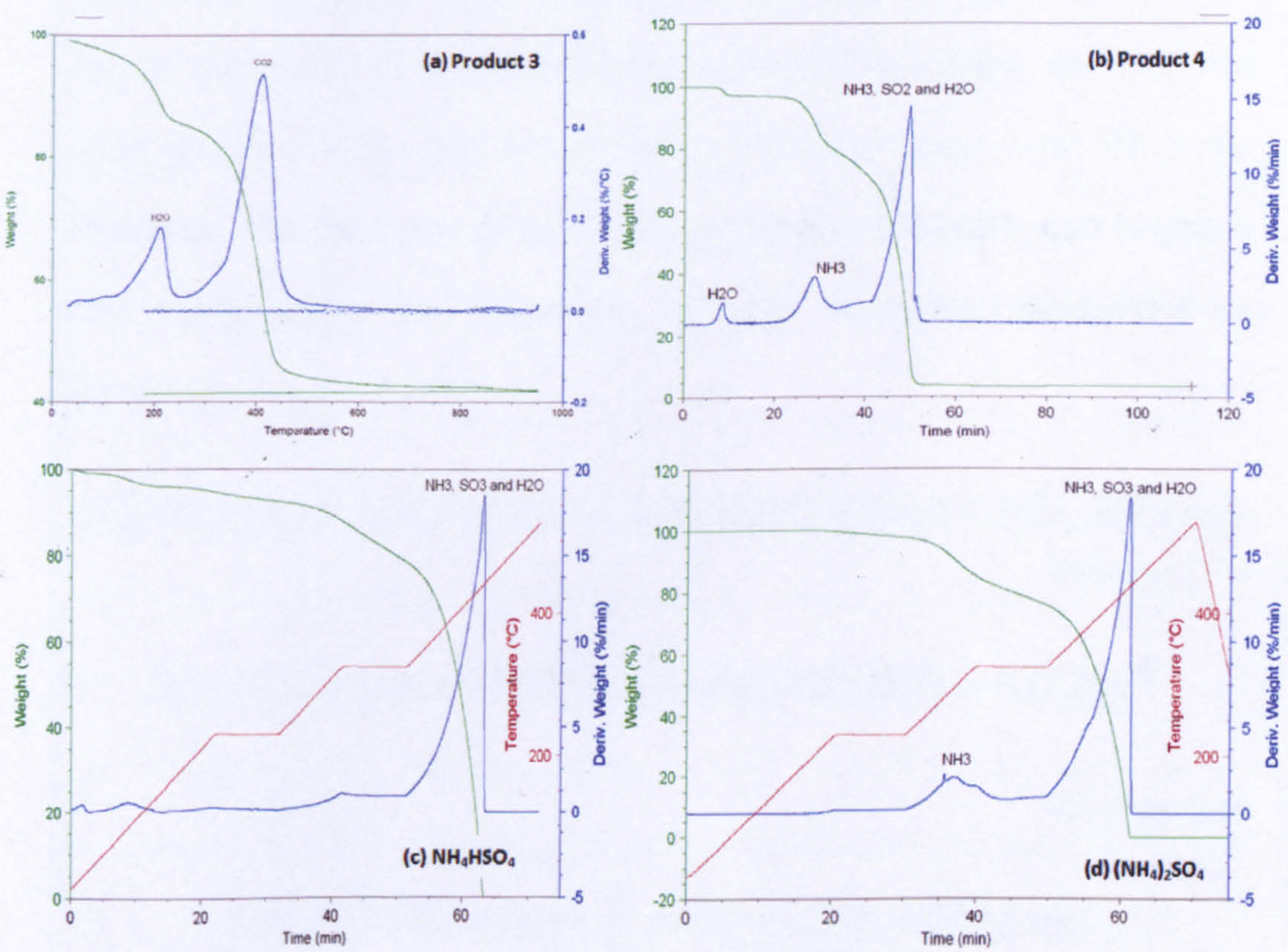

Figure 4-15: TGA profiles of product 3 and product 4 from experiment 7, NH_4HSO_4 and $(NH_4)_2SO_4$

Improving carbonation by adding NH_3

During the carbonation step, the Mg ions firstly react with HCO_3^- to form $Mg(HCO_3)_2$ (Eq. 4-11) that then thermally decomposes into insoluble nesquehonite at above 70 °C, followed by the transformation of nesquehonite into hydromagnesite (Eq. 4-8). It must be pointed out that in the thermal decomposition reaction of

$Mg(HCO_3)_2$ into $MgCO_3 \bullet 3H_2O$ (Eq. 4-12), 1 mole of $Mg(HCO_3)_2$ is converted into 1 mole of insoluble $MgCO_3 \bullet 3H_2O$ and 1 mole of CO_2. This means that the maximum stoichiometry carbonation efficiency from soluble $Mg(HCO_3)_2$ into precipitated $MgCO_3 \bullet 3H_2O$ is only 50 %. As an example, in the preliminary experiment where no NH_3 was used (Table 4-3), the carbonation efficiency was only 25.5 %. However, the joint use of ammonia water and NH_4HCO_3 can improve the carbonation as described by the reactions presented in equations 4-10 – 4-17:

$$MgSO_4(aq) + NH_4HCO_3 \rightarrow Mg(HCO_3)_2(aq) + NH_4SO_4(aq)$$

Equation 4-10

$$Mg(HCO_3)_2(aq) + 2H_2O(l) \rightarrow MgCO_3 \bullet 3H_2O(s)\downarrow + CO_2(g)\uparrow$$

Equation 4-11

$$NH_3(g) + CO_2(g) + H_2O(l) \rightarrow NH_4HCO_3(aq)$$

Equation 4-12

$$NH_3(g) + NH_4HCO_3(aq) \rightarrow (NH_4)_2CO_3(aq)$$

Equation 4-13

$$MgSO_4(aq) + (NH_4)_2CO_3(aq) + 3H_2O(l) \rightarrow$$
$$MgCO_3 \bullet 3H_2O(s)\downarrow + (NH_4)_2SO_4(aq)$$

Equation 4-14

$$MgSO_4(aq) + 2NH_3 \bullet H_2O(aq) \rightarrow Mg(OH)_2(s)\downarrow + (NH_4)_2SO_4(aq)$$

Equation 4-15

$$Mg(OH)_2(s) + 2CO_2(g) \rightarrow Mg(HCO_3)_2$$

Equation4-16

$$Mg(OH)_2(s) + Mg(HCO_3)_2(aq) + 4H_2O(l) \rightarrow 2MgCO_3 \bullet 3H_2O(s)\downarrow$$

Equation 4-17

Ammonia captures CO_2 to produce NH_4HCO_3 (Eq. 4-12), as known in CO_2 capture technology (Zhang Yun, 2003; Kim *et al.*, 2008). Ammonia can convert NH_4HCO_3 into $(NH_4)_2CO_3$ (Eq. 4-13), which can directly produce $MgCO_3$ (Eq. 4-14). Ammonia can also react with $MgSO_4$ to form insoluble $Mg(OH)_2$ when the pH value is above 10, as shown in equation 4-15 (Teir *et al.*, 2007b). Once the CO_2 is released from the decomposition of $Mg(HCO_3)_2$ (Eq. 4-11), $Mg(OH)_2$ can react with CO_2 to form $Mg(HCO_3)_2$ (Eq. 4-16). Moreover, the $Mg(OH)_2$ can also react with $Mg(HCO_3)_2$ directly to precipitate $MgCO_3$ (Eq. 4-17). Therefore, the carbonation efficiency can be improved by addition of ammonia water to the high Mg concentration solution. This is the case of experiments 1 - 10, where ammonia water was added in all experiments, the carbonation efficiency reached 95.9 % (Table 4-3).

Prevention of precipitation of magnesium ammonium carbonate

The precipitation of magnesium ammonium carbonate ($MgCO_3 \bullet (NH_4)_2CO_3 \bullet 4H_2O$) can reduce the carbonation efficiency, as $MgCO_3 \bullet (NH_4)_2CO_3 \bullet 4H_2O$ is generated from the reaction of NH_3 and NH_4HCO_3 with Mg ions at temperatures below 60 °C (Eq. 4-18) (Cesca, 1971). It can be seen from Figure 4-16 that the Mg concentration decreased until the temperature reached 60 °C during the first 15 mins. However, $MgCO_3 \bullet (NH_4)_2CO_3 \bullet 4H_2O$ decomposes quickly to produce $Mg(HCO_3)_2$, and NH_3 gas when the temperature is above 60 °C (Eq. 4-19).

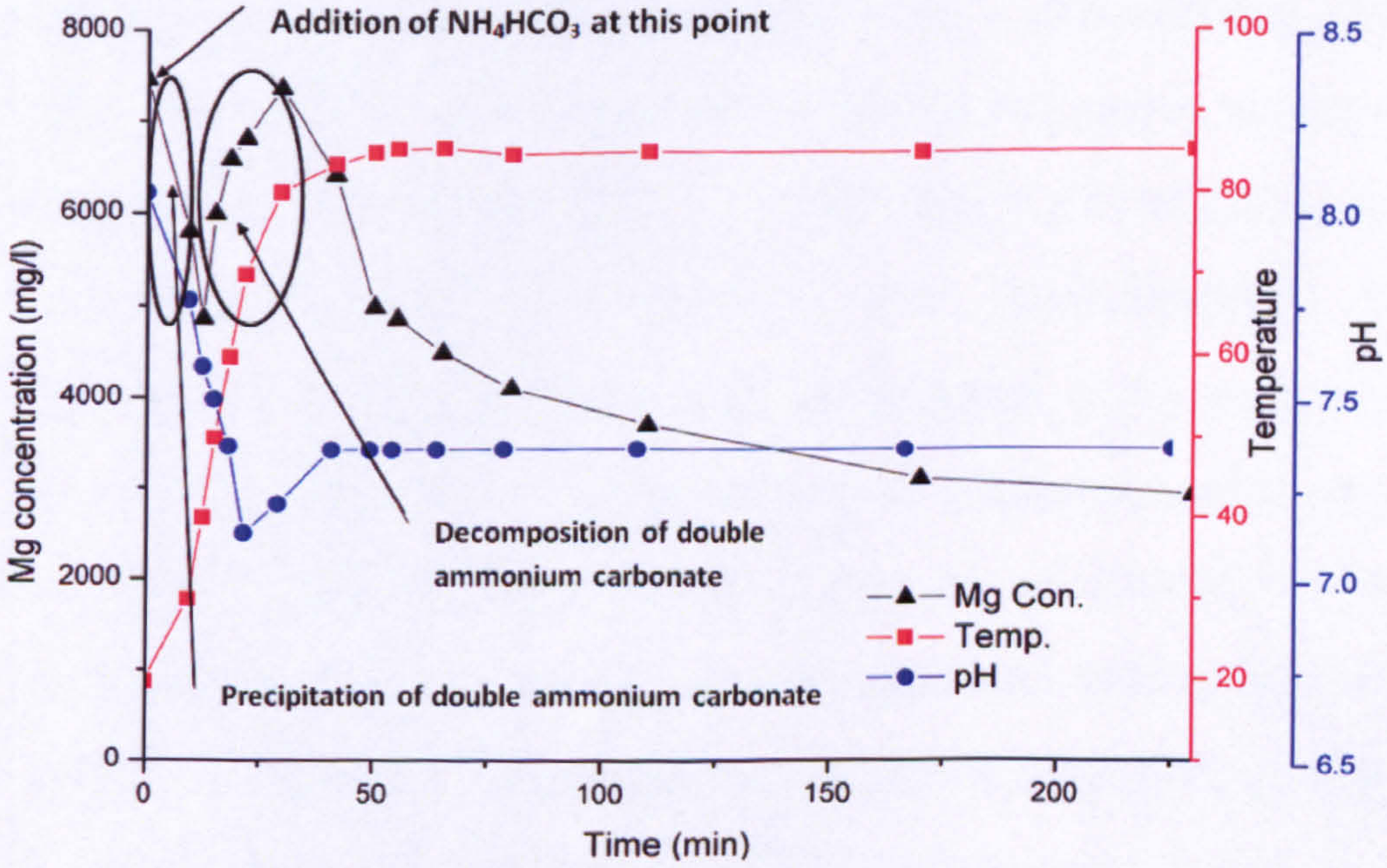

Figure 4-16: Temperature, time, pH and concentration of Mg in solution during the course of a carbonation experiment when double ammonium carbonate precipitates (Experiment 4)

$$MgSO_4(aq) + NH_4HCO_3(aq) + NH_3 \bullet H_2O$$
$$+3H_2O \rightarrow MgCO_3 \bullet (NH_4)_2CO_3 \bullet 4H_2O(s) \downarrow$$

Equation 4-18

$$MgCO_3 \bullet (NH_4)_2CO_3 \bullet 4H_2O(s) \rightarrow$$
$$Mg(HCO_3)_2(aq) + 2NH_3(g) \uparrow + 5H_2O(l)$$

Equation 4-19

It can be seen from equation 4-19 that NH_3 is produced and this would decrease the carbonation efficiency due to shortage of NH_3. Therefore, the precipitation of $MgCO_3 \bullet (NH_4)_2CO_3 \bullet 4H_2O$ should be prevented in order to maintain high carbonation efficiency. Taking experiment 4 as an example, the precipitation of $MgCO_3 \bullet (NH_4)_2CO_3 \bullet 4H_2O$ is indicated on the top left corner of Figure 4-16. When the temperature increased above 60 °C, the Mg concentration increases, indicating the decomposition of $MgCO_3 \bullet (NH_4)_2CO_3 \bullet 4H_2O$. The subsequent decrease of Mg ions after 30 minutes indicates the precipitation of hydromagnesite. The carbonation efficiency of experiment 4 is as low as 53.4 % due to the shortage of NH_3 gas which escaped from the reaction system during the thermal decomposition of $MgCO_3 \bullet (NH_4)_2CO_3 \bullet 4H_2O$. Comparing experiments 4 and 9 using the same mass ratio of Mg-NH_4HCO_3-NH_3 and same experimental conditions, the carbonation efficiency decreased from 91.5 % to 53.4 % when there was

precipitation of $MgCO_3 \bullet (NH_4)_2CO_3 \bullet 4H_2O$ (Table 4-3). Therefore, in order to prevent low carbonation efficiency caused by precipitation of magnesium ammonium carbonate, NH_4HCO_3 should preferably be added into solution above 60°C.

4.2.2.4 Thermal decomposition of $(NH_4)_2SO_4$

Product 4 is obtained from the carbonation step by evaporating the filtrate 3 (Figure 3-1). The product 4 was used to generate NH_3 and NH_4HSO_4 by thermal decomposition in oven at 330 °C for 20 mins. The released gas (NH_3) was collected using water to produce ammonia water. The solid residue after heating was NH_4HSO_4. These results were verified by conducting TGA studies, as described here. Studies of thermal conversion of ammonium sulphate to ammonium bisulphate can be found in several patents (Brennan, 1975; Bretherick, 1975 and Montgomery, 1962). As an example in this work, the thermal decomposition of product 4 from experiment 7, as studied by TGA, is shown in Figure 4-15 (b). The TGA profile shows two peaks, where the first weight loss below 330 °C is about 21.7 wt. %, corresponding to the release of NH_3 and the formation of NH_4HSO_4. The second weight loss between 350 °C and 500 °C is 75.8 wt. % and is due to further decomposition of NH_4HSO_4. In total, the weight loss of product 4 is 97.5 wt. %, and the residual 2.5 wt % is due to the presence of $MgSO_4$ which did not react during carbonation. The TGA profile of pure $(NH_4)_2SO_4$ (purchased from

Fisher Scientific) is presented in Figure 4-15 (c), where two peaks appear at the same temperature range as those for the TGA profile of product 4 (Figure 4-15 (b)). The TGA curve of NH_4HSO_4 is presented in Figure 4-15 (d) and shows only one peak between 330 °C and 500 °C due to decomposition into NH_3, H_2O and SO_3. The NH_4HSO_4 and NH_3 regeneration efficiency from $(NH_4)_2SO_4$ has been reported to be nearly 97 % (Brennan, 1975; Bretherick, 1975 and Montgomery, 1962). In this work, the regeneration efficiency of NH_4HSO_4 and NH_3 from product 4 is 95 %. These TGA results indicate that the reaction of thermal decomposition of $(NH_4)_2SO_4$ should not be conducted above 330 °C to avoid further decomposition, since NH_4HSO_4 can decompose into NH_3, SO_3 and H_2O above 330 °C.

4.2.2.5 The effect of mass ratio of Mg-NH_4HCO_3-NH_3 to carbonation

The mass ratio of Mg:NH_4HCO_3:NH_3 is the key factor controlling carbonation efficiency. The stoichiometric mass ratio of Mg: NH_4HCO_3 is 1:2, but experiment 5 shows that when the stoichiometric ratio 1:2 is used, the carbonation efficiency is only 41.5 % (Table 4-3). Increasing the Mg: NH_4HCO_3 ratio can improve the carbonation efficiency, as presented in Table 4-3, where the carbonation efficiency increase to 72%, 78 % and 90 %, when the ratio of Mg:NH_4HCO_3:NH_3 is 1:3, 1:4 and 1:5, respectively. This can

be explained by the thermal decomposition of NH_4HCO_3 (Eq. 4-20), and reported by Zhang *et al.* (2003). NH_4HCO_3 can regenerate NH_3 and release CO_2 when the temperature is above 70 °C. The two reactions (Eq. 4-6 and Eq. 4-20) compete for NH_4HCO_3, and this may cause low carbonation efficiency due to the shortage of NH_4HCO_3.

$$NH_4HCO_3(aq) \rightarrow NH_3(g)\uparrow + CO_2(g)\uparrow + H_2O(l)$$

Equation 4-20

Moreover, adding ammonia water can increase the carbonation efficiency, as discussed in Section 4.2.2.3. In comparison with the preliminary experiment, experiments 1 and 2 show that carbonation efficiencies increase from 25.5 % to 53 % and then 71.6 % when the mass ratio of $Mg:NH_4HCO_3:NH_3$ increases from 1:3:0 to 1:3:0.5 and then 1:3:1, respectively. This trend was also found in experiments 6, 8 and 9. However, when the ratio increases to 1:4:3, the carbonation efficiency does not increase any further.

In this work, the optimum mass ratio of $Mg:NH_4HCO_3:NH_3$ was determined. A 3D graph (Figure 4-17) is used to show the relationship of the four variables, including mass of Mg, mass of NH_4HCO_3, mass of NH_3 and carbonation efficiency. Figure 4-17 clearly shows that a low summit of 71.6 % carbonation efficiency appears when the mass ratio of $Mg:NH_4HCO_3:NH_3$ is 1:3:1 and a

high summit of 95.9% carbonation efficiency appears when the mass ratio of Mg:NH_4HCO_3:NH_3 is 1:4:2. Continuously increasing both NH_4HCO_3 and NH_3 does not result in a further significant rise of the carbonation efficiency. However, an optimum amount of NH_4HCO_3 and NH_3 are needed to achieve the highest carbonation efficiency due to the loss of CO_2 and NH_3 in an open system.

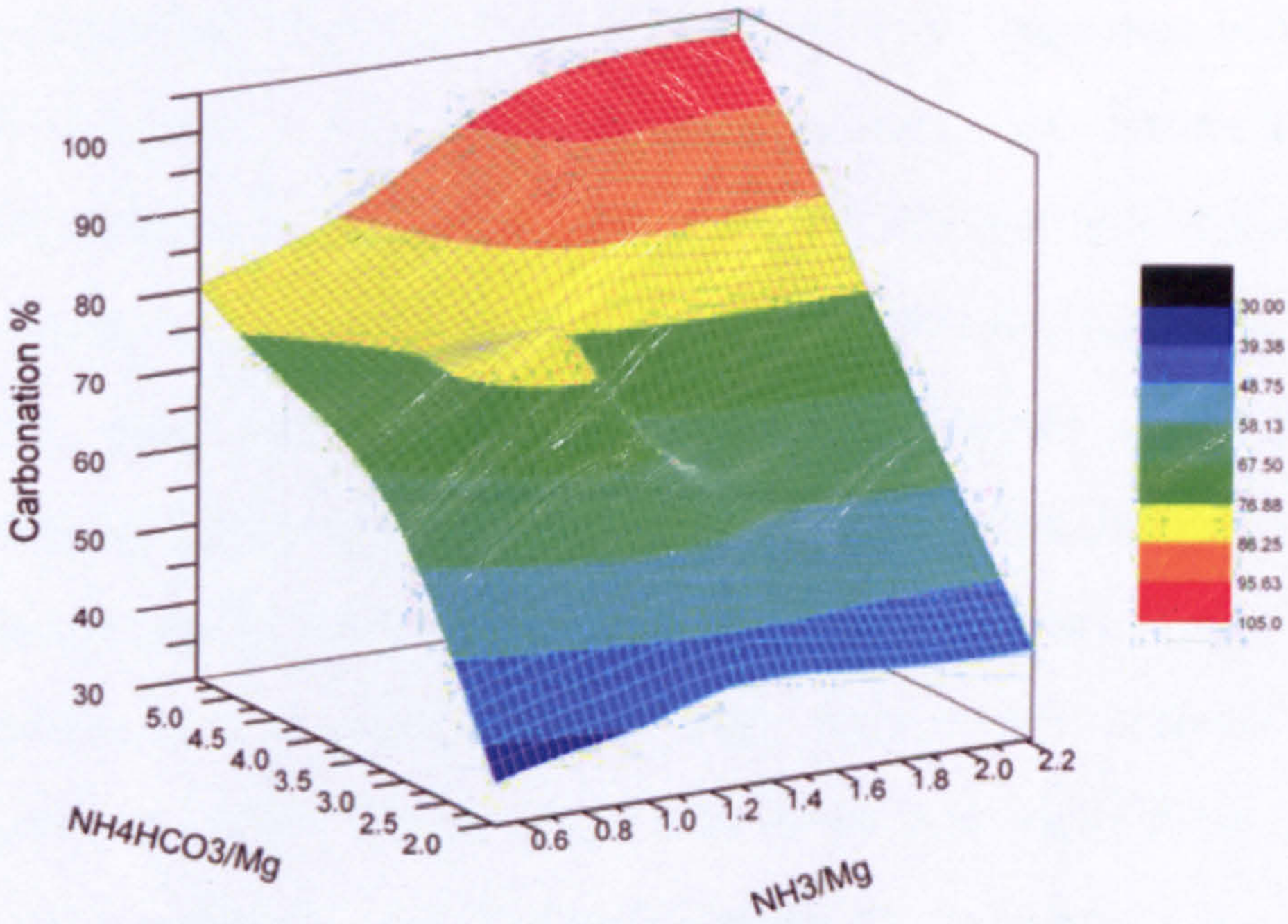

Figure 4-17: Plotted data of carbonation efficiency vs. molar ratio of Mg-NH_4HCO_3-NH_3

The process studied here presents higher carbonation efficiency than that reported by other researchers' work (Gerdemann *et al.*, 2007; Teir *et al.*, 2007b). For example, in Gerdemann *et al.* work (2007), 64 % carbonation efficiency was achieved in direct carbonation of heat treated serpentine at 155 °C and 115 bars in 0.64 M $NaHCO_3$ and 1 M NaCl solution. In Teir's work (2007b), the

conversion of magnesium ions to hydromagnesite was 94 % using HNO_3 and 79 % using HCl at pH value of 9 with addition of NaOH (1.1 g NaOH / g precipitate). In this study, the highest carbonation efficiency is 95.9 % at 85 °C and ambient pressure within 30 mins by using NH_4HCO_3 and NH_3.

4.2.2.6 Mass balance

To examine the distribution of Mg released from serpentine in the solids formed in the process (products 1, 2 and 3) and filtrate 3, a mass balance was constructed based on the XRF and ICP-AES and the results are presented in Fig 4-18. It can be seen that most of the Mg from the original mineral serpentine ends up in the precipitated hydromagnesite (product 3). The use of additives at the optimized ratio to improve carbonation conversion results in less Mg remaining in the final solution after carbonation (filtrate 3, experiments 6-10). Longer dissolution times may leach more Mg from the serpentine and therefore reduce the amount present in product 1 (Park and Fan, 2004). In addition, the presence of Mg in product 2 can be minimised by hot water washing (Everingham, 1976). The mass balance for Si and Fe is presented in Table 4-5, as the concentration of these two elements in filtrate 3 is very small. It can be seen that most of the Si remains in the residue after dissolution (product 1). In contrast, most of the Fe ends up in both the residue after dissolution (product 1) and the precipitate after

pH-swing (product 2) depending on the dissolution efficiency. The concentration of Si and Fe in filtrate 3 is negligible (Table 4-4). The total mass balances of Mg from filtrate 3 and product 1, 2 and 3 are 99-100% of the mass of Mg in original mineral is accounted for.

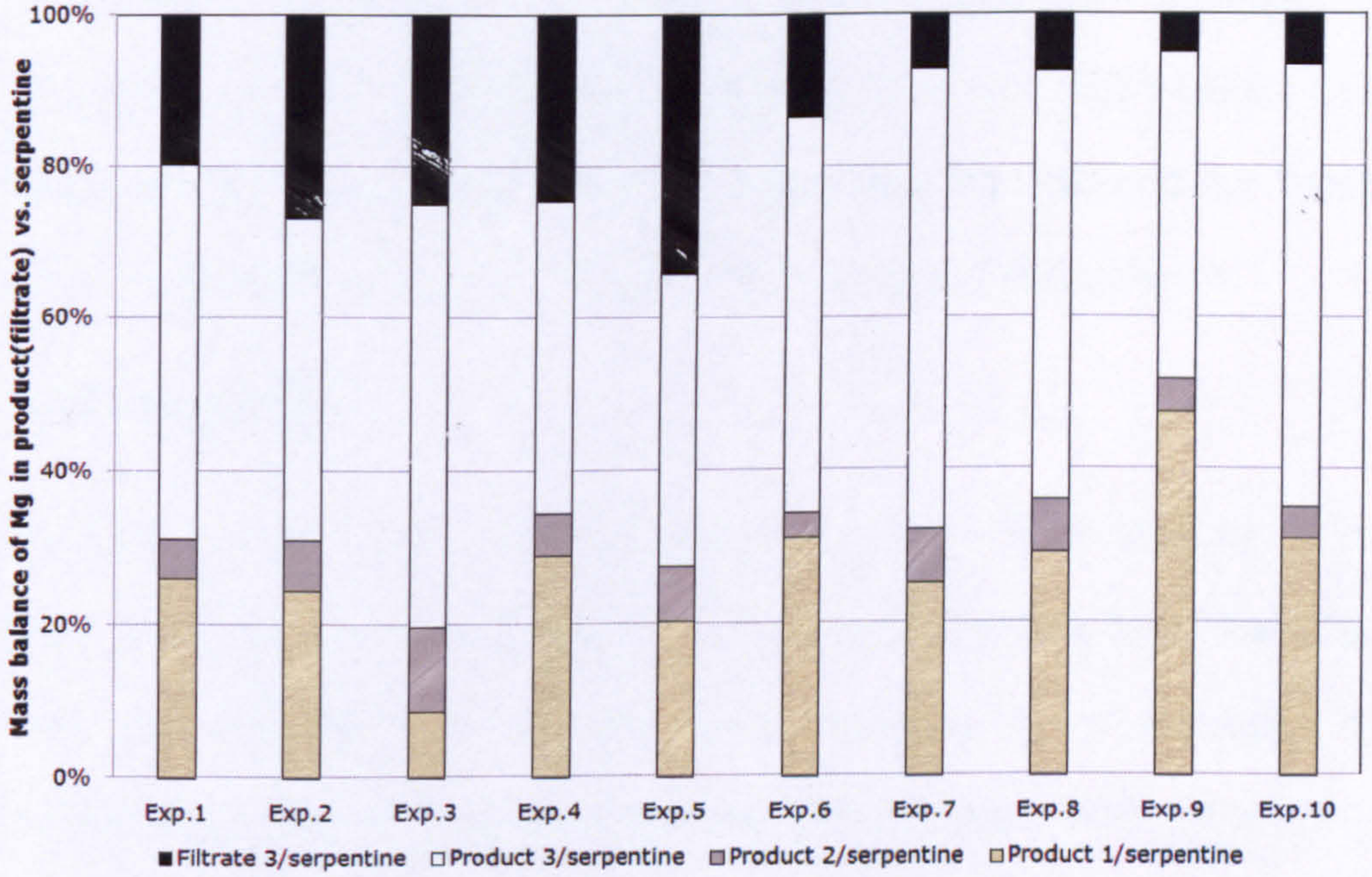

Figure 4-18: Mass balance of Mg in product 1, 2 and 3 and filtrate 3 in relation to serpentine

Considering that the dissolution efficiency can achieve 90 % at 100 °C and 2 h and that the carbonation efficiency is 95.9 % when the molar ratio of Mg:NH_4HCO_3:NH_3 is 1:4:2, the net conversion of serpentine to hydromagnesite is calculated to be 86.3 %. Taking this into account, about 2.63 t of serpentine, 8.48 t of NH_4HSO_4, 2.31 t of NH_4HCO_3 and 0.5 t of NH_3 are required to sequester 1 t CO_2, and 2.95 t of hydromagnesite is produced. If the 95 % regeneration efficiency of NH_4HSO_4 and NH_3 is considered, 0.12 t of

NH_4HSO_4 and 0.025 t of NH_3 is consumed to sequester 1 t CO_2. All the chemicals used in this process can be obtained from $(NH_4)_2SO_4$. Considering the current price for $(NH_4)_2SO_4$ is 90 US$/t (ICIS, 2010), the cost for make-up chemicals of this process is estimated to be 18 US$/t CO_2. However, in Teir's work (2007b), the cost for make-up chemicals is 1300 US$/t CO_2 when using HCl and 1600 US$/t CO_2 when using HNO_3. Moreover, the cost could be reduced by using high solid/liquid ratio and this will be the focus of future work.

4.2.3 Summary

In the Section 4.2, the precipitation of hydromagnesite from prepared high Mg concentration solution by using NH_3 and NH_4HCO_3 and the regeneration of NH_3 and NH_4HSO_4 were studied. In conclusion, pure hydromagnesite can be produced from serpentine with regenerated ammonium salts with a net conversion of 86.3 %. Amorphous silica can be obtained from the dissolution step. By-products with maximum 27.5 wt. % Fe content were obtained from the pH regulation and removal of impurities step. The additives used, NH_4HSO_4 and NH_3, can be regenerated by thermal decomposition of $(NH_4)_2SO_4$ at 330 °C. The addition of ammonia water before carbonation could significantly improve the carbonation efficiency. It must be pointed out that NH_4HCO_3 should be added into solution after 60 °C to prevent the production of magnesium ammonium carbonate. The mass ratio of Mg:NH_4HCO_3:NH_3 is the key factor to

control the carbonation efficiency, and it was found that when the mass ratio of $Mg:NH_4HCO_3:NH_3$ was 1:4:2, the carbonation efficiency achieved 95.9 %. From the TGA studies, the regeneration efficiency of NH_4HSO_4 in this process was found to be 95 %. According to the mass balance, about 2.63 t of serpentine, 0.12 t of NH_4HSO_4, 2.31 t of NH_4HCO_3 and 0.025 t of NH_3 are required to sequester 1 t CO_2, and 2.95 t of hydromagnesite is produced.

Chapter 5. CCSM Process route at high solid to liquid ratio condition

In Chapter 4, the author discussed the CCSM process route at low solid to liquid ratio condition (50 g/l) using recyclable ammonium salts, where 90% dissolution efficiency at 90 °C for 3 h, and 90% carbonation efficiency at 80 °C for 1h were achieved. Based on these results and the used solid to liquid ratio (50 g/l), 50-56 t of water is required to sequester 1 t CO_2. Since water evaporation is the most energy intensive step in the process (typical energy consumption for mechanical vapour recompression (MVR) evaporator system is 10-36 kWh/t evaporated water (Karasek, 2010), the water usage need to be minimised to make this process economically feasible. Therefore, the CCSM process was investigated at high solid liquid ratio (above 200 g/l). The process was described in Section 3.1.2 and the schematic of the process is presented in Figure 3-2. In this section, the autoclave pressure reactor was used to solve problems such as volume expansion and the loss of ammonia vapour. The effects of using different solid to liquid ratios on the dissolution efficiency and carbonation conversion were investigated. The comparison of carbonation conversions using different ammonium salts, the amount of residual NH_4HSO_4 after

dissolution and the pH increase were studied. Finally, the mass balance of all streams is reported.

5.1 Experimental methods

5.1.1 Dissolution of serpentine using recyclable ammonium salts at high solid/liquid ratio

In Section 3.4, the author showed that NH_4HSO_4 is suitable for dissolving magnesium from serpentine, as presented in Eq. 4-2.

Magnesium sulfate's solubility in water is reported to be 33.7 g/100 g water at 20 °C and increased to 52.9 g/100 g water at 90 °C (Solubility Database, 2011). Therefore, magnesium sulfate ($MgSO_4$) would precipitate in the dissolution of serpentine using NH_4HSO_4 when the solid to liquid ratio is above 280 g/l [14]. However, $MgSO_4$ was found to precipitate when the solid to liquid ratio was above 100 g/l (Section 4.1.6). This is explained as the solubility of $MgSO_4$ is lower in a mixture solution than in pure water solution due to the activity of other dissolved species, such as NH_4^+ and SO_4^{2-} and HSO_4^-. In this study, solid to liquid ratio values of 200 g/l and 300 g/l were used.

In this study, the same serpentine sample with particle size fraction between 75-150 μm was used as in Chapter 4. The dissolution

[14] 33.7 g/100 g water × 1000g water × 24/120/24 %, 1000 g water is 1 litre water, 24 and 120 is molecular weight of Mg and MgSO4, 24 % is the weight % of Mg in serpentine, assuming 100 % dissolution efficiency

experiments were carried out in a stirred 300 ml T316 stainless steel autoclave reactor from Parr Instrument Company. The reactor system (shown in Figure 5-1) includes a heating system with heating mantel, and a temperature control box (Parr 4843 controller) to accurately maintain a stable heating environment from ambient to 225°C, mechanical stirring and a cooling water system. The solutions were mixed by using mechanical stirring. A pressure of 1 bar during the experiment was generated due to the water vapour from solution.

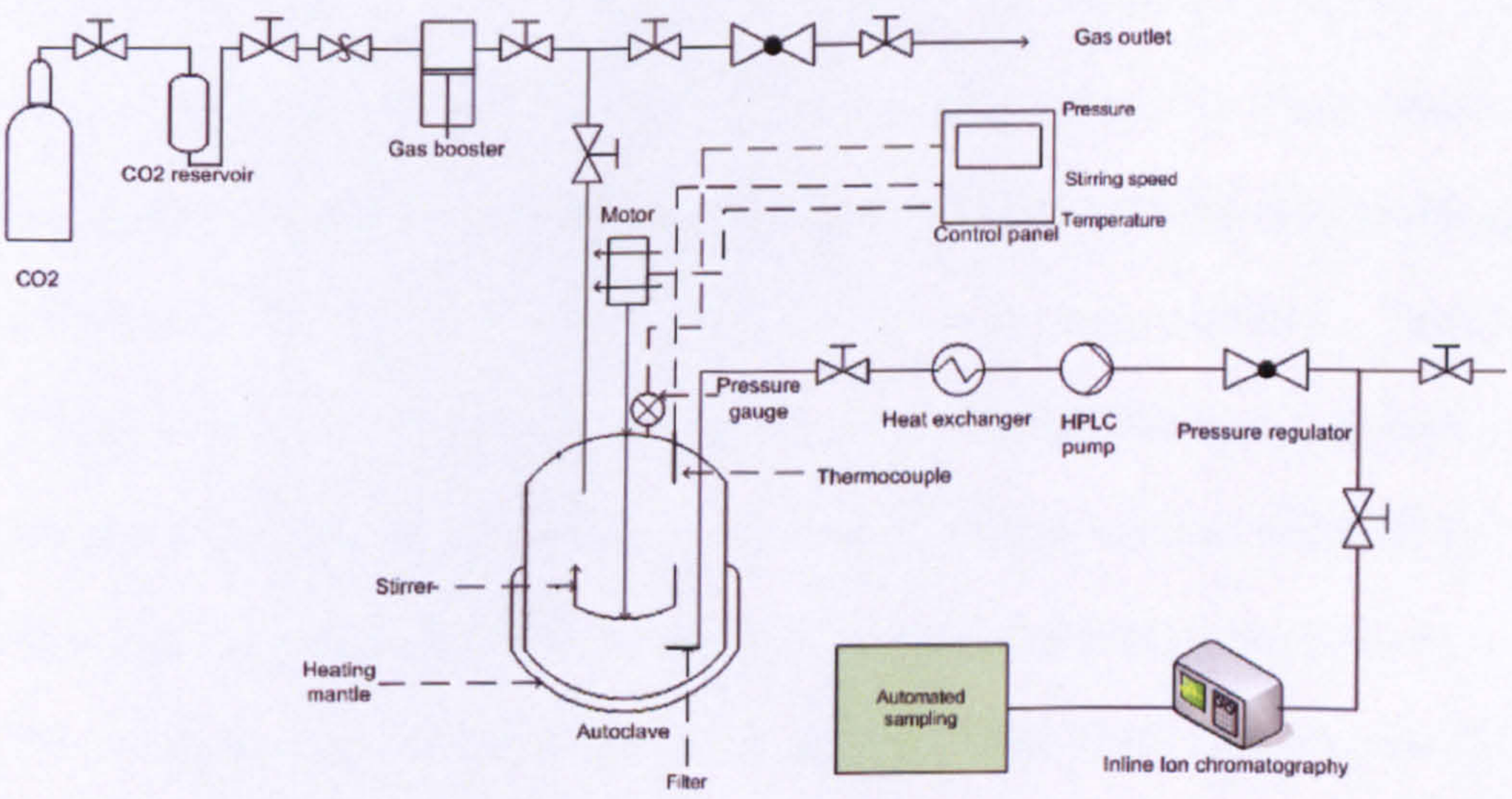

Figure 5-1: Schematic diagram of autoclave reactor used in this study.

The concentration of NH_4HSO_4 in this study was established based on the stoichiometric amount, where 2 parts of NH_4HSO_4 are consumed to dissolve 1 part of Mg from serpentine. For example, 40 g of serpentine (containing 24 wt % of magnesium) required ammonium bisulfate as follows:

$$C_{NH_4HSO_4} = \frac{2 \times 40(g) \times 24\%}{24(g/mol) \times 0.2(l)} = 4(mol/l)$$

Equation 5-1

Therefore, 4 mol/l NH_4HSO_4 was used for experiments where the solid to liquid ratio was 200 g/l. Thus 6 mol/l NH_4HSO_4 was used for the experiments where the solid to liquid ratio was 300 g/l.

The matrix of dissolution experiments conducted at different conditions is listed in Table 5-1. In order to compare the dissolution efficiency when using different types of reactors (glass and autoclave), two experiments were conducted using the glass reactor for the two solid to liquid ratios. The same procedure was used as presented in Section 4.1.1 for these two experiments. Typical dissolution experiments in the autoclave reactor were performed as follows. A serpentine sample was placed into a vessel with 200 ml NH_4HSO_4 solution at the corresponding concentration depending on the solid to liquid ratio used. The reactor was then sealed and the stirring was started at the speed of 800 rpm. Once reaching 100 °C, the reaction time was started for 3 h. At the end of the experiment, the vessel was cooled down quickly to room temperature by immersing the vessel in an ice bath. Once the reactor was opened, the slurry was washed and transferred into a 1500 ml glass beaker, where Millipore water was used to dissolve the precipitated $MgSO_4$. After 30 mins, the slurry was filtered using a 0.45 µm syringe filter

unit. The filtrate was prepared in a 10% HNO_3 solution for Inductively Coupled Plasma – Atomic Emission Spectroscopy (ICP-AES) analyzer for determining the concentrations of Mg, Ca, Fe, Al and Si.

Table 5-1: Matrix of dissolution experiments at different conditions.

Expt no.	reactor	Solid/liquid ratio (g/l)	Stirring	Sample weight (g)	Conc. of NH_4HSO_4 (mol/l)
D1	glass	200	1500 rpm	40	4
D2	glass	300	1500 rpm	80	6
D3	autoclave	200	mechanical	40	4
D4	autoclave	300	no	80	6
D5	autoclave	300	mechanical	80	6

For the carbonation experiments, the same dissolution experiment procedure as described above was followed to prepare Mg-rich slurry. The reactor vessel was moved to a fume cupboard for pH regulation after dissolution (see Section 5.1.2).

5.1.2 Measuring the amount of residual NH_4HSO_4 and pH regulation

After the dissolution, the pH values of the solution were acidic (0.9~1.2) due to the presence of residual NH_4HSO_4. Because the carbonation reaction is favourable at high pH values, it was necessary to increase the pH of the solution to alkaline values by

adding ammonia water (see Eq. 4-3). The reason for using ammonia water is that the acid/base reaction produces ammonium sulphate, which can be converted back to NH_3 and NH_4HSO_4 in the regeneration step in order to realize the recycling of the additives (Figure 3-2). Some impurities, such as Fe, Al, Cr, Zn, Cu and Mn, can also react with the added ammonia water to produce some solid products (see Eq.4-4 and 4-5).

Typical pH-swing experiments were performed as follows. Ammonia water (35 wt. %) was added into the slurry from the dissolution step until the pH value was neutral. The ammonia water consumed was recorded by reading the scale (ml) on a buret. During this process, the solution was stirred and an in-situ pH probe (Orion 720APlus pH meter) was used to measure the pH value. The residual amount of NH_4HSO_4 in the slurry was determined from the stoichiometric amount of ammonia water consumed in the acid/base reaction. The concentration of residual NH_4HSO_4 in slurry was calculated as follows:

$$C_r = \frac{1000\rho(g/ml)w\%}{M(g/mol)} \times \frac{V_1(ml)}{V_2(ml)}$$

Equation 5-2

C_r is the concentration of residual NH_4HSO_4 in the slurry. V_1 is the volume of the ammonia water used to regulate the pH to neutral. V_2 is the volume of slurry as 200 ml. p is the density of ammonia

water (0.88 g/ml). w% is the weight percentage of ammonia in ammonia water (35 %). M is the molecular weight of ammonia (35 g/mol). The overall uncertainty from the measured data is estimated to be ~1% as determined from the duplicate experiments. The uncertainty stems from errors in four measured quantities, i.e., the evaporation of ammonia water in storage, the loss of slurry, the reading of V_1 on buret and the analysis error of the pH meter.

5.1.3 Production of magnesite using NH_4HCO_3 or $(NH_4)_2CO_3$

The reaction of the production of magnesite by reacting $MgSO_4$ with NH_4HCO_3 and $(NH_4)_2CO_3$ is presented in Eq. 5-3 and 5-4. Once the dissolved aqueous $MgSO_4$ was consumed in these carbonation reactions, the suspended solid $MgSO_4$ dissolved into aqueous $MgSO_4$ (shown in Eq. 5-5) to supply the consumed $MgSO_4$.

$$MgSO_4(aq)+2NH_4HCO_3(aq)+2H_2O(l)\rightarrow$$
$$MgCO_3\bullet 3H_2O(s)\downarrow+(NH_4)_2SO_4(aq)+CO_2(g)\uparrow$$

Equation 5-3

$$MgSO_4(aq)+(NH_4)_2CO_3(aq)+3H_2O(l)\rightarrow$$
$$MgCO_3\bullet 3H_2O\downarrow(s)+(NH_4)_2SO_4(aq)$$

Equation 5-4

$$MgSO_4(s)\rightarrow MgSO_4(aq)$$

Equation 5-5

$$5MgCO_3 \bullet 3H_2O(s) \rightarrow 4MgCO_3 \bullet Mg(OH)_2 \bullet 4H_2O(s) \downarrow + 10H_2O(l) + CO_2(g) \uparrow$$

Equation 5-6

$$4MgCO_3 \bullet Mg(OH)_2 \bullet 4H_2O(s) + CO_2(g) \rightarrow 5MgCO_3 \downarrow (s) + 4H_2O(l)$$

Equation 5-7

The formation of magnesium carbonate species depends on temperature and pressure (Hänchen *et al.*, 2008). Nesquehonite ($MgCO_3 \bullet 3H_2O$) can precipitate from aqueous solutions at ambient temperature, as described in Eq. 5-6 and 5-7, while at higher temperatures (50 and 100 °C), nesquehonite is transformed into hydromagnesite ($4MgCO_3 \bullet Mg(OH)_2 \bullet 5H_2O$), as presented in Eq. 5-6. For temperatures above 100 °C or high pressure (>20 bar), hydromagnesite is transformed into magnesite ($MgCO_3$) as presented in Eq. 5-7 (Sandengen *et al.*, 2008). In this study, magnesite was produced as the experiments were conducted at 80 °C and a pressure above 20 bar.

The pressure in these experiments was caused by the decomposition of NH_4HCO_3 and $(NH_4)_2CO_3$. The increase of pressure was accompanied with an increase in temperature and stabilized once the temperature was constant. The reactions of the

decomposition of NH_4HCO_3 and $(NH_4)_2CO_3$ are presented in Eq. 5-8 and 5-9.

$$(NH_4)_2CO_3(aq) \rightarrow NH_4HCO_3(aq) + CO_2(g)\uparrow$$

Equation 5-8

$$NH_4HCO_3(aq) \rightarrow NH_3(g) + CO_2(g) + H_2O(l)$$

Equation 5-9

After carbonation, the temperature was cooled down and the pressure was decreased with the drop of temperature. The pressure also decreased resulting from the reaction between NH_3 and CO_2 gases and water (Eq. 5-10 and 5-11).

$$NH_3(g) + CO_2(g) + H_2O(l) \rightarrow NH_4HCO_3(aq)$$

Equation 5-10

$$NH_4HCO_3(aq) + CO_2(g) \rightarrow (NH_4)_2CO_3(aq)$$

Equation 5-11

For the carbonation experiments, after pH regulation the corresponding mass of NH_4HCO_3 or $(NH_4)_2CO_3$ was added. The mass of NH_4HCO_3 or $(NH_4)_2CO_3$ was weighed to established the stoichiometric amount according to the carbonation reaction (Equation 5-3 and 5-4). For example, for the 200 g/l solid to liquid ratio, assuming 100 % dissolution efficiency, 2 mol/l Mg^{2+} required

2 mol/l $(NH_4)_2CO_3$. The matrix of carbonation experiments conducted at different conditions is listed in Table 5-2.

Table 5-2: Matrix of dissolution experiments at different conditions.

Expt. no	Solid liquid ratio (g/l)	Ammonium salts	Conc. of salts (mol/l)	Temperature	Reaction time (h)
C1	200	$(NH_4)_2CO_3$	2	80	1
C2	300	$(NH_4)_2CO_3$	3	80	1
C3	200	NH_4HCO_3	2	80	1
C4	300	NH_4HCO_3	3	80	1

In order to compare the carbonation efficiency using different ammonium salts, the same amount of NH_4HCO_3 was used in experiments C3 and C4. After addition of ammonium salts, the vessel was sealed and heated to the required temperature. When the temperature was stabilized, the solution was kept at that temperature for 1 h. At the end of the experiment, the vessel was cooled down to room temperature using an ice bath and the residual pressure was released through a gas outlet valve. The reacted slurry was filtered with 0.45 µm Pall syringe filters and the filtrate is referred to as filtrate 1 (Figure 3-2). The solid residue was dried at 105 °C overnight and is referred to as product 1 (Figure 3-2). The composition of the product 1 was analyzed using XRF and the mineral phases were identified by XRD. The filtrate 1 was acidified

with HNO_3 for subsequent ICP-AES analysis to measure the concentration of elements such as Mg, Fe and Si.

The carbon content of the product 1 was measured by a Flash EA 1112 series elemental analyzer. The carbon fixation efficiency of the original mineral serpentine to magnesite is defined as follows:

$$Carbon\ fixation\ efficiency\ (\%) = \frac{C\ content\ (wt\%) \times 24 \times m}{12 \times m_{batch} \times w_{Mg}} \times 100$$

Equation 5-12

Where C content (wt. %) is measured by the elemental analyzer (EA). m is the mass (grams) of product 1 from carbonation experiment, m_{batch} is the mass of serpentine sample added. w_x is the initial weight percentage of mass of element x over the total mass of solid present in the original mineral sample. 24 and 12 are the molecular weight of Mg and C in magnesite, respectively.

5.2 Results and discussion

5.2.1 Dissolution of serpentine using recyclable ammonium salts at high solid/liquid ratio

The dissolution efficiencies of Mg, Si, Fe and Ca from serpentine using NH_4HSO_4 at high solid to liquid ratio (experiments D1-D5) are presented in Figure 5-2.

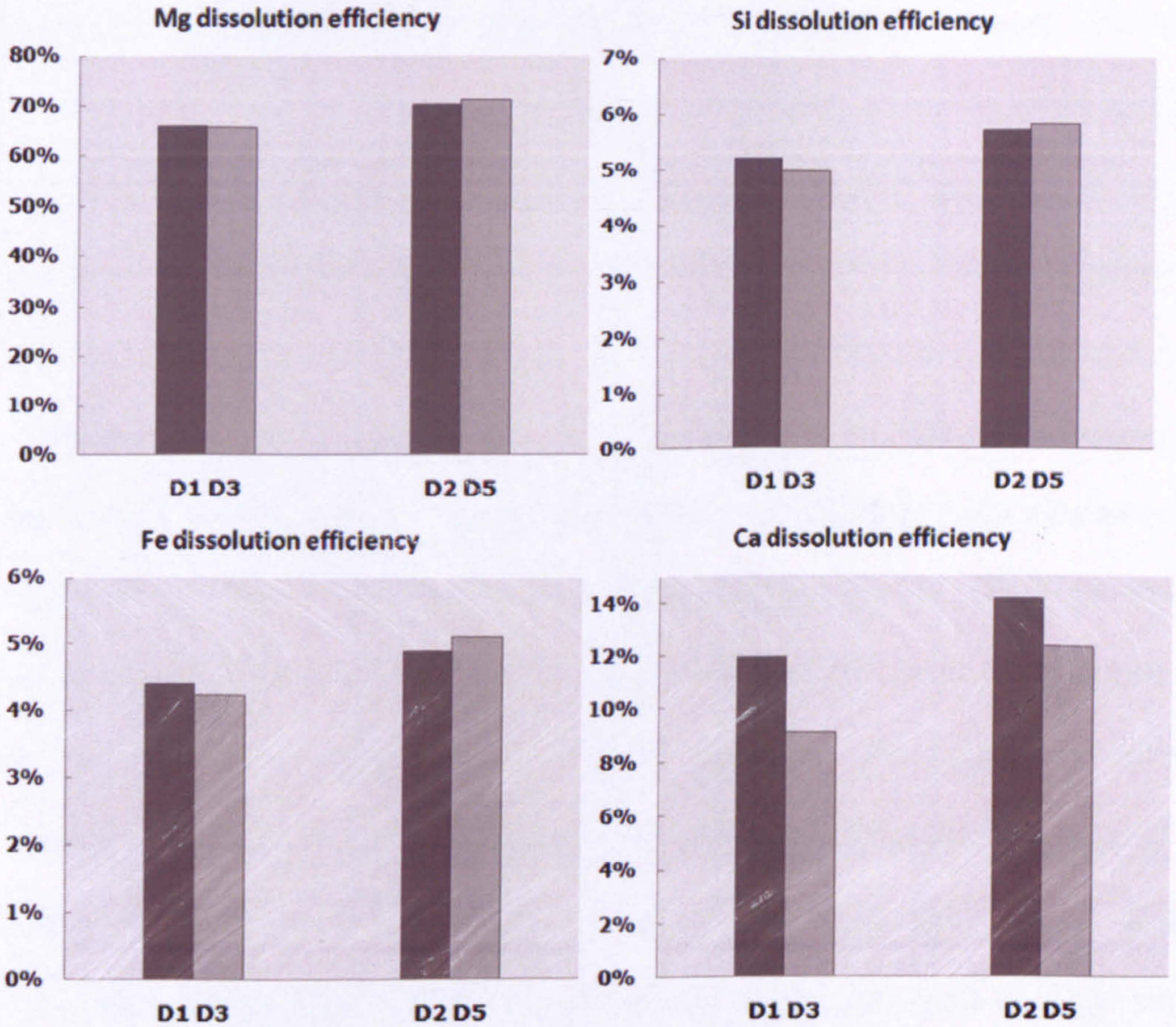

Figure 5-2: The effect of solid to liquid ratio to dissolution efficiencies of elements from serpentine (D1 and D3 are 200 g/l, D2 and D5 are 300 g/l).

It is found that around 64-72 % Mg was dissolved, while most of Si, Fe and Ca remained in the serpentine. Taking D5 (300 g/l solid to liquid ratio in the autoclave reactor) as an example, the dissolution efficiency of Mg from serpentine was 71.3 % at 100 °C for 3 h. However, only 5.5 % Si, 5.1 % of Fe and 12.3 % of Ca were dissolved in this experiment. This result is different with the previous dissolution studies at low solid to liquid ratio, where the dissolution efficiencies of Mg, Si and Fe from serpentine were 100 %, 17.6 % and 98 %, respectively, under the same temperature and

reaction time and using 50 g/l solid to liquid ratio (Figure 4-2 in Section 4.1.2). The decrease of dissolution efficiencies at high solid to liquid ratio is probably due to the precipitated $MgSO_4$ on the surface of mineral particles. With the progress of serpentine dissolution, the concentration of aqueous $MgSO_4$ continuously increases. When the concentration of aqueous $MgSO_4$ exceeds its solubility, the aqueous $MgSO_4$ precipitate as solid $MgSO_4$ (Reverse reaction of Eq. 5-5). The solid $MgSO_4$ precipitates onto to the surface of mineral particles, thus blocking the diffusion of NH_4HSO_4 in to the pore space of mineral particles. In addition, the stoichiometric molar ratio between NH_4HSO_4 and Mg (2:1) used for these dissolution experiments in this section can also cause the decrease of Mg dissolution in comparison with previous dissolution experiments in Section 4.1.2, where the excess mole ratio (2.8:1) was used.

The dissolution efficiency of serpentine is therefore influenced by the solid to liquid ratio used. The comparison of dissolution efficiencies of Mg, Si, Fe and Ca at different solid to liquid ratios (200 and 300 g/l) is also presented in Figure 5-2. It is found that the dissolution efficiencies of all elements increase slightly when the solid to liquid ratio increased from 200 g/l to 300 g/l. For example, the dissolution efficiency of Mg increased from 65.6 % to 71.3 % when using the autoclave reactor and from 66 % to 70.2 % for the experiments conducted in the glass reactor. This may be due the

intensive particle-particle interaction at high solid to liquid ratio. More collision at high solid to liquid ratio may break down particles or remove the product layer, and thus increasing the diffusion of NH_4HSO_4 into the pore space of the mineral particles. The effect of intensive particle-particle interaction at high solid to liquid ratio is probably similar to the effect of internal grinding reported by Park and Fan (2004). It can be seen from Figure 5-2 that the dissolution efficiency using different reactors is very similar. The main experimental difference between both reactors is the pressure, where 1 bar water vapour was obtained in the autoclave reactor. Thus the small pressure increase does not affect the dissolution of elements from serpentine.

In addition, the dissolution efficiency of serpentine is influenced by stirring. The comparison of dissolution efficiencies of Mg, Si, Fe and Ca at different stirring conditions is presented in Figure 5-3. It can be seen that dissolution efficiencies of the experiment with mechanical stirring (D5) is higher than that without stirring (D4) for the same solid to liquid ratio of 300 g/l. This indicates that the effect of stirring is probably similar to the particle-particle interaction, in that removal of the product layer and thus improves the dissolution efficiency (Bearat *et al.*, 2006).

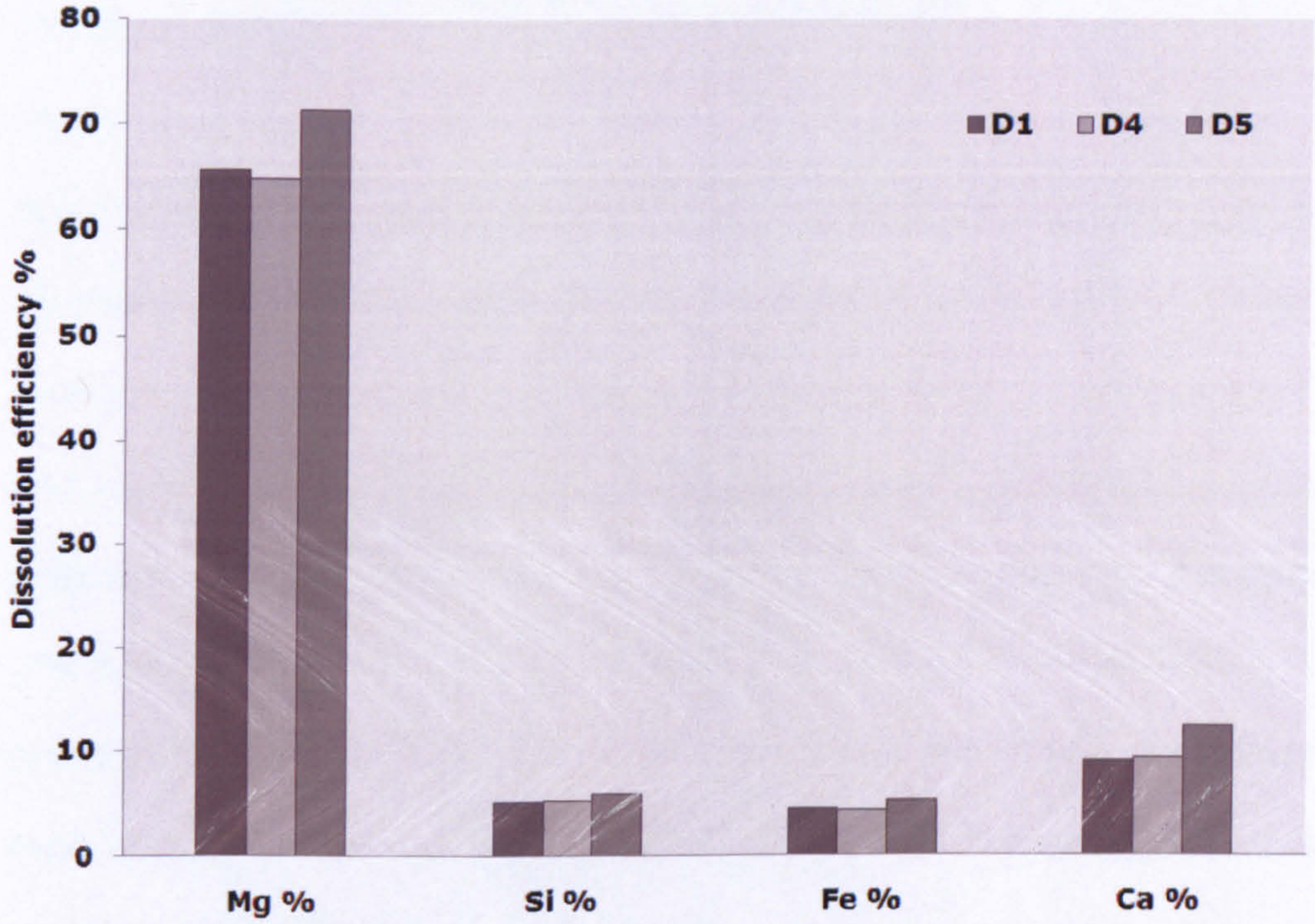

Figure 5-3: The effect of stirring to dissolution efficiencies of elements from serpentine (D1 used 1500 rpm stirring rate, D4 didn't use stirring and D5 used mechanical stirring).

At high solid to liquid ratio, the deposition of precipitated $MgSO_4$ on the surface of particles was thought to be the main reason for decreasing the dissolution efficiency (see the XRD results of product 1 from dissolution in Figure 5-8). It is believed that this problem can be overcome to some extent by intensive internal grinding (Park and Fan, 2004).

5.2.2 Measuring the amount of residual NH_4HSO_4 and pH regulation

It was found that after adding ammonia water (35 wt. %) to the slurry from the dissolution step, no particles precipitated. The presence of double ammonium salts ($(NH_4)_2Fe_2(SO_4)2•6H_2O$,

$(NH_4)_2Mg_2(SO_4)_2 \cdot 6H_2O$ and $(NH_4)_2Zn_2(SO_4)_2 \cdot 6H_2O$) have been reported in previous Section 4.2.2.2. But in this study, due to the lower dissolution of impurities such as Fe, Ca and other metal elements, the double ammonium salts did not precipitate and the ammonia water reacted with residual NH_4HSO_4 to form $(NH_4)_2SO_4$ and increased the pH. The residual concentrations of NH_4HSO_4 were measured by titration with ammonia water after the dissolution step. The comparison of initial and residual concentrations of NH_4HSO_4 is presented in Figure 5-4. The concentration of NH_4HSO_4 decreased from 6 mol/l to 1.6-1.7 mol/l at 300 g/l and from 4 mol/l to 1.1-1.2 mol/l at 200 g/l after dissolution. Therefore, around 70-72.8 % of NH_4HSO_4 was consumed in the dissolution step compared to the stoichiometric value of 100 %, probably because of the blockage of the diffusion of NH_4HSO_4 in the pore space of inner fresh mineral caused by the deposition of precipitated $MgSO_4$.

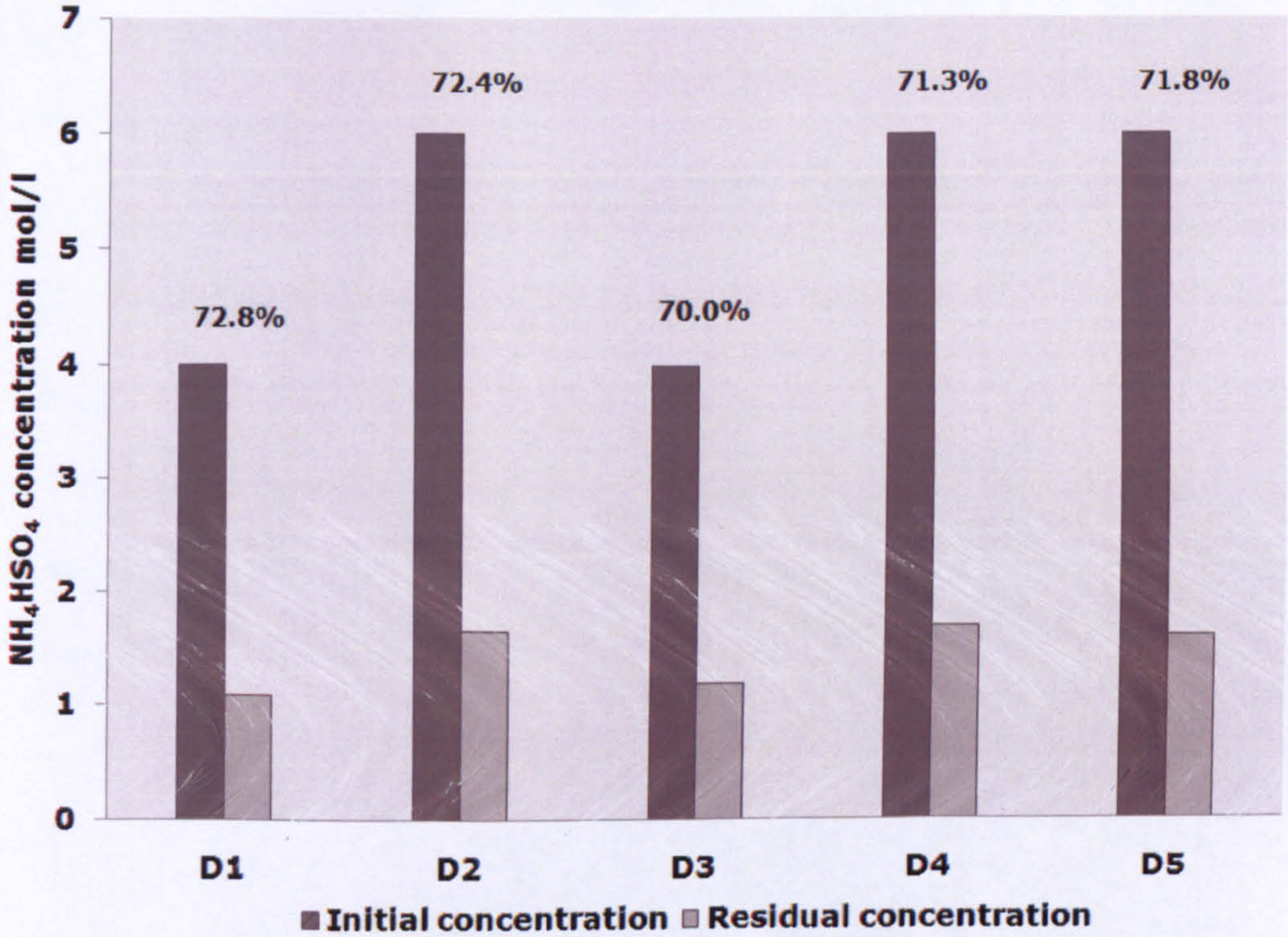

Figure 5-4: Comparison of concentration of NH_4HSO_4 before and after dissolution. (Initial concentration is 4 mol/l at 200 g/l and 6 mol/l at 300 g/l, the % value in figure is defined by the consumed NH_4HSO_4 concentration over initial concentration.)

After regulating the pH value to 7, NH_4HCO_3 and $(NH_4)_2CO_3$ were added into the slurry. The pH change of the slurry is presented in Figure 5-5. It is found that the pH increased from 7 to 8.2-8.5 when using $(NH_4)_2CO_3$ and was constant at the value of 7 when using NH_4HCO_3 because of the higher alkalinity of $(NH_4)_2CO_3$ (pH of 1 M solution is around 8.5) than that of NH_4HCO_3 (pH of 1 M solution is around 7.5). The higher pH value will be helpful for the subsequent carbonation reactions as the CO_3^{2-} ions are dominant when the pH is above 6.5. The CO_3^{2-} ions can directly react with Mg^{2+} to precipitate $MgCO_3$, while HCO_3^- ions firstly react with Mg^{2+} to form $Mg(HCO_3)_2$ and then convert into $MgCO_3$ when heated. The amount of NH_4HCO_3

and $(NH_4)_2CO_3$ added is based on the stoichiometric amount required in the carbonation reaction assuming 100 % dissolution of Mg ions from the original mineral serpentine. However, only 70 % Mg dissolution efficiency was achieved, and therefore, there will be excess of NH_4HCO_3 and $(NH_4)_2CO_3$ in the carbonation. The excess of NH_4HCO_3 and $(NH_4)_2CO_3$ can improve the carbonation efficiency, as a high content of reactive component enhances the probability of interaction between molecules.

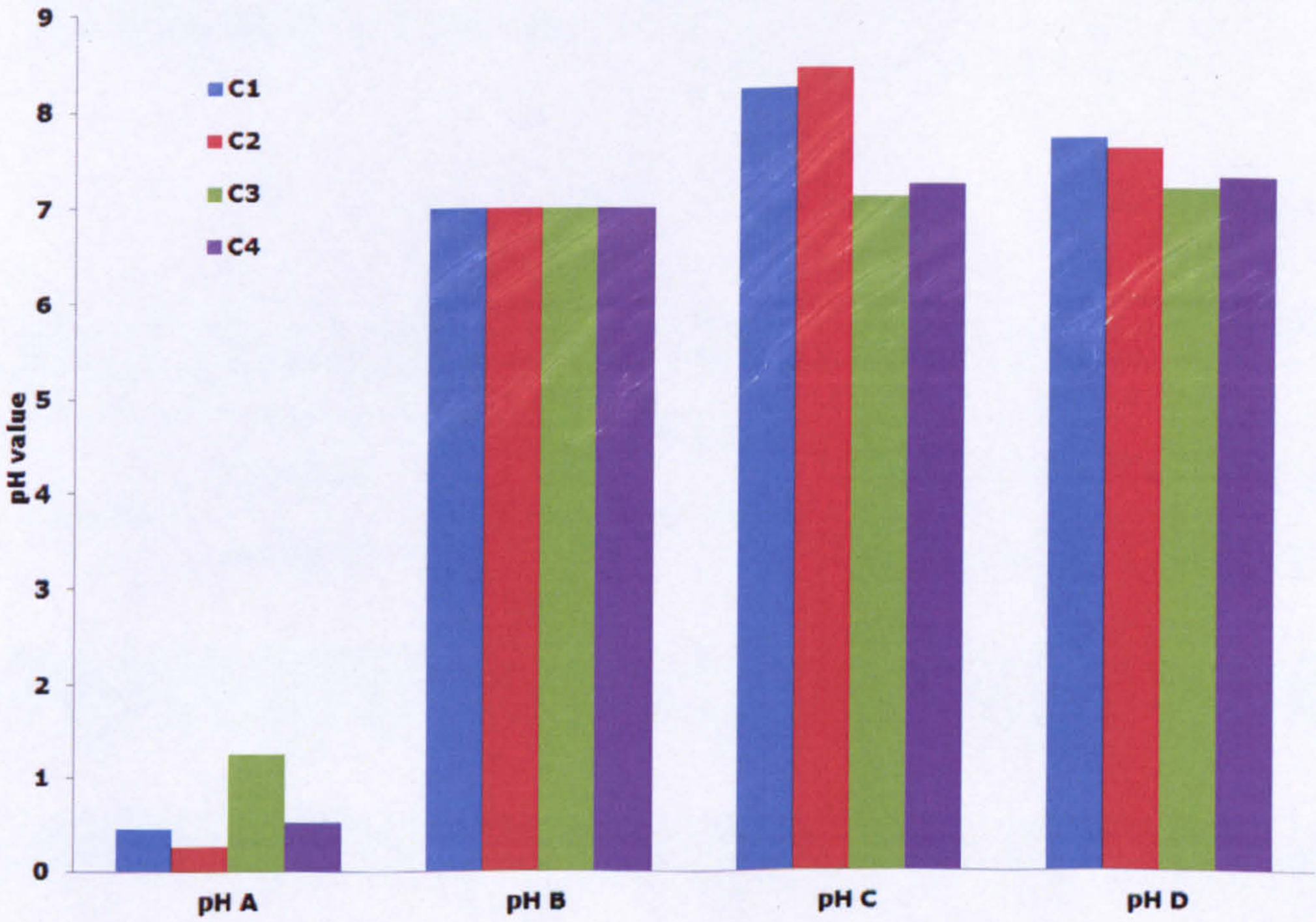

Figure 5-5: pH change of slurry at high solid liquid ratio condition. (pH A was measured after dissolution, pH B was 7 and measured after pH-regulation, pH C was measured after adding NH_4HCO_3 or $(NH_4)_2CO_3$ before carbonation and pH D was measured after carbonation.)

5.2.3 Production of magnesite using NH_4HCO_3 or $(NH_4)_2CO_3$

Four carbonation experiments were carried out using different solid to liquid ratios of 200 and 300 g/l and different additives of NH_4HCO_3 and $(NH_4)_2CO_3$, as shown in Table 5-3. The carbon content of product 1 and Mg concentrations of filtrate 1 from carbonation experiments are presented in Table 5-3 as well. The carbonation efficiency was calculated based on the following equation:

$$Carbonation\ efficiency = \frac{Carbon\ Fixation\ efficiency}{Dissolution\ efficiency} \quad [15]$$

Equation 5-13

Table 5-3: Carbon contain of product 1, Mg concentration of filtrate 1, fixation efficiency, dissolution and carbonation efficiencies in experiment C1-C4.

Expt No.	Carbon % (EA)	Mg conc. in filtrate 1 (mol/l)	Fixation efficiency %	Dissolution efficiency %	Carbonation efficiency %
C1	3.3	601.0	44	66	67
C2	2.8	361.5	47	71	65
C3	1.3	1238.5	18	66	27
C4	1.7	530.6	22	71	31

It can be seen from Table 5-3 that the highest fixation efficiency of 47% was achieved for the experiment C2, where the solid to liquid ratio was 300 g/l and using $(NH_4)_2CO_3$. The fixation efficiency of

[15] The carbon fixation and dissolution efficiencies are defined in Equation 5-12 and 4-1, respectively.

experiment C1 is relatively lower than that of C2 of 44 %. However, when NH_4HCO_3 was used for experiment C3 and C4, the fixation efficiency decreased to 18 % and 22 %, respectively. In order to understand the reason for the high fixation efficiency using $(NH_4)_2CO_3$, the thermodynamic properties of the reactions of $MgSO_4$ with $(NH_4)_2CO_3$ and NH_4HCO_3 were determined by using HSC 5.1 software and the results are presented in Table 5-4. The enthalpy of reaction of $MgSO_4$ with $(NH_4)_2CO_3$ is negative, which means that the reaction is exothermic and releases 36.15 kJ/mol. However, the enthalpy of reaction of $MgSO_4$ with NH_4HCO_3 is positive, which means that the reaction is endothermic and needs 53.06 kJ/mol. For the Free Gibbs energy, the reaction of $MgSO_4$ with $(NH_4)_2CO_3$ releases heat at 54.96 kJ/mol, which is higher than for the reaction of $MgSO_4$ with NH_4HCO_3 (47.28 kJ/mol). In addition, the reaction rate (Log K) of $MgSO_4$ with $(NH_4)_2CO_3$ is faster than reaction of $MgSO_4$ with NH_4HCO_3. Thus, the carbon fixation efficiency is significantly improved when using $(NH_4)_2CO_3$ compared to that using NH_4HCO_3.

Table 5-4: Thermodynamic properties of reactions of $MgSO_4$ with $(NH_4)_2CO_3$ and NH_4HCO_3

Reaction	T(°C)	ΔH(kJ)
$MgSO_4(aq)+(NH_4)_2CO_3(aq)\rightarrow MgCO_3\downarrow+(NH_4)_2SO_4(aq)$	80	-36.15
$MgSO_4(aq)+2NH_4HCO_3(aq)\rightarrow MgCO_3\downarrow+(NH_4)_2SO_4(aq)+H_2O(l)+CO_2\uparrow$	80	53.06

The XRD results of product 1 from C2 and C3 are presented in Figures 5-6 and 5-7, respectively. Magnesite and lizardite (mineral phase of serpentine) were identified in product 1 from C2. However, additional phases of $(NH_4)_2SO_4$ and $(NH_4)_2Mg(SO_4)_2 \cdot 6H_2O$ as mascagnite and boussingaultite, respectively, were identified in product 1 from C3. The reason for the presence of these solid sulfate salts is because of the low carbonation efficiency (27-30 %) of the experiments using NH_4HCO_3. Magnesite was found for the high solid to liquid ratio experiments (C1 and C2) instead of hydromagnestie for the low solid to liquid ratio experiments (C3 and C4). This can be explained by the CO_2 pressure (>20 bar, see Figure 5-8), as reported by Hanchen *et al.* (2008). The pressure increased due to the decomposition of $(NH_4)_2CO_3$ and NH_4HCO_3 at a temperature above 60 °C, as described in Eq. 5-8 and 5-9. The pressure change of C1-C4 was recorded and presented in Figure 5-8. It can be found that for C1 and C2, where $(NH_4)_2CO_3$ was used, the pressure raised sharply from 0 to 320 psi when the temperature was increased from ambient to 80 °C, and then went up continually from 320 psi to 440 psi after 60 mins and finally decreased to 125 psi when the temperature cooled down to ambient. However, for C3 and C4, where NH_4HCO_3 was used, the pressure raised from 0 to 602 psi when the temperature increased from ambient to 80 °C, and then went up continually from 602 psi to 758 psi after 60 mins and finally decreased to 424 psi when the temperature cooled down

to ambient. The higher pressure obtained when NH_4HCO_3 was used compared to that using $(NH_4)_2CO_3$ can be explained by the CO_2 produced from the carbonation reaction of $MgSO_4$ with NH_4HCO_3. It has been reported that high pressure can help the carbonation reaction due to the high solubility of CO_2 at high pressure (O'Connor, 2004; Alexander *et al.*, 2007). However, since the carbonation rate limiting step in this study is thought to be the diffusion of un-dissolved $MgSO_4$ and ammonium salts ($(NH_4)_2CO_3$ and NH_4HCO_3) in liquid phase, the high pressure will not help the carbonation reaction.

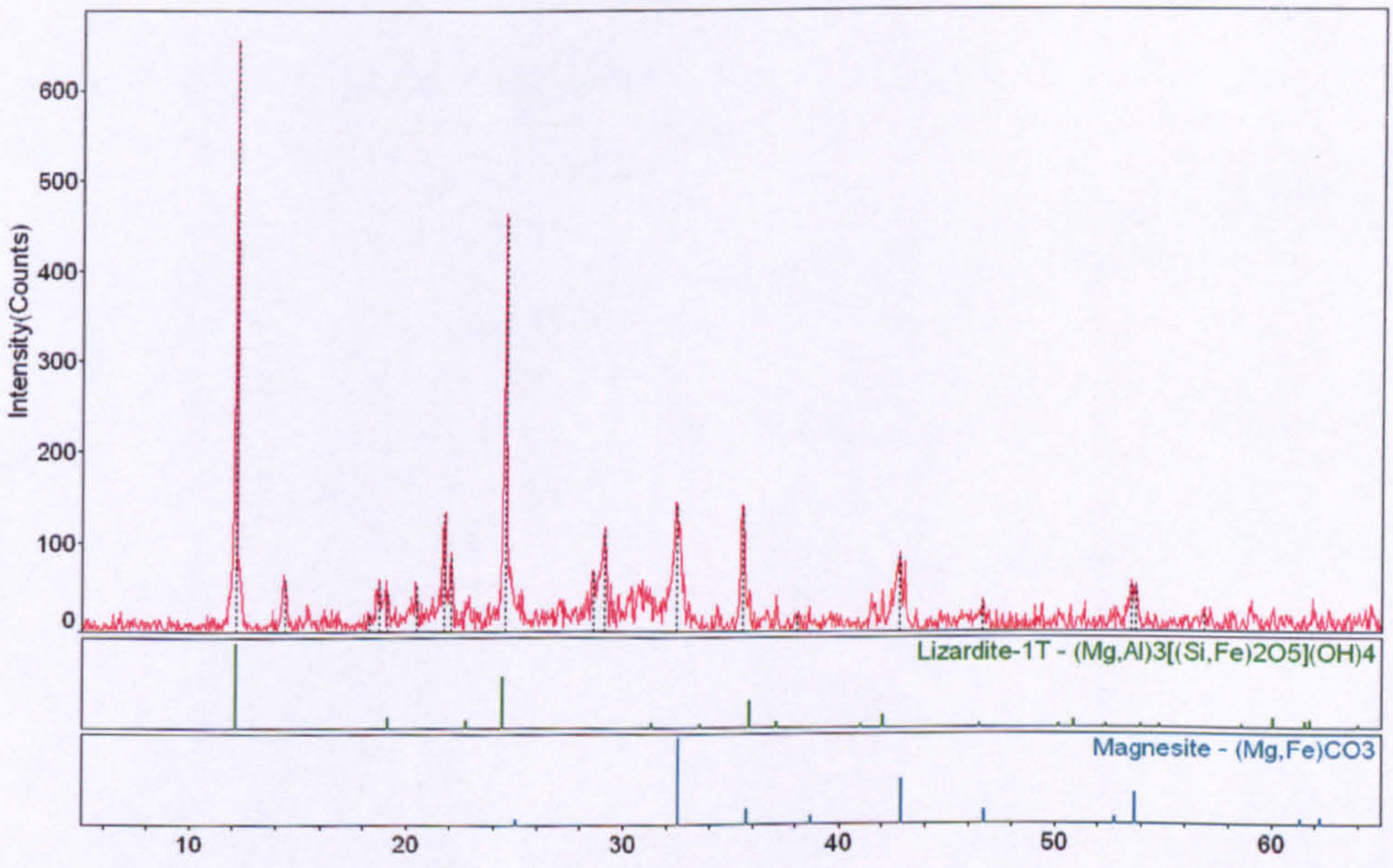

Figure 5-6: XRD of product 1 from C2.

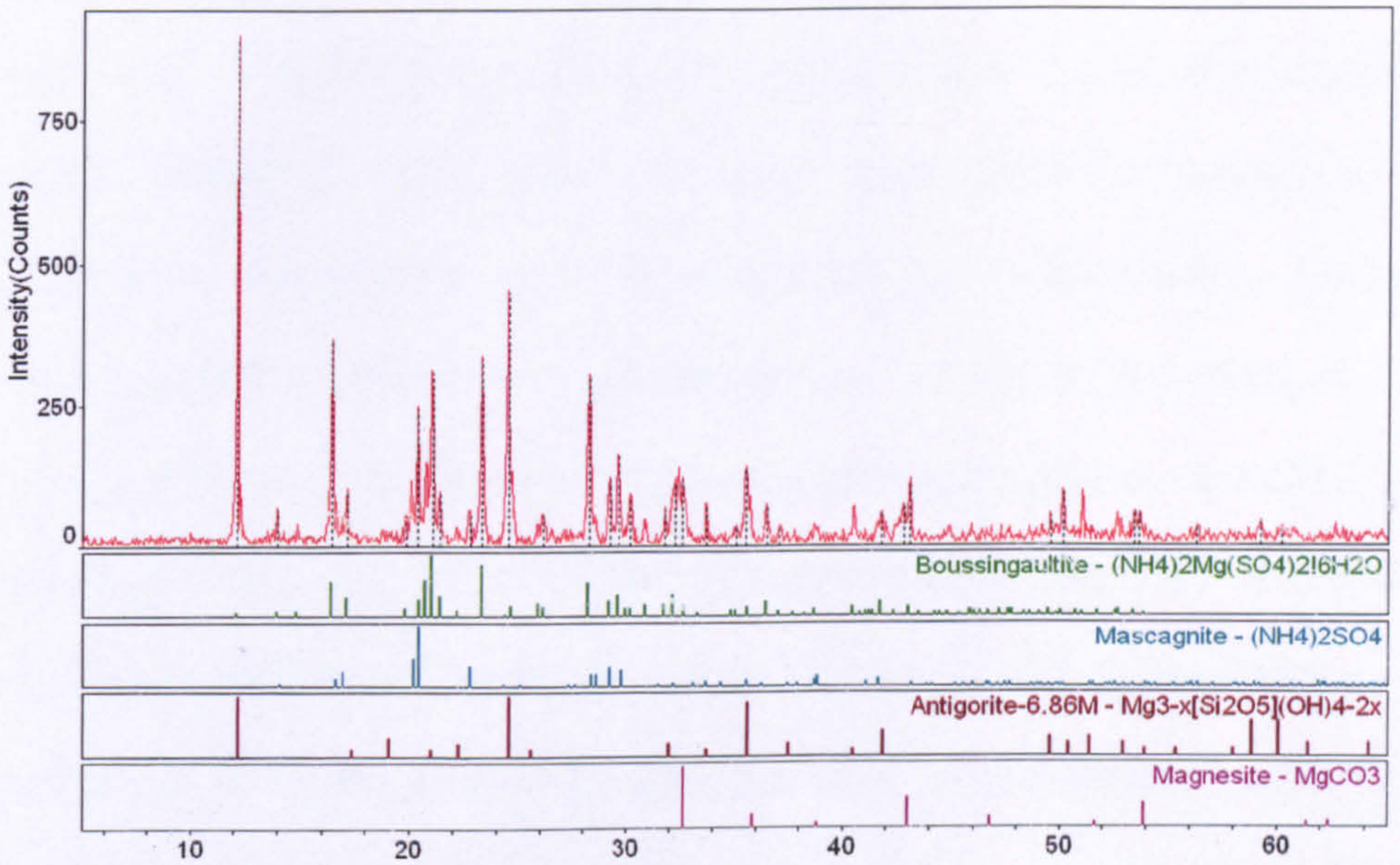

Figure 5-7: XRD of product 1 from C3.

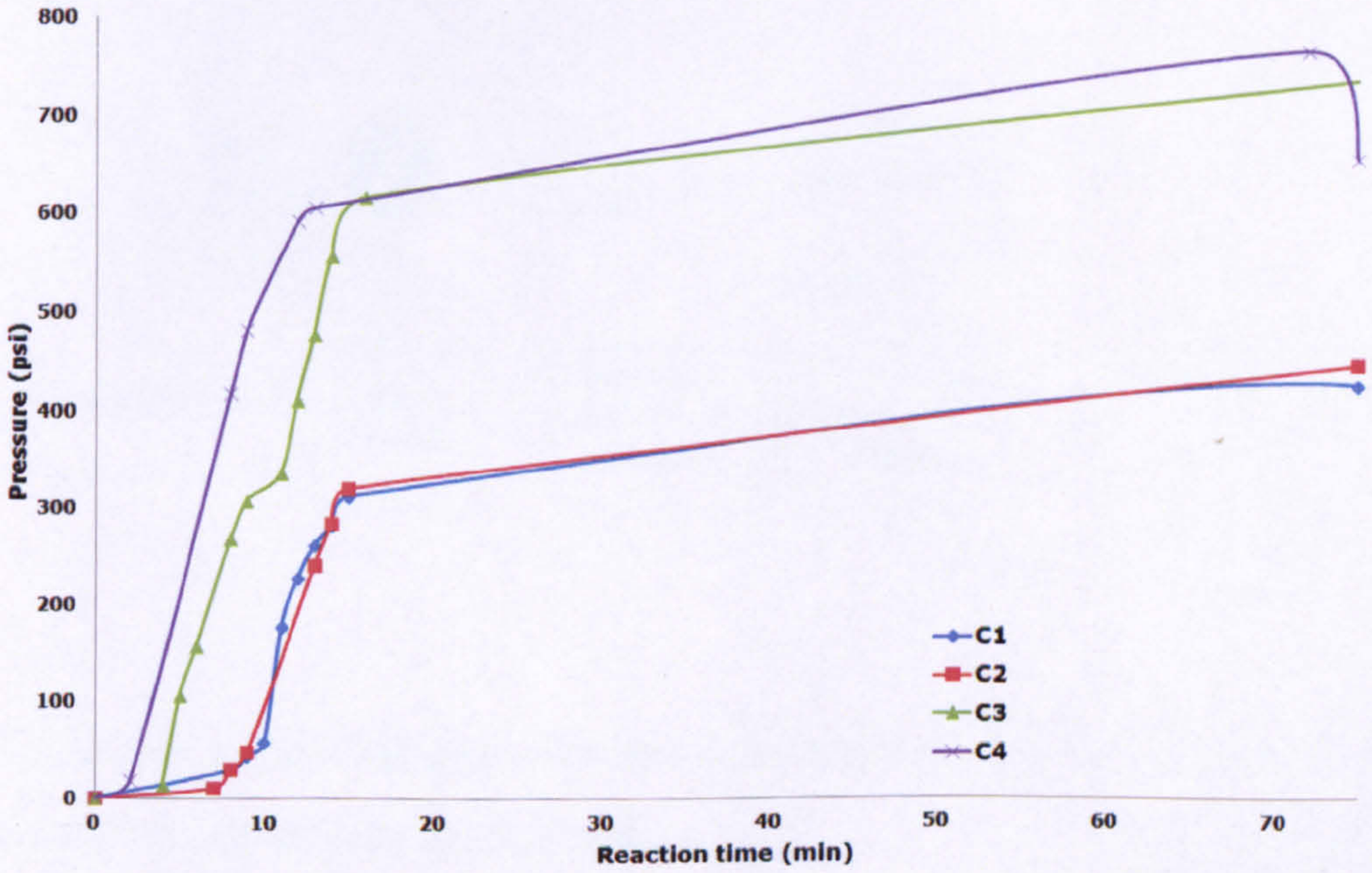

Figure 5-8: Pressure change vs. reaction time in C1-C4.

5.2.4 Mass Balance

When the solid to liquid ratio of 300 g/l was used, the carbon fixation efficiency was 46.6 %, with dissolution efficiency and carbonation efficiencies of 71.2 and 65.4 %, respectively. Taking this into account, about 4.9 t of serpentine, 11.3 t of NH_4HSO_4, 4.7 t of $(NH_4)_2CO_3$ and 16 t of water are required to sequester 1 t CO_2, as presented in Figure 5-9. If 95 % regeneration efficiency of NH_4HSO_4 and NH_3 is considered as for previous Section 4.2.2.4, then 0.6 t of NH_4HSO_4 is consumed to sequester 1 t CO_2. In comparison with the results from Section 4.2.2.6, 0.5 t of NH_4HSO_4 is required and 36.6 t of water can be saved at high solid to liquid ratio conditions.

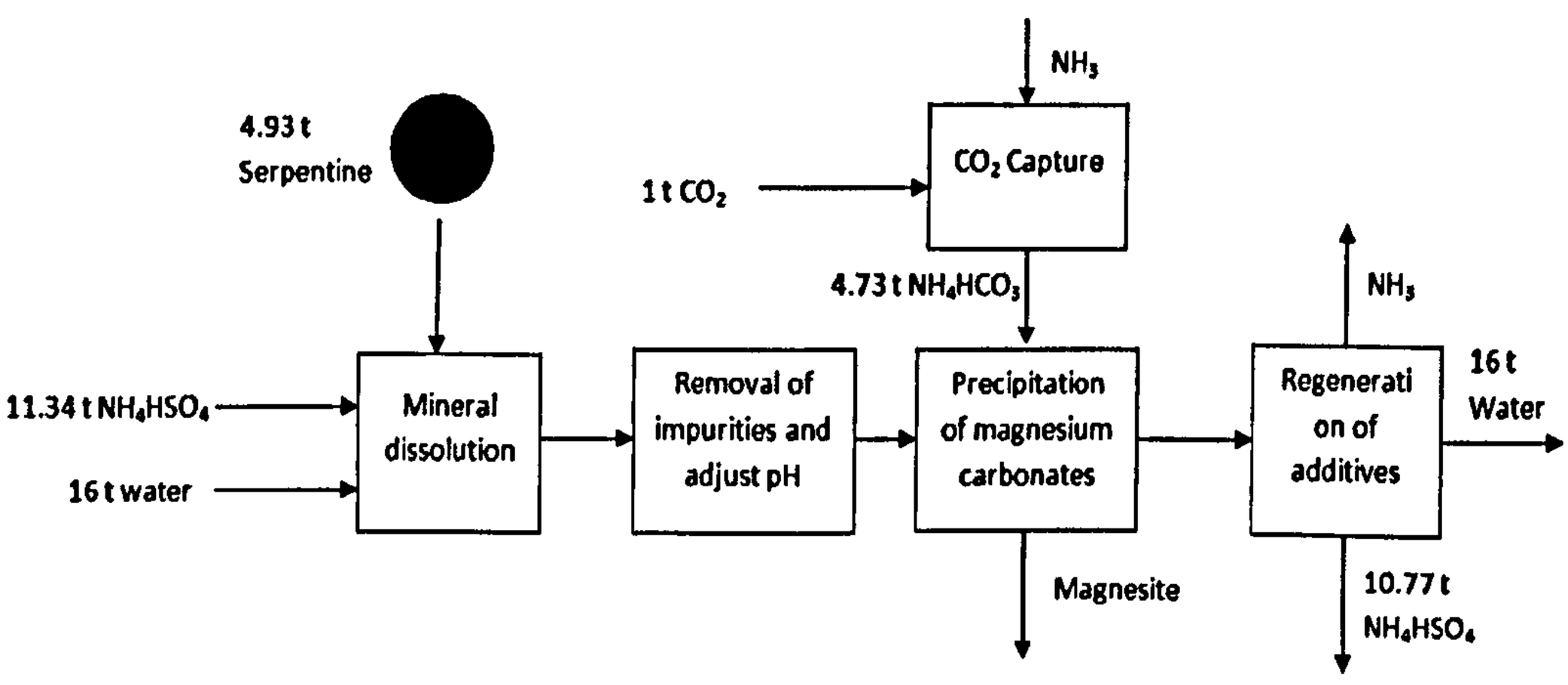

Figure 5-9: A simplified process scheme for sequestering 1 t of CO_2 by CCSM process at 300 g/l solid to liquid ratio.

5.3 Summary

In this chapter, the author has studied the CCSM process route with recyclable ammonium salts at high solid to liquid ratio conditions. In conclusion, the increase of dissolution efficiency when the solid to liquid ratio increased from 200 g/l to 300 g/l could be explained by particle-particle interaction. Magnesite instead of hydromagnesite was found due to the CO_2 pressure caused by the decomposition of ammonium salts at high temperature. The carbon fixation efficiency was significantly improved by using $(NH_4)_2CO_3$ compared to NH_4HCO_3 for the same concentration. At solid to liquid ratio of 300 g/l, the highest carbon fixation efficiency achieved was 46.6 %. According to the mass balance, about 4.9 t of serpentine, 0.6 t of NH_4HSO_4, 4.7 t of $(NH_4)_2CO_3$ and 16 t of water are required to sequester 1 t CO_2.

Chapter 6. Process evaluation and optimization

In this chapter, a preliminary evaluation was conducted to evaluate the OPEX[16] of the two process routes described in Chapters 4 and 5. A block diagram of the process scheme is shown in Figure 6-1. Firstly, the hot flue gas at a temperature of 900-1300 °C (depend on the fuel used and combustion technologies applied, 900 °C is used in this study) from the combustor passes through the thermal decomposition tower, where ammonium sulfate is decomposed into ammonium bisulfate and ammonia gas. After passing through a heat exchanger, ammonia gas and water vapour are condensed as aqueous ammonia and the flue gas is sent into an adsorption tower, where CO_2 is absorbed by a high concentration of aqueous ammonia into CO_2 containing ammonium salts (NH_4HCO_3, $(NH_4)_2CO_3$ and $NH_4NH_2CO_2$). The mineral is grinded to particle size between 75-150 μm and mixed with water from the mechanical vapour recompression (MVR) evaporator and NH_4HSO_4 from the thermal decomposition tower. The Mg ions are dissolved from the mixed slurry in the dissolution reactor. After filtering the solid residue (consisting mainly of amorphous silica), the pH of the Mg-rich solution is regulated by adding ammonia water to a pH value of 7 and a Fe-rich precipitate is produced with increasing pH. After

[16] Including energy consumption, chemical cost and mineral cost

filtering the Fe-rich precipitate, the Mg-rich solution reacted with CO_2 containing ammonium salts from the capture step to precipitate magnesite. After filtering the carbonate product, the remaining solution consisting mainly of ammonium sulfate is sent to the MVR evaporator. Dry ammonium sulfate solid is collected for the thermal decomposition and water is recycled.

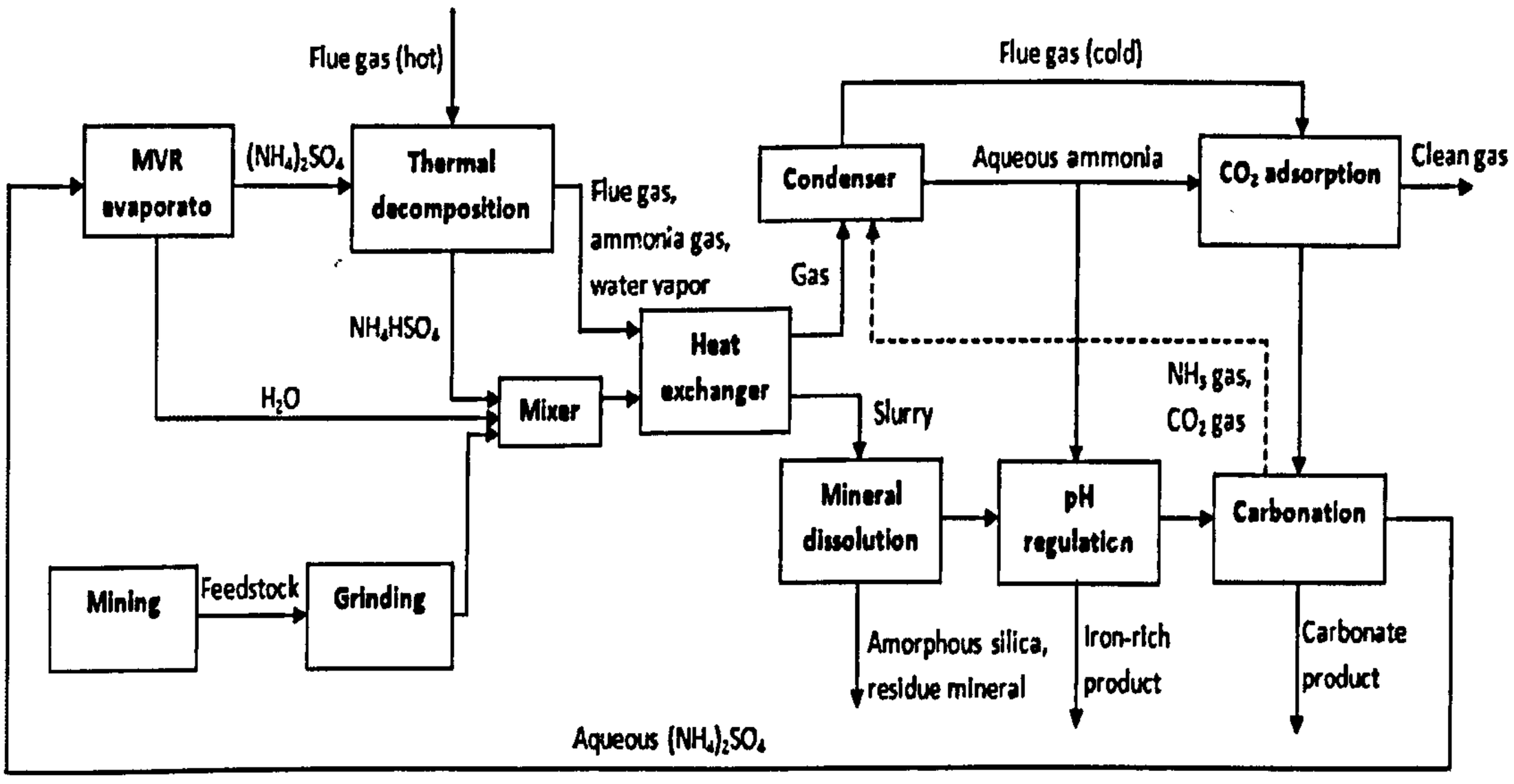

Figure 6-1: Block diagram of the CCSM process with recyclable ammonium salts.

The steps of capture, filtering, water evaporation and regeneration of ammonium salts are not the focus of this study. The technologies regarding these steps are mature and have been demonstrated in large scale projects (Kothandaraman, 2010). Therefore, a literature review was conducted to assess the potential applicability of these technologies to this study and identify the energy consumption for these steps in the process (Section 6.1). A preliminary cost

evaluation of the two process routes studied in Chapters 4 and 5 was conducted based on the mass balance from the experimental work and energy consumption from the literature review (Section 6.2). The conditions related to the cost reduction of the process, such as solid to liquid ratio and reaction time, were determined by using the results from the preliminary evaluation. Finally, the optimization experiments were conducted to further reduce the energy and cost of the process (Section 6.3).

6.1 Literature review of technologies regarding carbon dioxide capture, filtering, water evaporation and regeneration of ammonium salts

6.1.1 Carbon capture step

As described in Chapter 3, ammonia water was used to absorb CO_2 and produce $(NH_4)_2CO_3$ or NH_4HCO_3 in solid or liquid phase. The solid or liquid ammonium salts are then reacted with alkaline metal ions such as Mg/Ca to permanently store CO_2 as carbonate. In comparison with conventional aqueous ammonia carbon capture process, the energy intensive thermal regeneration of CO_2 and the high pressure CO_2 compression for transportation are avoided. Since the aqueous ammonia carbon capture has been intensively studied in recent years, there is a large body of publications available to assess the potential applicability of the aqueous ammonia process to

this study (Zhang *et al.*, 2003; Kim *et al.*, 2008; Kothandaraman, 2010; Huang, 2002; Corti, 2004; GAL, 2006). However, some variations in the capture step need to be investigated in order to match the requirements of the CCSM process with recyclable ammonium salts. For example, the output concentration of $(NH_4)_2CO_3$ and NH_4HCO_3 in the stream from the CO_2 capture step is a very important factor for the carbonation reaction. 2 mol/l NH_4HCO_3 and 3 mol/l $(NH_4)_2CO_3$ are required in the process studied in Chapters 4 and 5. In considering the reduction of water usage in order to minimise the energy consumption of water evaporation, $(NH_4)_2CO_3$ and NH_4HCO_3 are preferred to be either solid phase or high concentration of liquid phase. Therefore, high initial concentration of NH_3 is necessary for the capture step in this study. In addition, the output streams from the capture step typically contain both $(NH_4)_2CO_3$ and NH_4HCO_3, where the proportion of products is dependent on the process parameters (reaction time, CO_2 loading, flow rate of CO_2 and reaction temperature) (Zhang, 2003, Kim *et al.*, 2008).

6.1.1.1 High concentration of NH_3

The CO_2 absorption efficiency is closely related to the concentration of NH_3. Zhang *et al.* (2003) investigated the relationship between CO_2 absorption efficiency and NH_3/CO_2 molar ratio, where the absorption efficiency of CO_2 increased with higher NH_3

concentrations. The CO_2 absorption efficiency was reported to be improved from 76 % to 92 %, when the initial concentration of NH_3 increased from 1.8 mol/l to 2.4 mol/l, respectively. Besides, the high concentration of NH_3 can prolong the residence time of NH_3 in the absorber and increase the CO_2 absorption capacity. Kim *et al.* (2008) showed that increasing the NH_3 concentration can result in longer breakthrough times, where the time to achieve 95 % CO_2 removal efficiency doubled from 2 h to 4 h when using 7 wt. % and 17 wt. % of NH_3 solutions, respectively. Kim *et al.* (2008) also investigated the change of CO_2 sorption capacity with different aqueous ammonia concentration. It was reported that 13 wt. % (6.7 mol/l) aqueous ammonia was thought as the optimum concentration to maximise CO_2 sorption capacity (2.8 mol/kg).

6.1.1.2 Output concentration of $(NH_4)_2CO_3$ and NH_4HCO_3 concentration and composition in the stream from CO2 capture step

According to Kim *et al.* (2008), the output concentration of total CO_2 containing species from CO_2 absorption with 13 wt. % aqueous ammonia can achieve 3.4 mol/l, containing 35 % ammonium carbamate, 41 % ammonium bicarbonate and 24 % ammonium carbonate. It is thought that the higher concentration of aqueous ammonia used in absorption can generate higher concentration of CO_2 containing species.

6.1.1.3 Ammonia loss

Resnik *et al.* (2004) found that ammonia is lost to the gas phase during absorption, and the higher the initial concentration of aqueous ammonia increases the relative loss of NH_3 in capacity. For environmental reasons, the loss of ammonia must be kept to a minimum.

6.1.1.4 Energy consumption of current CO_2 ammonia process

CO_2 capture with aqueous ammonia has been studied at laboratory scale (Zhang *et al.*, 2003; Kim *et al.*, 2008). However there is no published information about energy consumption. A similar process using chilled ammonia has been successfully demonstrated for coal-fired power plants in a collaborative project by Alstom, the Electric Power Research Institute (EPRI) and We Energies in 2007 (0.1 Mt CO_2/year) (GAL, 2006). According to the study of Kothandaraman (2010), the energy consumption for 85% of capture of CO_2 in the chilled ammonia system was estimated to be 477 kWh/t CO_2, where 44% of the energy consumption from using the chilled ammonia system arises from the refrigeration process, 27 % of the energy consumption comes from the cooling of ammonia in the absorption process and 25 % of the energy consumption was due to the compression process. For the CCSM process with recyclable ammonium salts, the energy consumption of the capture step is 19

kWh/t CO_2, which is only 4 % of the energy required in the chilled ammonia system because compression, cooling and desorption are not necessary (considering that 4 % of 477 kWh/t).

6.1.2 Filtering, water evaporation and regeneration of ammonium salts

The two most energy intensive steps of CCSM with recyclable ammonium salts process are water evaporation and thermal decomposition. Both of the two steps are related to water usage, which is controlled by the solid to liquid ratio used. In this section, suitable technologies for filtering, water evaporation and thermal decomposition for CCSM within the recyclable ammonium salts process are identified and described, and their energy consumption is estimated.

6.1.2.1 Filtering

The slurries after dissolution, pH regulation and carbonation require separation of the solid from the liquid. The costs of filtering are related to the particle size and the concentration of the slurry. Large particles and a higher concentration of slurry can reduce the costs. It is reported that the energy required to dewater a magnesite concentrate from the beneficiation of taconite is 0.2 kWh/t of water removed (Eimco water technologies, 2011).

The filtering step of the CCSM process with recyclable ammonium salts process can be regarded as similar to filtering/dewatering in the mining processing industry. Hydrocyclones are therefore considered suitable for the CCSM process, since the particle sizes required for CCSM are matched with the working particles size range of hydrocyclone from 75 to 300 μm (Eimco water technologies, 2011). For the other choice of filtering equipment can be investigated in future work, such as the gravity filtering.

6.1.2.2 Water evaporation

CCSM wet technologies require a final drying step, which is a water thermal evaporation process. Thermal removal of water from slurries is a highly energy intensive technique. The new Mechanical Vapour Recompression (MVR) technology provides a low energy solution with typical power consumption of 8-12 kWh/t of clean water (Karasek, 2010; Windsor MVR Evaporation System, 2011).

MVR evaporators have been applied in food, paper and chemical industries (Karasek, 2010; Windsor MVR Evaporation System, 2011). Therefore, MVR are considered suitable for the CCSM process with recyclable ammonium salts.

6.1.2.3 Thermal decomposition of ammonium slats

Ammonium sulfate can be converted into ammonium bisulfate and ammonia gas by heating, as shown in the following equation:

$$(NH_4)_2SO_4(s) \rightarrow NH_3 \uparrow + NH_4HSO_4(s)$$

Equation 6-1

It is essential to control the temperature above 250 °C to initiate the decomposition, and no higher than 500 °C to prevent the formation of pyrosulfate ($(NH_4)_2S_2O_7$), which further decomposes into ammonia gas, sulphur dioxide and nitrogen at above 500 °C. The decomposition rate of $(NH_4)_2SO_4$ is slower when the temperature is below 300 °C. Moreover, the decomposition reaction is endothermic, absorbing 110 KJ/mol heat (value calculated using HSC 5.1). Finally, numerous processes for the thermal decomposition processes for ammonium sulphate have been suggested (Brennan, 1975; Montgomery, 1962; Bretherick, 1975).

The single step water evaporation and thermal decomposition of ammonium sulphate designed by Albert *et al.* (1972) proposed to inject a fluid mixture comprising of ammonium sulphate and water into a stream of hot flue gas (1300 °C) in an evaporation zone, where water is evaporated. The mixture of hot flue gas (500 °C), water vapor and ammonium sulphate flow into a decomposition zone, where ammonium sulphate was converted into ammonium bisulphate and ammonia.

In addition of the wet method described above, a dry method has been reported by Brennan (1975) and Furkert (1973), where 99-

100% NH_4HSO_4 was produced from a mixture of salts comprised of 50 % NH_4HSO_4, steam inlet temperature of 450-470 °C and liquid to gas ratio from 0.66 to 1. The mixture of ammonium bisulfate with ammonium sulphate in the feed has been reported to improve the conversion rate of ammonium sulphate to ammonium bisulfate (Welty, 1972; Montgomery, 1962; Furkert, 1973).

There is no data reported in the literature for the energy consumption of thermal decomposition of ammonium sulphate. However, a similar thermal process using rotary kiln for production of Portland cement can be considered as a comparable example. Worrell *et al.* (2008) reported that the thermal energy consumption for a rotary kiln is generally 3.1 GJ/t (1450 °C) and the power consumption for pumping was 6 to 9 kWh/t (IEA, 2010b). Taking this into consideration, the thermal decomposition of ammonium sulphate is estimated to require 0.85 GJ/t (400 °C). This heat penalty is high and makes the CCSM process costly. Recovering waste heat from flue gas from a power plant can reduce this heat penalty. Currently, the waste heat from flue gas from a power plant is only used in air pre-heater, and the majority of waste heat is not recovered. In contrast, a heat recovering system has been applied in the steel industry successfully (Huaiwei and Xin, 2011; Rautenbach et al., 1979). The heat capacity the flue gas (10 vol. % of CO_2) leaving the boiler at 900 °C is around 1.3 KJ/Nm^3, or in other words, 1 t CO_2 can provide 30 GJ of heat. Therefore, the heat

from the flue gas is sufficient for the thermal decomposition step, and only 6 to 9 kWh of power consumption for pumping is needed to decompose 1 t of ammonium sulphate. The use of waste heat from flue gas in power plant is very important for the CCSM process, and if this is not used the theoretical value of energy consumption for thermal decomposition of ammonium salts would rise to 236 kWh per tonne ammonium sulphate (value obtained from HSC software simulation). In order to supply enough heat for thermal decomposition of ammonium salts, a heat exchanger, such as shell and tube, should be placed after boiler (900 °C) and before selective catalyst reduction (SCR), where the minimum operation temperature of SCR is ~280 °C (Williams, 2009). For the other existing air pollution control system (APCs), electrostatic precipitator (ESP) and flue gas desulphurisation (FGD) do not have specific temperature requirements (Shanthakumar *et al.*, 2008). Additionally, the aqueous ammonia capture step of the CCSM process has the potential to convert SO_2 and NO_x into ammonium salts, and this may resolve the heat requirement of both thermal decomposition of CCSM and SCR. The integration of SO_2, NO_x and CO_2 capture by ammonia has already been reported by Powerspan (2011) and Cansolv (2011).

6.2 Preliminary cost analysis

A preliminary cost analysis of OPEX, including energy consumption, chemical consumption and feedstock cost, was developed based on the experimental results discussed in Chapters 4 and 5 (see Table 6-1). For the analysis, several assumptions were made based on the experimental results were made to simplify the work.

- The analysis was based on sequestering 1 t of CO_2.
- Serpentine consists of 24 wt. % of Mg.
- For the low solid to liquid ratio scenario, the 50 g/l was used.

  According to the results from Chapter 4, the total CO_2 fixation efficiency is 77 %, with 100 % and 96 % of dissolution and carbonation efficiencies, respectively.

- For the high solid to liquid ratio scenario, the 300 g/l was used.

  According to the results from Chapter 5, the total CO_2 fixation efficiency is 47 %, with 71 and 65 % are the dissolution and carbonation efficiencies, respectively.

The conditions applied for each step of the process are summarised in Appendix 1. The input and output of the two process routes were calculated and are presented in Table 6-1. The input and output streams of each step are listed in Appendix 2.

Table 6-1: Mass balance of the two process routes described in Chapters 4 and 5.

	50 g/l (t)	**300 g/l (t)**
Input		
CO_2	1	1
Serpentine	3.0	4.9
H_2O	-4.2[1]	-0.7[1]
NH_4HSO_4	0.2	1.5
NH_3	0.2	-0.3[1]
Output		
$NH_4HCO_3/(NH_4)_2CO_3/NH_4NH_2CO_2$	2.2	2.2
$MgSO_4$	0.2	1.4
$(NH_4)_2SO_4$	0.1	0.1
Product 1	1.3	
Product 2	0.3	
Residual solid		3.1
Hydromagnesite	2.8	
Magnesite		1.9

[1]Negative values indicate these chemicals are produced from the process.

According to the mass balance, the energy consumption for each step was calculated (Table 6-2) based on the following energy penalties. The details can be seen in Appendix 2.

- Grinding: 13 kWh/t is used to grind mineral to 75 -150 μm particle size (O'Connor, 2005).

- CO_2 capture: 19 kWh is used to capture 1 t CO_2 in the aqueous ammonia capture step with recyclable ammonium salts process (Section 6.1.1).

- Water evaporation: MVR evaporator was selected and 8 kWh/t water evaporated (Section 6.1.2.2).

- Filtering: Hydrocyclone was selected and 0.2 kWh/t solution filtered (Section 6.1.2.1).

- Pumping: 1.47 kWh/t solution pumped.

- Thermal decomposition: 6 kWh/t ammonium salts for pumping, cooling and preheating for the thermal decomposition of ammonium salts, if heat recovered from the flue gas is applied (Section 6.1.1).

- The electricity price is 0.03 US$/kWh

Table 6-2: Energy consumption (kWh) of the two process routes.

	50 g/l (kWh)	300 g/l (kWh)
Grinding	39	63
CO_2 capture	95	28
MVR evaporation	701	169
Filtering	49	19
Pumping	76	78
Thermal decomposition	128	43
Total energy	1088	400

The chemical requirements for the two process routes are presented in Table 6-3. It is assumed that $(NH_4)_2SO_4$ is supplied to produce NH_4HSO_4 and NH_3 by thermal decomposition with 95 % efficiency. Any excess NH_4HSO_4 or NH_3 can be used in the process, and this is considered in the calculation of chemical costs.

Table 6-3: Chemical requirements (t) and costs (US$) of the two process routes.

	Amount in 50 g/l scenario (t)	**Amount in 300 g/l scenario (t)**
NH_4HSO_4	0.2	1.5
NH_3(capture + mineralisation)	0.2	-0.3
$(NH_4)_2SO_4$ (equal, 99 % purity) [a]	1.9	1.7
NH_3 (generation from $(NH_4)_2SO_4$)	0.0	-0.5
NH_4HSO_4	-1.4[d]	0.0
Cost of $(NH_4)_2SO_4$ *(US$)*	172.1	154.5
Cost of NH_3 [b] *(US$)*	0.0	-84.3
Cost of NH_4HSO_4 [c] *(US$)*	-127.4	0.0
Total Chemical cost (US$)	44.7	70.2

[a] Price of NH_3 is 180 US$/t.
[b] Price of NH_4HSO_4 is 90 US$/t.
[c] Price of $(NH_4)_2SO_4$ is 90 US$/t.
[d] Negative value means excess amount is produced.

The OPEX of the two process routes is shown in Table 6-4.

Table 6-4: OPEX of the two process routes.

	50 g/l scenario (US/t_{CO2} sequestered)	**300 g/l scenario (US/t_{CO2} sequestered)**
Energy cost [a]	33	12
Chemical cost	45	70
Mineral cost [b]	15	24
Transport cost (100km) [c]	7	12
Total cost	100	119

[a] Electricity price is 0.03 US$/kWh.
[b] Price of serpentine is 5 US$/t.
[c] Transportation cost is 2.5 US$/t for 100 km.

The total costs for sequestering 1 t CO_2 are 100 US$ and 119 US$ t at 50 g/l and 300 g/l solid to liquid ratios, respectively. In both cases, the highest cost come from the chemical and accounting for 59-65 % of the total cost. The MVR evaporation is the most energy intensive step, with up to 702 kWh/t CO_2 sequestered for the 50 g/l case. The costs of feedstock are closely related to the carbon fixation efficiency, where increasing efficiency can reduce the feedstock cost. In addition, it can be seen that the solid liquid ratio has a strong influence on the energy consumption. Low solid to liquid ratio resulted in a large amount of water evaporated that subsequently needs to be filtered and pumped. However, both dissolution and carbonation efficiencies decreased at high solid to liquid ratio, and therefore, more serpentine and chemicals are required. Moreover, dissolution efficiency influences the required

amount of serpentine and the amount of products, while carbonation influences the required net amount of NH_3 and NH_4HSO_4 and the energy consumption on CO_2 capture.

Based on this preliminary cost analysis the following recommendations are made for the process to improve its economical viability. The low solid to liquid ratio case is better than the high solid to liquid ratio scenario in terms of total cost. However, the solid to liquid ratio should be maximised without exceeding the solubility limit of ammonium sulphate. The input of ammonium salts should be reduced, but the carbonation efficiency should be maintained. In addition, it is also suggested that the carbonation step should be conducted using an autoclave reactor instead of an open glass reactor to produce magnesite instead of hydromagnesite (Section 5.2.3). Another important parameter to be considered is the reaction time, where longer reaction times give high dissolution efficiency, but they demands a large reactor size and therefore increase the capital cost. It is also important to limit the dissolution time to 1 h considering the trade off between the cost and the efficiency.

The carbon footprint of production of the chemical used and mining of raw materials need to be considered, it is suggested to do the life cycle carbon footprint assessment of the CCSM process in future work.

6.3 Process optimization

According to the suggestions from the previous section, optimization experiments were carried out to reduce the total cost of the proposed CCSM process with recyclable ammonium salts. The Data shown in Section 6.2 suggested that the low solid liquid ratio case gave better performance on cost evaluation. In the boundary of low solid to liquid ratio (without exceeding the solubility), the maximise value of solid to liquid ratio is 100 g/l (this value was obtained from dissolution experiments in Section 4.1.6), and this value was selected as the optimum value. 40 % excess of NH_4HSO_4 (2.8 M) was used for the dissolution experiments, as for the previous studies described in Chapter 4. Serpentine with 75-150 μm particle size was dissolved at 100 °C for 1 h. A mixture of NH_4HCO_3 and $(NH_4)_2CO_3$ solution was used instead of NH_4HCO_3 aiming at simulating the different CO_2 containing ammonium salts solution coming from the CO_2 capture step. The mixture solution used contains 1.7 M NH_4HCO_3 and 1.7 M $(NH_4)_2CO_3$ (see Section 6.1.1), where the output concentration of total CO_2 containing species from aqueous ammonia was 3.4 mol/l. Finally, an autoclave reactor was used for the carbonation step.

6.3.1 Experimental methods

The dissolution step for the optimization experiments was conducted following by the procedure presented in Section 5.1.1. The solid to

liquid ratio was increased to 100 g/l, and the concentration of NH_4HSO_4 to 2.8 M, while the reaction time was reduced to 1 h. The pH regulation step and carbonation steps were carried out following the methods described in Section 4.2.1.2. and 5.1.3., respectively. The mixture solution of 1.7 M NH_4HCO_3, 1.7 M $(NH_4)_2CO_3$ and ammonia water (13 wt. %) was added to the solution obtained from the dissolution step. The amounts of mixture solution of NH_4HCO_3 or $(NH_4)_2CO_3$ and ammonia water were determined by the molar ratio of Mg ions in filtrate 2: CO_2 containing ammonium salts: NH_3. The matrix of carbonation experiments conducted at different ratios is listed in Table 6-5.

Table 6-5: Matrix of carbonation experiments conducted at different ratios

	OP1	**OP2**	**OP3**	**OP4**
Mg in filtrate 2 : CO_2 containing ammonium salts	1:1	1:1.5	1:1	1:1.5
Mg in filtrate 2 : NH_3	1:1	1:1	1:2	1:2

6.3.2 Results and discussions

According to the results from the ICP-AES analyses of the filtrate 1 from OP1-OP4, the dissolution efficiency of Mg is around 80 % (see Table 6-6), compared to 100 % for the dissolution experiments presented in Section 4.1.2. The decrease of dissolution efficiency at 100 g/l solid to liquid ratio is probably due to the Si passive layer on the surface of the serpentine particle, as the rate limiting step is

product layer diffusion control at this solid to liquid ratio (see Section 4.1.3).

The overall reaction for the carbonation step is presented below:

$$2MgSO_4 + NH_4HCO_3 + (NH_4)_2CO_3 + NH_3 \rightarrow 2MgCO_3 \downarrow + 2(NH_4)_2SO_4$$

ΔH=-43.59 KJ, ΔG=-102.99 KJ (80 °C) Equation 6-2

The enthalpy and Gibbs free energy of this reaction are both negative, indicating that it is an endothermic reaction. Due to the low thermal stability of ammonium bicarbonate and ammonium carbonate (decomposition happens at 80 °C), it is necessary to supply excess amount of ammonium bicarbonate and ammonium carbonate for the carbonation reaction to be completed. The presence of ammonia can slow down the decomposition reaction and help the carbonation reaction by maintaining a pH above 8 for precipitation, reacting with CO_2 to regenerate ammonium bicarbonate and then to regenerate ammonium carbonate.

Table 6-6 also shows that the molar ratio of Mg: NH^{4+} salts: NH_3 is the key factor controlling carbonation efficiency. When the molar ratio of Mg: NH^{4+} salts: NH3 is 1:1:1 (Experiment OP 1), the carbonation efficiency is 80.9 % (Table 6-6). Increasing the Mg: NH^{4+} salts ratio to 1:1.5 (Experiment OP 2) can improve carbonation efficiency to 85.9 %. Further increasing the Mg: NH_3

ratio to 1:2 (Experiment OP 3) can improve the carbonation efficiency to 89.7 %. The improvement of carbonation efficiency by adding ammonia water has been discussed in Section 4.2.2.3. It is thought that ammonia water can react with NH_4HCO_3 into $(NH_4)_2CO_3$ and thus increases the carbonation efficiency. The comparison between the reaction kinetics of $(NH_4)_2CO_3$ with $MgSO_4$ and NH_4HCO_3 with $MgSO_4$ was also discussed in Section 5.2.3. The highest carbonation efficiency of 96 % was obtained when the molar ratio of Mg: NH^{4+} salts: NH_3 was 1:1.5:2 (Experiment OP 4).

Table 6-6: ICP-AES results of Mg concentration from OP1-4.

	Filtrate 1 (ppm)	**Filtrate 2 (ppm)**	**Filtrate 3 (ppm)**	**Dissolution efficiency %**	**Carbonation efficiency %**
OP1	19149	18999	3605	79.8	80.9
OP2	18908	18778	2652	78.8	85.9
OP3	19012	18891	1939	79.2	89.7
OP4	19201	19083	761	80.0	96.0

The CO_2 from the decomposition of ammonium bicarbonate and ammonium carbonate can increase the pressure of the system. The XRD pattern of product 3 from experiment OP 4 in Figure 6-2 confirms that magnesite is produced from the carbonation step. Therefore, hydromagnesite is transformed into magnesite at high pressure condition.

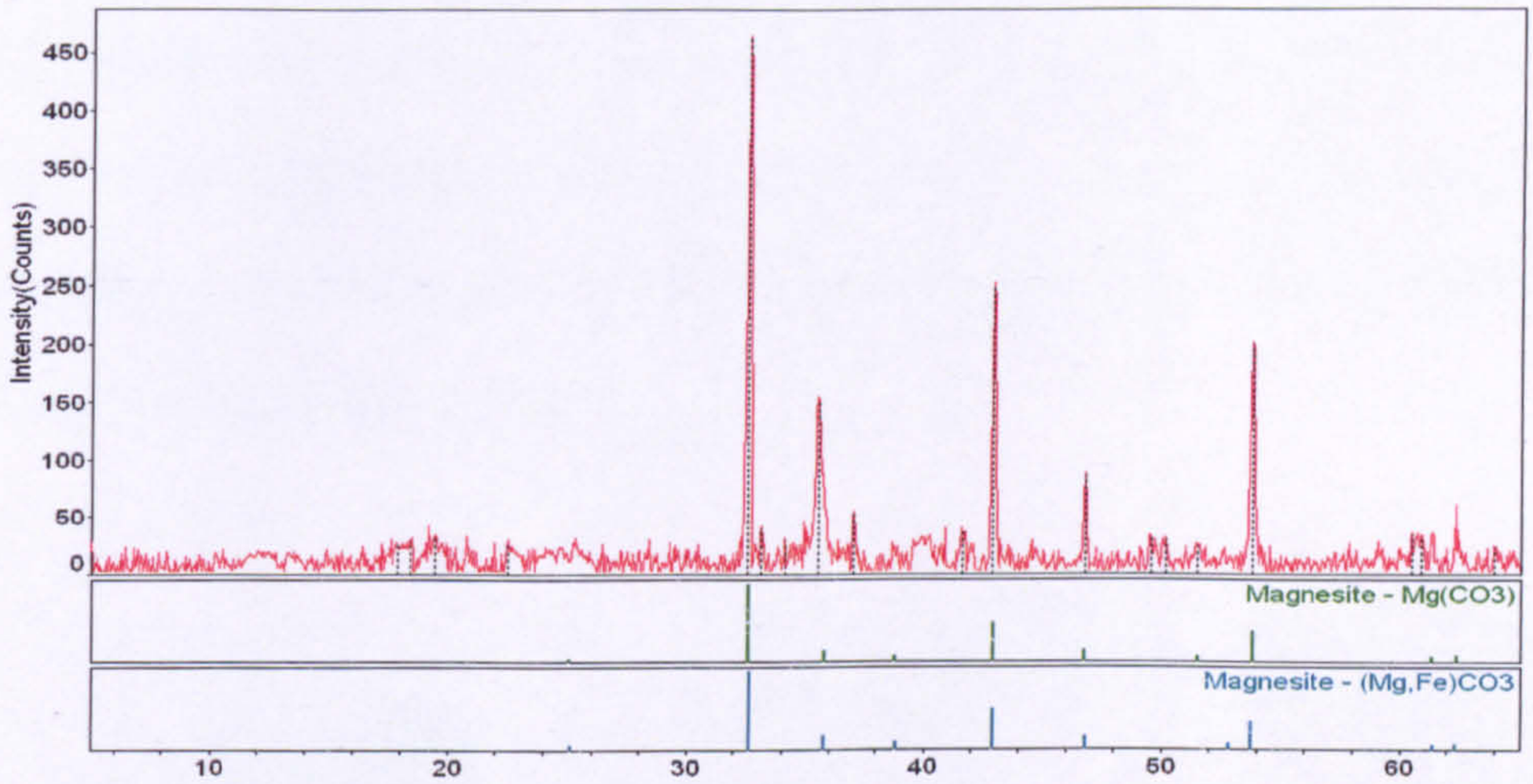

Figure 6-2: XRD pattern of product 3 from experiment OP 4.

The process was re-evaluated and the cost analysis was estimated based on the optimization experimental work. The input and output streams in each step, energy consumption and chemical cost are presented in Appendix 3. The OPEX of the four optimization experiments is shown in Table 6-7. It can be seen that Experiment OP 4 shows the lowest total cost.

Table 6-7: OPEX of four optimization experiments.

	OP1	OP2	OP3	OP4
Unit		***US$/$t_{CO2}$ sequestered***		
Energy cost	17	17	16	16
Chemical cost	55	46	37	25
Mineral cost	17	17	16	15
Transport cost (100km)	9	8	8	7
Total cost	98	88	77	63

A simplified process scheme of the best case is presented in Figure 6-3, where approximately 3.0 t of serpentine, 0.2 t of NH_4HSO_4 and 0.1 t of NH_3 are required to sequester 1 t of CO_2 and 1.9 t of magnesite, 1 t of high Si contain by-product and 0.3 t of high Fe contain product are produced.

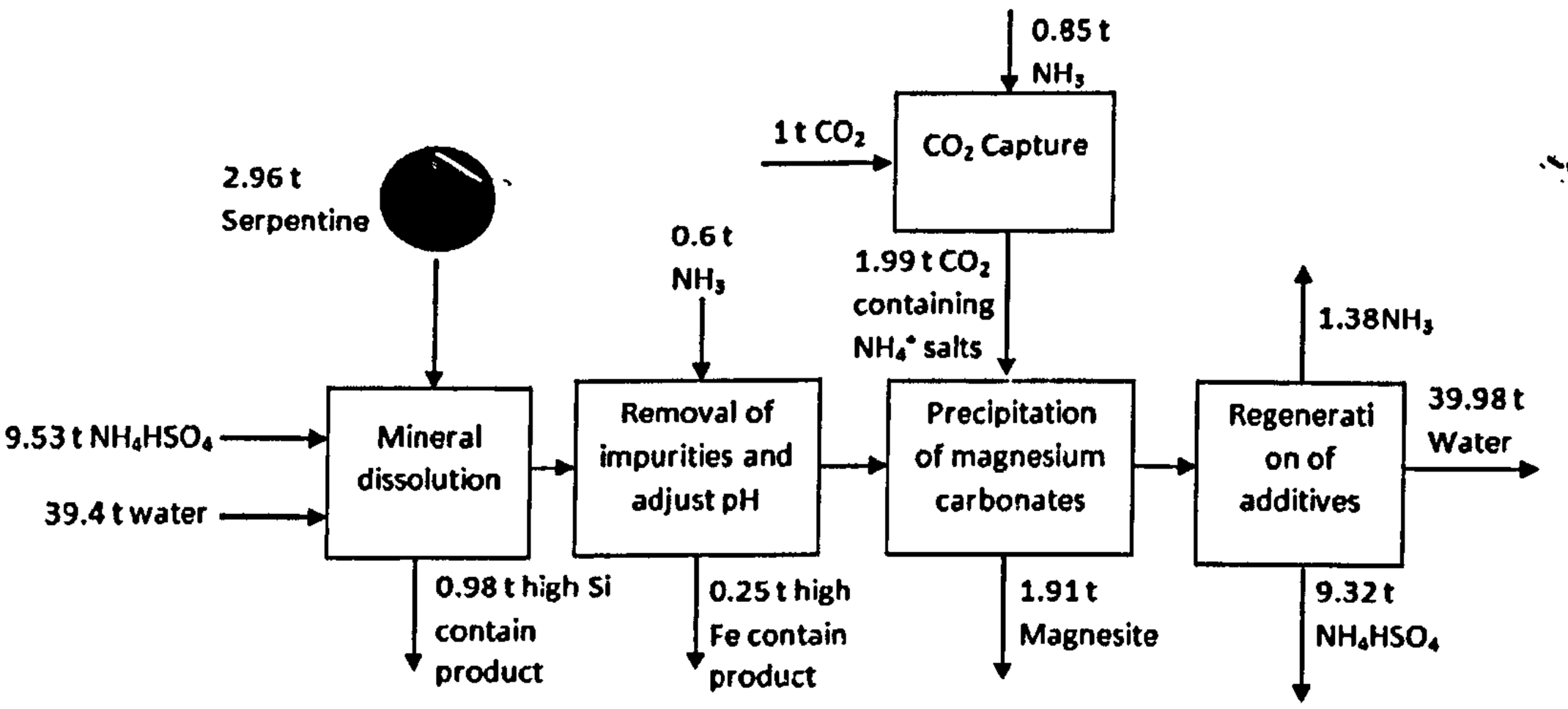

Figure 6-3: A simplified process scheme for sequestering 1 t of CO_2 by CCSM process at optimized condition.

Table 6-7 shows that the total cost to sequester 1 t CO_2 decreased from 98 US$ to 63 US$ with the increase of carbonation efficiency at different molar ratio of Mg: NH^{4+} salts: NH_3. Taking the OP 4 as an example, the cost of energy consumption is 532 kWh or 16 US$ (see Appendix 3), which accounts for 25 % of the total cost. The feed stock cost is 22 US$ (35 % of the total), while the cost of chemical represented the highest cost (40 % of the total), as presented in Figure 6-4. For the energy consumption shown in Figure 6.5 and Appendix 3, MVR evaporation consumes the largest

energy of 312 kWh, which accounts for 59 % of the total. Then in increasing order of energy consumption, there is pumping, thermal decomposition, grinding, CO_2 capture and filtering. It is confirmed that increasing the carbonation efficiency can significantly reduce the chemical cost, while increasing the solid to liquid ratio can largely reduce the energy consumption. In comparison with other researchers' work, the energy consumption of this study is relatively lower than the best result of 1009 kWh/t CO_2 from Gerdemann *et al.* (2007), where serpentine was sequestered at 155 °C and 115 bar (Gerdemann *et al.*, 2007). The chemical cost of this study is significantly lower than Teir *et al.* reported 1300-1600 US$/t CO_2 sequestered using serpentine and un-recyclable HCl or HNO_3 and NaOH (Teir *et al.*, 2007b).

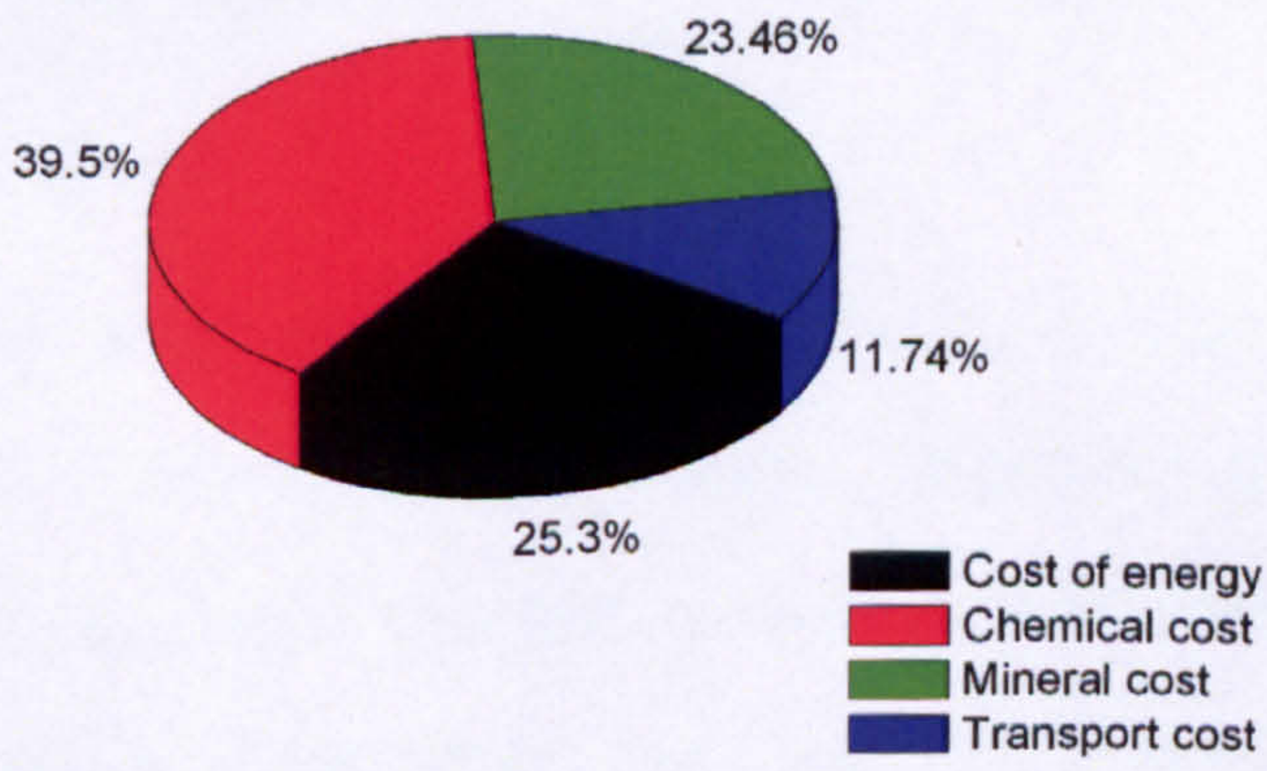

Figure 6-4: Percentages accounted of energy, chemical, mineral and transport in total cost.

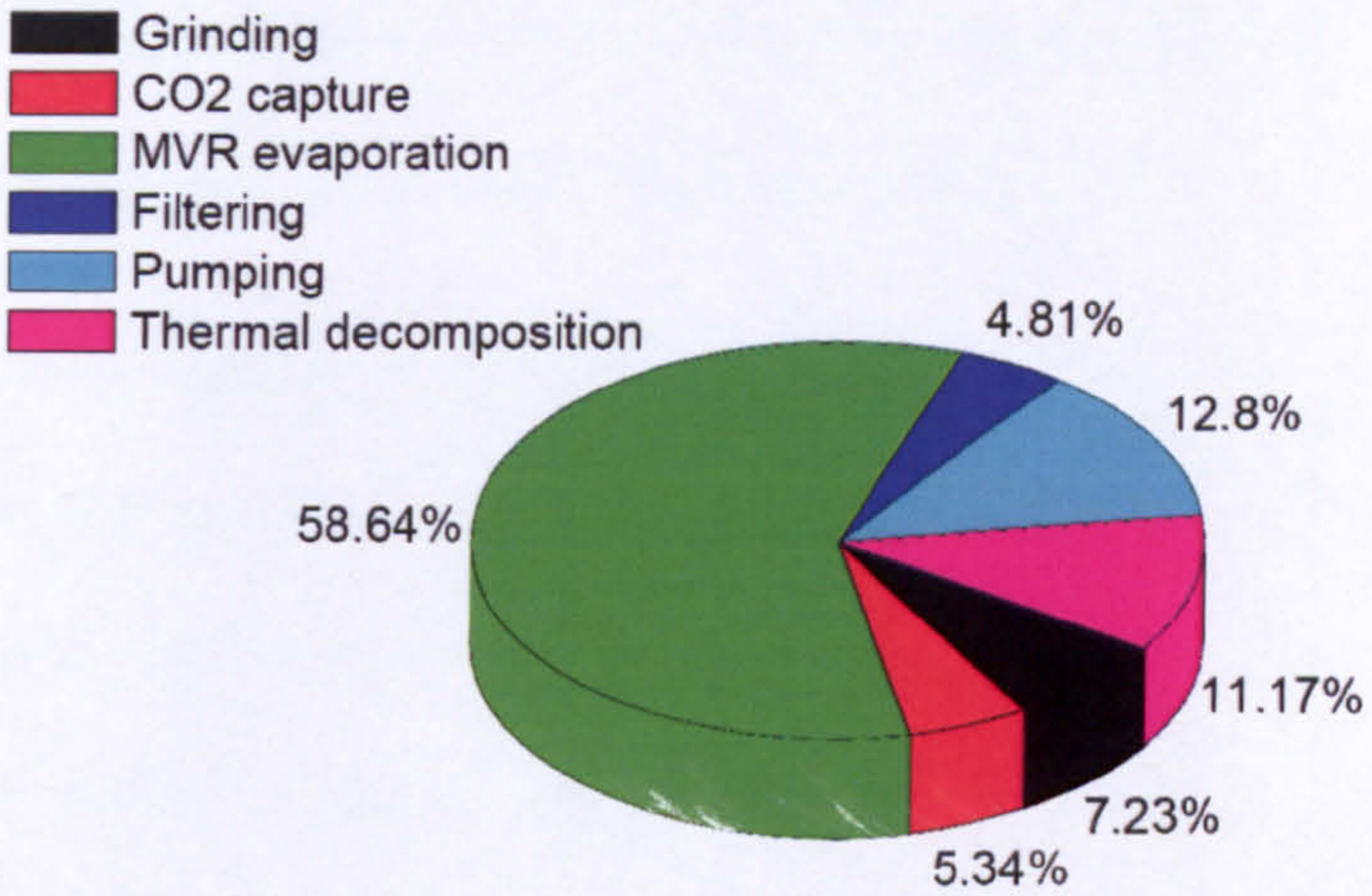

Figure 6-5: Percentages accounted of grinding, CO_2 capture, MVR evaporation, filtering, pumping and thermal decomposition in total energy consumption.

6.4 Summary

Most of the process units used are mature technologies. Additionally, it was found that the using waste heat from flue gas to supply the heat required for the thermal decomposition of ammonium salts is very important for the success of the CCSM process with recyclable ammonium salts.

The preliminary cost analysis evaluated the OPEX of the two process routes in terms of energy consumption, chemical costs and feedstock cost. It was found that the solid liquid ratio has a large influence on the energy consumption cost. The results show that the total cost to sequestering 1 t CO_2 is 100 US$ at 50 g/l case and 119 US$ at 300 g/l case. Using low solid to liquid ratio (50 g/l) resulted in large streams in the process, and thus resulting in a high energy

consumption. However, high solid to liquid ratio (300 g/l) decreases the dissolution and carbonation efficiencies.

The optimization experiments were conducted according to the recommendations from the preliminary cost analysis. The dissolution efficiency of Mg from serpentine using 2.8 M NH_4HSO_4 at 100 g/l solid to liquid ratio for 1 h was around 80 %. The decrease in dissolution efficiencies is because of the Si passive layer on the surface of serpentine particle. The molar ratio of Mg: NH^{4+} salts: NH_3 is the key factor controlling carbonation efficiency, and when using the molar ratio of Mg: NH^{4+} salts: NH_3 is 1:1.5:2, the carbonation efficiency was 96 %.

Chapter 7 Cost evaluation

Chapter 6 described the optimization of the operating variables of the CCSM process using recyclable ammonium salts. The variables studied included reaction temperature (T), reaction time (t), particle size of feedstock (d), solid to liquid ratio (S/L) and molar ratio of Mg^{2+}:NH^{4+}:NH_3 (R). It was shown that serpentine can be dissolved (80% efficiency) and subsequently carbonated (96% efficiency) within 1 h. The cost of additives and energy consumption were reduced to 25 US$ and <532 kWh, respectively. Chapter 7 describes the cost evaluation (CAPEX[17] and OPEX) to assess the economic feasibility of the CCSM process with recyclable ammonium salts.

There are several papers published on the costs of mineral carbonation (Gerdemann *et al.*, 2007; Huijgen *et al.*, 2007; Teir *et al.*, 2009). Huijgen's study represents the most comprehensive cost evaluation, including investment cost, energy cost, chemical cost and feedstock cost. However, Huijgen used wollastonite and steel slags as feedstock, which have limited capacity. Gerdemann *et al.* (2007) reported that the energy costs for olivine and serpentine were 54 and 250 US$/t CO_2 sequestered, respectively. These costs seem substantially higher than other CCS technologies (e.g. costs of geological storage are typically 0.7-8 US$/t CO_2 sequestered (IPCC,

[17] Capital cost including purchase equipments, construction, labour and other surcharge

2005). Gerdemann et al. (2007) assumed that the $NaHCO_3$ and NaCl were recycled in their process; however, this has not been proved. Teir *et al.* (2009) reported that the cost of chemicals was estimated to be 1300-1600 US$/t CO_2 sequestered using serpentine and un-recyclable HCl or HNO_3 and NaOH. These costs are significantly high, but Teir mentioned the potential for beneficial use of the products made from his process.

The aim of this chapter is therefore to assess the economic feasibility of CO_2 capture and storage costs by CCSM process with recyclable ammonium salts. A basic design of the process by Aspen plus was made to estimate CAPEX cost, including investment and depreciation costs and fixed costs (e.g. labour and maintenance). Finally, a sensitivity analysis was performed to investigate how the process conditions and assumptions may affect the costs and to identify opportunities for cost reduction.

7.1 CCSM process with recyclable ammonium salts

Aspen plus 11.1 flow sheeting software was used in this study. The CCSM process with recyclable ammonium salts requires several classical unit operations, including crusher, heat exchanger, autoclave reactor with stirrer, absorber, mixer and feed pump. Figure 7-1 shows a simplified Aspen flow diagram of the CCSM process with recyclable ammonium salts. The process was designed to sequester CO_2 emitted from a 100 MW power plant (assuming

CO_2 emission of 0.60 kg/kWh and operation time of 8000 h/yr). The simulation was performed using the experimental results from the optimization study described in Chapter 6 (80% and 90% dissolution and carbonation efficiency, respectively). In addition, the process conditions used for dissolution were d (particle size) =75-150 µm, t= 1 h and T=100°C, while for carbonation, S/L=100 g/l, t=1 h, T= 80°C and Mg^{2+}:NH^{4+}:NH_3 (R) was 1:1.5:2.

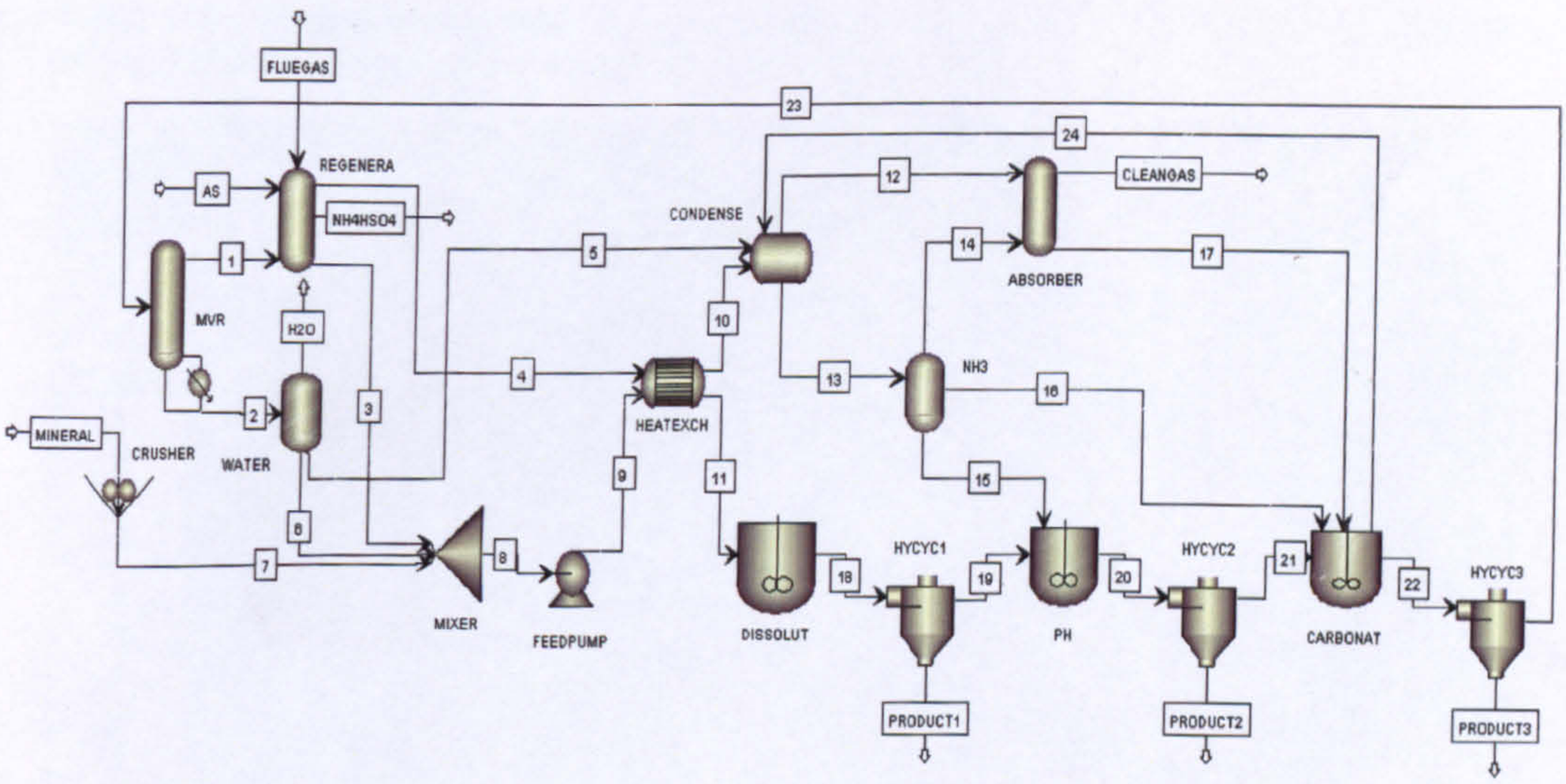

Figure 7-1: Simplified Aspen flow diagram of CCSM process with recyclable ammonium salts

The resulting composition and physical properties of the streams (stream numbers are presented in Figure 7-1) are given in Table 7-1. It was found that the CO_2 removal efficiency was 93 % (CO_2 input and output 60 and 4 t, respectively). The heat and power consumptions (unit names are given in Figure 7-1) are shown in Table 7-2. The flue gas from the boiler typically contains 1800 GJ of heat (assuming 900 °C, 10 vol. % CO_2 and 1.2667 kJ/Nm^3 of flue

gas) (Coskun, 2009). The total heat consumed in the process was 697.9 GJ (Table 7-2). The demand heats of regenerator and heat exchanger (698 GJ) are only 39 % of the heat of flue gas (1800 GJ). Therefore, using waste heat from flue gas can fully compensate the required heat of the process. The total power consumption was 30 MW representing around 30 % of the 100 MW plant with 93 % of CO_2 removal efficiency.

Table 7-1: Properties (temperature and pressure) and composition of the streams of the CCSM process with recyclable ammonium salts

Stream number	T (°C)	P(bar)	Mass flow (t/ h)											
			H_2O	CO_2	$Mg_3Si_2O_5(OH)$	$MgSO_4$	Magnesite	SiO_2	Fe2+	FeO	NH_4HSO_4	$(NH_4)_2SO_4$	NH_3	NH_4HCO_3/ $(NH_4)_2CO_3$
Flue gas	900	1		60										
Mineral	25	1			168.72									
$(NH_4)_2SO_4$	25	1										30.78		
1	25	1										646.95		
2	25	1	2221.9											
3	25	1									543.21			
4	450	1		60									82.7	
5	25	1	860.13											
6	25	1	1329.8											
7	25	1			168.72									
8	25	1	1329.8		168.72						543.21			
9	25	1	1329.8		168.72						543.21			
10	25	1		60									82.7	
11	100	1	1329.8		168.72						543.21			
12	25	1		85.1										
13	25	1	860.13										133	
14	25	1	413.82										65	
15	25	1	229.14										34.2	
16	25	1	217.17										32.5	
17	25	1	400.14										13.1	160.17
18	80	1	1370.3		33.63	161.88		56	8.6		232.56	177.84		
19	80	1	1370.3			161.88			8.6		232.56	177.84		
20	80	1	1594.9			161.88				14		445.17		
21	80	1	1594.9			161.88						445.17		
22	80	1	2221.9			6.27	108.9					616.17		
23	80	1	2221.9									616.17		
24	80	30		25.1									50.2	
Clean gas	25	1		3.99										
NH_4HSO_4	450	1									76.95			
H_2O	25	1	9.69											
Product 1	80	1			33.63			56						
Product 2	80	1								14				
Product 3	80	1					108.9							

Table 7-2: Heat and power consumption of CCSM process with recyclable ammonium salts

	Power flow (MW)	**Heat flow input (GJ)**
Regenerator	4	578
MVR	18	
Feed pump	3	
Crusher	2	
Heat exchanger		433
Absorber	2	
Dissolution		-85
Carbonation		-228
HYCYC1,2,3[18]	1	
Total	30	698

7.2 Cost evaluation

On the basis of the simulated process shown in Figure 7-1 and the flow sheeting in Table 7-1, the variable and fixed capture and storage costs of all the operation units were estimated.

7.2.1 CAPEX costs

The CAPEX costs were estimated using a detailed factorial cost estimation method as described by Sinnott (1997). The price of

[18] Hydrocyclone 1, 2 and 3

each major unit operation in the process was calculated taking into consideration the following:

- Because of possible corrosion due to the use of ammonia water and ammonium bisulfate, AISI 316 stainless steel was selected for the construction of MVR, regenerator, feed pump heat exchanger, condenser, absorber, HYCYC1 and carbonation reactor. The crusher, water tank and HYCYC 2, 3 are made of stainless steel, while the dissolution and pH reactors are made of glass. The NH_3 tank is made of linear low-density polyethylene (LLDPE).
- Reference equipment was selected for which price information was available in the public literature (DACE, 2005). The size of the reference equipment was chosen as close as possible to the actual designed equipment size.
- The cost of the reference equipment was adjusted for the actual size of the equipment type using an apparatus-specific scale factor, which was calculated from the costs data available in the public literature (Peters, 1991).
- The price of the scaled reference equipment was corrected for the operating pressure as well as the materials of construction. On the basis of data presented in Huijgen's work (Huijgen *et al.*, 2007), prices given for equipment operating at ambient pressure were corrected by a factor of 1.6 in an operating pressure of around 35 bar. In this study, the operation

pressure is 1 bar except for the carbonation reactor, where a maximum pressure of 35 bars is used.

Table 7-3: Surcharge factors used for various equipment (Sinnott, 1997)

Direct associated investments (% of equipment cost)	
Equipment erection	45
Instrumentation	25
Piping	45
Process building	10
Storages	20
Utilities	45
Ancillary building	20
Site development	5
Sum	215
Indirect associated investments (% of equipment cost)	
Design and engineering	25
Contractor's fee	5
Contingency	10
Sum	40

After calculation of the costs for the major process equipment units, these costs were multiplied individually with specific factors to include direct associated costs (Table 7-3). For each major unit operation, the sum of direct associated costs was determined to be 215 % of equipment cost and the sum of indirect associated costs was determined to be 40 % of equipment cost. The total direct associated costs and indirect associated costs were added, resulting

in the total fixed capital costs. Finally, 10 % of the total fixed capital costs was reserved as working capital. The investment costs of the mineral carbonation plant were determined as the sum of the fixed and working capital.

Table 7-4 shows the calculation of the CAPEX costs of the process, including the costs of the reference equipment selected for the major unit operations and possible scale and correction factors used. The total CAPEX costs of a mineral carbonation plant with a CCSM process with recyclable ammonium salts are 39 million US$, of which 35.6 million US$ is fixed capital. Total equipment costs are 10 MUS$, of which the most expensive equipment units are the carbonation reactor (2.6 million US$), MVR evaporator (1.3 million US$) and HYCYC 3 (1.2 million US$). The costs of feed pump, absorber, water tank and NH_3 tank are small compared to the other investment costs. Taking into consideration 8000 operating h/yr and the depreciation time of 10 years, the CAPEX cost is 9 US$/t CO_2 sequestered.

A number of units contribute to a small extent to the total CAPEX cost. For example, the total cost contribution for the crushers, feed pump, absorber, condenser, NH_3 tank and water tank is approximately 11 % (Figure 7-2). These common components present therefore very little opportunity for cost reduction and optimization.

The cost of HYCYC 1, 2 and 3 can be significant and accounts for up to 30 % of total CAPEX cost (Figure 7-2). The cost of HYCYC is controlled by the amount of slurry processed per tonne of CO_2. The increase of solid to liquid ratio or fixation efficiency can reduce the required size of HYCYC. HYCYC equipment has been utilized in industry for a long time and its performance has been largely optimized. Therefore, there is little opportunity for cost reduction and optimization on this unit.

Figure 7-2: CAPEX Cost structure of CCSM process.

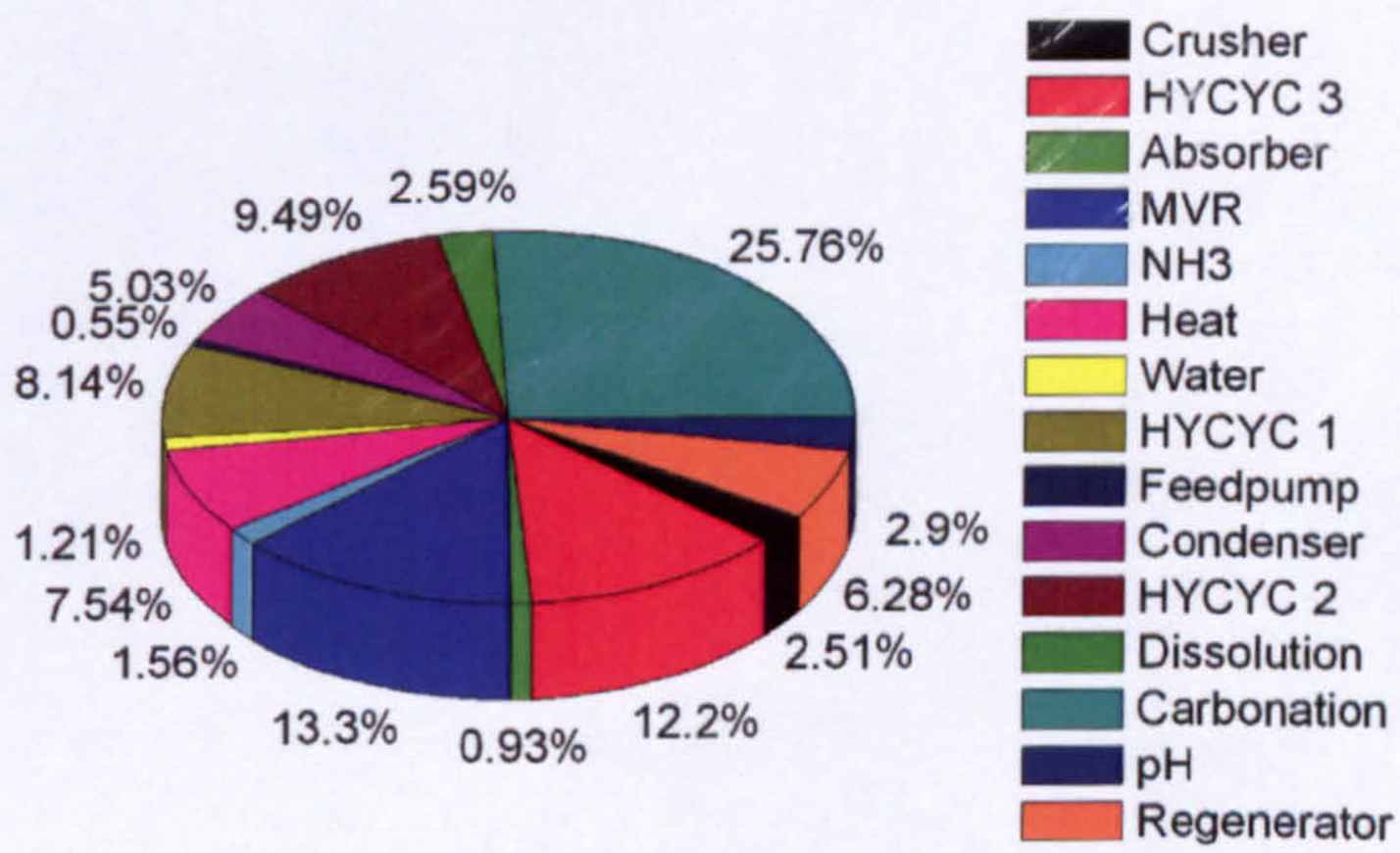

The cost of the carbonation reactors is primarily controlled by the residence/hold time; therefore, faster carbonation kinetics enables lower cost. The cost of the carbonation reactors is also dependent on the solid to liquid ratio, where increasing the solid to liquid ratio from 50 g/l to 100 g/l lowers by 50 % the carbonation reactor cost.

Pressure also effects the cost, where as an example the cost decreases from 2583 kUS$ to 260 kUS$ when the pressure decreases from 34 bars to 1 bar (Table 7-4). Overall, the cost of the carbonation reactor takes account for the major CAPEX cost, and therefore the enhancement of carbonation kinetics and conditions optimization, such as S/L ratio and pressure, present significant cost reduction opportunities.

Table 7-4: CAPEX costs for CCSM process with recyclable ammonium salts

Name of unit	Reference equipment from the literature				Flow-sheeting results			Cost calculation				Price (kUS$)	
	Equipment type	Price (kUS$)	Relevant size	materials	Relevant size	Pressure (bar)	Number in series	Correction factor: Scale	Pressure	other	PCE[19]	surcharge: Direct	Indirect
Crusher	Cone crusher	65	60 t/h	Stainless steel	168.72	NA	3			1.29	251.55	540.83	100.62
MVR	Leke MVR evaporator	92	600 t/h	AISI 316	2838.03	NA	5	0.78			1333.8	2867.67	533.52
Regenerator	Welded plate heat exchanger	342	1000 m^3	AISI 316	677.73	1-34	1		1.6	1.15	629.28	1352.95	251.71
Water tank	SMC water tank	3.3	180 t/h	Stainless steel	2221.9	NA	13	0.78			121.68	261.61	48.67

[19] PCE: Purchase cost of equipment

Feedpump	Single stage centrifugal pump	11	250 t/h	AISI 316	2041.73	NA	9	0.14	4	55.44	119.20	22.18
Heat exchanger	Shell and tube heat exchanger	28	1000 m^3	AISI 316	2184.39	NA	3			756	1625.4	302.4
Condenser	Shell and tube heat exchanger	28	1000 m^3	AISI 316	1576.2	NA	2			504	1083.6	201.6
Absorber	Ammonia scrubber	20	100 t/h	AISI 316	563.88	NA	6	0.78		93.6	201.24	37.44
NH_3 tank	Ammonia tank	10	100 t/h	LLDPE	992.94	NA	10	0.78		156	335.4	62.4
Dissolution reactor	CSTR	10	120 m^3	Glass	2041.73	1-2	17	0.45		260.1	559.22	104.04
HYCYC 1	Hydrocyclone separator	2	350t/h	AISI 316	2040.7	NA	6	0.66		815.76	1753.88	326.30

pH reactor	CSTR	10	120 m^3	Glass	2214.45	NA	19	0.45		290.7	625.01	116.28
HYCYC 2	Hydrocyclone separator	2	350t/h	Stainless steel	2216.16	NA	7	0.66		951.72	2046.20	380.69
Carbonation reactor	CSTR	18	120 m^3	AISI 316	3024.99	1-35	26	0.45	1.6	2583.36	5554.22	1033.34
HYCYC 3	Hydrocyclone separator	2	350t/h	Stainless steel	2953.17	NA	9	0.66		1223.64	2630.83	489.46
Sum										10026.63	21557.25	4010.65

Fixed capital	35594.54
Working capital	3559.45
Total investment	39153.99

7.2.2 CO_2 capture and storage costs

The total CO_2 capture and storage costs for the CCSM process with recyclable ammonium salts are listed in Table 7-5, including the CAPEX, energy, chemical and feedstock costs. The total cost is 72 US$/t CO_2 sequestered, when excluding product sale. The largest costs are associated with chemical costs (35 %) (Figure 7-3), followed by energy costs (22 %) and feedstock costs (21 %). In comparison, CAPEX costs (12 %) and transportation costs (10 %) are relatively small. The amount of feedstock required not only has an influence on the costs of feedstocks, but also affect the transportation costs. Also, the value of the products from the process is an important parameter for the costs, since the mass of products is 3.8 times larger than the mass of CO_2 sequestered (212.5 t products compared to 56 t CO_2). However, the value of the products and the market size are uncertain, since no assessment of possible markets have been reported so far. If product sale of 20 US$/t of product 1 (>46.9 wt. % Si), 130 US$/t of product 2 (>60 wt. % Fe) and 400 US$/t of magnesite are included, this would reduce the total costs substantially (e.g. from spend of 71.79 US$/t CO_2 sequestered to a profit 681.30 US$/t CO_2 sequestered) (see Table 7-5). It should be noted that the current market sizes of these products is relatively small compared to the large amounts produced by the CCSM process.

Table 7-5: CO_2 capture and storage costs for CCSM process with recyclable ammonium slats

		Costs (US$/t CO_2)
Energy costs		16
Chemical costs		25
Mineral costs		15
Transportation costs (100 km)		7
CAPEX cost US$/t CO_2		9
Total cost exclude product sale		**72**
Benefits from product sale		
	Product 1	-20 [a]
	Product 2	-33 [a]
	Magnesite	-764 [a]
Total profit from product sale		-816 [a]
Total cost include product sale		-681 [a]

[a] Negative value means the profit from the sale of products.

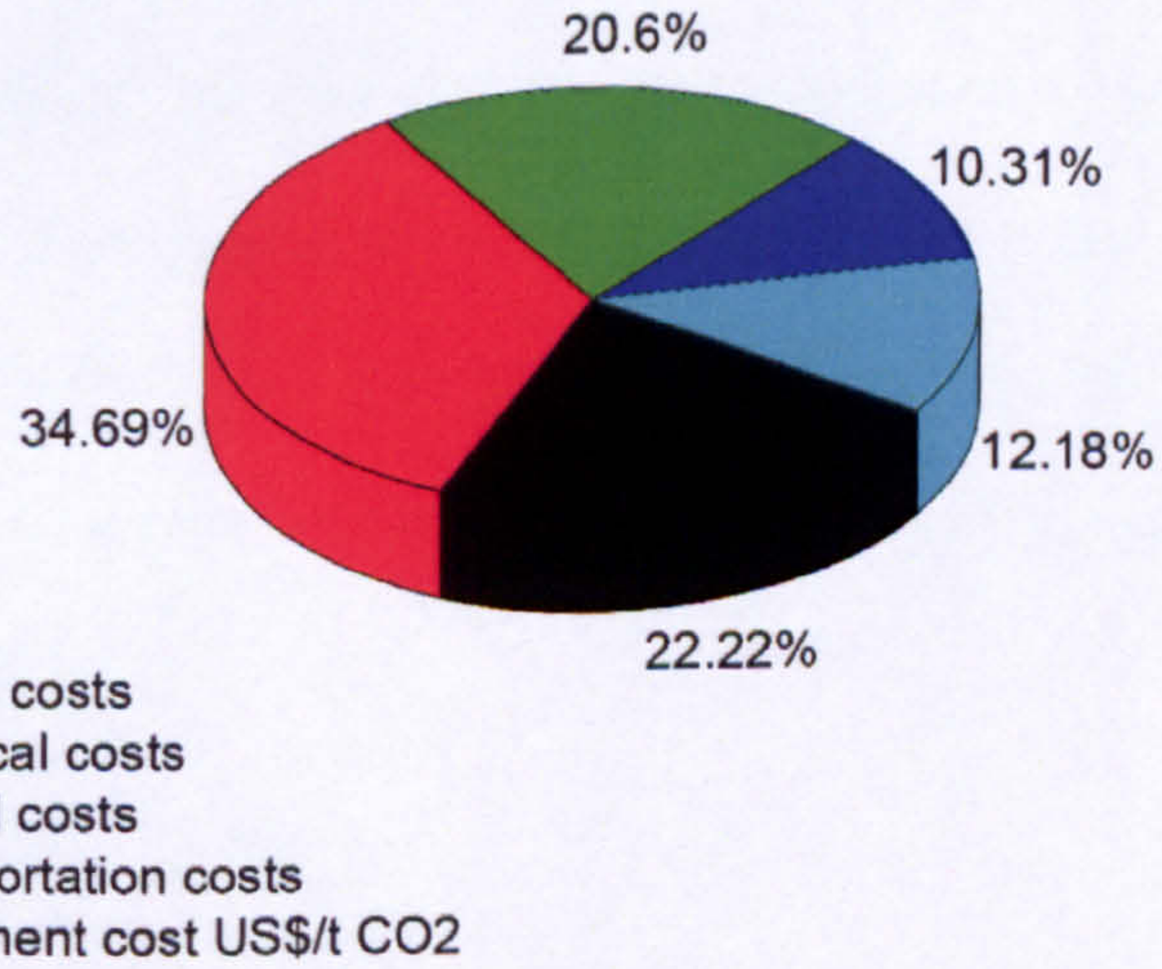

Figure 7-3: Pie chart of costs in CCSM process with recyclable ammonium salts

7.3 Sensitivity analysis and influence of the process conditions

A sensitivity analysis was conducted and the results are presented in Table 7-6 and Figure 7-4. Three different values have been selected for each parameter (standard, minimum and maximum values). The effect of these different parameter values on the total cost/t_{CO2} sequestered (including CAPEX and OPEX) can be seen clearly. Within the ranges studied, the largest variables on the reported costs are associated with the value of the carbonation efficiency (72-109 US$/t), molar ratio of Mg:$NH_4$ salts: NH_3 (72-101 US$/t), dissolution efficiency (63-87 US$/t), electricity price (61-82 US$/t), price of feedstock (63-81 US$/t) and solid to liquid ratio (72-86 US$/t). Table 7-7 shows the influence of solid to liquid ratio, reaction time, particles size, molar ratio of Mg:NH_4 salts: NH_3 and excess of NH_4HSO_4 on the dissolution efficiency and carbonation efficiency. The economically optimum set of process conditions is presented in Table 7-6 (scenario 1). However, the economically optimum set of process conditions may not be the most efficient set (scenarios 7 and 9).

Table 7-6: Parameters studied with a standard, minimum and maximum value.

#	Parameters	Standard	Min	Max
1	**Dissolution efficiency (%)**	80	60	100
2	**Carbonation efficiency (%)**	96	81	
3	**Solid to liquid ratio (g/l)**	100	50	
4	**Reaction time (h)**	1		3
5	**Mg: NH_4 salts: NH_3 (molar ratio)**	1:1.5:2	1:1:1	
6	**Particle size (µm)**	75-150	<38	150-300
7	**Feedstock (US$/t)**	5	2	8
8	**Cost of $(NH_4)_2SO_4$ (US$/t)**	90	70	110
9	**MVR energy cost (kWh/t)**	8	4	12
10	**Thermal decomposition (kWh/t)**	6	0	12
11	**CO_2 capture (kWh/t)**	19	10	28
12	**Electricity (US$/kWh)**	0.03	0.01	0.05
13	**Operation time (hr/yr)**	8000	7500	8500
14	**Depreciation time (yr)**	10	5	15

Combing the information about the effect of parameters on cost (Figure 7-4) and the effect of parameters on efficiency (Table 7-7), it is found that the carbonation efficiency is the most important parameter. Increasing the carbonation efficiency from 81 to 96 %

results in cost reduction from 109 to 72 \$/t CO_2 sequestered. Although, addition of NH_3 in carbonation (from 0 to 0.07 t) is required in order to get high carbonation efficiency, it can save consumption of NH_4HSO_4 from 0.71 to 0.20 t.

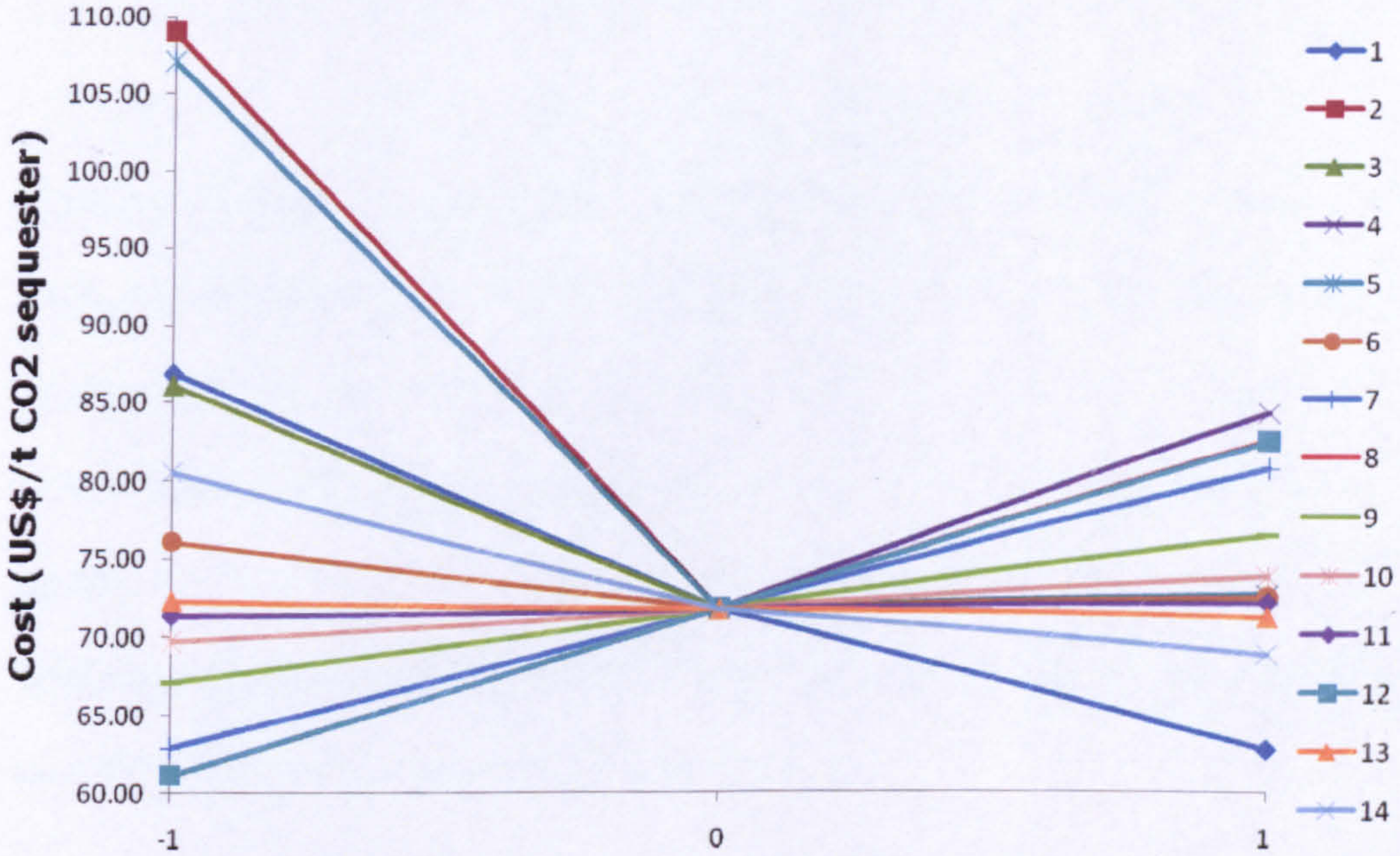

Figure 7-4: Sensitivity analysis of CO_2 capture and storage costs for CCSM process with recyclable ammonium salts (1. Dissolution efficiency (%), 2. Carbonation efficiency (%), 3. Solid to liquid ratio (g/l), 4. Reaction time (h), 5. Mg: NH4 salts: NH3 (molar ratio), 6. Particle size (μm), 7. Feedstock (US$/t), 8. Cost of (NH4)2SO4 (US$/t), 9. MVR energy cost (kWh/t), 10. Thermal decomposition (kWh/t), 11. CO2 capture (kWh/t), 12. Electricity (US$/kWh), 13. Operation time (hr/yr), 14. Depreciation time (yr); there is no maximum value for 2, 3 and 5, since the selected standard value is already high, the detail information can be seen in Table 7-6)

The dissolution efficiency is affected by reaction time, solid to liquid ratio and particle size of feedstock. The high dissolution efficiency needs a small amount of feedstock, thus decreasing the feedstock,

transportation costs and reducing the amount of additive (NH_4HSO_4) used. Normally, high dissolution efficiency requires longer reaction time (3 h), low solid to liquid ratio (50 g/l) and small particle size. When decreasing S/L from 100 to 50 g/l, the dissolution efficiency increases from 80 % to 90 %. However, low S/L resulted in larger streams of materials and thereby requires a larger size of equipment and high energy consumption. For example, when the amount of water input increases from 39 to 64.7 t, the size of all equipment nearly doubles. Besides, low S/L increases the energy consumption for water evaporation and the amount of additives used. It can be seen from Figure 7-4 (Parameter 3) that the cost/t_{CO2} sequestered decreases from 94 to 72 US$/t, when the solid to liquid ratio increases from 50 to 100 g/l.

Table 7-7: Influence of process conditions on dissolution and carbonation efficiency.

Scenario #	**1**	**2**	**3**	**4**	**5**	**6**	**7**	**8**	**9**	**10**
Solid to liquid ratio (g/l)	100	100	100	100	100	100	100	50	50	50
Reaction time (h)	1	1	1	1	1	1	3	1	3	3
Particle size (µm)	75-150	75-150	75-150	75-150	38	150-300	75-150	75-150	75-150	75-150
Mg:NH_4 salts: NH_3 (molar	1-1.5-2	1-1-1	1-1.5-1	1-1-2	1-1.5-2	1-1.5-2	1-1.5-2	1-1.5-2	1-1.5-2	1-1.5-2

ratio)										
Excess of NH_4HSO_4	40%	40%	40%	40%	40%	40%	40%	40%	40%	0%
Dissolution efficiency (%)	80	80	80	80	83	77	100	90	100	90
Carbonation efficiency (%)	96	81	86	90	96	96	96	96	96	96

When increasing the reaction time from 1 to 3 h, the dissolution efficiency raised slightly from 80 % to 90 %. However, long reaction times significantly increase the size of equipment by as much as 3 times and the investment costs will increase from 9 to 26 US$/t. Small particle size (<38 μm) increases the dissolution efficiency slightly (3 %), but raises the grinding power consumption from 13 to 83 kWh/t, and thus increasing the total cost to 76 US$/t. Therefore, small particle size and long reaction time are not preferred in terms of cost reduction.

The energy consumptions of several steps, such as CO_2 capture, MVR evaporation and thermal decomposition present small variations on cost (no more than 10 US$), because the technologies used in these steps have been optimized and their energy penalties are relatively low. The electricity price has a large influence on the total costs (61-82 US$/t CO_2 sequestered) and this is dependent on the types of fuel source (coal or natural gas) and the technologies

applied (coal-fired, IGCC, supercritical combustion and NGCC). It was assumed that electricity is supplied from the power plant to the mineral carbonation plant at a low price (0.03 US$/kWh). The long depreciation time reduces the total costs, since the investment costs are spread out over long time periods.

7.4 Comparison to other cost analysis

This section compares the costs of the studies process with other reported mineralisation processes (Table 7-8). For the direct aqueous mineral carbonation process using serpentine, the Albany Research Center (ARC) calculated total costs of 250 US$/t CO_2 sequestered excluding chemical cost and investment cost. The main difference between the ARC process and this study is due to the large energy consumption of the heat treatment of serpentine (283 kWh/t serpentine) and high energy consumption resulting from high temperature and high pressure applied (155 °C and 115 bar) (Gerdemann *et al.*, 2007). For the indirect aqueous mineral carbonation process using serpentine, Teir *et al.* (2009) calculated total costs of 1300-1600 US$/t CO_2 sequestered using serpentine and un-recyclable HCl or HNO_3 and NaOH, excluding energy cost and investment cost. The high costs of Teir's work resulted from the unrecyclable nature of the chemicals used. The direct aqueous mineral carbonation using wollastonite and steel slags studied by Huijgen (2007) resulted in costs of 86 and 64 US$/t CO_2

sequestered (Table 7.8). Additionally, the costs reported by all the other processes exclude the carbon capture step.

Table 7-8: Comparison of costs reported for mineral carbonation and other carbon capture and storage technologies

Costs mineral carbonation (US$/t CO_2 sequestered)	**Feedstock**	**Process route**	**Chemical used**	**Reference**
250	Serpentine	Direct aqueous	$NaHCO_3$ and NaCl	Gerdemann *et al.*, 2007
54	Olivine	Direct aqueous	$NaHCO_3$ and NaCl	Gerdemann *et al.*, 2007
91	Wollastonite	Direct aqueous	water	Gerdemann *et al.*, 2007
1300-1600	Serpentine	Indirect aqueous	HCl (HNO_3) and NaOH	Teir *et al.*, 2009
86	Wollastonite	Direct aqueous	Water	Huijgen *et al.*, 2007
72 (including capture)	serpentine	Indirect aqueous	Ammonium salts	This study

Overall, the CCSM process with recyclable ammonium salts has the lowest costs of 72 US$/t CO_2 sequestered among the current available mineral carbonation processes using serpentine. The CO_2 capture costs are included in the total cost of the CCSM process. Representative CO_2 capture cost reported for different types of power plants range from 25-75 US$/t CO_2 (IPCC, 2005). Therefore, the integration of the mineral carbonation process with the CO_2

capture process into the CCSM process with recyclable ammonium salts successfully lower the overall costs of CO_2 capture and storage costs.

7.5 Summary

A comprehensive cost evaluation (CAPEX and OPEX) of the CCSM process with recyclable ammonium salts has reported 72 US$/t CO_2 sequestered. The major costs were found to be associated with chemical costs, energy costs and feedstock costs. Sensitivity analysis have shown that influential parameters in the total costs are the possible value of products, carbonation efficiency, molar ratio of Mg:NH_4 salts: NH_3, dissolution efficiency, electricity price, price of feedstock and solid to liquid ratio. Generally, total costs were affected by the dissolution efficiency and carbonation efficiency. Carbonation efficiency was affected by molar ratio of Mg: NH_4 salts: NH_3. Dissolution efficiency was affected by the solid to liquid ratio, reaction time and particle size. The optimized process conditions were determined in this study to obtain the lowest total costs.

Research on cost reduction should focus on carbonation reactor, which is the major CAPEX cost contributor identified in this study. The faster carbonation kinetics can significantly reduce the residence time, thus reducing the CAPEX cost of the carbonation reactor.

Chapter 8. Conclusions and future work

8.1 Conclusions

Carbon dioxide capture and storage by mineralisation (CCSM) is considered as one of the main solutions for reducing anthropogenic CO_2. However, low efficiency of mineral dissolution and unrecyclable use of additives are two key barriers for the development of CCSM. In this thesis, a novel pH-swing mineral carbonation process has been developed to improve the dissolution and carbonation efficiencies using a recyclable ammonium salts. This process is unique in using CO_2 containing ammonium salts from aqueous ammonia capture technology, instead of direct CO_2 gas. The advantages of using CO_2 containing ammonium salts include avoiding CO_2 desorption in the capture step and subsequent CO_2 compression for transportation that are energy intensive steps of the conventional CCS process. The integration of carbon capture and mineral carbonation in this process has not been explored before. Two process routes at different solid to liquid ratios were developed to couple the aqueous ammonia carbon capture step with the subsequent carbonation step. Hence, this thesis provides novel information on the dissolution and carbonation experiments with recyclable ammonium salts at different parameters as well as the

regeneration of ammonium salts. And the reaction conditions were carefully selected to maximize the efficiencies.

8.1.1 Serpentine dissolution with ammonium salts

The dissolution of serpentine using ammonium salts was investigated (Section 4.1). The incongruent leaching of Mg and Si created a passive silicon layer on the surface of the particles preventing further leaching of Mg. The applications of internal grinding and fluidized bed are expected to remove the product layer. The solvent concentration, particle size and solid to liquid ratio was carefully selected through the experimental studies. The Mg dissolution from serpentine achieved 100 % in 3 hours when dissolving serpentine with particle size fraction of 75-150 μm and using 1.4 M ammonium bisulfate solution at 50 g/l solid to liquid ratio.

8.1.2. Carbonation with ammonium salts

The precipitation of hydromagnesite from prepared high Mg concentration solution was studied by using NH_3 and NH_4HCO_3 in the multistep process route with pure products (Section 4.2). Pure hydromagnesite, amorphous silica and iron by-products were obtained. The integration of carbon capture with mineralization was successful and show high efficiency. The mass ratio of $Mg:NH_4HCO_3:NH_3$ was the key factor controlling carbonation efficiency. The additives used, NH_4HSO_4 and NH_3, were regenerated

by the thermal decomposition of $(NH_4)_2SO_4$ at 330 °C with 95 % efficiency.

8.1.3. CCSM process route at high solid to liquid ratio

The dissolution and carbonation experiments with recyclable ammonium salts at high solid to liquid ratio conditions were studied in Chapter 5. The dissolution efficiency increased when the solid to liquid ratio increased from 200 g/l to 300 g/l due to particle-particle interactions; magnesite instead of hydromagnesite was found after the carbonation step due to the CO_2 pressure evolved (20 bar); and the carbon fixation efficiency was significantly improved by using $(NH_4)_2CO_3$ rather than using NH_4HCO_3.

8.1.4. Preliminary cost evaluation

Most of the process units are mature technologies, excluding the unit for thermal decomposition of ammonium salts. Additionally, it was found that the use of waste heat from flue gas to supply the heat required for the thermal decomposition of ammonium salts is very important for the success of the CCSM process with recyclable ammonium salts.

A preliminary cost analysis of the developed CCSM process was conducted to evaluate the OPEX of the two process routes (high and low solid-to-liquid ratio) in terms of energy consumption, chemical costs and feedstock cost (Section 6.2). It was found that high solid to liquid ratios resulted in less streams in the process, and thus

lower energy consumption, but it also decreases the dissolution and carbonation efficiencies. It was suggested that dissolution and carbonation efficiencies at the low solid to liquid ratio scenario was better than those at the high solid to liquid ratio.

8.1.5. Optimization work and cost evaluation

The optimization process conditions were determined according to the results from the process evaluation (Section 6.3). A series of experiments were then conducted at the optimization process conditions to maximize the efficiencies. The dissolution efficiency of Mg from serpentine using 2.8 M NH_4HSO_4 at 100 g/l solid to liquid ratio for 1 h was 80 %. The carbonation efficiency was 96 % when the molar ratio of Mg: NH^{4+} salts: NH_3 was 1:1.5:2. Finally, a comprehensive cost evaluation (CAPEX and OPEX) of the CCSM process with recyclable ammonium salts was made by using Aspen plus software (Chapter 7). It was found that 93 % of the CO_2 can be sequestered by the process with an energy consumption of 30 %. The total capture and storage costs were calculated to be 72 US$/t CO_2 sequestered in this process. The reaction time and equipment cost still have potential to be reduced. The full life cycle carbon footprint of this CCSM process is needed to show the net CO_2 reduction.

8.2 Future work

Based on the results and conclusions from this research, there are several areas that are worthy of further investigation which could contribute significantly to the development of the CCSM process with recyclable ammonium salts.

a) To investigate the dissolution experiments in a fluidized bed reactor or pipeline looping reactor, where particle-particle interactions can improve the dissolution efficiency;
b) To improve the carbonation efficiency in the high solid to liquid ratio conditions by adding ammonia water, which can enhance the carbonation kinetics;
c) To investigate the potential use of a continuous process instead of batch process to reduce the reaction time;
d) To measure the species of CO_2 containing ammonium salts at higher NH_3 concentration (>13 wt. %) in the CO_2 absorption step;
e) To investigate the thermal decomposition of ammonium salts with hot gas which mimics the temperature and chemical composition of flue gas from a boiler in a power plant;
f) To use waste materials from industries instead of serpentine with the CCSM process with recyclable ammonium salts.
g) To investigate the re-use of products from the process, especially, the re-use of carbonate products as supplementary

cementitious material (SCM) to make cement or other construction materials;

h) To investigate the co-removal of SO_2, NO_X and Hg in the capture and the carbonation steps.

i) To do the full life cycle carbon footprint of this CCSM process is needed to show the net CO_2 reduction.

j) The choice of equipment for filtering, drying and the other steps need to be investigated to reduce the cost.

References

2050CEACES (2009) China's Low Carbon Development Pathways by 2050: Scenario Analysis of Energy Demand and Carbon Emissions. Energy Research Institute National Development and Reform Commission, China science press, Beijing, China.

ADIAC (2004) Available: ftp://adiac.oral.gov/pub/trends/co2/vostok.icecore.co2 [Accessed 24th March 2011].

ALBERT B. and WELTY, W. (1972) Process for decomposiong ammmonium sulfate into ammonium bisulfate and ammonia, United States Patent: 3674427

ALEXANDER, G., MERCEDES MAROTO-VALER, M. and GAFAROVA-AKSOY, P. (2007) Evaluation of reaction variables in the dissolution of serpentine for mineral carbonation. *Fuel,* 86, 273-281.

APGTF (2009) Cleaner Fossil Power Generation in the 21st Century: A Technology Strategy for Carbon Capture and Storage. UK Advanced Power Generation Technology Forum (APGTF).

APOSTOLIDIS, C. I. and DISTIN, P.A. (1978) The kinetics of the sulfuric acid leaching of nickel andmagnesium fromreduction roasted serpentine. *Hydrometallurgy,* 3.

BACIOCCHI, R. (2008) Ex-situ Mineral Carbonation. *Accelerated Carbonation for Environmental and Materials Engineering 2008.* Roma, Italy.

BACIOCCHI, R., POLETTINI, A., POMI, R., PRIGIOBBE, V., VONZEDWITZ, V.N., STEINFELD, A. (2006a) CO_2 sequestration by direct gas-solid carbonation of air pollution control (APC) residues. *Energy Fuels,* 20, 1933-1940.

BACIOCCHI, R., POLETTINI, A., POMI, R., PRIGIOBBE, V., ZEDTWITZ-NIKULSHYNA, V., STEINFELD, A. (2006b) Performance and kinetics of CO_2 sequestration by direct gas-solid carbonation of APC residues. *8th International Conference on Greenhouse Gas Control Technologies, 19-22 June,* Trondheim, Norway.

BALUCAN, R. D., KENNEDY, E. M., MACKIE, J. M., DLUGOGORSKI, B. Z. (2010) An Optimised Antigorite Heat Pre-treatment Strategy for CO2 Sequestration by Mineral Carbonation. *In:* the 3nd Int. Conf. on Accelerated Carbonation for Environmental and Materials Engineering, (ACEME10), Turku (Finland) Nov. 29-1 Dec., 2010.

BEARAT, H., MCKELVY, M. J., CHIZMESHYA, A. V. G., GORMLEY, D., NUNEZ, R., CARPENTER, R. W., SQUIRES, K. & WOLF, G. H. (2006) Carbon sequestration via aqueous olivine mineral carbonation: Role of passivating layer formation. *Environmental Science & Technology,* 40, 4802-4808.

BERR (2008) Towards Carbon Captuire and Storage: A Consultation Document. . Department for Business, Enterprise & Regulatory Reform (BERR), London, UK.

BERR (2009) Towards Carbon Captuire and Storage: A Consultation Document. . Department for Business, Enterprise & Regulatory Reform (BERR), London, UK.

BLENCOE JAMES G., P., DONALD A., ANOVITZ, LAWRENCE M., BEARD, JAMES S. (2004) *Carbonation of metal silicates for long-term CO_2 sequestration*

BRADSHAW, J., DANCE, T. (2004) Mapping geological storage prospectivity of CO_2 for the world's sedimentary basins and regional source to sink matching. *In:* IN E.S. RUBIN, D. W. K. A. C. F. G. E., ed. Proceedings of 7th International Conference on Greenhouse Gas Control Technologies, Vol. 1, Peer-Reviewed Papers and Plenary Presentations, IEA Greenhouse Gas Programme, Cheltenham, UK.

BUTT, D. P., LACKNER, K.S., WENDT, C.H. (1998)The kinitics of binding carbon dioxide in magnesium carbonate. *In:* 23rd international conference on coal utilization and fuel systems, Clearwater, FL (U.S.), 9.-13. Mar, 1998.

COSKUN, Z. O. and ILTEN N. (2009) A new approach for simplifying the calculation of flue gas specific heat and specific exergy value depending on fuel composition. *Energy,* 34, 1898-1902.

CANSOLV (2011) Integrated SO_2-CO_2 System. Available: http://www.cansolv.com/en/multipollutant.ch2 [Accessed 27th March 2011].

CESCA, T. (1971) Process for the production of magnesium oxide. US Patent: 3615201.

CHEN, Y., BRANTLEY, S.L. (2000) Dissolution of forsteritic olivine at 65 °C and 2 < pH < 5. Chemical Geology, 165, 267 - 281.

CHEN, Z. Y., O'CONNOR, W. K. & GERDEMANN, S. J. (2006) Chemistry of aqueous mineral carbonation for carbon sequestration and explanation of experimental results. *Environmental Progress,* 25, 161-166.

CLASS, H., EBIGBO, A., HELMIG, R., DAHLE, H. K., NORDBOTTEN, J. M., CELIA, M. A., AUDIGANE, P., DARCIS, M., ENNIS-KING, J., FAN, Y. Q., FLEMISCH, B., GASDA, S. E., JIN, M., KRUG, S., LABREGERE, D., BENI, A. N., PAWAR, R. J., SBAI, A., THOMAS, S. G., TRENTY, L. & WEI, L. L. (2009) A benchmark study on problems related to CO_2 storage in geologic formations. *Computational Geosciences,* 13, 409-434.

DACE, D. A. (2005) *DACE price booklet 25rd ed,* DACE prijzenboekje, in Dutch.

DAVAL, D., MARTINEZ, I., CORVISIER, J., FINDLING, N., GOFF , B. & GUYOT, F. (2009) Carbonation of Ca-bearing silicates, the case of wollastonite: Experimental investigations and kinetic modeling. *Chemical Geology,* 265, 63-78.

DECC (2009) Climate Change Act 2008: Impact Assessment. Department of Energy and Climate Change (DECC), London, UK.

DEVLEENA MANI, S. N. C. A. B. K. (2008) Assessment of carbon dioxide sequestration potential of ultramafic rocks in the greenstone belts of southern India. *Current science* 94, 124-134.

DUFAUD, F., MARTINEZ, I. and SHILOBREEVA, S. (2009) Experimental study of Mg-rich silicates carbonation at 400 and 500 °C and 1 kbar. *Chemical Geology,* 265, 79-87.

OELKERS, E. H. and MATTER J. (2008) Mineral Carbonation of CO2 *Elements,* 4.

BRENNAN EARL D (1975) Method for the thermal conversion of ammonium sulfate to ammonium bisulfate, US Patent: 3929977.

EIMCO WATER TECHNOLOGIES. (2011) Sustainable biosolids solutions [Online]. Available: Available from http://www.treatmentequipment.com/files/products/cin_brochure.pdf. [Accessed 4th April 2011].

ELONEVA, S. (2010) Reduction of CO_2 emission by *mineral carboantion: steelmarking slag raw material with a pure calcium carboanteend product.* Doctor of Science in Technology, Aalto University

ELONEVA, S., PUHELOINEN, E. M., KANERVA, J., EKROOS, A., ZEVENHOVEN, R. & FOGELHOLM, C. J. (2010) Co-utilisation of CO_2 and steelmaking slags for production of pure $CaCO_3$ - legislative issues. *Journal of Cleaner Production,* 18, 1833-1839.

ELONEVA, S., TEIR, S., REVITZER, H., SALMINEN, J., SAID, A., FOGELHOLM, C. J. and ZEVENHOVEN, R. (2009) Reduction of CO_2 Emissions from Steel Plants by Using Steelmaking Slags for Production of Marketable Calcium Carbonate. *Steel Research International,* 80, 415-421.

ELONEVA, S., TEIR, S., SALMINEN, J., FOGELHOLM, C.J. and ZEVENHOVEN, R. (2008) Fixation of CO_2 by carbonating calcium derived from blast furnace slag. *Energy,* 33, 1461-1467.

ERNST WORRELL. (2008) Energy Efficiency Improvement Opportunities for the Cement Industry. Environmental Energy Technologies Division, Lawrence Berkeley National Laboratory.

EVERINGHAM, J. R., HOENKE, KARL A. (1976) Lawn moss control with ferric ammonium sulfate-ammonium sulfate double salts. U.S. patent: 3964893.

EXPERIENCE NDUAGU, R. Z. (2010) Production of magnesium hydroxide from magnesium silicate for the purpose of CO_2 mineralisation and increasing ocean alkalinity: effect of reaction parameters, ACEME 10, Turku, Finland.

FAGERLUND, J., TEIR, S., NDUAGU, E. & ZEVENHOVEN, R. (2009) Carbonation of magnesium silicate mineral using a pressurised gas/solid process. *Energy Procedia,* 1, 4907-4914.

FAUTH, D. J., SOONG, Y., KNOER, J. P., HOWARD, B. H., GRAHAM, W. J., MAROTO-VALER, M. M., ANDRESEN, J. M. & BALTRUS, J. P. (2001) Conversion of silicate minerals with carbon dioxide producing environmentally benign and stable carbonates. *Abstracts of Papers of the American Chemical Society,* 221, 88.

FOUDA, M. F. R., AMIN, R.E.-S., ABD-ELZAHER, M.M. (1996) Extraction of magnesia from Egyptian serpentine ore via reaction with different acids. II. Reaction with nitric and acetic acids. *Bull. Chem. Soc. Jpn.* , 69, 1913-1916.

FURKERT, H. (1973) Process for the cracking of ammonium sulfte. U.S. patent: 3761575.

GAL, E. (2006) Ultra clearing of combustion gas including the removal of CO_2. Patent no. WO/2006/022885.

GCCSI (2010) THE GLOBAL STATUS OF CCS. Available: http://www.globalccsinstitute.com/resources/publications/global-status-ccs-2010 [Accessed 9th March 2011].

GERDEMANN, S. J., O'CONNOR, W. K., DAHLIN, D. C., PENNER, L. R. & RUSH, H. (2007) Ex situ aqueous mineral carbonation. *Environmental Science & Technology,* 41, 2587-2593.

GIAMMAR, D. E., BRUANT, J. R. G. and PETERS, C. A. (2005) Forsterite dissolution and magnesite precipitation at conditions relevant for deep saline aquifer storage and sequestration of carbon dioxide. *Chemical Geology,* 217, 257-276.

GISLASON, S. R., WOLFFBOENISCH, D., STEFANSSON, A., OELKERS, E. H., GUNNLAUGSSON, E., SIGURDARDOTTIR, H., SIGFUSSON, B., BROECKER, W. S., MATTER, J. M., STUTE, M., AXELSSON, G. & FRIDRIKSSON, T. (2010) Mineral sequestration of carbon dioxide in basalt: A pre-injection overview of the CarbFix project. *International Journal of Greenhouse Gas Control,* 4, 537-545.

GOFF F, L. K. (1998) Carbon dioxide sequestering using ultramafic rocks. *Environmental Geoscience,* 5, 89-101.

GUNNING, P. J., HILLS, C. D. & CAREY, P. J. (2010) Accelerated carbonation treatment of industrial wastes. *Waste Management,* 30, 1081-1090.

HENCHEN, M., KREVOR, S., MAZZOTTI, M. & LACKNER, K. S. (2007) Validation of a population balance model for olivine dissolution. *Chemical Engineering Science,* 62, 6412-6422.

HENCHEN, M., PRIGIOBBE, V., BACIOCCHI, R. & MAZZOTTI, M. (2008) Precipitation in the Mg-carbonate system-effects of temperature and CO_2 pressure. *Chemical Engineering Science,* 63, 1012-1028.

HENCHEN, M., PRIGIOBBE, V., STORTI, G., SEWARD, T. M. & MAZZOTTI, M. (2006) Dissolution kinetics of fosteritic olivine at 90-150 °C including effects of the presence of CO_2. *Geochimica et Cosmochimica Acta,* 70, 4403-4416.

HAUG, T. A., KLEIV, R. A. & MUNZ, I. A. (2010) Investigating dissolution of mechanically activated olivine for carbonation purposes. *Applied Geochemistry,* 25, 1547-1563.

HERZOG, H. (2002) Carbon Sequestration via Mineral Carbonation: Overview and Assessment. MIT Laboratory for Energy and the Environment, , Cambridge, MA, US.

HUAIWEI, Z. & XIN, H. (2011) An overview for the utilization of wastes from stainless steel industries. *Resources, Conservation and Recycling,* 55, 745-754.

HUIJGEN, W. J. J., COMANS, R. N. J. & WITKAMP, G.J. (2007) Cost evaluation of CO_2 sequestration by aqueous mineral carbonation. *Energy Conversion and Management,* 48, 1923-1935.

HUIJGEN, W. J. J., WITKAMP, G.-J. & COMANS, R. N. J. (2006) Mechanisms of aqueous wollastonite carbonation as a possible CO_2 sequestration process. *Chemical Engineering Science,* 61, 4242-4251.

STASIULAITIENE, G. D. (2007) Lithuanian serpentines as potential carbon dioxide binders. *In: The Proceedings of the 32nd International Technical Conference on Coal Utilization & Fuel Systems, June 10–15, 2007, Sharaton Sand Key, Clearwater, Florida, U.S.*.

ICIS (2010) *Chemical price report* [Online]. Available: http://www.icis.com/staticpages/generalpriceslanding.htm?cp=KNC-CHPR-Generalprices_2010&sfid=70120000000Hu8n&mode=icispricing [Accessed 12th March 2011].

IEA (2007) World Energy Outlook 2007. International Energy Agency, OECD/IEA, Paris, France [Online]. Available: www.iea.org/textbase/nppdf/free/2007/weo_2007.pdf [Accessed 23th February 2011].

IEA (2008) Energy Technology Perspectives, International Energy Agency, Paris: France [Online]. Available: www.iea.org/textbase/nppdf/free/2008/etp2008.pdf [Accessed 23th February 2011].

IEA (2009) World Energy Outlook 2009 (WEO 2009), OECD/IEA, Paris, France [Online]. Available: http://www.worldenergyoutlook.org/docs/weo2009/WEO2009_es_english.pdf [Accessed 23th February 2011].

IEA. (2010a) CO_2 emission from fuel combustion Highlights 2010 Edition, International Energy Agency [Online]. Available: www.iea.org/co2highlights/co2highlights.pdf [Accessed 23th February 2011].

IEA (2010b0 Energy technology system analysis programe: Cement Production. http://www.etsap.org/E-techDS/PDF/I03_cement_June%202010_GS-gct.pdf. [Accessed 23th February 2011]

IPCC (2005) Working Group III of the Intergovernmental Panel on Climate Change (Metz, B., O. Davidson, H. C. de Coninck, M. Loos, and L. A. Meyer (eds.). IPCC special report on carbon dioxide capture and storage. Cambridge, United Kingdom and New York, NY, U.S.: Cambridge University Press.

IPCC (2007) Climate Change 2007: Mitigation. Contribution of Working Group III to the Fourth Assessment Report of the Intergovernmental Panel on Climate Change, Metz, B., O. Davidson, H. C. de Coninck, M. Loos, and L. A. Meyer (eds.), Cambridge University Press, Cambridge, UK

BLENCOE, J. G., BEARD, J. S. AND PALMER D. A. (2003) Carbonation of Serpentine for Long-Term CO2 Sequestration. ENGINEERING SCIENCE AND TECHNOLOGY.

LEE, W. K. D. (2005) Characteristic study of korean magnesium silicate for CO_2 mineral carbonation. 22nd annual international Pittsburgh coal conference, 12-15 September, Pittsburgh, PA, U.S..

JARVIS, K., CARPENTER, R. W., WINDMAN, T., KIM, Y., NUNEZ, R. & ALAWNEH, F. (2009) Reaction Mechanisms for Enhancing Mineral Sequestration of CO_2. *Environmental Science & Technology,* 43, 6314-6319.

KAKIZAWA, M., YAMASAKI, A. & YANAGISAWA, Y. (2001) A new CO_2 disposal process via artificial weathering of calcium silicate accelerated by acetic acid. *Energy,* 26, 341-354.

KARASEK, G. (2010) Evaporation Technology - Evaporation, Crystallization and Rectification [Online]. Available: http://www.gigkarasek.at/assets/images/content/EVT-englisch-NEU.pdf [Accessed 24th April 2011].

KELEMEN, P. (2010) In situ mineral carbonation in peridotite for CO_2 capture & storage [Online]. Available: http://eps.mcgill.ca/~courses/c666/Kelemen%20Report_final.pdf [Accessed 2th May 2011].

KIM, Y. J., YOU, J. K., HONG, W. H., YI, K. B., KO, C. H. & KIM, J. N. (2008) Characteristics of CO2 absorption into aqueous ammonia. *Separation Science and Technology,* 43, 766-777.

KLAUS S. LACKNER, D. P. B., CHRISTOPHER H. WENDT (1998) Binding Carbon Dioxide in Mineral Form: A Critical Step Towards a Zero-Emission Coal Power Plant. Los Alamos National Laboratory.

KODAMA, S., NISHIMOTO, T., YAMAMOTO, N., YOGO, K. & YAMADA, K. (2008) Development of a new pH-swing CO_2 mineralization process with a recyclable reaction solution. *Energy,* 33, 776-784.

KOHLMANN, J. (2001) Removal of CO_2 from flue gases using magnesium silicates in Finland. Helsinki university of technology department of mechanical engineering, Espoo, TKKENY-3.

KOTHANDARAMAN, A. (2010) Carbon Dioxide Capture by Chemical Absorption: A Solvent Comparison Study. Doctor of Philosophy in Chemical Engineering Practice, Massachusetts Institute of Technology.

KREVOR, S. C. & LACKNER, K. S. (2009) Enhancing process kinetics for mineral carbon sequestration. *Energy Procedia,* 1, 4867-4871.

KREVOR, S. C. M., LACKNER, KLAUS S. (2011) Enhancing serpentine dissolution kinetics for mineral carbon dioxide sequestration. *International Journal of Greenhouse Gas Control,* In Press, Corrected Proof.

KUNZIG, R. (2009) The Canadian oil boom: Scraping Bottom. *National Geographic* 215, 38-59.

LACKNER, K. S. (2002) CARBONATE CHEMISTRY FOR SEQUESTERING FOSSIL CARBON. *Annual Review of Energy and the Environment,* 27, 193-232.

LACKNER, K. S., BUTT, D. P. & WENDT, C. H. (1997) Progress on binding CO_2 in mineral substrates. *Energy Conversion and Management,* 38, S259-S264.

LACKNER, K. S., WENDT, C. H., BUTT, D. P., JOYCE, E. L. & SHARP, D. H. (1995) Carbon dioxide disposal in carbonate minerals. *Energy,* 20, 1153-1170.

LACKNER, K. S. Z., H. J. (2000) From low to no emissions. *Modern Power Systems,* 20, 31-32.

LAOUTID, F., GAUDON, P., TAULEMESSE, J. M., LOPEZ CUESTA, J. M., VELASCO, J. I. & PIECHACZYK, A. (2006) Study of hydromagnesite and magnesium hydroxide based fire retardant systems for ethylene-vinyl acetate containing organo-modified montmorillonite. *Polymer Degradation and Stability,* 91, 3074-3082.

LARRY PENNER, W. K. O. C., DAVID C. DAHLIN, STEVE GERDEMANN, GILBERT E. RUSH (2004) Mineral Carbonation: Energy Costs of Pretreatment Options and Insights Gained from Flow Loop Reaction Studies. ARE.

LEVENSPIEL, O. (1972) *Chemical reaction engineering*, Second Ed., John Wiley and Sons, New York, U.S.;.

LI, W., LI, W., LI, B. & BAI, Z. (2009) Electrolysis and heat pretreatment methods to promote CO2 sequestration by mineral carbonation. *Chemical Engineering Research and Design,* 87, 210-215.

LUCE, R. W., BARTLETT, R.W., PARKS, G.A. (1972) Dissolution kinetics of magnesium silicates. *Geochim. Cosmochim. Acta,* 36, 35-50.

MATTER, J. M., BROECKER, W. S., STUTE, M., GISLASON, S. R., OELKERS, E. H., STEF NSSON, A., WOLFF-BOENISCH, D., GUNNLAUGSSON, E., AXELSSON, G. & BJ RNSSON, G. (2009) Permanent Carbon Dioxide Storage into Basalt: The CarbFix Pilot Project, Iceland. *Energy Procedia,* 1, 3641-3646.

MATTER, J. M., KELEMEN, PETER B., AND STREIT, ELISABETH (2009) Permenant carbon dioxide storage and mineral carbonation geologic reservorirs. *Portland GSA Annual Meeting* Portland, Oregon, U.S..

MCKELVY, M. J., CHIZMESHYA, A. V. G., DIEFENBACHER, J., BEARAT, H. & WOLF, G. (2004) Exploration of the role of heat activation in enhancing serpentine carbon sequestration reactions. *Environmental Science & Technology,* 38, 6897-6903.

MCKINSEY, C. (2008) Carbon Capture and Storage: Assessing the Economics, McKinsey & Company [Online]. Available:

http://www.mckinsey.com/clientservice/sustainability/pdf/CCS_Assessing_the_Economics.pdf [Accessed 6th April 2011].

MERCEDES MAROTO-VALER, M., FAUTH, D. J., KUCHTA, M. E., ZHANG, Y. & ANDR SEN, J. M. (2005) Activation of magnesium rich minerals as carbonation feedstock materials for CO_2 sequestration. *Fuel Processing Technology,* 86, 1627-1645.

MERCEDES MAROTO-VALER, Z., YINZHI, KUCHTA, MATTHEW E., ANDRESEN, JOHN M., FAUTH, DAN J. (2005) *Process for sequestering carbon dioxide and sulfur dioxide*

MICHAEL J. MCKELVY, A. V. G. C., KYLE SQUIRES, RAY W. CARPENTER, HAMDALLAH B ARAT (2006) A new approach to mineral carbonation: enhancing carbonation while avoiding mineral pre-treatment process cost. DOE, report number: DE-FG26-04NT42124, Submitted by Arizona State University. Center for Solid State Science and Department of Mechanical and Aerospace Engineering.

MONTGOMERY, J. C. (1962) Apparatus for decomposing solid ammonium sulfate. U.S. patent: 3047369

MUNZ, I. A., KIHLE, J., BRANDVOLL, O., MACHENBACH, I., CAREY, J. W., HAUG, T. A., JOHANSEN, H. & ELDRUP, N. (2009) A continuous process for manufacture of magnesite and silica from olivine, CO_2 and H_2O. *Energy Procedia,* 1, 4891-4898.

MUSVOTO, E. V., WENTZEL, M. C. & EKAMA, G. A. (2000) Integrated chemical-physical processes modelling--II. simulating aeration treatment of anaerobic digester supernatants. *Water Research,* 34, 1868-1880.

NORDKALY, O. (2004) Price data. Supplied by Nordkalk Oy, June 2004.

NZEC (2009) China-UK Near Zero Emission Coal (NZEC) initiative [Online]. Available: http://www.nzec.info/en/assets/Reports/CCS-Activities-in-China.pdf [Accessed 5th March 2011].

O'CONNOR W.K., D. D. C., RUSH G.E., GERDEMANN S.J., PENNER L.R. (2004) Energy and Economic Evaluation of Ex-Situ Aqueous Mineral Carbonation. ARE, DOE/ARC-2004-028.

O'CONNOR, W. K., DAHLIN, D. C., RUSH, G. E., DAHLIN, C. L. & COLLINS, W. K. (2002) Carbon dioxide sequestration by direct mineral carbonation: process mineralogy of feed and products. *Minerals & Metallurgical Processing,* 19, 95-101.

O'CONNOR, W. K., DAHLIN, D.C., NILSEN, D.N., RUSH, G.E., WALTERS, R.P. & TURNER, P.C. (2001) Carbon dioxide sequestration by direct mineral carbonation: results from recent studies and current status. *In:* 1st National Conference on Carbon Sequestration, Alexandria, VA, U.S..

O'CONNOR, W. K., DAHLIN, D.C., RUSH, G.E., GERDEMANN, S.J., PENNER, L.R. & NILSEN, D.N. (2004) Aqueous mineral carbonation: mineral availability, pretreatment, reaction parametrics and process studies,. DOE/ARC-TR-04-002, Albany Research Center, Albany, OR, U.S..

O'CONNOR, W. K., DAHLIN, D.C., RUSH, G.E., GERDEMANN, S.J., PENNER, L.R. & NILSEN, D.N. (2005) Aqueous mineral carbonation: mineral availability, pretreatment, reaction parametrics and process studies,. DOE/ARC-TR-04-002, Albany Research Center, Albany, OR, U.S..

OELKERS, E.H. (2001) An experimental study of forsterite dissolution rates as a function of temperature and aqueous Mg and Si concentrations. Chemical Geology, 175, 48-494.

ORMOND BRETHERICK, CALIF, B. (1975) Method for converting ammonium sulfate to ammonium bisulfate. U.S. patent: 3911092.

PARK, A. H. (2008) Enabling Sustainable Fossil Fuel Energy Conversion Systems: CO_2 and SO_2 Mineral Sequestration and Utilization of Solid Byproducts. *In:* Presented at the 2nd Int. Conf. on Accelerated Carbonation for Environmental and Materials Engineering, (ACEME08), Rome (Italy) October 1-3, 2008.

PARK, A. H. A. & FAN, L. S. (2004) CO_2 mineral sequestration: physically activated dissolution of serpentine and pH swing process. *Chemical Engineering Science,* 59, 5241-5247.

PETER B. KELEMEN, J. M. (2008) In situ carbonation of peridotite for CO_2 storage *Proc. Nat. Acad. Sci. U.S., 105 (45), 17295-17300.*

PETERS MS, T. K. (1991) Plant design and economics for chemical engineers. , New York: McGraw-Hill.

POKROVSKY, O.S., SCHOTT, J. (2000) Kinetics and mechanism of forsterite dissolution at 25 °C and pH from 1 to 12. Geochim. Cosmochim. Acta 64, 3313-3325.

POWERSPAN (2011) ECO-SO_2 & ECO_2 Process Flow [Online]. Available: http://www.powerspan.com/uploadedFiles/Technology/ECO2/Powerspan_Integrated_ECO-SO2-ECO2_Process_Flow.pdf [Accessed 16th May 2011].

PRIGIOBBE, V., COSTA, G., BACIOCCHI, R., H NCHEN, M. & MAZZOTTI, M. (2009a) The effect of CO_2 and salinity on olivine dissolution kinetics at. *Chemical Engineering Science,* 64, 3510-3515.

PRIGIOBBE, V., H NCHEN, M., WERNER, M., BACIOCCHI, R. & MAZZOTTI, M. (2009b) Mineral carbonation process for CO_2 sequestration. *Energy Procedia,* 1, 4885-4890.

PUNDSACK, F. L. (1967) Recovery of silica, iron oxide and magnesium carbonate from the treatment of serpentine with ammonium bisulfate. United States Patent 3338667.

RAUTENBACH, R., MONHEIM, P. & ZEBROWSKI, D. (1979) MSF-Seawater desalination plants using waste heat from electric-arc furnaces in the steel industry. *Desalination,* 31, 197-206.

RENDEK, E., DUCOM, G. & GERMAIN, P. (2006) Carbon dioxide sequestration in municipal solid waste incinerator (MSWI) bottom ash. *Journal of Hazardous Materials,* 128, 73-79.

ROSKILL INFORMATION SERVICES, L. (2008) *The Economics of Precipitated Calcium Carbonate, 7th Edition.*

ROSSO, J.J., RIMSTIDT, J.D. (2000) A high resolution study of forsterite dissolution rates. Geochim. Cosmochim. Acta 64, 797 - 811.

S.C. KREVOR, C. R. G., B.S. VAN GOSEN, AND A.E. MCCAFFERTY (2009) Mapping the Mineral Resource Base for Mineral Carbon-Dioxide Sequestration in the Conterminous United States. U.S. Geological Survey, Reston, Virginia.

SANDENGEN, K., JOSANG, L. O. & KAASA, B. (2008) Simple Method for Synthesis of Magnesite ($MgCO_3$). *Industrial & Engineering Chemistry Research,* 47, 1002-1004.

SEIFRITZ, W. (1990) CO_2 disposal by means of silicates. *Nature,* 345, 486.

SHANTHAKUMAR, S., SINGH, D. N. & PHADKE, R. C. (2008) Flue gas conditioning for reducing suspended particulate matter from thermal power stations. *Progress in Energy and Combustion Science,* 34, 685-695.

SHOGENOVA, A., SLIAUPA, S., SHOGENOV, K., SLIAUPIENE, R., POMERANCEVA, R., VAHER, R., UIBU, M. & KUUSIK, R. (2009) Possibilities for geological storage and mineral trapping of industrial CO_2 emissions in the Baltic region. *Energy Procedia,* 1, 2753-2760.

SINNOTT RK (1997) *Chemical engineering design. 2nd ed. Coulson &Richardson's chemical engineering vol. 6.* , Butterworth-Heinemann Ltd.

SOLUBILITY DATABASE (2011) *International Union of Pure and Applied Chemistry / National Institute of Standards and Technology* [Online]. Available: http://srdata.nist.gov/solubility/index.aspx [Accessed 4th April 2011].

STERN, N. (2006) The economics of climate change: The Stern review. Cambridge University Press, Cambridge, UK.

TEIR, S., ELONEVA, S. & ZEVENHOVEN, R. (2005) Production of precipitated calcium carbonate from calcium silicates and carbon dioxide. *Energy Conversion and Management,* 46, 2954-2979.

TEIR, S., ELONEVA, S., FOGELHOLM, C. J. & ZEVENHOVEN, R. (2006) Stability of calcium carbonate and magnesium carbonate in rainwater and nitric acid solutions. *Energy Conversion and Management,* 47, 3059-3068.

TEIR, S., ELONEVA, S., FOGELHOLM, C. J. & ZEVENHOVEN, R. (2007a) Dissolution of steelmaking slags in acetic acid for precipitated calcium carbonate production. *Energy,* 32, 528-539.

TEIR, S., KUUSIK, R., FOGELHOLM, C. J. & ZEVENHOVEN, R. (2007b) Production of magnesium carbonates from serpentinite for long-term storage of CO_2. *International Journal of Mineral Processing,* 85, 1-15.

TEIR, S., REVITZER, H., ELONEVA, S., FOGELHOLM, C. J. & ZEVENHOVEN, R. (2007c) Dissolution of natural serpentinite in mineral and organic acids. *International Journal of Mineral Processing,* 83, 36-46.

TEIR, S., ELONEVA, S., FOGELHOLM, C. J. & ZEVENHOVEN, R. (2009) Fixation of carbon dioxide by producing hydromagnesite from serpentinite. *Applied Energy,* 86, 214-218.

THAMBIMUTHU, K. (2008) Conference Summary for the 9th International Conference on Greenhouse Gas Control Technologies (GHGT9). Washington DC, 16-20 November 2008.

VALENTINA PRIGIOBBE, M. W., MARCO MAZZOTTI (2010) Enhanced Olivine Dissolution using Organic Salts. *oral presentation at GHGT10, 10th Greenhouse Gas Control Technologies Conference, Sep 19-23, 2010, Amsterdam, The Netherlands.*

VAN ESSENDELFT, D. T. & SCHOBERT, H. H. (2009a) Kinetics of the Acid Digestion of Serpentine with Concurrent Grinding. 1. Initial Investigations. *Industrial & Engineering Chemistry Research,* 48, 2556-2565.

VAN ESSENDELFT, D. T. & SCHOBERT, H. H. (2009b) Kinetics of the Acid Digestion of Serpentine with Concurrent Grinding. 2. Detailed Investigation and Model Development. *Industrial & Engineering Chemistry Research,* 48, 9892-9901.

VAN ESSENDELFT, D. T. & SCHOBERT, H. H. (2010) Kinetics of the Acid Digestion of Serpentine with Concurrent Grinding. 3. Model Validation and Prediction. *Industrial & Engineering Chemistry Research,* 49, 1588-1590.

W.J.J. HUIJGEN, R. N. J. C. (2003) Carbon dioxide sequestration by mineral carbonation Literature Review. ECN.

WEBER, M. (2000) Mineral flame retardant-overview & future trends. *Industrial Minerals,* 389, 19-27.

WILLIAMS, J. (2009) *Optimization of Emissions Reduction Equipment (SCR)* [Online]. Available: http://www.emersonprocessxperts.com/papers/Optimization-of-Emissions-Reduction-Equipment-SCR.pdf [Accessed 15th March 2011].

WINDSOR MVR EVAPORATION SYSTEM. (2011) *MVR EVAPORATION SYSTEMS* [Online]. Available: http://www.windsorsathyam.com/faq.html#S [Accessed 24th April 2011].

WOLF, G. H., CHIZMESHYA, A. V. G., DIEFENBACHER, J. & MCKELVY, M. J. (2004) In situ observation of CO_2 sequestration reactions using a novel microreaction system. *Environmental Science & Technology,* 38, 932-936.

XIAOLONG WANG, Mercedes Maroto-Valer (2010a) Dissolution of serpentine using recyclable ammonium salts for CO_2 mineral carbonation. *FUEL,* 90, 1229-1237.

XIAOLONG WANG, Mercedes Maroto-Valer (2010b) Integration of CO_2 capture and storage based on pH–swing mineral carbonation using recyclable ammonium salts. *Energy Procedia.*

YANG, H., XU, Z., FAN, M., GUPTA, R., SLIMANE, R. B., BLAND, A. E. & WRIGHT, I. (2008) Progress in carbon dioxide separation and capture: A review. *Journal of Environmental Sciences,* 20, 14-27.

ZEP (2011) CO_2 capture costs, Report January 2011, European Technology Platform for Zero Emission Fossil Fuel Power Plants [Online]. Available: www.zeroemissionplatform.eu. [Accessed 15th May 2011].

ZEVENHOVEN, RON (2001) CO_2 SEQUESTRATION BY MAGNESIUM SILICATE MINERAL CARBONATION IN FINLAND. *Second Nordic Minisymposium on Carbon Dioxide Capture and Storage.* Göteborg, October 26, 2001.

ZEVENHOVEN, RON (2002) Direct Dry Mineral Carbonation for CO_2 Emissions Reduction in Finland. *27th International Technical Conference on Coal Utilization & Fuel Systems Clearwater* FL, U.S., March 4-7, 2002.

ZEVENHOVEN, R., ELONEVA, S. & TEIR, S. (2006) Chemical fixation of CO_2 in carbonates: Routes to valuable products and long-term storage. *Catalysis Today,* 115, 73-79.

ZEVENHOVEN, R., SIPIL , J., TEIR, S. (2008) Motivations for carbonating magnesium silicates using a gas-solid process route. *In:* In: Proc. of the 2nd Int. Conf. on Accelerated Carbonation for Environmental and Materials Engineering, (ACEME08), Rome (Italy) October 1-3, 2008, 45-54, 2008.

ZEVENHOVEN, R., TEIR, S. & ELONEVA, S. (2008) Heat optimisation of a staged gas-solid mineral carbonation process for long-term CO_2 storage. *Energy,* 33, 362-370.

ZEVENHOVEN, Ron, JOHAN FAGERLUND, INES ROMAO, JAMES HIGHFIELD, BU JIE (2010) Assessment & improvement of a stepwise magnesium silicate carbonation route via $MgSO_4$ & $Mg(OH)_2$. *ACEME 10.* Turku, Finland.

ZHANG YUN, L. Z.Z., LI XIN, DONG JIANG-XUN, WANG YANG, SCOTT M. SMOUSE AND JAMES M. EKMANN (2003) Preliminary Study to Capture CO_2 in Flue Gas by Spraying Aqueous Ammonia to Produce NH_4HCO_3. National Power Plant Combustion Engineering Technology Research Center, Shenyang, P.R. China; U.S. Department of Energy, National Energy Technology Laboratory.

Appendix 1:

The detail of conditions applied in the modelling of mass flow

Dissolution step	For 50 g/l scenario, 1.4 mol/l NH_4HSO_4 (15 wt. %) was used to dissolve serpentine with particle size of 75-150 μm. The Mg dissolution efficiency achieved 100 % after 3 h at 100 °C. 90 % of Fe was dissolved. Product 1 (contain 46.9 wt. % of Si) was filtered after dissolution. For 300 g/l scenario, 6 mol/l NH_4HSO_4 (53 wt. %) was used to dissolve serpentine with particle size of 75-150 μm. The dissolution efficiency achieved 71 % after 3 h at 100 °C.
pH swing step	1 mol NH_4HSO_4 react with 1 mol NH_3 to produce 1 mol $(NH_4)_2SO_4$. Assuming that the iron ions precipitate does not consume ammonia water. 13 wt. % NH_3 was used. Product 2 (60 wt. % Fe) was filtered after pH-swing at 50 g/l scenario.
Capture step	According to Kim's work, 13 wt. % of NH_3 used in aqueous ammonia CO_2 capture can achieve 95 % absorption efficiency and produce 3.4 mol/l total CO_2 containing ammonium salts (41 % NH_4HCO_3, 24 % $(NH_4)_2CO_3$ and 35 % $NH_4NH_2CO_2$, molecular weight is 82.52) after breakthrough point of 6 h (Kim *et al.*, 2008). In the other way, capturing 1 t CO_2 requires 0.76 t NH_3 and 5.01 t H_2O and produces 1.88 t of CO_2 containing ammonium salts (where contains 35 % ammonium carbamate, 41 % ammonium bicarbonate and 24 % ammonium carbonate).

Appendix 2

Input and output streams in each step of the two process routes.

		Mass at 50 g/l scenario (t)	Mass at 300 g/l scenario (t)
Mineral dissolution step	Input		
	Serpentine	2.96	4.88
	NH_4HSO_4	9.54	11.22
	H_2O	54.91	10.16
	Output		
	$MgSO_4$	3.55	4.17
	$(NH_4)_2SO_4$	3.91	4.59
	NH_4HSO_4	2.73	3.23
	H_2O	55.80	11.20
	Product 1 (46.9 wt. % Si)	1.27	0.00
	Serpentine	0.00	
	Fe^{2+}	0.15	
	Residual solid (including serpentine and SiO_2)		3.07
pH-swing step	*Input*		
	$MgSO_4$	3.55	4.17
	$(NH_4)_2SO_4$	3.91	4.59
	NH_4HSO_4	2.73	3.23
	H_2O	58.49	14.40
	Fe^{2+}	0.15	
	NH_3 for pH-swing	0.40	0.48
	Residual solid		3.07
	output		

	$MgSO_4$	3.55	4.17
	$(NH_4)_2SO_4$	7.04	8.30
	H_2O	58.39	14.40
	Product 2 (60 wt. % Fe)	0.25	0.00
	Residual solid		3.07
Capture step	*input*		
	CO_2	4.99	1.46
	NH_3 (13 wt. %)	3.82	1.12
	H_2O	24.21	7.10
	output (95 % efficiency, 6 h)		
	$NH_4HCO_3/(NH_4)_2CO_3/NH_4NH_2CO_2$	9.36	2.75
	NH_3	0.76	0.22
	H_2O	23.05	6.76
	CO_2	0.61	0.18
Carbonation step	*input*		
	$MgSO_4$	3.55	4.17
	$(NH_4)_2SO_4$	7.04	8.30
	$NH_4HCO_3/(NH_4)_2CO_3/NH_4NH_2CO_2$	9.36	2.75
	NH_3 for carbonation	1.01	0.00
	Residual solid		3.07
	H_2O	88.18	21.16
	output		
	$(NH_4)_2SO_4$	10.79	11.30
	Hydromagnesite	2.75	
	NH_3	0.52	
	$MgSO_4$	0.15	1.44
	$NH_4HCO_3/(NH_4)_2CO_3/NH_4NH_2CO_2$	7.12	0.56
	NH_3		

		CO_2	
		H_2O	
	Magnesite		1.91
	Residual solid		3.07
	H_2O	87.67	21.16
	input		
	$(NH_4)_2SO_4$	10.79	11.30
	H_2O	87.67	21.16
Regener	*output*		
ation	NH_4HSO_4	9.30	9.74
	NH_3	1.38	1.44
	$(NH_4)_2SO_4$	0.11	0.11
	H_2O	87.67	21.16
	Serpentine	2.96	4.88
	H_2O	-4.18	-0.70
	NH_4HSO_4	0.23	1.48
	NH_3	0.24	-0.25
	$NH_4HCO_3/(NH_4)_2CO_3/NH_4NH_2CO_2$	2.24	2.18
Sum	$MgSO_4$	0.15	1.44
	$(NH_4)_2SO_4$	0.11	0.11
	Product 1	1.27	
	Product 2	0.25	
	Residual solid		3.07
	hydromagnesite	2.75	
	magnesite		1.91

Appendix 3.

Input and output streams in each step, the energy consumption, and chemical cost of the four optimization experiments,

		OP 1	OP2	OP 3	OP 4
Mineral dissolution step	Input				
	Serpentine	3.50	3.32	3.15	2.96
	NH_4HSO_4	11.26	10.69	10.14	9.53
	H_2O	27.58	26.16	24.83	23.33
	Output				
	$MgSO_4$	3.36	3.19	3.02	2.84
	$(NH_4)_2SO_4$	3.69	3.50	3.33	3.12
	NH_4HSO_4	4.83	4.58	4.35	4.08
	H_2O	28.42	26.96	25.58	24.04
	Product 1 (46.9 wt. % Si)	1.16	1.10	1.05	0.98
	Serpentine	0.70	0.66	0.63	0.59
	Fe^{2+}	0.18	0.17	0.16	0.15
	Residual solid (including serpentine and SiO_2)				
pH-swing step	*Input*				
	$MgSO_4$	3.36	3.19	3.02	2.84
	$(NH_4)_2SO_4$	3.69	3.50	3.33	3.12
	NH_4HSO_4	4.83	4.58	4.35	4.08
	H_2O	33.19	31.49	29.88	28.08
	Fe^{2+}	0.18	0.17	0.16	0.15
	NH_3 for pH-swing	0.71	0.68	0.64	0.60
	Residual solid				

	output				
	$MgSO_4$	3.36	3.19	3.02	2.84
	$(NH_4)_2SO_4$	9.24	8.76	8.31	7.81
	H_2O	33.07	31.37	29.77	27.98
	Product 2 (60 wt. % Fe)	0.30	0.28	0.27	0.25
	Residual solid				
	input				
	CO_2	1.18	1.68	1.06	1.50
	NH_3 (13 wt. %)	0.90	1.28	0.81	1.14
	H_2O	5.72	8.14	5.15	7.26
Captur	*output*				
e step	$NH_4HCO_3/(NH_4)_2CO_3/NH_4NH_2CO_2$	2.21	3.15	1.99	2.81
	NH_3	0.18	0.25	0.16	0.23
	H_2O	5.44	7.75	4.90	7.02
	CO_2	0.14	0.21	0.13	0.07
	input				
	$MgSO_4$	3.36	3.19	3.02	2.84
	$(NH_4)_2SO_4$	9.24	8.76	8.31	7.81
	$NH_4HCO_3/(NH_4)_2CO_3/NH_4NH_2CO_2$	2.21	3.15	1.99	2.81
Carbo	NH_3 for carbonation	0.48	0.45	0.86	0.80
nation	Residual solid				
step	H_2O	40.51	40.44	39.33	38.86
	output				
	$(NH_4)_2SO_4$	12.24	11.76	11.31	10.81
	Hydromagnesite				

	NH_3	0.28	0.26	0.66	0.61
	$MgSO_4$	0.63	0.46	0.30	0.11
	$NH_4HCO_3/(NH_4)_2CO_3/NH_4NH_2CO_2$	0.22	1.16	0.00	0.82
	NH_3	0.07	0.38	0.00	0.27
	CO_2	0.12	0.62	0.00	0.44
	H_2O	0.03	0.16	0.00	0.12
	Magnesite	1.91	1.91	1.91	1.91
	Residual solid				
	H_2O	40.51	40.44	39.33	38.86
Regeneration	*input*				
	$(NH_4)_2SO_4$	12.24	11.76	11.31	10.81
	H_2O	40.51	40.44	39.33	38.98
	output				
	NH_4HSO_4	10.55	10.14	9.76	9.32
	NH_3	1.56	1.50	1.44	1.38
	$(NH_4)_2SO_4$	0.12	0.12	0.11	0.11
	H_2O	40.51	40.44	39.33	38.98
Sum	Serpentine	3.50	3.32	3.15	2.96
	H_2O	-0.44	-0.29	-0.40	-0.48
	NH_4HSO_4	0.71	0.54	0.38	0.20
	NH_3	0.00	0.02	0.04	0.07
	$NH_4HCO_3/(NH_4)_2CO_3/NH_4NH_2CO_2$	1.99	1.99	1.99	1.99
	$MgSO_4$	0.63	0.46	0.30	0.11
	$(NH_4)_2SO_4$	0.12	0.12	0.11	0.11
	Product 1	1.16	1.10	1.05	0.98
	Product 2	0.30	0.28	0.27	0.25

	magnesite	1.91	1.91	1.91	1.91
Energy consumption (kWh/t CO_2)	Grinding	45.48	43.14	40.94	38.47
	CO_2 capture	22.40	31.87	20.16	28.42
	MVR evaporation	324.05	323.51	314.65	311.80
	Filtering	28.82	27.95	26.60	25.56
	Pumping	78.36	74.33	70.54	68.08
	Thermal decomposition	62.38	62.85	59.60	59.40
	Total energy	561.49	563.66	532.49	531.74
	Cost of energy (US$)	16.84	16.91	15.97	15.95
Chemical consumption	NH_4HSO_4	0.71	0.54	0.38	0.20
	NH_3(capture + mineralisation)	0.00	0.02	0.04	0.07
	$(NH_4)_2SO_4$ (equal, 99 %)	0.83	0.63	0.44	0.54
	Cost of $(NH_4)_2SO_4$	74.26	56.57	39.91	48.19
	NH_3 (reduce amount generated from above)	-0.11	-0.06	-0.01	0.00
	Cost of NH_3	-19.52	-10.72	-2.43	0.00
	NH_4HSO_4	0.00	0.00	0.00	-0.26
	cost of NH_4HSO_4	0.00	0.00	0.00	-23.29
	Chemical cost (US$)	54.74	45.85	37.48	24.90